Gmelin Handbook of Inorganic and Organometallic Chemistry

N

SUPPLEMENT VOLUME B2

COMPOUNDS WITH NOBLE GASES AND HYDROGEN

1993

Periodic Table of the Elements with

1 H																	2 He
3 Li	4 Be											5 B	6 C	7 N	8 O	9 F	10 Ne
11 Na	12 Mg											13 Al	14 Si	15 P	16 S	17 Cl	18 Ar
19 * K	20 Ca	21 Sc	22 Ti	23 V	24 Cr	25 Mn	26 Fe	27 Co	28 Ni	29 Cu	30 Zn	31 Ga	32 Ge	33 As	34 Se	35 Br	36 Kr
37 Rb	38 Sr	39 Y	40 Zr	41 Nb	42 Mo	43 Tc	44 Ru	45 Rh	46 Pd	47 Ag	48 Cd	49 In	50 Sn	51 Sb	52 Te	53 I	54 Xe
55 Cs	56 Ba	57** La	72 Hf	73 Ta	74 W	75 Re	76 Os	77 Ir	78 Pt	79 Au	80 Hg	81 Tl	82 Pb	83 Bi	84 Po	85 At	86 Rn
87 Fr	88 Ra	89*** Ac	104	105													* NH_4

**Lanthanides	58 Ce	59 Pr	60 Nd	61 Pm	62 Sm	63 Eu	64 Gd	65 Tb	66 Dy	67 Ho	68 Er	69 Tm	70 Yb	71 Lu
***Actinides	90 Th	91 Pa	92 U	93 Np	94 Pu	95 Am	96 Cm	97 Bk	98 Cf	99 Es	100 Fm	101 Md	102 No	103 Lr

A Key to the Gmelin System is given on the Inside Back Cover

Gmelin Handbook of Inorganic and Organometallic Chemistry

8th Edition

Gmelin Handbook of Inorganic and Organometallic Chemistry

8th Edition

Gmelin Handbuch der Anorganischen Chemie

Achte, völlig neu bearbeitete Auflage

PREPARED AND ISSUED BY
Gmelin-Institut für Anorganische Chemie
der Max-Planck-Gesellschaft
zur Förderung der Wissenschaften
Director: Ekkehard Fluck

FOUNDED BY
Leopold Gmelin

8TH EDITION
8th Edition begun under the auspices of the
Deutsche Chemische Gesellschaft by R. J. Meyer

CONTINUED BY
E. H. E. Pietsch and A. Kotowski, and by
Margot Becke-Goehring

Springer-Verlag Berlin Heidelberg GmbH 1993

Gmelin-Institut für Anorganische Chemie
der Max-Planck-Gesellschaft zur Förderung der Wissenschaften

GMELIN HANDBOOK

Dr. J. von Jouanne

Dr. L. Berg, Dr. H. Bergmann, Dr. J. Faust, J. Füssel, Dr. H. Katscher, Dr. R. Keim, Dipl.-Phys. D. Koschel, Dr. A. Kubny, Dr. P. Merlet, Dr. M. Mirbach, Prof. Dr. W. Petz, Dr. F. A. Schröder, Dr. A. Slawisch, Dr. W. Töpper

Dr. R. Albrecht, Dr. G. Bär, D. Barthel, Dr. N. Baumann, Dr. K. Behrends, Dr. W. Behrendt, D. Benzaid, Dr. R. Bohrer, K. D. Bonn, Dipl.-Chem. U. Boßlet, Dr. U. Busch, A.-K. Castro, Dipl.-Ing. V. A. Chavizon, E. Cloos, A. Dittmar, Dipl.-Geol. R. Ditz, R. Dowideit, Dr. H.-J. Fachmann, B. Fischer, Dr. D. Fischer, Dipl.-Ing. N. Gagel, Dr. K. Greiner, Dipl.-Bibl. W. Grieser, Dr. R. Haubold, Dipl.-Min. H. Hein, Dipl.-Phys. C. Heinrich-Sterzel, H.-P. Hente, H. W. Herold, U. Hettwer, G. Hoell, Dr. G. Hönes, Dr. W. Hoffmann, G. Horndasch, Dr. W. Huisl, Dr. M. Irmler, B. Jaeger, Dr. R. Jotter, Dipl.-Chem. P. Kämpf, Dr. B. Kalbskopf, H.-G. Karrenberg, Dipl.-Phys. H. Keller-Rudek, Dipl.-Chem. C. Koeppel, Dr. M. Körfer, R. Kolb, Dr. M. Kotowski, E. Kranz, E. Krawczyk, Dipl.-Chem. I. Kreuzbichler, Dr. V. Kruppa, Dr. W. Kurtz, M. Langer, Dr. B. Ledüc, H. Mathis, E. Meinhard, M. Meßer, C. Metz, K. Meyer, E. Mlitzke, Dipl.-Chem. B. Mohsin, Dr. U. Neu-Becker, K. Nöring, Dipl.-Min. U. Nohl, Dr. U. Ohms-Bredemann, Dr. H. Pscheidl, Dipl.-Phys. H.-J. Richter-Ditten, E. Rudolph, G. Rudolph, Dr. B. Sarbas, Dr. H. Schäfer, Dr. R. Schemm, Dr. D. Schiöberg, V. Schlicht, Dipl.-Chem. D. Schneider, E. Schneider, A. Schwärzel, Dr. B. Schwager, R. Simeone, Dr. F. Stein, Dr. C. Strametz, Dr. G. Swoboda, Dr. D. Tille, A. Tuttas, Dipl.-Phys. J. Wagner, R. Wagner, M. Walter, Dr. E. Warkentin, Dr. C. Weber, Dr. A. Wietelmann, Dr. M. Winter, Dr. B. Wöbke, K. Wolff

GMELIN ONLINE

Dr. R. Deplanque

Dr. P. Kuhn, Dr. G. Olbrich

Dr. R. Baier, Dr. B. Becker, Dipl.-Chem. E. Best, Dr. H.-U. Böhmer, Dipl.-Phys. R. Bost, Dr. A. Brandl, Dr. R. Braun, Dr. T. Buck, Dipl.-Chem. R. Durban, R. Hanz, Dr. S. Kalwellis-Mohn, Dr. A. Kirchhoff, Dipl.-Chem. H. Köttelwesch, Dr. M. Kunz, Dr. L. Leichner, Dipl.-Chem. R. Maass, Dr. K. Müller, Dr. A. Nebel, Dipl.-Chem. R. Nohl, Dr. M. Nohlen, H. Reinhardt, Dr. B. Rempfer, Dipl.-Ing. H. Vanecek

Volumes published on "Nitrogen" (Syst. No. 4)

Main Volume 1
History. Occurrence. The Element — 1934

Main Volume 2
Compounds of Nitrogen with Hydrogen — 1935

Main Volume 3
Compounds of Nitrogen with Oxygen — 1936

Main Volume 4
Compounds with Oxygen — 1936

Supplement Volume B2
Compounds with Noble Gases and Hydrogen — 1993 (present volume)

Gmelin Handbook of Inorganic and Organometallic Chemistry

8th Edition

N

Nitrogen

Supplement Volume B 2

Compounds with Noble Gases and Hydrogen
(continued)

With 2 illustrations

AUTHORS Reinhard Haubold, Claudia Heinrich-Sterzel, Peter Merlet,
Ulrike Ohms-Bredeman, Carol Strametz, Astrid Wietelmann

EDITORS Dieter Koschel, Peter Merlet, Astrid Wietelmann

CHIEF EDITOR Peter Merlet

System Number 4

Springer-Verlag Berlin Heidelberg GmbH 1993

LITERATURE CLOSING DATE: MID 1992
IN SOME CASES MORE RECENT DATA HAVE BEEN CONSIDERED

Library of Congress Catalog Card Number: Agr 25-1383

ISBN 978-3-662-06338-5 ISBN 978-3-662-06336-1 (eBook)
DOI 10.1007/978-3-662-06336-1

Originally published by Springer-Verlag, Berlin in 1993.
Softcover reprint of the hardcover 8th edition 1993

Preface

"Nitrogen" Suppl. Vol. B2 continues the description of binary compounds composed of nitrogen and hydrogen (nitrogen hydrides). While "Nitrogen" Suppl. Vol. B1 covers mononitrogen compounds, the present volume comprises compounds having two, three, four, or more nitrogen atoms. Hydrazine, N_2H_4, and its ions $N_2H_5^+$ and $N_2H_6^{2+}$ were not included. (Reference is made to a voluminous monograph: E.W. Schmidt, Hydrazine and its Derivatives: Preparation, Properties, Applications, Chichester 1984, 1088 pages.)

Among the dinitrogen compounds, the diazenyl cation, N_2H^+, has been extensively investigated, especially in regards to spectroscopic and kinetic properties, because of its occurrence in interstellar space. Chemically well-characterized are diazene, N_2H_2, the simplest unsaturated nitrogen hydride which is used as a hydrogenation reagent, and the hydrazyl radical, N_2H_3, which is frequently present as an intermediate during the formation and decay of nitrogen-hydrogen compounds.

The major portion of this volume is taken up by hydrogen azide or hydrazoic acid, HN_3, the first member in the series of trinitrogen compounds. Known to be highly explosive in pure form, it can be safely handled when diluted. Thus, a great deal of information is available mainly on its properties as a chemical reagent and its decomposition processes.

Other compounds with three or more nitrogens which are stable at room temperature include 2-tetrazene, N_4H_4, ammonium azide, NH_4N_3, and hydrazinium azide, $N_2H_5N_3$. Cyclotriazane, c-N_3H_3, and triazane, N_3H_5, were isolated as Ag^+ complexes. The aminodiazonium ion, $N_3H_2^+$, and the triazanium ion, $N_3H_6^+$, form isolable salts. Some other nitrogen hydrides such as triazene, N_3H_3, 1,3-tetrazadiene, N_4H_2, and tetrazane, N_4H_6, were thought to form only as intermediates. Occasionally they were identified by physical techniques. In several cases, where the binary nitrogen hydrides cannot be isolated other than in the form of organic derivatives, the data available for the organic derivatives were included when they were thought to be characteristic for the particular unsubstituted N-H parent compound. A series of other, hypothetical nitrogen hydrides have so far only been studied by quantum-chemical methods.

The volume closes with a few ternary compounds composed of nitrogen, hydrogen, and noble gases.

Frankfurt am Main
September 1993

Peter Merlet

Table of Contents

Page

Compounds of Nitrogen with Hydrogen

(continued)

2.2 Dinitrogen Compounds

2.2.1 The Diazenyl Radical, N_2H

Other names: Hydrodinitrogen radical, hydrogen dinitride, dinitrogen hydride, hydroazine

CAS Registry Numbers: N_2H *[36882-13-0]*, N_2D *[120550-96-1]*, N_2T *[38326-92-0]*

There are no direct observations of the N_2H radical. Indirect evidence for its formation was obtained from experimental studies on the reaction $NH_2 + NO \rightarrow$ products and on the electron-transfer neutralization of N_2H^+. Theoretical arguments for its existence were once provided by kinetic models of ammonia combustion.

The radical has been the subject of about 30 quantum-chemical studies. Only the results of the more recent and extensive studies are considered in the following text. For other studies, consult the bibliography of ab initio calculations listed on pp. 16/17. Ab initio studies are generally in agreement in predicting that the ground-state radical is thermodynamically unstable with respect to dissociation to N_2 and H, but separated from them by a barrier.

Formation

Indirect evidence for the formation of the radical $N_2H(N_2D)$ by electron-transfer neutralization in the collision of a high-velocity, mass-resolved beam of $N_2H^+(N_2D^+)$ with a target metal gas M (Na, K, Mg, or Zn maintained at a few mTorr), according to $N_2H^+(N_2D^+) + M \rightarrow N_2H^*(N_2D^*) + M^+$, was obtained by monitoring the beam profile of N_2, assumed to arise from the dissociation of the $N_2H(N_2D)$ product. The kinetic energy distribution of N_2, determined from the maximum scattering angle of the N_2 beam profile, indicates that $N_2H(N_2D)$ is formed in the electronic ground state as well as in excited states (see below) depending on the metal target used. As no state of $N_2H(N_2D)$ was observed, an upper limit on the lifetime is given by the beam time-of-flight (5×10^{-7} s) [1].

The formation of an N_2H intermediate was proposed in kinetic modeling studies on the combustion of ammonia, specifically the selective reduction of nitric oxide by ammonia (thermal $DeNO_x$ process). It was assumed that N_2H, formed in one of the channels available to the key reaction of NH_2 with NO (see "Nitrogen" Suppl. Vol. B1), is important in driving subsequent chain reactions. Formation of N_2H in reactions of NH and of N_2H_2 with other species was also included in the reaction schemes; see for example [2 to 6]. Indirect experimental evidence, indicating that the branching of the $NH_2 + NO$ reaction into the $N_2H + OH$ channel is much lower than assumed at the time the combustion models were developed, has cast doubt on the proposed role of N_2H in combustion; see for example [7]. Moreover, an N_2H lifetime of 10^{-4} s, indicated by matching the model to observation, is much longer than experimental and theoretical predictions (see below), implying that N_2H is too short-lived to play an important role [8].

Formation of an N_2H intermediate in the isomerization and decomposition of N_2H_2 was considered in ab initio studies [9 to 13].

An N_2H intermediate was proposed to form during the photodecomposition of N_2H_2 [14] (see p. 61) and dissociation of N_2H_2O isomers [12]. Formation of a vibrationally excited N_2T intermediate in the reaction of recoil tritium with N_2 was suggested [15].

Some observations reported for the N_2H radical [16 to 18] have not been confirmed.

Molecular Properties

Electronic Ground State. The ground state X $^2A'$ of the asymmetric, bent N_2H radical (symmetry group C_s) arises from the electron configuration $(1a')^2$ $(2a')^2$ $(3a')^2$ $(4a')^2$ $(5a')^2$ $(1a'')^2$ $(6a')^2$ $7a'$. Qualitatively, the valence orbital 5a′ corresponds to the σ orbital of N_2, 6a′ to the combination of the bonding π_g orbital of N_2 and the 1s orbital of H, and 7a′ to the combination of the antibonding π_g orbital of N_2 and the 1s orbital of H [19 to 22]. According to MO theory, one NN π bond has been broken and an NH σ bond formed. A lengthening of the NN bond comparable to that of N_2 [21, 22] and an NNH angle Θ of $\sim 120°$ [20] are to be expected. The unpaired electron is localized on the outer nitrogen [11, 23].

The potential energy surface of $N_2H(X\ ^2A') \rightarrow N_2(^1\Sigma_g^+) + H(^2S)$ was characterized in ab initio studies at different levels of calculation: SCF (RHF and UHF) [21, 23 to 26], CASSCF [9], MP2 [27], CI [21], GVB-CI [11], MP4/MP3 [1, 22], and CASSCF/CCI [19, 28 to 30]. Table 1 gives the total energy E_t; dissociation energy D_e; dissociation energy with zero-point energy correction D_0; barrier to dissociation E_a; the geometrical parameters r(NH), r(NN), and Θ from complete geometry optimizations at a multiconfiguration level; and the fundamental frequencies ω_1 (NH stretch), ω_2 (NN stretch), and ω_3 (bend) from some of the more extensive calculations.

Table 1
N_2H. X $^2A'$ Electronic Ground State. Molecular Properties Derived from Various Ab Initio Calculations.

constants	method and basis set CASSCF/CCI ANO[a]	CASSCF/CCI ANO[b]	MP4/MP3 6-31G**	MP4/MP3 6-311G**
E_t in hartree	−109.86037[c]	−109.87596[c]	−109.74902	−109.79020
r(NH) in Å	1.067	1.062	1.045	1.060
r(NN) in Å	1.192	1.197	1.157	1.181
Θ	115°	116.3°	118°	115.8°
D_e in kJ/mol	−16.3	−12.6	−60.2	−59.4
D_0 in kJ/mol	–	−31.1	−86.6	–
E_a in kJ/mol	47.3	50.8	43.9	35.6
E_a^{corr} in kJ/mol[d]	–	35.5	24.3	–
ω_1 in cm^{-1}	–	2744	3077	–
ω_2 in cm^{-1}	–	1583	2619	–
ω_3 in cm^{-1}	–	1070	1079	–
Ref.	[29]	[19]	[22]	[1]

[a] [5s4p3d2f/4s3p2d]. — [b] [4s3p2d1f/3s2p1d]. — [c] Includes a multireference size-consistency (Davidson) correction. — [d] Includes the zero-point energy correction [19].

An anomalous behavior in the ω_2 frequency calculated using MP3 theory [22] led to the suggestion that the perturbation expansion may be inadequate for describing the multiply bonded N_2H species [19]. A high value of $D_e(-83.7$ kJ/mol) obtained in a GVB-CI calculation [11] is attributed to neglected spin-recoupling effects [28]. An analytical potential energy surface was obtained by fitting [31] to points calculated on CASSCF/CCI surfaces [19, 29]. In the majority of studies it was concluded that the N_2H species is thermodynamically unstable, lying above the N_2+H asymptote, but quasibound due to a barrier to dissociation E_a, occurring at the saddle point observed between the N_2H minimum and the N_2+H asymptote [1, 9, 11, 19, 22 to 24, 27, 29, 30].

An ionization potential of 8.15 eV was estimated in a recent ab initio study (MP2) [27]. Comparable values were predicted using SCF energies and using the equivalent core analogy [32]. A value of 7.6 eV was estimated using SCF energies and $\Delta_fH(N_2H^+)=992$ kJ/mol [33].

Experimental evidence based on a study of the neutralization of a beam of N_2H^+ by electron transfer was used to suggest that no state of N_2H has a lifetime longer than 5×10^{-7} s (see above) [1]. Theoretical unimolecular decay lifetimes of N_2H in its ten lowest vibrational states were obtained using converged coupled channel scattering calculations on an analytical potential energy surface fitted [31] to points on CASSCF/CCI surfaces [29]. The vibrational ground state (000) and the first excited state (001) were predicted to have lifetimes of 3×10^{-9} and 2×10^{-10} s, respectively [31]. Lifetimes of 10^{-9} to 10^{-11} s for N_2H [1, 19, 22] and 10^{-10} s for N_2D [1] were estimated using models for one-dimensional quantum-mechanical tunneling through a barrier [1, 19, 22].

Electronically Excited States. The lowest excited state is the $^2A''(\Pi)$ Renner-Teller component of a linear $^2\Pi$ state (symmetry group $C_{\infty v}$). It arises from the electronic configuration $(1a')^2$ $(2a')^2$ $(3a')^2$ $(4a')^2$ $(5a')^2$ $(1a'')^2$ $(6a')^2$ $2a''$ [21, 34]. Potential energy surfaces for the linear $^2A''(\Pi)$, a bent 2 $^2A'$, and linear n = 3 Rydberg states associated with N_2H^+ were characterized in extensive ab initio calculations, CASSCF/CCI with an ANO basis [4s3p2d1f/3s*2p] that was augmented in the case of the Rydberg states with diffuse orbitals. The $^2A''(\Pi)$ and 2 $^2A'$ states were calculated to lie 155 and about 243 kJ/mol above the $N_2(^1\Sigma_g^+)+H(^2S)$ asymptote. The zero-point energy correction was found to raise the former value to 183 kJ/mol. The n = 3 Rydberg states were calculated to lie, after correcting them for the zero-point energy, 544 to 711 kJ/mol (5.7 to 7.2 eV) above the $N_2(^1\Sigma_g^+)+H(^2S)$ asymptote. In this calculated manifold of states, the X $^2A'$ ground state lies 16.3 kJ/mol above the $N_2(^1\Sigma_g^+)+H(^2S)$ asymptote (see Table 1 above). The geometrical parameters of the linear $^2A''(\Pi)$ state, r(NH) = 0.995 Å and r(NN) = 1.188 Å, were determined at the CASSCF level of calculation. It was noted [34] that the $^2A''(\Pi)$, 2 $^2A'$, and the n = 3 Rydberg states lie energetically in the range of excited states of N_2H that could be formed in a resonant electron-transfer process, occurring in experiments in which a beam of N_2H^+ is neutralized by alkali metal targets [1]; see above. Radiative transitions that could occur in such experiments were discussed [1, 34].

Thermodynamic Properties

The enthalpy of formation, $\Delta_fH_0^\circ=255$ kJ/mol [35, 36] and $\Delta_fH_{298}^\circ=252$ kJ/mol, the Gibb's free energy of formation, $\Delta_fG_{298}^\circ=262$ kJ/mol, and values of Δ_fG° at 600, 1200, and 2000 K [36] were obtained using the MP4-BAC method (MP4 energies adjusted by using empirical bond additivity correction factors) [35, 36]. The values $\Delta_fH_0^\circ=322$ kJ/mol and $\Delta_fH_{298}^\circ=319$ kJ/mol, based on an estimated N_2H zero-point energy of 36 kJ/mol, were obtained from GVB-CI results that predict a high value of D_0 (106 kJ/mol) [11].

The entropy $S_{298}^\circ=224$ $J\cdot mol^{-1}\cdot K^{-1}$ was obtained from MP2 calculations [37].

Chemical Behavior

Dissociation $N_2H \rightarrow N_2 + H$. Enthalpy and entropy changes for the $N_2H \rightarrow N_2 + H$ system were obtained from ab initio electronic energies and vibrational frequencies using statistical mechanics [19, 22]. The values $\Delta H^\circ_{298} = -26.2$ kJ/mol and $\Delta S^\circ_{298} = 81.5$ $J \cdot mol^{-1} \cdot K^{-1}$ were based on the results of CASSCF/CCI calculations [19]; the values $\Delta H^\circ_{298} = -81.6$ kJ/mol [22] and $\Delta S^\circ_{298} = 85.4$ $J \cdot mol^{-1} \cdot K^{-1}$ [19] were based on MP4/MP3 calculations [22]. For the potential energy surface $N_2H(X\ ^2A') \rightarrow N_2(^1\Sigma_g^+) + H(^2S)$, see above.

Reactions. Ab initio calculations of reactant and product energies were reported for reactions of N_2H with N_2H_3 [13], O [38], OH [39], and H [24]. For an ab initio study on the $N_2H + H$ potential energy surface, see [28]. Rate constants for the reactions of N_2H with various species were estimated in modeling studies on the oxidation of ammonia in flames; see for example [2 to 4].

References:

[1] Selgren, S. F.; McLoughlin, P. W.; Gellene, G. I. (J. Chem. Phys. **90** [1989] 1624/9).
[2] Miller, J. A.; Smooke, M. D.; Green, R. M.; Kee, R. J. (Combust. Sci. Technol. **34** [1983] 149/76).
[3] Miller, J. A.; Branch, M. C.; Kee, R. J. (Combust. Flame **43** [1981] 81/98).
[4] Dean, A. M.; Chou, M.-S.; Stern, D. (Int. J. Chem. Kinet. **16** [1984] 633/53).
[5] Dean, A. M.; Hardy, J. E.; Lyon, R. K. (Symp. Int. Combust. Proc. **19** [1982] 97/105).
[6] Branch, M. C.; Kee, R. J.; Miller, J. A. (Combust. Sci. Technol. **29** [1982] 147/65).
[7] Unfried, K. G.; Glass, G. P.; Curl, R. F. (Chem. Phys. Lett. **173** [1990] 337/42).
[8] Miller, J. A.; Kee, R. J.; Westbrook, C. K. (Annu. Rev. Phys. Chem. **41** [1990] 345/87, 374/5).
[9] Jensen, H. J. A.; Joergensen, P.; Helgaker, T. (J. Am. Chem. Soc. **109** [1987] 2895/901).
[10] Pasto, D. J.; Chipman, D. M. (J. Am. Chem. Soc. **101** [1979] 2290/6).

[11] Casewit, C. J.; Goddard, W. A., III (J. Am. Chem. Soc. **102** [1980] 4057/62).
[12] Casewit, C. J.; Goddard, W. A., III (J. Am. Chem. Soc. **104** [1982] 3280/7).
[13] Pasto, D. J. (J. Am. Chem. Soc. **101** [1979] 6852/7).
[14] Willis, C.; Back, R. A.; Parsons, J. M. (J. Photochem. **6** [1977] 253/64).
[15] Johnston, A. J.; Urch, D. S. (J. Chem. Soc. Chem. Commun. **1972** 585/6).
[16] Bian, J.; Vandooren, J.; Van Tiggelen, P. J. (Symp. Int. Combust. Proc. **21** [1988] 953/63).
[17] Breuer, H. D. (Mol. Galactic Environ. Proc. Symp., Green Bank, W.Va., 1971 [1973], pp. 381/8).
[18] Papazian, H. A. (J. Chem. Phys. **32** [1960] 456/60).
[19] Walch, S. P.; Duchovic, R. J.; Rohlfing, C. M. (J. Chem. Phys. **90** [1989] 3230/40).
[20] Peyerimhoff, S. D.; Buenker, R. J. (Ber. Bunsen-Ges. Phys. Chem. **78** [1974] 119/27).

[21] Vasudevan, K.; Peyerimhoff, S. D.; Buenker, R. J. (J. Mol. Struct. **29** [1975] 285/97).
[22] Curtiss, L. A.; Drapcho, D. L.; Pople, J. A. (Chem. Phys. Lett. **103** [1984] 437/42).
[23] Baird, N. C. (J. Chem. Phys. **62** [1975] 300/1).
[24] Baird, N. C.; Kathpal, H. B. (Can. J. Chem. **55** [1977] 863/8).
[25] Lathan, W. A.; Curtiss, L. A.; Hehre, W. J.; Lisle, J. B.; Pople, J. A. (Prog. Phys. Org. Chem. **11** [1974] 175/261).
[26] Yu, H.; Zhu, Z. (Chengdu Keji Daxue Xuebao **1989** No. 4, p. 76).
[27] Pople, J. A.; Curtiss, L. A. (J. Chem. Phys. **95** [1991] 4385/8).
[28] Walch, S. P. (J. Chem. Phys. **91** [1989] 389/94).
[29] Walch, S. P. (J. Chem. Phys. **93** [1990] 2384/92).
[30] Brandemark, U.; Siegbahn, P. E. M. (Theor. Chim. Acta **66** [1984] 217/32).

[31] Koizumi, H.; Schatz, G. C.; Walch, S. P. (J. Chem. Phys. **95** [1991] 4130/5).
[32] Hitchcock, A. P.; Brion, C. E. (Chem. Phys. **37** [1979] 319/31).
[33] Willis, C.; Lossing, F. P.; Back, R. A. (Can. J. Chem. **54** [1976] 1/3).
[34] Walch, S. P. (J. Chem. Phys. **95** [1991] 4277/83).
[35] Melius, C. F.; Binkley, J. S. (Chem. Phys. Processes Combust. **1983** Paper 39, 4 pp.; C.A. **100** [1984] No. 216703).
[36] Melius, C. F.; Binkley, J. S. (Symp. Int. Combust. Proc. **20** [1985] 575/83).
[37] McKee, M. L.; Stanbury, D. M. (J. Am. Chem. Soc. **114** [1992] 3214/9).
[38] Harrison, J. A.; Maclagan, R. G. A. R. (J. Chem. Soc. Faraday Trans. **86** [1990] 3519/23).
[39] Harrison, J. A.; Maclagan, R. G. A. R.; Whyte, A. R. (J. Phys. Chem. **91** [1987] 6683/6).

2.2.2 The Diazenyl Cation, N_2H^+

Systematic name: Diazynium

CAS Registry Numbers: N_2H^+ *[12357-66-3]*, $N^{15}NH^+$ *[58000-02-5]*, $^{15}NNH^+$ *[58000-01-4]*, N_2D^+ *[12132-97-7]*, $^{15}NND^+$ *[80560-24-3]*, $^{15}N_2D^+$*[80668-08-2]*, N_2T^+ *[123319-92-6]*

2.2.2.1 Interstellar Sources

Spectral lines of N_2H^+ were first detected in 1974. A triplet of lines centered near 93174 MHz in the spectrum of a dense interstellar cloud [1] was identified as the hyperfine structure of the $J=1\rightarrow 0$ transition [2, 3]. Further observations on N_2H^+ and some of its isotopomers in various interstellar sources were reported; see for example [4 to 8]. It belongs to the most abundant interstellar ions; see for example [9, 10].

The formation and destruction of N_2H^+ are important for understanding the chemistry of interstellar clouds, comets, and planetary atmospheres. It is generally assumed that the N_2H^+ ion in interstellar clouds arises mainly from the reactions $H_3^+ + N_2 \rightarrow N_2H^+ + H_2$ and $N_2^+ + H_2 \rightarrow N_2H^+ + H$ and that dissociative recombination $N_2H^+ + e^- \rightarrow N_2 + H$ and proton transfer reactions with abundant interstellar species such as CO are the major loss processes; see for example [11 to 15].

References:

[1] Turner, B. E. (Astrophys. J. **193** [1974] L83/L87).
[2] Green, S.; Montgomery, J. A., Jr.; Thaddeus, P. (Astrophys. J. **193** [1974] L89/L91).
[3] Hillier, I. H.; Kendrick, J. (J. Chem. Soc. Chem. Commun. **1975** 526/7).
[4] Lovas, F. J. (J. Phys. Chem. Ref. Data **21** [1992] 181/272).
[5] Mauersberger, R.; Guelin, M.; Martin-Pintado, J.; Thum, C.; Cernicharo, J.; Hein, H.; Navarro, S. (Astron. Astrophys. Suppl. Ser. **79** [1989] 217/61).
[6] Turner, B. E.; Thaddeus, P. (Astrophys. J. **211** [1977] 755/71).
[7] Womack, M.; Ziurys, L. M.; Wyckoff, S. (Astrophys. J. **387** [1992] 417/29).
[8] Mauersberger, R.; Henkel, C. (Astron. Astrophys. **245** [1991] 457/66).
[9] Opendak, M. G.; Varshalovich, D. A. (Astron. Zh. **63** [1986] 458/64; Sov. Astron. [Engl. Transl.] **30** [1986] 274/7).
[10] Linke, R. A.; Guelin, M.; Langer, W. D. (Astrophys. J. **271** [1983] L85/L88).

[11] Prasad, S. S.; Huntress, W. T., Jr. (Astrophys. J. Suppl. Ser. **43** [1980] 1/35).
[12] Dalgarno, A.; Black, J. H. (Rep. Prog. Phys. **39** [1976] 573/612).
[13] Smith, D. (Philos. Trans. R. Soc. [London] A **324** [1988] 257/73).

[14] Pineau des Forets, G.; Roueff, E.; Flower, D. R. (Mon. Not. R. Astron. Soc. **244** [1990] 668/74).
[15] Nejad, L. A. M.; Williams, D. A.; Charnley, S. B. (Mon. Not. R. Astron. Soc. **246** [1990] 183/90).

2.2.2.2 Formation

2.2.2.2.1 Survey

The N_2H^+ species is usually generated via the fast ion-molecule reactions

1) $H_3^+ + N_2 \rightarrow N_2H^+ + H_2$, 2) $H_2^+ + N_2 \rightarrow N_2H^+ + H$, and 3) $N_2^+ + H_2 \rightarrow N_2H^+ + H$

that follow ionization of gaseous mixtures containing H_2 and N_2 or follow addition of N_2 or H_2 gas to a gas stream containing hydrogen ions or nitrogen ions. In spectroscopic studies, it is typically generated by the $H_3^+ + N_2$ reaction using a glow discharge [1 to 7] (lengthening of the negative glow region by applying a longitudinal magnetic field to enhance N_2H^+ production by two orders of magnitude [6, 7]) or hollow cathode discharge [8 to 15] in a mixture of N_2 in H_2 at a total pressure ranging from a few to several hundred mTorr.

Ion-molecule reactions that lead to N_2H^+ formation are treated in Sections 2.2.2.2.2, 2.2.2.2.3, and 2.2.2.2.4 according to the type of reaction. Rate constants measured for the $HX^+ + N_2 \rightarrow N_2H^+ + X$ (protonation of N_2) and $N_2^+ + HX \rightarrow N_2H^+ + X$ (hydrogen atom abstraction by N_2^+) reactions are summarized in Tables 2 (p. 8) and 3 (p. 11). Other product channels such as charge transfer (e.g., $HX^+ + N_2 \rightarrow N_2^+ + HX$ and $N_2^+ + HX \rightarrow HX^+ + N_2$) are available to the reactants. Experimentally determined branching fractions for the N_2H^+ product channel are given in the text. Additional information on the kinetics of the tabulated and further reactions is given in the text. Ionization of an N_2-H_2 mixture yields H_2^+ and N_2^+ ions, so that N_2H^+ can be formed in the protonation and abstraction reactions. To differentiate between these concurrent reactions, techniques such as ion ejection or ion trapping were applied. The rate constants generally refer to thermal or near-thermal measurements at room temperature. Pressures typically used for these reactions were: ca. 10^{-6} Torr in ion cyclotron resonance studies; ca. 10^{-4} Torr in low-pressure mass spectrometer studies; a few up to several hundred mTorr in flowing afterglow, drift tube, hollow cathode discharge, and high-pressure mass spectrometer studies; and ca. 30 Torr up to 1 atm in corona discharge studies. For an overview of these experimental techniques, see for example [16, 17].

Collision rate constants for reactions resulting in N_2H^+ formation were predicted by classical theories such as the Langevin ion-induced dipole theory, the locked dipole theory, and the average dipole orientation theory. These rate constants, often compared with experimentally determined rate constants to estimate the reaction efficiency, are not treated in the following text. In case of N_2 protonation, see for example [18 to 21], and in case of hydrogen atom abstraction by N_2^+, see [18, 19, 22 to 26].

References:

[1] Nesbitt, D. J.; Petek, H.; Gudeman, C. S.; Moore, C. B.; Saykally, R. J. (J. Chem. Phys. **81** [1984] 5281/7).
[2] Sastry, K. V. L. N.; Helminger, P.; Herbst, E.; De Lucia, F. C. (Chem. Phys. Lett. **84** [1981] 286/7).
[3] Saykally, R. J.; Dixon, T. A.; Anderson, T. G.; Szanto, P. G.; Woods, R. C. (Astrophys. J. **205** [1976] L101/L103).

[4] Owrutsky, J. C.; Gudeman, C. S.; Martner, C. C.; Tack, L. M.; Rosenbaum, N. H.; Saykally, R. J. (J. Chem. Phys. **84** [1986] 605/17).

[5] Gudeman, C. S.; Begemann, M. H.; Pfaff, J.; Saykally, R. J. (J. Chem. Phys. **78** [1983] 5837/8).

[6] De Lucia, F. C.; Herbst, E.; Plummer, G. M.; Blake, G. A. (J. Chem. Phys. **78** [1983] 2312/6).

[7] Cazzoli, G.; Corbelli, G.; Degli Esposti, C.; Favero, P. G. (Chem. Phys. Lett. **118** [1985] 164/6).

[8] Sasada, H.; Amano, T. (J. Chem. Phys. **92** [1990] 2248/50).

[9] Foster, S. C.; McKellar, A. R. W. (J. Chem. Phys. **81** [1984] 3424/8).

[10] Verhoeve, P.; Zwart, E.; Versluis, M.; Drabbels, M.; Ter Meulen, J. J.; Meerts, W. L.; Dymanus, A.; McLay, D. B. (Rev. Sci. Instrum. **61** [1990] 1612/25).

[11] Nakanaga, T.; Ito, F.; Sugawara, K.; Takeo, H.; Matsumura, C. (Chem. Phys. Lett. **169** [1990] 269/73).

[12] Pursell, C. J.; Weliky, D. P.; Oka, T. (J. Chem. Phys. **93** [1990] 7041/8).

[13] Ho, W. C.; Pursell, C. J.; Weliky, D. P.; Tagaki, K.; Oka, T. (J. Chem. Phys. **93** [1990] 87/93).

[14] Sears, T. J. (J. Opt. Soc. Am. B Opt. Phys. **2** [1985] 786/9).

[15] Amano, T. (J. Chem. Phys. **92** [1990] 6492/501).

[16] McDaniel, E. W.; Cermak, V.; Dalgarno, A.; Ferguson, E. E.; Friedman, L. (Ion-Molecule Reactions, Wiley-Interscience, London 1970, 374 pp.).

[17] Farrar, J. M.; Saunders, W. H., Jr. (Techniques for the Study of Ion-Molecule Reactions, Techniques of Chemistry, Volume XX, Wiley, New York 1988, 652 pp.).

[18] Bowers, M. T.; Elleman, D. D. (J. Chem. Phys. **51** [1969] 4606/17).

[19] Bowers, M. T.; Elleman, D. D.; King, J., Jr. (J. Chem. Phys. **50** [1969] 1840/5).

[20] Ryan, K. R. (J. Chem. Phys. **61** [1974] 1559/70).

[21] Rakshit, A. B. (Int. J. Mass Spectrom. Ion Phys. **41** [1982] 185/97).

[22] Gioumousis, G.; Stevenson, D. P. (J. Chem. Phys. **29** [1958] 294/9).

[23] Warneck, P. (Ber. Bunsen-Ges. Phys. Chem. **76** [1972] 413/20).

[24] Lias, S. G. (Int. J. Mass Spectrom. Ion Phys. **20** [1976] 123/37).

[25] Karpas, Z.; Anicich, V.; Huntress, W. T., Jr. (J. Chem. Phys. **70** [1979] 2877/81).

[26] Schultz, R. H.; Armentrout, P. B. (J. Chem. Phys. **96** [1992] 1036/45).

2.2.2.2.2 Protonation of N_2

The formation of N_2H^+ resulting from the protonation of N_2, according to $H^+ + N_2 \rightarrow N_2H^+$ and $HX^+ + N_2 \rightarrow N_2H^+ + X$, is treated in this section. Rate constants for these reactions are summarized in Table 2.

$H^+ + N_2$. The negative of the room-temperature enthalpy change of the reaction $H^+ + N_2 \rightarrow N_2H^+$ is defined as the proton affinity A_p of N_2. This quantity is not well established experimentally. Recommended values are $A_p = 494.5$ kJ/mol [1, 2], obtained using a ladder of proton affinity differences [1], and $A_p \leq 497.9 \pm 3.8$ kJ/mol, obtained using the appearance potential of N_2H^+ arising from *trans*-N_2H_2 ($\Delta_fH_0^\circ(N_2H_2) \leq 195.0 \pm 3.3$ kJ/mol) [3]. For a summary of experimental and theoretical values of A_p, see [3]. The quantities $-T\Delta S_{298} = 29.3$ kJ/mol and $\Delta G_{298} = -465.3$ kJ/mol for the reaction were calculated using statistical mechanics [4].

$H_2^+ (D_2^+, HD^+) + N_2$. The branching ratios 0.96 and 0.04 for the proton transfer and for the charge transfer channels available to the $H_2^+ + N_2$ reaction at thermal collision energies were determined in an ion cyclotron resonance study [12].

Table 2
Rate Constants k (in $cm^3 \cdot molecule^{-1} \cdot s^{-1}$) for the Protonation of N_2.

reaction	10^9 k	experimental technique	Ref.
$H_2^+ + N_2 \rightarrow N_2H^+ + H$	2.0 ± 0.3	ion cyclotron resonance (ion trapping)	[12]
	1.95	ion cyclotron resonance (ion ejection)	[11]
	2.8 ± 0.2	mass spectrometer ion source (ion trapping)	[10]
$D_2^+ + N_2 \rightarrow N_2D^+ + D$	1.61	ion cyclotron resonance (ion ejection)	[11]
$HD^+ + N_2 \rightarrow N_2H^+ + D$	0.80	ion cyclotron resonance (ion ejection)	[11]
$HD^+ + N_2 \rightarrow N_2D^+ + H$	0.82	ion cyclotron resonance (ion ejection)	[11]
$H_3^+ + N_2 \rightarrow N_2H^+ + H_2$	1.8 ± 0.7	selected-ion drift chamber	[5]
	1.8 ± 0.4	flowing afterglow	[6]
	2.0 ± 0.4	selected-ion flow tube	[7]
	1.7 ± 0.1	ion cyclotron resonance	[8]
	1.9 ± 0.3	flow-drift tube	[9]
	1.95 ± 0.05	mass spectrometer ion source (ion trapping)	[10]
$D_3^+ + N_2 \rightarrow N_2D^+ + D_2$	0.75	ion cyclotron resonance (ion ejection)	[11]
$NH^+ + N_2 \rightarrow N_2H^+ + N$	~1	flowing afterglow	[13]
	0.65	selected-ion flow tube	[14]
$OH^+ + N_2 \rightarrow N_2H^+ + O$	0.22 ± 0.04	selected-ion flow tube	[6]
	0.36 ± 0.07	selected-ion flow tube	[15]
	0.23 ± 0.09	flowing afterglow	[16]
	0.19	ion cyclotron resonance	[17]
$HeH^+ + N_2 \rightarrow N_2H^+ + He$	1.7 ± 0.3	selected-ion flow tube	[7]
$KrH^+ + N_2 \rightarrow N_2H^+ + Kr$	0.58 ± 0.12	flowing afterglow	[6]
$XeH^+ + N_2 \rightarrow N_2H^+ + Xe$	0.011 ± 0.003	flowing afterglow	[6]
$O_2H^+ + N_2 \rightarrow N_2H^+ + O_2$	0.8	flow-drift tube	[18]
$CD_4^+ + N_2 \rightarrow N_2D^+ + CD_3$	0.148	mass spectrometer ion source (ion trapping)	[19]
	0.12	mass spectrometer ion source	[20]

Ion cyclotron resonance investigations revealed that the rate constants for the proton and deuteron transfer reactions decrease with increasing H_2^+ [11] and D_2^+ [21] energy in the range from thermal up to a few eV [11, 21]. Collision experiments (ion-beam target-gas) showed the cross section for the N_2H^+ product channel to fall off faster than classical collision theory predicts, that is, an $E^{-1/2}$ energy dependence [22, 23]. Similar studies with state-selected reactant ions (H_2^+, D_2^+ [23 to 25], and HD^+ [24] in the electronic ground state X $^2\Sigma_g^+$, v=0 to 4 [23], 0 to 7 [24, 25]) showed the vibrational dependence of the cross section for proton (deuteron) transfer at a low center-of-mass collision energy (2.5 eV [24], 0.5 to 3 eV [23]) to be weak in comparison with that of the charge transfer channel. As the collision energy was increased, the vibrational dependence of the cross section for proton transfer increased, mirroring that for charge transfer at 6 eV [23], whereas the cross section for deuteron transfer remained less sensitive [25]. It was suggested that the proton (deuteron) transfer reaction proceeds on a potential energy surface correlating with that of $H_2^+(D_2^+, HD^+) + N_2$ at infinite separation without a nonadiabatic crossover to the charge-transfer surface $N_2^+ + H_2$ [23, 24]. For an overview, see [26].

The values $\Delta H = -212$ kJ/mol [27] and -232 kJ/mol [28] were estimated for the reaction $H_2^+ + N_2 \rightarrow N_2H^+ + H$.

$H_3^+(D_3^+)+N_2$. The ions were obtained from hydrogen or deuterium by electron bombardment [6, 8, 10, 11], by electric discharge [7], and in reactions with rare gas ions or metastable atoms [5, 9]. The tabulated rate constant determined with the flowing afterglow technique [6] supersedes previous values [29 to 31]. A decrease in the rate constant for the proton transfer reaction with increasing H_3^+ internal energy was suggested to explain the observed pressure [8, 10] and energy [9] dependencies of the rate constant. An increase in the rate constant for the deuteron transfer reaction with increasing D_3^+ internal energy was observed by ion cyclotron double resonance [11].

The equilibrium constant $K \leq (7.4 \pm 2.7) \times 10^8$ at 296 ± 2 K for the reaction $H_3^+ + N_2 \rightleftharpoons N_2H^+ + H_2$ was measured using a flowing afterglow apparatus. For the rate constant of the back direction, see p. 31. With $\Delta G° = -50.6 \pm 0.8$ kJ/mol (from K) and $\Delta S° = -8.4 \pm 2.9$ $J \cdot mol^{-1} \cdot K^{-1}$, $\Delta H° = -53.1 \pm 1.7$ kJ/mol was obtained [6].

$OH^+ + N_2$. The equilibrium constant $K = 1.7 \pm 0.5$ at 296 ± 2 K was determined from independent measurements of the forward and reverse rate constants (see p. 31). Using $\Delta G° = -1.30 \pm 0.75$ kJ/mol (from K) and $\Delta S° = -13.8 \pm 2.5$ $J \cdot mol^{-1} \cdot K^{-1}$(from the entropies of the individual species), $\Delta H° = -5.4 \pm 2.1$ kJ/mol was obtained [6].

$ArD^+ + N_2$. The dependence of the reaction cross section for the deuteron transfer on the center-of-mass collision energy (0 to 15 eV) was studied mass spectrometrically [32].

$XeH^+ + N_2$. For the equilibrium constant, see p. 32.

$O_2H^+ + N_2$. A flow-drift tube experiment showed the rate constant to decrease to about one-half its thermal value on raising the center-of-mass collision energy from thermal energy (0.05 eV) to 1.5 eV. A reaction enthalpy of −54 kJ/mol was estimated [18].

$H_2F^+ + N_2$. The equilibrium constant $K = 3.3 \pm 1.0$ for the reaction $H_2F^+ + N_2 \rightarrow N_2H^+ + HF$ was determined using the ion cyclotron resonance trapped-ion technique. A reaction enthalpy of -4.6 ± 0.8 kJ/mol was estimated [33].

$CD_4^+ + N_2$. A rate constant determined in a mass spectrometer ion source [34] was quoted to be too small by a factor of two [20]. A reaction enthalpy of 50 kJ/mol was estimated [19].

$HCl^+ + N_2$. The formation of N_2H^+ in the proton transfer reaction from excited states of HCl^+ ($^2\Pi_{3/2}$, v=1; $^2\Pi_{1/2}$, v=1; and $^2\Pi_{1/2}$, v=0) to N_2 was observed in an ion cyclotron resonance study on the relaxation of HCl^+ [35].

$HOC^+ + N_2$. The proton transfer from HOC^+ to N_2 was suggested to be a source of N_2H^+ in interstellar sources [36].

References:

[1] Lias, S. G.; Liebmann, J. F.; Levin, R. D. (J. Phys. Chem. Ref. Data **13** [1984] 695/808).

[2] Lias, S. G.; Bartmess, J. E.; Liebman, J. F.; Holmes, J. L.; Levin, R. D.; Mallard, W. G. (J. Phys. Chem. Ref. Data Suppl. **17** [1988] 1/861).

[3] Ruscic, B.; Berkowitz, J. (J. Chem. Phys. **95** [1991] 4378/84).

[4] DeFrees, D. J.; McLean, A. D. (J. Comput. Chem. **7** [1986] 321/33).

[5] Rakshit, A. B. (Int. J. Mass Spectrom. Ion Phys. **41** [1982] 185/97).

[6] Bohme, D. K.; Mackay, G. I.; Schiff, H. I. (J. Chem. Phys. **73** [1980] 4976/86).

[7] Adams, N. G.; Smith, D. (Int. J. Mass Spectrom. Ion Phys. **21** [1976] 349/59).

[8] Kim, J. K.; Thread, L. P.; Huntress, W. T., Jr. (Chem. Phys. Lett. **32** [1975] 610/4).

[9] Fehsenfeld, F. C.; Lindinger, W.; Albritton, D. L. (J. Chem. Phys. **63** [1975] 443/5).

[10] Ryan, K. R. (J. Chem. Phys. **61** [1974] 1559/70).

[11] Bowers, M. T.; Elleman, D. D. (J. Chem. Phys. **51** [1969] 4606/17).
[12] Kim, J. K.; Huntress, W. T., Jr. (J. Chem. Phys. **62** [1975] 2820/5).
[13] Fehsenfeld, F. C.; Schmeltekopf, A. L.; Ferguson, E. E. (J. Chem. Phys. **46** [1967] 2802/8).
[14] Adams, N. G.; Smith, D.; Paulson, J. F. (J. Chem. Phys. **72** [1980] 288/97).
[15] Jones, J. D. C.; Berkinshaw, K.; Twiddy, N. D. (Chem. Phys. Lett. **77** [1981] 484/8).
[16] Fehsenfeld, F. C. (private communication from Anicich, V. G.; Huntress, W. T., Jr.; Astrophys. J. Suppl. **62** [1986] 553/672).
[17] Huntress, W. T., Jr.; McEwan, M. J.; Karpas, Z.; Anicich, V. G. (Astrophys. J. Suppl. Ser. **44** [1980] 481/8).
[18] Lindinger, W.; Albritton, D. L.; Fehsenfeld, F. C.; Schmeltekopf, A. L.; Ferguson, E. E. (J. Chem. Phys. **62** [1975] 3549/53).
[19] Li, Y. H.; Harrison, A. G. (Int. J. Mass Spectrom. Ion Phys. **28** [1978] 289/96).
[20] Harrison, A. G.; Myher, J. J. (J. Chem. Phys. **46** [1967] 3276/7).

[21] Bowers, M. T.; Elleman, D. D.; King, J., Jr. (J. Chem. Phys. **50** [1969] 1840/5).
[22] Giese, C. F. (J. Chem. Phys. **39** [1963] 739/48).
[23] Anderson, S. L.; Turner, T.; Mahan, B. H.; Lee, Y. T. (J. Chem. Phys. **77** [1982] 1842/54).
[24] Koyano, I.; Tanaka, K.; Kato, T.; Suzuki, S. (Faraday Discuss. Chem. Soc. No. 84 [1987] 265/79).
[25] Koyano, I.; Tanaka, K.; Kato, T. (in: Lorents, D. C.; Meyerhof, W. E.; Peterson, J. R.; Electronic and Atomic Collisions, Elsevier, Amsterdam 1986, p. 529).
[26] Koyano, I.; Tanaka, K. (Adv. Chem. Phys. **82** [1992] 263/307).
[27] Smith, R. D.; Futrell, J. H. (Int. J. Mass Spectrom. Ion Phys. **20** [1976] 347/78).
[28] Smith, R. D.; Futrell, J. H. (J. Phys. Chem. **81** [1977] 195/9).
[29] Burt, J. A.; Dunn, J. L.; McEwan, M. J.; Sutton, M. M.; Roche, A. E.; Schiff, H. I. (J. Chem. Phys. **52** [1970] 6062/75).
[30] Bohme, D. K.; Hemsworth, R. S.; Rundle, H. W.; Schiff, H. I. (J. Chem. Phys. **58** [1973] 3504/18).

[31] Schiff, H. I.; Bohme, D. K. (Int. J. Mass Spectrom. Ion Phys. **16** [1975] 167/89).
[32] Malkhasyan, R. T.; Zhurkin, E. S.; Tunitskii, N. N. (Dokl. Akad. Nauk Arm. SSR **59** [1974] 281/5; C.A. **83** [1975] No. 36498).
[33] Foster, M. S.; Beauchamp, J. L. (Inorg. Chem. **14** [1975] 1229/32).
[34] Shannon, T. W.; Harrison, A. G. (J. Chem. Phys. **43** [1965] 4201/6).
[35] Mauclaire, G.; Heninger, M.; Fenistein, S.; Wronka, J.; Marx, R. (Int. J. Mass Spectrom. Ion Processes **80** [1987] 99/113).
[36] Woods, R. C. (Astrophys. J. **270** [1983] 583/8).

2.2.2.2.3 Hydrogen Atom Abstraction by N_2^+

The formation of N_2H^+ resulting from hydrogen atom abstraction by N_2^+ via $N_2^+ + HX \rightarrow N_2H^+ + X$ is treated in this section. Rate constants for these reactions are summarized in Table 3.

$N_2^+ + H_2(D_2, HD)$. The formation of N_2H^+ by the reaction of N_2^+ with H_2, following electron bombardment of a 1:5 N_2-H_2 mixture (at 8×10^{-3} Torr) in a mass spectrometer ion source, was reported early [16]. The H abstraction by N_2^+ was observed to dominate the competing charge transfer channel ($N_2^+ + H_2 \rightarrow H_2^+ + N_2$) [6, 8, 17 to 19]. Complete branching into the N_2H^+ product channel was observed for ground-state $N_2^+(X\ ^2\Sigma_g^+)$ ions [6, 8]. Electronic excitation of N_2^+ increased the branching into the charge transfer channel [13, 17 to 19]. The rate constant for the abstraction reaction $N_2^+ + H_2$ was measured at low temperatures (20 and 70 K [20] and below 15 K [21]) using a free jet flow reactor technique [20, 21]. A

Table 3
Rate Constants k (in $cm^3 \cdot molecule^{-1} \cdot s^{-1}$) for the Hydrogen Atom Abstraction by N_2^+.

reaction	10^9 k	experimental technique	Ref.
$N_2^+ + H_2 \rightarrow N_2H^+ + H$	2.4	selected-ion flow tube	[1]
	2.1	mass spectrometer ion source	[2]
	1.7	flowing afterglow	[3]
	1.41 ± 0.28	ion cyclotron resonance (ion ejection)	[4]
	1.7 ± 0.2	mass spectrometer ion source (ion trapping)	[5]
	1.73 ± 0.05	ion cyclotron resonance (ion trapping)	[6]
	1.45	mass spectrometer ion source	[7]
	2.1 ± 0.4	selected-ion flow tube	[8]
$N_2^+ + D_2 \rightarrow N_2D^+ + D$	1.26 ± 0.19	ion cyclotron resonance (ion ejection)	[4]
	1.15	ion cyclotron resonance	[9]
	1.0	ion cyclotron resonance (ion ejection)	[10]
$N_2^+ + HD \rightarrow N_2H^+ + D$	0.56 ± 0.11	ion cyclotron resonance (ion ejection)	[4]
	0.65	ion cyclotron resonance	[9]
$N_2^+ + HD \rightarrow N_2D^+ + H$	0.55 ± 0.11	ion cyclotron resonance (ion ejection)	[4]
	0.69	ion cyclotron resonance	[9]
$N_2^+ + H_2O \rightarrow N_2H^+ + OH$	0.5	ion cyclotron resonance	[11]
	0.5	ion cyclotron resonance (ion trapping)	[12]
	0.6	selected-ion flow tube	[13]
$N_2^+ + CD_4 \rightarrow N_2D^+ + CD_3$	0.23	mass spectrometer ion source	[14]
$N_2^+ + HBr \rightarrow N_2H^+ + Br$	0.300 ± 0.035	ion cyclotron resonance	[15]
$N_2^+ + HCl \rightarrow N_2H^+ + Cl$	0.22 ± 0.02	ion cyclotron resonance	[15]
$N_2^+ + NH_3 \rightarrow N_2H^+ + NH_2$	0.02	ion cyclotron resonance	[11]

decrease in the rate constant with decreasing temperature from 300 to 20 K was found to fit the relation $k = 3.9 \times 10^{-10} T^{0.29}$ $cm^3 \cdot molecule^{-1} \cdot s^{-1}$ well [20]. At 15 K the rate constant passes through a minimum and increases with decreasing temperature [21].

The cross sections for the abstraction reactions were measured as a function of the N_2^+ translational energy by ion-beam target-gas [17, 22 to 30] and crossed-beam techniques [31, 32]; see discussion below. For mass spectrometer ion source studies (N_2^+ mean translational energies), see [33 to 38]. The cross sections for the abstraction reactions $H_2 + N_2^+ \rightarrow N_2H^+ + H$ and $D_2 + N_2^+ \rightarrow N_2D^+ + D$ were observed to be equal for center-of-mass collision energies from 1.5 to 7 eV [28], 0.01 to 10 eV [17], and 0.078 to 14 eV [29]. Furthermore, between 0.01 and 10 eV (center-of-mass), the total cross sections for $N_2^+ + HD \rightarrow N_2H^+ + D$ and $N_2^+ + HD \rightarrow N_2D^+ + H$ were observed to be equal to the cross sections for the abstraction reactions with H_2 and D_2 [17]. The abstraction reaction with HD showed an isotope effect. Below 0.1 eV center-of-mass collision energy, the formation of N_2D^+ is slightly favored, while above 0.1 eV, formation of N_2H^+ is favored by increasing amounts, reaching 90% at 10 eV. The cross sections for the abstraction reactions of N_2^+ with the hydrogen isotopes were observed to show a rapid fall-off with increasing N_2^+ translational energy [17, 22, 23, 25 to 31, 38], for example, from >100 Å^2 at thermal center-of-mass collision energy (~0.01 eV) to 1 Å^2 at superthermal energies (10 eV) [17]. A high-resolution crossed-beam technique showed the fall-off in the range from 0.025 to 2 eV to be structured with a broad shoulder that showed an isotope effect, appearing at different collision energies for the H and D abstractions [32]. The cross section determined in [27] was suggested to be too high [17, 38]. The energy dependence of the cross section at center-of-mass kinetic energies in the range from 0.01 to 0.02 eV was given by $E^{-1/2}$, from 0.02 to about 0.6 eV by $E^{-0.31\pm0.01}$, from 1.3 to 5 eV by $E^{-0.95\pm0.06}$, and between 5 and 10 eV by $E^{-2.9\pm0.03}$. The onset of the more rapid fall-off was observed at about 0.6 eV [17]. Reaction via a nonadiabatic transfer to the potential energy surface correlating with H_2^+ (D_2^+, HD^+) + N_2 at infinite separation was proposed to explain the greater than predicted energy dependence of the cross sections on the translational energy [17, 32].

The dependence of the cross section on the vibrational excitation of N_2^+ in the electronic ground X $^2\Sigma_g^+$ and excited A $^2\Pi$ states at center-of-mass collision energies of $\leq$1.3 eV was investigated using an ion-beam target-gas technique. The cross sections for the reactions of N_2^+(X $^2\Sigma_g^+$, v = 0 to 3) with D_2 were observed to be almost independent of the vibrational state of N_2^+, whereas the cross sections for the reactions of N_2^+(A $^2\Pi$, v = 0 to 3) showed a decrease for the v = 0 to 1 excitation and a slight increase for the v = 1 to 2 and 2 to 3 excitations. Abstraction via a D_2^+-N_2 charge transfer complex (see above) is consistent with this vibrational energy dependence [18]. For an overview, see [19].

A strong forward scattering of N_2H^+ and N_2D^+ from the reactions of N_2^+ with the isotopic hydrogens was observed in the angular distributions that were determined for collision energies ranging from intermediate (as low as 0.1 eV center-of-mass [39]) to superthermal (as high as 14 eV center-of-mass [29]) using ion-beam target-gas [22, 25, 28, 29, 40 to 42] and crossed-beam [25, 31, 39, 43] techniques. The N_2H^+ and N_2D^+ product angular distributions from the reactions of N_2^+ with H_2 and D_2 were found to be similar at center-of-mass collision energies from 3.1 to 11.2 eV. The N_2^+ + HD reaction (3.4 to 11.6 eV) was observed to show an isotope effect in favoring N_2H^+ formation by large factors over N_2D^+ at small scattering angles and in favoring N_2D^+ by small factors at large angles. The energy distributions of the products show that the internal excitation of N_2H^+(N_2D^+) from N_2^+ + H_2(D_2) is very high and that it decreases with increasing scattering angle [22]. The difference between the initial and final kinetic energies of the reactants and products (translational ergicity) in the reactions of N_2^+ with H_2 [25, 29], HD [25], and D_2 [25, 39, 41, 42] as a function of N_2^+ translational energy were calculated for a wide range of collision energies [25, 29, 39, 41, 42]. For a discussion of the reaction mechanism for the N_2H^+(N_2D^+) product channel, spectator stripping (direct reaction) versus collision complex, see for example [17, 29].

The following reaction enthalpies for the abstraction reactions of N_2^+ with H_2, D_2, and HD are based on previously reported thermodynamic data in the case of N_2H^+ [44] or spectroscopic data in the case of N_2D^+ [45, 46]: $N_2^+ + H_2 \rightarrow N_2H^+ + H$, $\Delta H = -250$ kJ/mol; $N_2^+ + D_2 \rightarrow N_2D^+ + D$, $\Delta H = -239$ kJ/mol; $N_2^+ + HD \rightarrow N_2H^+ + D$, $\Delta H = -246$ kJ/mol; $N_2^+ + HD \rightarrow N_2D^+ + H$, $\Delta H = -243$ kJ/mol [17].

$N_2^+ + H_2O(D_2O)$. The abstraction channel is dominated by the charge transfer channel. The branching ratio for abstraction was determined to be 0.22 (ion cyclotron resonance (ion ejection)) [12], 0.24 (ion cyclotron resonance) [11], 0.19 (selected-ion flow tube) [13].

An ion-beam target-gas study showed a fall-off in the cross sections for the H and D abstractions with increasing collision energy and an isotope effect, favoring the abstraction of H over D at center-of-mass energies from 1 to 15 eV. Time-of-flight measurements on N_2H^+ showed a large amount of forward translational energy [30]. A strong forward scattering in the product angular velocity distribution of N_2D^+ for center-of-mass energies from 1 to 16 eV was observed in an ion-beam target-gas study [47].

N_2^+ + $CH_4(CD_4)$. The rate constant $k = 0.22 \times 10^{-12}$ $cm^3 \cdot molecule^{-1} \cdot s^{-1}$ for the H abstraction reaction, determined in a mass spectrometer ion source study on N_2-CH_4 mixtures [7], seems to be unreliable due to the isobaricity of N_2H^+ and $C_2H_5^+$, arising from the $CH_3^+ + CH_4$ reaction [48]. A rate constant for the D abstraction reaction determined in a mass spectrometer ion source [49] was noted to be incorrect [14]. A similar determination with ion trapping showed that the abstraction channel is dominated by a dissociative charge transfer channel. A branching of only 2±2% into the D abstraction channel was determined [48].

The total cross section as well as the product velocity and angular distributions of $N_2H^+(N_2D^+)$ at center-of-mass collision energies from 9 to 47 eV (to 25 eV for D abstraction) were determined using an ion-beam target-gas technique [50]. The product velocity distribution for N_2^+ energies from about 1 to 50 eV was determined using the same technique [42, 50]. Forward scattering of N_2H^+ [50] and N_2D^+ [42, 50] as well as a large isotope effect favoring abstraction of H over D were observed [50].

$N_2^+ + NH_3$. An ion cyclotron resonance study showed that only 1% of the $N_2^+ + NH_3$ reactive collisions branch into the N_2H^+ product channel [11].

$N_2^+ + H_2S$. An ion cyclotron resonance study showed that only 2% of the $N_2^+ + H_2S$ reactive collisions branch into the N_2H^+ product channel [51].

References:

[1] Adams, N. G.; Smith, D. (Int. J. Mass Spectrom. Ion Phys. **21** [1976] 349/59).
[2] Aquilanti, V.; Galli, A.; Giardini-Guidoni, A.; Volpi, G. G. (J. Chem. Phys. **43** [1965] 1969/73).
[3] Fehsenfeld, F. C.; Schmeltekopf, A. L.; Ferguson, E. E. (J. Chem. Phys. **46** [1967] 2802/8).
[4] Bowers, M. T.; Elleman, D. D. (J. Chem. Phys. **51** [1969] 4606/17).
[5] Ryan, K. R. (J. Chem. Phys. **61** [1974] 1559/70).
[6] Kim, J. K.; Theard, L. P.; Huntress, W. T., Jr. (J. Chem. Phys. **62** [1975] 45/52).
[7] Warneck, P. (Ber. Bunsen-Ges. Phys. Chem. **76** [1972] 413/20).
[8] Smith, G. P.; Adams, N. G.; Millar, T. M. (J. Chem. Phys. **69** [1978] 308/18).
[9] Bowers, M. T.; Elleman, D. D.; King, J., Jr. (J. Chem. Phys. **50** [1969] 1840/5).
[10] Karpas, Z.; Anicich, V.; Huntress, W. T., Jr. (J. Chem. Phys. **70** [1979] 2877/81).

[11] Huntress, W. T., Jr.; McEwan, M. J.; Karpas, Z.; Anicich, V. G. (Astrophys. J. Suppl. Ser. **44** [1980] 481/8).
[12] Karpas, Z.; Anicich, V. G.; Huntress, W. T., Jr. (Chem. Phys. Lett. **59** [1978] 84/6).
[13] Tichy, M.; Rakshit, A. B.; Lister, D. G.; Twiddy, N. D.; Adams, N. G.; Smith, D. (Int. J. Mass Spectrom. Ion Phys. **29** [1979] 231/47).
[14] Harrison, A. G.; Myher, J. J. (J. Chem. Phys. **46** [1967] 3276/7).
[15] Lias, S. G. (Int. J. Mass Spectrom. Ion Phys. **20** [1976] 123/37).
[16] Eltenton, G. C. (Nature **141** [1938] 975/6).
[17] Schultz, R. H.; Armentrout, P. B. (J. Chem. Phys. **96** [1992] 1036/45).
[18] Koyano, I.; Tanaka, K.; Kato, T.; Suzuki, S. (Faraday Discuss. Chem. Soc. No. 84 [1987] 265/79).
[19] Koyano, I.; Tanaka, K. (Adv. Chem. Phys. **82** [1992] 263/307).
[20] Rowe, B. R.; Marquette, J.-B.; Rebrion, C. (J. Chem. Soc. Faraday Trans. II **85** [1989] 1631/41).

[21] Randeniya, L. K.; Smith, M. A. (J. Chem. Phys. **94** [1991] 351/6).
[22] Gentry, W. R.; Gislason, E. A.; Mahan, B. H.; Tsao, C. W. (J. Chem. Phys. **49** [1968] 3058/70).
[23] Henglein, A.; Lacmann, K.; Knoll, B. (J. Chem. Phys. **43** [1965] 1048/9).
[24] Henglein, A. (Adv. Chem. Ser. **58** [1966] 63/79).

[25] Gentry, W. R.; Gisalon, E. A.; Yuan-Tseh Lee; Mahan, B. H.; Chi-Wing Tsao (Discuss. Faraday Soc. No. 44 [1967] 137/45).
[26] Homer, J. B.; Lehrle, R. S.; Robb, J. C.; Thomas, D. W. (Nature **202** [1964] 795/7).
[27] Giese, C. F. (J. Chem. Phys. **39** [1963] 739/48).
[28] Lacmann, K.; Henglein, A. (Ber. Bunsen-Ges. Phys. Chem. **69** [1965] 292/6).
[29] Hierl, P. M.; Strattan, L. W.; Wyatt, J. R. (Int. J. Mass Spectrom. Ion Phys. **10** [1972] 385/403).
[30] Dressler, R. A.; Gardner, J. A.; Salter, R. H.; Wodarczyk, F. J.; Murad, E. (J. Chem. Phys. **92** [1990] 1117/25).

[31] Turner, B. R.; Fineman, M. A.; Stebbings, R. F. (J. Chem. Phys. **42** [1965] 4088/96).
[32] Tosi, P.; Dmitrijev, O.; Bassi, D. (J. Chem. Phys. **97** [1992] 3333/40).
[33] Stevenson, D. P.; Schissler, D. O. (J. Chem. Phys. **29** [1958] 282/93).
[34] Gutbier, H. (Z. Naturforsch. **12a** [1957] 499/507).
[35] Moran, T. F.; Friedman, L. (J. Chem. Phys. **42** [1965] 2391/405).
[36] Kubose, D. A.; Hamill, W. H. (J. Am. Chem. Soc. **85** [1963] 125/7).
[37] Hutchison, D. A.; Kuppermann, A.; Pobo, L. G. (TID-18176 [1962] 26 pp.; C.A. **61** [1964] 1283).
[38] Hyatt, D.; Lacmann, K. (Z. Naturforsch. **23a** [1968] 2080/3).
[39] Herman, Z.; Kerstetter, J.; Rose, T. (Discuss. Faraday Soc. No. 44 [1967] 123/36).
[40] Giese, C. F. (Phenom. Ioniz. Gases Contrib. Pap. 8th Int. Conf., Vienna 1967, p. 17; C.A. **70** [1969] No. 61050).

[41] Doverspike, L. D.; Champion, R. L.; Bailey, T. L. (J. Chem. Phys. **45** [1966] 4385/91).
[42] Ding, A.; Henglein, A.; Hyatt, D.; Lacmann, K. (Z. Naturforsch. **23a** [1968] 2084/90).
[43] Herman, Z.; Kerstetter, J. D.; Rose, T. L.; Wolfgang, R. (J. Chem. Phys. **46** [1967] 2844/5).
[44] Lias, S. G.; Bartmess, J. E.; Liebman, J. F.; Holmes, J. L.; Levin, R. D.; Mallard, W. G. (J. Phys. Chem. Ref. Data Suppl. **17** [1988] 1/861).
[45] Owrutsky, J. C.; Gudeman, C. S.; Martner, C. C.; Tack, L. M.; Rosenbaum, N. H.; Saykally, R. J. (J. Chem. Phys. **84** [1986] 605/17).
[46] Sasada, H.; Amano, T. (J. Chem. Phys. **92** [1990] 2248/50).
[47] Felder, W.; Sbar, N.; Dubrin, J. (Chem. Phys. Lett. **6** [1970] 385/8).
[48] Li, Y. H.; Harrison, A. G. (Int. J. Mass Spectrom. Ion Phys. **28** [1978] 289/96).
[49] Shannon, T. W.; Harrison, A. G. (J. Chem. Phys. **43** [1965] 4201/6).
[50] Gislason, E. A.; Mahan, B. H.; Tsao, C. W.; Werner, A. S. (J. Chem. Phys. **50** [1969] 142/50).

[51] Anicich, V. G.; Huntress, W. T., Jr. (Astrophys. J. Suppl. Ser. **62** [1986] 553/672).

2.2.2.2.4 Other Ion-Molecule Reactions

$N^+ + NH_3$, $NH^+ + NH_3$. Formation of N_2H^+ was observed following electron beam ionization of gaseous ammonia (at pressures up to 0.6 Torr) in the ion source of a mass spectrometer. The cross sections 0.89 Å^2 and 1.1 Å^2 were reported for the $NH^+ + NH_3 \rightarrow N_2H^+ + H + H_2$ and $N^+ + NH_3 \rightarrow N_2H^+ + H_2$ reactions, respectively [1]. In the $N^+ + NH_3$ system, the N_2H^+ product channel (branching fraction 0.1) was found to be dominated by the charge transfer channel [2 to 4].

$NH^+ + NO$. The product distribution for the reaction of NH^+ with NO was determined using the selected-ion flow tube technique to be 0.20 for N_2H^+ from $NH^+ + NO \rightarrow N_2H^+ + O$ and 0.80 for NO^+ from the charge transfer channel $NH^+ + NO \rightarrow NO^+ + NH$ [3].

$N_3^+ + H_2$. The rate constant k≈2×10^{-13} $cm^3\cdot molecule^{-1}\cdot s^{-1}$ for the reaction $N_3^+ + H_2 \rightarrow N_2H^+ + NH$ was determined using a selected-ion flow tube technique. Only branching into the N_2H^+ product channel was observed [2].

$N_4^+ + H_2(HD, D_2)$. An ion-beam target-gas study showed that the $N_4^+ + D_2 \rightarrow N_2D^+ + N_2 + D$ channel dominates other available reaction channels; in addition to N_2D^+, only a comparatively small amount (<5%) of N_2^+ from collision-induced dissociation was detected [5]. Drift tube studies showed significantly more (13%) [2] or only N_4H^+ (100%) [6] to be formed in $N_4^+ + H_2$ reactive collisions. The difference in product distributions is attributed [5] to the single [5] and multiple collision [2, 6] conditions that were present. Thermal rate constants at 300 K for the N_2H^+ and N_2D^+ product channels in the reactions of N_4^+ with H_2 and D_2, $k=(2.4\pm1.2)\times10^{-12}$ $cm^3\cdot molecule^{-1}\cdot s^{-1}$ [7] and $k=(1.6\pm0.8)\times10^{-12}$ $cm^3\cdot molecule^{-1}\cdot s^{-1}$ [5, 7], respectively, were determined using a flow-drift tube [7] and the ion-beam target-gas techniques [5]. Other measurements at thermal collision energies also indicate that the reactions with H_2 [2, 8, 9], D_2 [9], and HD [7] proceed slowly despite a reaction enthalpy estimated to be −145 kJ/mol.

The energy dependence of the cross sections for the reactions of thermal N_4^+ ions with H_2, HD, and D_2 was determined for center-of-mass collision energies from thermal up to 5 eV using the ion-beam target-gas technique. The total cross section for the reactions with HD ($N_4^+ + HD \rightarrow N_2H^+(N_2D^+) + D(H)$) is equal to the cross sections for the reactions with H_2 and D_2. An isotope effect was observed in the reaction with HD: at energies above 0.1 eV, formation of N_2D^+ over N_2H^+ is favored [5].

Typical for reactions with a barrier, the cross sections for the N_2H^+ and N_2D^+ product ions rise with increasing collision energy up to 3 eV. Above 3 eV the cross sections decrease, possibly due to dissociation of the product ion. For the reactions with H_2, D_2, and HD, an activation energy of 0.09±0.03 eV at 0 K was obtained from the reaction thresholds which were determined in ion-beam target-gas experiments [5]. From Arrhenius plots of temperature-dependent [7] and collision-energy-dependent [9] drift tube data, the following activation energies were obtained: H_2, 0.15±0.01 [7], 0.16±0.01; D_2, 0.17±0.01 eV [9].

$N_2O^+ + H_2$, $H_2^+ + N_2O$. The reaction channels (a) $N_2O^+ + H_2 \rightarrow N_2H^+ + OH$ and (b) $H_2^+ + N_2O \rightarrow N_2H^+ + OH$ were observed in an ion cyclotron double-resonance study of reactions occurring in N_2O-H_2 mixtures. They are of negligible importance compared to the competitive channels $N_2O^+ + H_2 \rightarrow N_2OH^+ + H$ and $H_2^+ + N_2O \rightarrow N_2OH^+ + H$. The rate constants $k_a = 1.4\times10^{-10}$ $cm^3\cdot molecule^{-1}\cdot s^{-1}$ and $k_b = 4.7\times10^{-10}$ $cm^3\cdot molecule^{-1}\cdot s^{-1}$ were estimated [10].

$C_2N^+ + NH_3$. An ion cyclotron resonance study showed that 10% of the $C_2N^+ + NH_3$ reactive collisions yield N_2H^+ and C_2H_2 ($-\Delta H = 444$ kJ/mol estimated) [11].

References:

[1] Derwish, G. A. W.; Galli, A.; Gardini-Guidoni, A.; Volpi, G. G. (J. Chem. Phys. **39** [1963] 1599/605).
[2] Smith, G. P.; Adams, N. G.; Millar, T. M. (J. Chem. Phys. **69** [1978] 308/18).
[3] Adams, N. G.; Smith, D.; Paulson, J. F. (J. Chem. Phys. **72** [1980] 288/97).
[4] Tichy, M.; Rakshit, A. B.; Lister, D. G.; Twiddy, N. D.; Adams, N. G.; Smith, D. (Int. J. Mass Spectrom. Ion Phys. **29** [1979] 231/47).
[5] Schultz, R. H.; Armentrout, P. B. (J. Chem. Phys. **96** [1992] 1046/52).
[6] McCrumb, J. L.; Rakshit, A. B.; Warneck, P. (Ber. Bunsen-Ges. Phys. Chem. **84** [1980] 677/80).

[7] Lindinger, W.; Dotan, I.; Albritton, D. L.; Fehsenfeld, F. C. (J. Chem. Phys. **68** [1978] 2607/11).

[8] Dreyer, J. W.; Perner, D.; Roy, C.; Volz, A. (Ber. Bunsen-Ges. Phys. Chem. **79** [1975] 270/7).

[9] Tichy, M.; Twiddy, N. D.; Wareing, D. P.; Adams, N. G.; Smith, D. (Int. J. Mass Spectrom. Ion Processes **81** [1987] 235/46).

[10] McAllister, T. (Int. J. Mass Spectrom. Ion Phys. **10** [1973] 419/24).

[11] McEwan, M. J.; Anicich, V. G.; Huntress, W. T., Jr.; Kemper, P. R.; Bowers, M. T. (Int. J. Mass Spectrom. Ion Phys. **50** [1983] 179/87).

2.2.2.2.5 Dissociative Ionization of Compounds Containing Nitrogen and Hydrogen

Formation of N_2H^+ following electron impact ionization [1 to 5] or photoionization [6] of compounds containing nitrogen and hydrogen was observed with a mass spectrometer. The appearance potentials, AP, of N_2H^+ arising from various parent compounds are summarized below:

compound	AP in eV	Ref.	compound	AP in eV	Ref.
trans-N_2H_2	10.954 ± 0.019	[6]	N_2H_4	14.8 ± 0.3	[5]
trans-N_2H_2	10.89 ± 0.8	[3]	$CH_3N_2H_3$	13.3 ± 0.3	[5]
trans-N_2H_2	10.98 ± 0.05	[2]	HN_3	13.8 ± 0.2	[4]

AP = 10.93 eV for N_2H^+ arising from N_2H_2 was obtained in an ab initio calculation (G2) [7]. For the formation of N_2H^+ from N_2H, see [1, 7].

References:

[1] Wiberg, N.; Fischer, G.; Bachhuber, H. (Z. Naturforsch. **34b** [1979] 1385/90).

[2] Willis, C.; Lossing, F. P.; Back, R. A. (Can. J. Chem. **54** [1976] 1/3).

[3] Foner, S. N.; Hudson, R. L. (J. Chem. Phys. **68** [1978] 3169/71).

[4] Franklin, J. L.; Dibeler, V. H.; Reese, R. M.; Krauss, M. (J. Am. Chem. Soc. **80** [1958] 298/302).

[5] Dibeler, V. H.; Franklin, J. L.; Reese, R. M. (J. Am. Chem. Soc. **81** [1959] 68/73).

[6] Ruscic, B.; Berkowitz, J. (J. Chem. Phys. **95** [1991] 4378/84).

[7] Pople, J. A.; Curtiss, L. A. (J. Chem. Phys. **95** [1991] 4385/8).

2.2.2.3 Molecular Properties

Quantum-chemical studies on the structure of N_2H^+ have paralleled experimental and radioastronomical studies. Only those ab initio studies that supplement the experimental results or that provide lacking information are considered in the following section. For other quantum chemistry studies, see the following bibliography:

Richards, W. G.; Walker, T. E. H.; Hinkley, R. K.; A Bibliography of ab initio Molecular Wave Functions, Clarendon Press, Oxford 1971.

Richards, W. G.; Walker, T. E. H.; Farnell, L.; Scott, P. R.; Bibliography of ab initio Molecular Wave Functions. Supplement for 1970-1974, Clarendon Press, Oxford 1974.

Richards, W. G.; Scott, P. R.; Colburn, E. A.; Marchington, A. F.; Bibliography of ab initio Molecular Wave Functions. Supplement for 1974-1977, Clarendon Press, Oxford 1978.

Richards, W. G.; Scott, P. R.; Sackwild, V.; Robins, S. A.; A Bibliography of Ab Initio Molecular Wave Functions. Supplement for 1978-1980, Clarendon Press, Oxford 1981.

Ohno, K.; Morokuma, K.; Quantum Chemistry Literature Data Base-Bibliography of Ab Initio Calculations for 1978-1980, Elsevier, Amsterdam 1982.

Annual Supplements appeared in the following volumes of the Journal of Molecular Structure: **91** [1982], **106** [1983], **119** [1984], **134** [1985], **148** [1986], **154** [1987], **182** [1988], **203** [1989], **211** [1990], **252** [1991], **298** [1992].

Electron Configuration. Electronic States

The asymmetric cation N≡N-H$^+$ with ten valence electrons is linear ($C_{\infty v}$) in the electronic ground state and may be bent (C_s) in excited states. The electronic ground state $^1\Sigma^+$ is represented by the MO configuration $(1\sigma)^2$ $(2\sigma)^2$ $(3\sigma)^2$ $(4\sigma)^2$ $(5\sigma)^2$ $(1\pi)^4$. For the lowest electronic state $^1A'$ of the bent molecule, this configuration correlates with $(1a')^2$ $(2a')^2$ $(3a')^2$ $(4a')^2$ $(5a')^2$ $(1a'')^2$ $(6a')^2$. An examination of the ground-state MOs showed that the 1σ and 2σ MOs are essentially the 1s AOs localized at the respective nitrogen centers and that they correlate with the $1\sigma_g$ and $1\sigma_u$ MOs of the N_2 molecule as the proton separates. Likewise the 3σ MO corresponds to a distorted $2\sigma_g$ MO of N_2. The 4σ orbital correlates with $2\sigma_u$ of N_2 and shows significant mixing with the hydrogen 1s AO. The next most stable orbital 5σ correlates with the $3\sigma_g$ MO of N_2 and mixes less strongly with the hydrogen 1s species. The 1π MO, correlating with the $1\pi_u$ in N_2, is forbidden by symmetry to mix with the hydrogen 1s but is polarized towards the inner nitrogen [1].

Apparently, no electronic spectrum of N_2H^+ has been observed yet. Vertical excitation energies for transitions from the ground state to low-lying excited states of N_2H^+ were obtained in ab initio CI (configuration interaction) calculations. The values, calculated at roughly the ground-state geometry, are 7.83, 9.17, 10.07, 10.34, 10.86, 17.65, 8.38, and 10.81 eV for transitions to the $^3\Sigma^+(2\pi\leftarrow1\pi)$, $^3\Delta(2\pi\leftarrow1\pi)$, $^3\Sigma^-(2\pi\leftarrow1\pi)$, $^1\Sigma^-(2\pi\leftarrow1\pi)$, $^1\Delta(2\pi\leftarrow1\pi)$, $^1\Sigma^+(2\pi\leftarrow1\pi)$, $^3\Pi(2\pi\leftarrow5\sigma)$, and $^1\Pi(2\pi\leftarrow5\sigma)$ states, respectively [1].

The N_2H^+ ground-state potential energy as a function of the NN and NH stretching coordinates [2] and as a function of the stretching and bending coordinates [3] was obtained in extensive ab initio calculations, CEPA-1 (coupled electron pair approximation) [2] and CI-SDQ [3]. The anharmonic parts of the latter potential [3] were noted to show large numerical errors [2]. Potential energy curves for the ground and several excited states were obtained at the CI-SD or SCF level [1].

The potential energy surface for the isomerization reaction, corresponding to the migration of H$^+$ around N_2 (NNH$^+ \rightarrow {}^+$HNN), was calculated by ab initio techniques (MO SCF and MPPT(3) (third-order Møller-Plesset pertubation theory)). A cyclic C_{2v} structure was located at the peak of the calculated barrier of 192 kJ/mol [4, 5].

The energy level spacing of a high-lying bending vibrational structure that can isomerize was calculated using a semirigid bender model [6].

Electric Moments. Polarizabilities and Hyperpolarizabilities

The electric dipole moment $\mu=(3.4\pm0.2)$ D was obtained from measurements of the rotational Zeeman effect using far-infrared laser spectroscopy. The isotope shifts of the splittings of the $J=7\rightarrow6$ rotational transition in the vibrational ground states of $^{15}NNH^+$, $N^{15}NH^+$, and N_2H^+ were measured at a high magnetic field strength of 5.444 T [7].

A number of ab initio quantum-chemical studies include the calculation of the dipole moment of N_2H^+. Most of the predicted μ values are around 3.4 D [2, 8 to 14]. The most extensive calculations, CEPA-1 and MPPT(4), give μ to be 3.374 D [2] and 3.375 D [8], respectively.

The quadrupole and octopole moments, the dipole polarizability, the first and second dipole hyperpolarizabilities, and the dipole-quadrupole and dipole-dipole-quadrupole polarizabilities were calculated using MPPT(4) theory [8].

Nuclear Quadrupole Coupling Constants

The following nuclear quadrupole coupling constants of the outer and inner nitrogen nuclei, eqQ_1 and eqQ_2, were derived from the hyperfine splitting of the $J=1\leftarrow0$ rotational transition in the vibrational ground state [15 to 17] and the (10^00) vibrational state [15]:

	N_2H^+				$N^{15}NH^+$
vibrational state	(00^00)	(00^00)	(00^00)	(10^00)	(00^00)
eqQ_1 [eqQ_2] in MHz	−5.88(10)	−5.75	−5.71(3) [−1.44(4)]	−5.71(17)	−5.75
remark	a)	b)	b)	a)	b)
Ref.	[15]	[17]	[16]	[15]	[17]

a) Infrared-microwave double-resonance spectroscopy. — b) Microwave spectroscopy.

The analysis of data from radioastronomical observations of the $J=1\rightarrow0$ transition in the vibrational ground state gave $eqQ_1=-5.69\pm0.2$ [18], -5.666 ± 0.012 MHz and $eqQ_2=-1.426\pm0.021$ MHz [19].

Spin-Rotation Coupling Constants

The following spin-rotation coupling constants due to the outer and inner nitrogen nuclei, c_1 and c_2, were derived from the hyperfine splitting of the $J=1\leftarrow0$ rotational transition in the vibrational ground state: N_2H^+, $c_1=0.012(4)$ [16], 0.012 MHz [17] and $c_2=0.011$ MHz [16]; $N^{15}NH^+$, $c_1=-0.026$ MHz [17]. The analysis of radioastronomical data gave $c_1=0.0147\pm0.0023$ MHz [19].

l-Type Doubling Constants

The double degeneracy of the rotational levels of N_2H^+ in the excited bending vibrational state v_2 ($v_2=1$, $l=1$) is removed by a rotation-vibration interaction (l-type doubling). The following l-type doubling constants q and centrifugal distortion corrections q_J (both in cm^{-1}) were obtained from the splitting of rotational levels:

species	vibrational state	q	q_J	Ref.
N_2H^+	v_2	0.00850475(37)	$0.944(6)\times10^{-7}$	[15]
		0.008541(13)	–	[20]
	v_1+v_2	0.00863637(106)	$1.05(22)\times10^{-7}$	[15]
		0.008661(13)	–	[20]
N_2D^+	v_2	0.007274(22)	–	[20]
	v_1+v_2	0.006563(22)	–	[20]

The l-type doubling constants of all isotopomers of the ion were obtained from ab initio (CI-SDQ) calculations [3].

Rotational Constants. Centrifugal Distortion Constants. Rotation-Vibration Interaction Constants

A simultaneous weighted least-squares fit of data for many J transitions in the ν_1 [20 to 22], ν_2 [23, 24], ν_3 [25] bands, the $\nu_1+\nu_2 \leftarrow \nu_2$ hot band [20, 22], and for pure rotational transitions in the vibrational ground state [26 to 29] yielded the following rotational (B), centrifugal distortion (D), and rotation-vibration interaction (α, γ) constants (in cm^{-1}) [20]. (Typographical errors in Table I of reference [20] were corrected.)

	N_2H^+	N_2D^+		N_2H^+	N_2D^+
B_e	1.562429(37)	1.291656(82)	α_1	0.0129204(76)	0.012359(39)
B_{000}	1.553971(20)	1.286047(51)	α_2	−0.003346(16)	−0.004146(42)
D_{000}	$2.927(18) \times 10^{-6}$	$2.027(83) \times 10^{-6}$	α_3	0.010999(50)	0.00797(10)
			γ_{12}	0.0003106(56)	0.000821(26)

An analysis of a Fourier transform infrared absorption spectrum gave $B_{000} = 1.5539707(16)$ and $D_{000} = 2.926(34) \times 10^{-6}$ [30].

The following effective rotational constants B_{000} (in MHz) were obtained from microwave data (see below): N_2H^+, 46586.871; $N^{15}NH^+$, 45603.038; $^{15}NNH^+$, 45132.080; $^{15}N_2H^+$, 44132.192; N_2D^+, 38554.757; $N^{15}ND^+$, 38009.274; $^{15}NND^+$, 37380.528 [31]; $^{15}N_2D^+$, 36817.76 [32].

Rotational and rotation-vibration constants for all isotopomers of the ion [3] and the rotational constant of $N^{15}NH^+$ [13] were obtained by ab initio (CI-SDQ) calculations [3, 13].

Constants for excited vibrational states are given in [20].

The sextic equilibrium centrifugal distortion constants of N_2H^+ and N_2D^+, $H_J = 50$ and 35 mHz, were estimated in an ab initio (CEPA-1) study [2].

Geometrical Structure

The equilibrium structural parameters $r_e(HN) = 1.03359(43)$ Å and $r_e(NN) = 1.092766(92)$ Å were obtained from the rotational constants [20]. The substitution structural parameters $r_s(HN) = 1.031426(56)$ Å and $r_s(NN) = 1.095415(6)$ Å, obtained from microwave data on several isotopomers [33], apparently supersede earlier r_s values which were determined in the same laboratory [17, 31, 32]. The geometric structure was also calculated from microwave data [32] using a mass-dependent scaling of the moments of inertia [34].

Molecular Vibrations. Force Constants

Fundamental Vibrations. There are three normal modes of vibration of the asymmetric linear cation ($C_{\infty v}$ symmetry): the N-H stretch ν_1, the doubly degenerate bend ν_2, and the N-N stretch ν_3.

The following **fundamental** frequencies ν_i (in cm^{-1}) were obtained from infrared [20, 22 to 25] and infrared Fourier transform [30] data:

species	ν_1		ν_2		ν_3	
N_2H^+	3233.9608(2)	[30]	685.2510(4)	[23]	2257.8667(13)	[25]
N_2D^+	2636.983(50)	[22]	544.46766(27)	[24]	2024.0141(13)	[25]

A 0.008 cm^{-1} lower fundamental ν_1 was reported in [20].

The following **harmonic** frequencies ω_i (in cm^{-1}) were determined by a simultaneous weighted least-squares fit of infrared data; they are regarded to be relatively crude approximations, since only the x_{12} anharmonicity constant could be evaluated [20]:

species	ω_1	ω_2	x_{12}
N_2H^+	3257.6	698.6	−23.7
N_2D^+	2655.2	552.3	−18.2

The anharmonicity constant $x_{11} = -65.6$ cm^{-1} was derived from the band origin of the $2\nu_1$ and ν_1 bands [35].

The spectroscopic search for the fundamentals of $N_2H^+(N_2D^+)$ was guided by high-quality ab initio calculations that gave estimates (empirical corrections of ab initio results) on the stretching [2, 3] and bending [3] frequencies. The anharmonicity constants x_{11}, x_{13}, and x_{33} for N_2H^+, N_2D^+, N_2T^+, $^{15}NNH^+$, $N^{15}NH^+$, $^{15}N_2H^+$ were calculated using the CEPA-1 method. Only stretching coordinates were considered in this calculation [2]. Anharmonicity constants obtained in an ab initio (CI-SDQ) investigation that included the stretching and bending coordinates [3] were questioned, since the anharmonic parts of the potential show numerical errors [2].

The following **force constants** (all in mdyn/Å) for N_2H^+ corresponding to the N-H stretch (F_{11}), N-N stretch (F_{33}), the interaction of these stretches (F_{13}), and the bend (F_{22}) were predicted by fitting a force constant expression to the potential energy surfaces from high-quality ab initio calculations:

F_{11}	F_{22}	F_{13}	F_{33}	method	Ref.
6.170	0.287	−0.218	23.712	CI-SDQ	[3, 36]
6.132	–	−0.208	24.124	CEPA-1	[2]

Only the dependence of the potential energy on the two stretching coordinates was considered in the CEPA-1 calculation [2]. The dependence on the bending and stretching coordinates was considered in the CI-SDQ calculation of the potential; however, the anharmonic parts of this potential [3] were noted to show large numerical errors [2].

Dissociation Energy

Theoretical values for the N_2H^+ ground-state dissociation energy $D_e(N_2\text{-}H^+)$ in the range 516 to 529 kJ/mol [1, 2, 36 to 39] were obtained using correlated wave functions from ab initio calculations, CEPA-1 [2], CI-SDQ [1, 36], MPPT(4) [37, 38], and MPPT(3) [39]. Estimated zero-point energies of 31 kJ/mol [37] and 42.1 kJ/mol [2] were used to obtain $D_0 = 492.9$ kJ/mol [37] and 488.1 kJ/mol [2]. $D_0(N_2H^+) = 495$ kJ/mol and $D_0(N_2D^+) = 490$ kJ/mol

[40] were derived based on previously reported thermodynamic data in the case of N_2H^+ [41] and spectroscopic data in the case of N_2D^+ [20, 35].

The enthalpy change of the dissociation reaction $N_2H^+ \rightarrow N_2 + H^+$ at 298 K is defined as the proton affinity of N_2 (see p. 7).

References:

[1] Vasudevan, K.; Peyerimhoff, S. D.; Buenker, R. J. (Chem. Phys. **5** [1974] 149/65).
[2] Botschwina, P. (Chem. Phys. Lett. **107** [1984] 535/41).
[3] Hennig, P.; Kraemer, W. P.; Diercksen, G. H. F. (MPI/PAE Astro-135 [1977]).
[4] Musaev, D. G.; Yakobson, V. V.; Charkin, O. P. (Zh. Strukt. Khim. **32** [1991] 3/11; J. Struct. Chem. [Engl. Transl.] **32** [1991] 61/8).
[5] Musaev, D. G.; Yakobson, V. V.; Charkin, O. P. (Mol. Strukt. **1990** 18/24; C.A. **114** [1991] No. 192928).
[6] Ross, S. C. (Chem. Phys. Lett. **107** [1984] 572/4).
[7] Havenith, M.; Zwart, E.; Meerts, W. L.; Ter Meulen, J. J. (J. Chem. Phys. **93** [1990] 8446/51).
[8] Maroulis, G. (Z. Naturforsch. **43a** [1988] 419/29).
[9] Montgomery, J. A., Jr.; Dykstra, C. E. (J. Chem. Phys. **71** [1979] 1380/4).
[10] Kraemer, W. P.; Bunker, P. R. (J. Mol. Spectrosc. **101** [1983] 379/94).

[11] Hillier, I. H.; Kendrick, J. (J. Chem. Soc. Chem. Commun. **1975** 526/7).
[12] Haese, N. N.; Woods, R. C. (Chem. Phys. Lett. **61** [1979] 396/8).
[13] DeFrees, D. J.; Loew, G. H.; McLean, A. D. (Astrophys. J. **257** [1982] 376/82).
[14] Green, S.; Montgomery, J. A., Jr.; Thaddeus, P. (Astrophys. J. **193** [1974] L89/L91).
[15] Ho, W. C.; Pursell, C. J.; Weliky, D. P.; Tagaki, K.; Oka, T. (J. Chem. Phys. **93** [1990] 87/93).
[16] Cazzoli, G.; Corbelli, G.; Degli Esposti, C.; Favero, P. G. (Chem. Phys. Lett. **118** [1985] 164/6).
[17] Gudeman, C. S. (Diss. Univ. Wisconsin 1982; Diss. Abstr. Int. B **43** [1983] 3255).
[18] Turner, B. E. (Astrophys. J. **193** [1974] L83/L87).
[19] Thaddeus, P.; Turner, B. E. (Astrophys. J. **201** [1975] L25/L26).
[20] Owrutsky, J. C.; Gudeman, C. S.; Martner, C. C.; Tack, L. M.; Rosenbaum, N. H.; Saykally, R. J. (J. Chem. Phys. **84** [1986] 605/17).

[21] Gudeman, C. S.; Begemann, M. H.; Pfaff, J.; Saykally, R. J. (J. Chem. Phys. **78** [1983] 5837/8).
[22] Nesbitt, D. J.; Petek, H.; Gudeman, C. S.; Moore, C. B.; Saykally, R. J. (J. Chem. Phys. **81** [1984] 5281/7).
[23] Sears, T. J. (J. Opt. Soc. Am. B Opt. Phys. **2** [1985] 786/9).
[24] Sears, T. J. (J. Chem. Phys. **82** [1985] 5757/8).
[25] Foster, S. C.; McKellar, A. R. W. (J. Chem. Phys. **81** [1984] 3424/8).
[26] Saykally, R. J.; Dixon, T. A.; Anderson, T. G.; Szanto, P. G.; Woods, R. C. (Astrophys. J. **205** [1976] L101/L103).
[27] Anderson, T. G.; Dixon, T. A.; Piltch, N. D.; Saykally, R. J.; Szanto, P. G.; Woods, R. C. (Astrophys. J. **216** [1977] L85/L86).
[28] Van den Heuvel, F. C.; Dymanus, A. (Chem. Phys. Lett. **92** [1982] 219/22).
[29] Sastry, K. V. L. N.; Helminger, P.; Herbst, E.; De Lucia, F. C. (Chem. Phys. Lett. **84** [1981] 286/7).
[30] Nakanaga, T.; Ito, F.; Sugawara, K.; Takeo, H.; Matsumura, C. (Chem. Phys. Lett. **169** [1990] 269/73).

[31] Warner, H. E. (Diss. Univ. Wisconsin 1988; Diss. Abstr. Int. B **49** [1988] 1737).

[32] Szanto, P. G.; Anderson, T. G.; Saykally, R. J.; Piltch, N. D.; Dixon, T. A.; Woods, R. C. (J. Chem. Phys. **75** [1981] 4261/3).

[33] Woods, R. C. (Phil. Trans. R. Soc. [London] A **324** [1988] 141/6).

[34] Berry, R. J.; Harmony, M. D. (J. Mol. Spectrosc. **128** [1988] 176/94).

[35] Sasada, H.; Amano, T. (J. Chem. Phys. **92** [1990] 2248/50).

[36] Kraemer, W. P.; Komornicki, A.; Dixon, D. A. (Chem. Phys. **105** [1986] 87/96).

[37] Del Bene, J. E.; Frisch, M. J.; Raghavachari, K.; Pople, J. A. (J. Phys. Chem. **86** [1982] 1529/35).

[38] DeFrees, D. J.; McLean, A. D. (J. Comput. Chem. **7** [1986] 321/33).

[39] Ikuta, S. (Chem. Phys. Lett. **109** [1984] 550/3).

[40] Schultz, R. H.; Armentrout, P. B. (J. Chem. Phys. **96** [1992] 1036/45).

[41] Lias, S. G.; Bartmess, J. E.; Liebman, J. F.; Holmes, J. L.; Levin, R. D.; Mallard, W. G. (J. Phys. Chem. Ref. Data Suppl. **17** [1988] 1/861).

2.2.2.4 Spectra

Rotational Spectrum

The pure rotational spectrum of N_2H^+ was discovered accidentally in the interstellar space. A triplet near 93174 MHz [1] was identified on the basis of ab initio calculations to be the $J=1\rightarrow0$ transition, split by electric quadrupole coupling due to the outer nitrogen nucleus [2, 3]. Detection of this triplet with microwave absorption spectroscopy confirmed this identification [4]. Subsequently, all seven of the hyperfine components due to the inner and outer nuclei were observed in a high-resolution microwave absorption spectrum [5].

Summarized in Table 4 are the frequencies of the pure rotational transitions up to $J=3\leftarrow2$ of N_2H^+ and isotopomers which were observed in the laboratory by absorption. Additionally, frequencies for the following transitions were reported: $N_2H^+(00^00)$, $J=1\leftarrow0$ [4, 6], $J=4\leftarrow3$, $5\leftarrow4$ [7], $J=11\leftarrow10$ [8], $J=6\leftarrow5$ up to $21\leftarrow20$ [9]; (10^00), $J=1\leftarrow0$ [10], $3\leftarrow2$, $4\leftarrow3$ [11]; $N_2D^+(00^00)$, $J=4\leftarrow3$ up to $6\leftarrow5$ [7]; $^{15}NNH^+$, $N^{15}NH^+(00^00)$, $J=7\leftarrow6$ [12]. $N_2H^+(N_2D^+)$ was produced in N_2-$H_2(D_2)$ gas mixtures in a hollow cathode discharge [8 to 11] or in a glow discharge [4 to 7, 13, 14] with liquid nitrogen cooling. The transitions measured in [10] are also reported in [15]. The frequency tabulated for the $J=1\leftarrow0$ transition of $^{15}NNH^+$ [6] supersedes an earlier value [14]. Frequencies from radioastronomical observations are given in [1, 16 to 19].

The central line frequency ν_0 of the $J=1\leftarrow0$ transition in the vibrational ground state was determined to be 93173.435(3) MHz [5], 93173.419(50) [6], and 93173.439(35) MHz [10]; in the (10^00) vibrational state, $\nu_0=92417.622(54)$ MHz [10]. The frequencies of the $J=1\leftarrow0$ transition in the vibrational ground state for all isotopomers of the ion were obtained from ab initio (CI-SDQ) calculations [20, 21].

The Einstein coefficient of spontaneous emission for the $J=1\rightarrow0$ transition, $A=3.6\times10^{-5}$ s^{-1} [22], was obtained from the spectroscopic data of [2].

A computer-accessible catalog of observed or predicted submillimeter, millimeter, and microwave spectral lines of many species includes 34 lines for N_2H^+ and 41 lines for N_2D^+ [23].

Estimations were given for the pressure-induced shifts of the $J=1\rightarrow0$ line [24].

For an overview of microwave spectroscopy of molecular ions, including N_2H^+, see for example [25, 26].

Table 4
Pure Rotational Transitions in the Vibrational Ground State $^1\Sigma^+(00^00)$.

species	$J' \leftarrow J''$	outer N $F' \leftarrow F''$	inner N $F' \leftarrow F''$	ν in MHz	Ref.
N_2H^+	$1 \leftarrow 0$	$0 \leftarrow 1$	–	93176.36(10)	[10]
			$1 \leftarrow 2$	93176.310	[5]
		$2 \leftarrow 1$	–	93173.78(10)	[10]
			$2 \leftarrow 1$	93173.505	[5]
			$3 \leftarrow 2$	93173.809	[5]
			$1 \leftarrow 1$	93174.016	[5]
		$1 \leftarrow 1$	–	93171.94(10)	[10]
			$0 \leftarrow 1$	93171.619	[5]
			$2 \leftarrow 2$	93171.947	[5]
			$1 \leftarrow 0$	93172.078	[5]
	$2 \leftarrow 1$	–	–	186344.874(100)	[7]
	$3 \leftarrow 2$	–	–	279511.671(50)	[7]
N_2D^+	$1 \leftarrow 0$	$1 \leftarrow 1$	–	77107.86 ± 0.09	[13]
		$2 \leftarrow 1$	–	77109.61 ± 0.08	[13]
		$1 \leftarrow 0$	–	$77112.2 \pm 0.1^{*)}$	[27]
	$2 \leftarrow 1$	–	–	154217.199(150)	[7]
	$3 \leftarrow 2$	–	–	231321.635(50)	[7]
$^{15}NNH^+$	$1 \leftarrow 0$	–	–	90263.833(30)	[6]
$N^{15}NH^+$	$1 \leftarrow 0$	$1 \leftarrow 1$	–	91204.328(30)	[6]
		$2 \leftarrow 1$	–	91205.999(10)	[6]
		$0 \leftarrow 1$	–	91208.663(70)	[6]
$^{15}N_2H^+$	$1 \leftarrow 0$	–	–	88264.083(10)	[6]

$^{*)}$ This component was only observed radioastronomically [27] and is centered on the laboratory frequency of the 2 ← 1 component [13].

Vibration-Rotation Spectrum

High-resolution vibration-rotation spectra of N_2H^+ and of N_2D^+ in plasmas were obtained by infrared and far-infrared absorption spectroscopy using tunable color-center [28 to 30], diode [31 to 33], and semiconductor [34] lasers. Velocity modulation of the ions formed in an ac glow discharge was employed to observe the ν_1 bands of N_2H^+ [28, 29] and N_2D^+ [30] as well as the $\nu_1+\nu_2 \leftarrow \nu_2$ hot bands, including l-type doublets, of N_2H^+ [29] and N_2D^+ [30]. Modulated hollow cathode discharges (modulation of the discharge current and hence the ion concentration) were used to observe the weaker ν_2 bands of N_2H^+ [31] and N_2D^+ [32], the even weaker ν_3 bands of N_2H^+ and N_2D^+ [33], and the $2\nu_1$ band of N_2H^+ [34]. The observed transition frequencies [28 to 33] were combined in a weighted least-squares analysis and are compiled in [29]. A high-resolution spectrum of the ν_1 band of N_2H^+ was also obtained by Fourier transform IR spectroscopy [35].

The fundamental frequencies are given on p. 20. The band center of the $2\nu_1$ band, $\nu_0 = 6336.6775(39)$ cm^{-1}, was obtained from measured wave numbers [34]. Frequencies for the ten lowest vibrational states that involve the stretching fundamentals ν_1 and ν_3 [36] and for overtones and combinations that also involve the bending fundamental ν_2 [6] were predicted for the isotopomers of N_2H^+ using high-quality ab initio calculations (CEPA-1) [36] and CI-SDQ [6].

An absolute integrated intensity of 1880(290) $cm^{-2} \cdot atm^{-1}$ at STP was determined for the ν_1 band of N_2H^+ using the technique of direct laser absorption spectroscopy in fast ion beams. This value [37] supersedes a previous value determined in the same laboratory [38]. Higher values were predicted by high-quality ab initio calculations, CEPA-1 [36] and CI-SDQ [39]. Integrated intensities for the ν_2 [39] and ν_3 [36, 39] bands of N_2H^+, for the ν_1 and ν_3 bands of N_2D^+ [36], and for bands from overtones and combinations of the ν_1 and ν_3 fundamentals of $N_2H^+(N_2D^+)$ were also predicted in the ab initio calculations [36, 39]. The ν_3 band was predicted to be about 140 times weaker than the ν_1 band [36], and the ν_2 band to be about five times weaker than the ν_1 band [39].

Values for the Einstein transition probabilities of spontaneous emission, $A_{nm} = 857$, 1592, and 2213 s^{-1} for the transitions $(00^00) \leftarrow (10^00)$, $(10^00) \leftarrow (20^00)$, and $(20^00) \leftarrow (30^00)$, respectively, were predicted in high-quality ab initio calculations (CEPA-1) [36].

References:

[1] Turner, B. E. (Astrophys. J. **193** [1974] L83/L87).

[2] Green, S.; Montgomery, J. A., Jr.; Thaddeus, P. (Astrophys. J. **193** [1974] L89/L91).

[3] Hillier, I. H.; Kendrick, J. (J. Chem. Soc. Chem. Commun. **1975** 526/7).

[4] Saykally, R. J.; Dixon, T. A.; Anderson, T. G.; Szanto, P. G.; Woods, R. C. (Astrophys. J. **205** [1976] L101/L103).

[5] Cazzoli, G.; Corbelli, G.; Degli Esposti, C.; Favero, P. G. (Chem. Phys. Lett. **118** [1985] 164/6).

[6] Gudeman, C. S. (Diss. Univ. Wisconsin 1982; Diss. Abstr. Int. B **43** [1983] 3255).

[7] Sastry, K. V. L. N.; Helminger, P.; Herbst, E.; De Lucia, F. C. (Chem. Phys. Lett. **84** [1981] 286/7).

[8] Van den Heuvel, F. C.; Dymanus, A. (Chem. Phys. Lett. **92** [1982] 219/22).

[9] Verhoeve, P.; Zwart, E.; Versluis, M.; Drabbels, M.; Ter Meulen, J. J.; Meerts, W. L.; Dymanus, A.; McLay, D. B. (Rev. Sci. Instrum. **61** [1990] 1612/25).

[10] Ho, W. C.; Pursell, C. J.; Weliky, D. P.; Tagaki, K.; Oka, T. (J. Chem. Phys. **93** [1990] 87/93).

[11] Warner, H. E. (Diss. Univ. Wisconsin 1988; Diss. Abstr. Int. B **49** [1988] 1737).

[12] Havenith, M.; Zwart, E.; Meerts, W. L.; Ter Meulen, J. J. (J. Chem. Phys. **93** [1990] 8446/51).

[13] Anderson, T. G.; Dixon, T. A.; Piltch, N. D.; Saykally, R. J.; Szanto, P. G.; Woods, R. C. (Astrophys. J. **216** [1977] L85/L86).

[14] Szanto, P. G.; Anderson, T. G.; Saykally, R. J.; Piltch, N. D.; Dixon, T. A.; Woods, R. C. (J. Chem. Phys. **75** [1981] 4261/3).

[15] Pursell, C. J.; Weliky, D. P.; Ho, W. C.; Takagi, K.; Oka, T. (J. Chem. Phys. **91** [1989] 7997/9).

[16] Turner, B. E.; Thaddeus, P. (Astrophys. J. **211** [1977] 755/71).

[17] Erickson, N.; Davis, J. H.; Evans, N. J., II; Loren, R. B.; Mundy, L.; Peters, W. L., III; Scholtes, M.; Vanden Bout, P. A. (Symp. Int. Astron. Union No. 87 [1980] 25/30; C.A. **94** [1981] No. 112221).

[18] Lovas, F. J. (J. Phys. Chem. Ref. Data **21** [1992] 181/272).

[19] Thaddeus, P.; Turner, B. E. (Astrophys. J. **201** [1975] L25/L26).

[20] Hennig, P.; Kraemer, W. P.; Diercksen, G. H. F. (MPI/PAE Astro-135 [1977]).

[21] Kraemer, W. P.; Hennig, P.; Diecksen, G. H. F. (Spectres Mol. Simples Lab. Astrophys. Commun. 21st Colloq. Int. Astrophys., Liege 1977 [1980], pp. 87/99; C.A. **93** [1980] No. 213004).

[22] Dickinson, A. S.; Flower, D. R. (Mon. Not. R. Astron. Soc. **196** [1981] 297/304).

[23] Poynter, R. L.; Pickett, H. M. (Appl. Opt. **24** [1985] 2235/40).

[24] Krupnov, A. F.; Skvortsov, V. A. (Izv. Vyssh. Uchebn. Zaved. Radiofiz. **29** [1986] 499/502; C.A. **105** [1986] No. 160990).

[25] Woods, R. C. (in: Miller, T. A.; Bondybey, V. E.; Molecular Ions: Spectroscopy, Structure and Chemistry, North Holland, Amsterdam 1983, pp. 11/47).

[26] Woods, R. C. (in: Maier, J. P.; Ion and Ion Cluster Spectroscopy and Structure, Elsevier, Amsterdam 1989, pp. 27/58).

[27] Snyder, L. E.; Hollis, J. M.; Buhl, D.; Watson, W. D. (Astrophys. J. **218** [1977] L61/L64).

[28] Gudeman, C. S.; Begemann, M. H.; Pfaff, J.; Saykally, R. J. (J. Chem. Phys. **78** [1983] 5837/8).

[29] Owrutsky, J. C.; Gudeman, C. S.; Martner, C. C.; Tack, L. M.; Rosenbaum, N. H.; Saykally, R. J. (J. Chem. Phys. **84** [1986] 605/17).

[30] Nesbitt, D. J.; Petek, H.; Gudeman, C. S.; Moore, C. B.; Saykally, R. J. (J. Chem. Phys. **81** [1984] 5281/7).

[31] Sears, T. J. (J. Opt. Soc. Am. B Opt. Phys. **2** [1985] 786/9).

[32] Sears, T. J. (J. Chem. Phys. **82** [1985] 5757/8).

[33] Foster, S. C.; McKellar, A. R. W. (J. Chem. Phys. **81** [1984] 3424/8).

[34] Sasada, H.; Amano, T. (J. Chem. Phys. **92** [1990] 2248/50).

[35] Nakanaga, T.; Ito, F.; Sugawara, K.; Takeo, H.; Matsumura, C. (Chem. Phys. Lett. **169** [1990] 269/73).

[36] Botschwina, P. (Chem. Phys. Lett. **107** [1984] 535/41).

[37] Keim, E. R.; Polak, M. L.; Owrutsky, J. C.; Coe, J. V.; Saykally, R. J. (J. Chem. Phys. **93** [1990] 3111/9).

[38] Owrutsky, J. C.; Keim, E. R.; Coe, J. V.; Saykally, R. J. (J. Phys. Chem. **93** [1989] 5960/3).

[39] Kraemer, W. P.; Komornicki, A.; Dixon, D. A. (Chem. Phys. **105** [1986] 87/96).

2.2.2.5 Enthalpy of Formation

The enthalpy of formation of N_2H^+ can be obtained from the proton affinity of N_2, $A_p(N_2)$, according to $\Delta_fH°(N_2H^+) = \Delta_fH°(N_2) + \Delta_fH°(H^+) - A_p(N_2)$. The quantity $A_p(N_2)$ is discussed on p. 7. Uncertainty in the value of $A_p(N_2)$ resulted in a range of $\Delta_fH°(N_2H^+)$ values [1 to 4]. The recommended value, 1035.5 kJ/mol [1, 2], was obtained from an updated assignment of absolute values [1] to a ladder of A_p differences [3]. $\Delta_fH°(N_2H^+) = 1038$ kJ/mol was obtained in a similar way [5].

Values of $\Delta_fH°$ were also obtained from the appearance potentials of N_2H^+ arising from nitrogen-hydrogen compounds (see p. 16). The recommended values are 1036.0 ± 3.8 [6] and 1035.5 kJ/mol [2]. Other values given in [7 to 10] infer an incorrect value of $A_p(N_2)$.

The values $\Delta_fH^\circ_{298}(N_2H^+) = 1041.8$ and $\Delta_fH^\circ_{298}(N_2D^+) = 1049.0$ kJ/mol [11] were derived from thermodynamic [2] and spectroscopic [12, 13] data.

The **entropy** of N_2H^+ at 298 K, $S° = 200 \pm 2$ [3] and 202 $J \cdot mol^{-1} \cdot K^{-1}$ [14], was calculated using statistical mechanics. Ab initio values of vibrational frequencies were used in the latter calculation [14]. Vibrational contributions to the entropy were neglected in the former calculation [3].

References:

[1] Lias, S. G.; Liebmann, J. F.; Levin, R. D. (J. Phys. Chem. Ref. Data **13** [1984] 695/808).

[2] Lias, S. G.; Bartmess, J. E.; Liebman, J. F.; Holmes, J. L.; Levin, R. D.; Mallard, W. G. (J. Phys. Chem. Ref. Data Suppl. **17** [1988] 1/861).

[3] Bohme, D. K.; Mackay, G. I.; Schiff, H. I. (J. Chem. Phys. **73** [1980] 4976/86).

[4] Li, Y. H.; Harrison, A. G. (Int. J. Mass Spectrom. Ion Phys. **28** [1978] 289/96).

[5] Smith, R. D.; Futrell, J. H. (J. Phys. Chem. **81** [1977] 195/9).

[6] Ruscic, B.; Berkowitz, J. (J. Chem. Phys. **95** [1991] 4378/84).

[7] Dibeler, V. H.; Franklin, J. L.; Reese, R. M. (J. Am. Chem. Soc. **81** [1959] 68/73).

[8] Dibeler, V. H.; Franklin, J. L.; Reese, R. M. (Adv. Mass Spectrom. **1** [1959] 443/57).

[9] Franklin, J. L.; Dibeler, V. H.; Reese, R. M.; Krauss, M. (J. Am. Chem. Soc. **80** [1958] 298/302).

[10] Willis, C.; Lossing, F. P.; Back, R. A. (Can. J. Chem. **54** [1976] 1/3).

[11] Schultz, R. H.; Armentrout, P. B. (J. Chem. Phys. **96** [1992] 1036/45).

[12] Owrutsky, J. C.; Gudeman, C. S.; Martner, C. C.; Tack, L. M.; Rosenbaum, N. H.; Saykally, R. J. (J. Chem. Phys. **84** [1986] 605/17).

[13] Sasada, H.; Amano, T. (J. Chem. Phys. **92** [1990] 2248/50).

[14] DeFrees, D. J.; McLean, A. D. (J. Comput. Chem. **7** [1986] 321/33).

2.2.2.6 Transport Phenomena

The reduced mobilities as a function of E/N (the ratio of the applied electrostatic field strength E to the neutral gas density N) were measured for N_2H^+ drifting through He at E/N = 3 to 130 Td (1 Townsend = 10^{-17} V·cm^2) [1], through Ar at E/N = 3 to 100 Td [1], and through N_2 at E/N = 2 to 260 Td [2] (smoothed data tabulated in [3]). Extrapolated zero-field reduced mobilites μ_0 (in $cm^{-2} \cdot V^{-1} \cdot s^{-1}$) are summarized below. The free-ion diffusion coefficients D, obtained from μ_0, are given as D·p (in $cm^2 \cdot Torr \cdot s^{-1}$, p is the neutral gas pressure) and D·N (in 10^{19} $cm^{-1} \cdot s^{-1}$, N is the neutral gas number density).

neutral gas	μ_0	D·p	D·N	remarks	Ref.
N_2	2.14 ± 0.11	46.2	0.149	flow-drift tube, 300 K	[2]
He	19.0 (± 4%)	403	1.20	flow-drift tube, 295 K	[1]
Ar	2.56 (± 4%)	54	0.16	flow-drift tube, 295 K	[1]
H_2	12.1 ± 0.1	–	–	drift tube, 293 K	[4]
H_2	11.07 ± 0.10	–	–	ion cyclotron resonance, 273 K	[5]

The reduced mobility of N_2H^+ drifting through N_2 as a function of the effective ion gas temperature was predicted using a kinetic theory [3].

References:

[1] Jones, T. T. C.; Jones, J. D. C.; Birkinshaw, K.; Twiddy, N. D. (Chem. Phys. Lett. **89** [1982] 443/5).

[2] Dotan, I.; Albritton, D. L.; Lindinger, W.; Pahl, M. (J. Chem. Phys. **65** [1976] 5028/30).

[3] Ellis, H. W.; McDaniel, E. W.; Albritton, D. L.; Viehland, L. A.; Lin, S. L.; Mason, E. A. (At. Data Nucl. Data Tables **22** [1978] 179/217).

[4] Elford, M. T. (J. Chem. Phys. **79** [1983] 5951/9).

[5] Ridge, D. P.; Beauchamp, J. L. (J. Chem. Phys. **64** [1976] 2735/46).

2.2.2.7 Energy Transfer

Vibrational Energy Transfer

Angular and velocity spectra of the inelastic scattering of N_2D^+ with He were investigated by using an ion-beam target-gas technique for center-of-mass collision energies in the range 8 to 18 eV. A vibrational-to-translational energy transfer from N_2D^+ to He was proposed. The energy transferred for 180° scattering was observed to increase with collision energy [1].

The rate constants for the vibrational relaxation of N_2H^+ by He, Ar, and Kr were estimated in a selected-ion flow tube study to be less than 1×10^{-13} (He) and 5×10^{-11} $cm^3 \cdot molecule^{-1} \cdot s^{-1}$ (Ar, Kr) [2].

Rotational Energy Transfer

$N_2H^+ + e^-$. Interest in the rotational excitation of N_2H^+ by electron impact was prompted by the observation of a $J = 1 \rightarrow 0$ emission of N_2H^+ in interstellar clouds [3].

Rate constants for the $\Delta J = +1$ ($J = 1 \leftarrow 0$ and $J = 2 \leftarrow 1$) and $\Delta J = +2$ ($J = 2 \leftarrow 0$) rotational excitations of N_2H^+ by electron impact were calculated using a semiclassical, first-order perturbation theory that treats only the electron-dipole term of the interaction potential. In the range 10 to 500 K, the maximum values $k(1 \leftarrow 0) = 20 \times 10^{-6}$ at 10 K and $k(2 \leftarrow 1) = 9.6 \times 10^{-6}$ $cm^3 \cdot molecule^{-1} \cdot s^{-1}$ at 20 K were calculated. The rate constants for the $J = 2 \leftarrow 0$ excitation were estimated to be lower by a factor of 6 to 7 [4]. Semiempirically calculated rate constants for $J = 1 \leftarrow 0$ and $1 \rightarrow 0$ transitions as a function of temperature in the range 10 to 1000 K were reported [5]. The temperature dependence of the $J = 1 \rightarrow 0$ deexcitation, which was predicted by the Glauber approximation [6], was shown to be inadequate and to differ substantially from the semiclassical results [5].

$N_2H^+ + X$ ($X = He$, Ar, and N_2). The rotational transitions of N_2H^+ induced by collisions with He, Ar, and N_2 were investigated using infrared-microwave four-level double-resonance spectroscopy. The $J = 1 \leftarrow 0$ transition was saturated by high-power microwave radiation. The transfer of this perturbation of the population from equilibrium to other rotational levels ($J' = 2$, 3, and 4) by rotationally inelastic collisions was probed by infrared radiation. In all three systems (He, Ar, and N_2), the ratios of the population change of level J' to the change of level $J'' = 1$ were observed to be positive and to decrease monotonically with increasing J'. This behavior is attributed to collisional selection rules for rotational energy transfer. The observed selection rules are suggested to arise from the interaction of a charge-induced dipole in the collision partner with the permanent dipole moment of N_2H^+ [7].

Rate constants for the rotational energy transfer in low-energy collisions of N_2H^+ and He at the low temperatures (5 to 40 K) of interstellar clouds were obtained using quantum close-coupling scattering approximations to describe the collision dynamics on an N_2H^+-He ab initio (SCF) potential energy surface. The rate constants for the transitions $|\Delta J| = |J' - J''| = 0$ up to 6 were reported ($k = 1.8 \times 10^{-10}$ $cm^3 \cdot molecule^{-1} \cdot s^{-1}$ for the $J = 1 \leftarrow 0$ excitation at 10 K). While single quantum jumps are most likely, the probability for multiple quantum jumps was observed to fall off slowly with increasing $|\Delta J|$. The rate constants for $|\Delta J| = 2$ transitions were observed to be generally smaller by a factor of 2 to 3 than those for $|\Delta J| = 1$ transitions. The calculated rate constants for the $J = 2, 3, 4 \leftarrow 1$ transitions [8], extrapolated to 100 K, predict rotational populations that agree with the experimental population probes [7] discussed above. Information theoretic surprisals of state-to-state ab initio cross sections as a function of the energy gap were reported for N_2H^+, rotationally excited by collisions with He at a total energy of 80 cm^{-1} [9]. Thermal rate constants at 10, 20, and 30 K for the multiple ΔJ transitions, $J''=0$ to 4 and $J'=1$ to 5, were predicted using T-matrix factorization based on the infinite-order sudden approximation [10].

References:

[1] Chiang, M. M. H. (LBL-474 [1972] 87 pp. from N.S.A. **26** [1972] No. 34435; C.A. **77** [1972] No. 118541).
[2] Villinger, H.; Futrell, J. H.; Saxer, A.; Richter, R.; Lindinger, W. (J. Chem. Phys. **80** [1984] 2543/7).
[3] Turner, B. E. (Astrophys. J. **193** [1974] L83/L87).
[4] Bhattacharyya, S. S.; Bhattacharyya, B.; Narayan, M. V. (Astrophys. J. **247** [1981] 936/40).
[5] Dickinson, A. S.; Flower, D. R. (Mon. Not. R. Astron. Soc. **196** [1981] 297/304).
[6] Gupta, G. P.; Mathur, K. C. (Phys. Rev. [3] A **21** [1980] 1350/1).
[7] Pursell, C. J.; Weliky, D. P.; Oka, T. (J. Chem. Phys. **93** [1990] 7041/8).
[8] Green, S. (Astrophys. J. **201** [1975] 366/72).
[9] Green, S. (Chem. Phys. **40** [1979] 1/10).
[10] Goldflam, R.; Kouri, D. J.; Green, S. (J. Chem. Phys. **67** [1977] 5661/75).

2.2.2.8 Chemical Behavior

2.2.2.8.1 Photodissociation. Decay

The upper limits of the cross sections for the photodissociation of N_2H^+ over a range of wavelengths were obtained with drift tube mass spectrometry: $\sigma<0.02$ Å^2, $\lambda=5309$ Å; $\sigma<0.11$ Å^2, $\lambda=4762$ Å; $\sigma<0.17$ Å^2, $\lambda=4680$ Å; and $\sigma<0.04$ Å^2, $\lambda\approx3507$Å [1].

The N_2H^+ formed following electron beam ionization of gaseous ammonia in the ion source of a mass spectrometer was observed to decay ($N_2H^+ \rightarrow$ products) with the cross section $\sigma\approx98$ Å^2 [2].

References:

[1] Smith, G. P.; Lee, L. C. (J. Chem. Phys. **69** [1978] 5393/9).
[2] Derwish, G. A. W.; Galli, A.; Giardini-Guidoni, A.; Volpi, G. G. (J. Chem. Phys. **39** [1963] 1599/605).

2.2.2.8.2 Electron-Ion Dissociative Recombination

The electron-ion dissociative recombination $N_2H^+ + e^-$ is an important loss process for N_2H^+ in laboratory plasmas and in interstellar gas clouds [1, 2].

A flowing afterglow study employing spectroscopic monitoring of the H-atom production showed that the dissociative recombination of N_2H^+ proceeds only through the channel a) $N_2H^+ + e^- \rightarrow N_2 + H$, even though the channel b) $N_2H^+ + e^- \rightarrow NH + N$ is energetically feasible [3]. Channel a) was considered in modeling studies of the gas phase chemistry of interstellar clouds; see for example [4 to 6].

The rate constants for the dissociative recombination process are summarized in Table 5. The rate constants, appropriate to plasmas in which the temperatures of the component species (electron, ion, and gas) are equal, are designated α_t and those appropriate to conditions for which the temperature of the electrons (T_e) is greater than that of ions and gas are designated α_e [1]. The tabulated rate constants, which were determined by spectroscopic monitoring on several vibration-rotation levels of N_2H^+ in a hollow cathode discharge, are rotationally averaged. No significant dependence on rotation was observed (rotational relaxation is much faster than dissociative recombination) [7]. An earlier version of the merged-beam work [8] reported α_e an order of magnitude smaller [9].

Table 5
Rate Constants α (in 10^{-7} $cm^3 \cdot molecule^{-1} \cdot s^{-1}$) for the Dissociative Recombination $N_2H^+(N_2D^+) + e^- \rightarrow N_2 + H(D)$.

ion	T in K	α_t	α_e	method	Ref.
N_2H^+	95	4.9 ± 1.0		flowing afterglow Langmuir probe	[1]
	100		15[d)]	merged beam	[8]
	110	15[a,b)]		hollow cathode discharge	[7]
	210	9[a,b)]		hollow cathode discharge	[7]
	273	7.0[a)]		hollow cathode discharge	[7]
	300	1.7 ± 0.3		flowing afterglow Langmuir probe	[1]
N_2D^+	95	4.4 ± 0.9		flowing afterglow Langmuir probe	[1]
	100		15[d)]	merged beam	[8]
	300		7.5[c)]	merged beam	[1]

[a)] N_2H^+ decay monitored spectroscopically on several vibration-rotation levels. — [b)] Average of the values reported. — [c)] Extrapolated from the data in [8]. — [d)] For an extrapolated cross section, see text.

The cross sections for the dissociative recombinations of N_2H^+ and N_2D^+, measured by a merged electron ion-beam technique for center-of-mass electron energies from 0.006 to 0.75 eV, showed a close to E^{-1} energy dependence between 0.006 and 0.05 eV [8]. At higher energies ($E > 0.06$ eV [9]), a stronger decrease of the cross section was found [8, 9]. From these data, rate constants between 10 to 10^4 K were calculated by extrapolating the E^{-1} behavior down to 0.001 eV and assuming a Maxwellian distribution of electron velocities. The rate constants show a $T_e^{-0.5}$ temperature dependence below 300 K [8]. A hollow cathode study indicated a $T_e^{-0.5}$ temperature dependence in the limited range 110 K to 273 K [7]. An approximate T^{-1} temperature dependence in the range 95 to 300 K was observed for the rate constants obtained using truly thermal, flowing afterglow Langmuir-probe data [1].

SCF values for the sum of the contributions of the electric moments and the sum of the contributions of the polarizabilities to the interaction energy of the system e^--N_2H^+ were calculated for different specified positions of the electron [10].

References:

[1] Adams, N. G.; Smith, D.; Alge, E. (J. Chem. Phys. **81** [1984] 1778/84).
[2] Adams, N. G.; Smith, D. (NATO ASI Ser. C **157** [1985] 657/9).
[3] Adams, N. G.; Herd, C. R.; Geoghegan, M.; Smith, D.; Canosa, A.; Gomet, J. C.; Rowe, B. R.; Queffelec, J. L.; Morlais, M. (J. Chem. Phys. **94** [1991] 4852/7).
[4] Swade, D. A. (Astrophys. J. **345** [1989] 828/52).
[5] Viala, Y. P. (Astron. Astrophys. Suppl. Ser. **64** [1986] 391/437).
[6] Brown, R. D.; Rice, E. H. N. (Mon. Not. R. Astron. Soc. **223** [1986] 405/28).
[7] Amano, T. (J. Chem. Phys. **92** [1990] 6492/501).

[8] Mul, P. M.; McGowan, J. W. (Astrophys. J. **227** [1979] L157/L159).
[9] McGowan, J. W.; Mul, P. M.; D'Angelo, V. S.; Mitchell, J. B. A.; Defrance, P.; Froelich, H. R. (Phys. Rev. Lett. **42** [1979] 373/5).
[10] Maroulis, G. (Z. Naturforsch. **43a** [1988] 419/29).

2.2.2.8.3 Electron-Transfer Neutralization

The electron-transfer reaction $N_2H^+(N_2D^+) + M \rightarrow N_2H^*(N_2D^*) + M^+$ (M = Na, K, Mg, or Zn) was studied using an ion-beam target-gas technique. Following electron impact ionization of N_2-$H_2(D_2)$ mixtures (ca. 1 Torr) at temperatures from 100 to 300 K, the $N_2H^+(N_2D^+)$ ions were accelerated to 5 keV and focused into a chamber containing a few mTorr of the target metal (M). The beam profiles of the N_2 dissociation product from $N_2H(N_2D) \rightarrow N_2 + H(D)$ was observed.

Reference:

Selgren, S. F.; McLoughlin, P. W.; Gellene, G. I. (J. Chem. Phys. **90** [1989] 1624/9).

2.2.2.8.4 Isotope-Exchange Reactions

The rate constants k (in 10^{-9} $cm^3 \cdot molecule^{-1} \cdot s^{-1}$) for the following isotope exchange reactions in the forward (k_f) and reverse (k_r) directions were obtained with a temperature-variable, selected-ion flow tube apparatus [1, 2]. (The accuracy was ± 20% at 292 K and ± 25% at 80 K [1]; ΔH is in kJ/mol.)

reaction	k_f		k_r		−ΔH	Ref.
	292 K	80 K	292 K	80 K		
$^{14}N_2H^+ + {}^{14}N^{15}N \rightleftharpoons {}^{14}N^{15}NH^+ + {}^{14}N_2$	4.1	4.6	4.1	4.1	0.07 ± 0.02	[1]
$^{14}N^{15}NH^+ + {}^{15}N_2 \rightleftharpoons {}^{15}N^2H^+ + {}^{14}N^{15}N$	4.1	4.6	4.1	4.1	0.07 ± 0.02	[1]
$^{14}N_2H^+ + {}^{15}N_2 \rightleftharpoons {}^{15}N_2H^+ + {}^{14}N_2$	4.1	4.8	4.1	4.1	0.10 ± 0.02	[1]
	300 K	120 K	300 K	120 K		
$N_2H^+ + D \rightleftharpoons N_2D^+ + H$	3	8	~0.1	0.25	4.6[a]	[2]

[a] Estimated value.

The $^{14}N/^{15}N$ reactions were proposed to proceed via proton transfer (the term isotope exchange is misleading in this case), since an $^{14}N^{15}NH^+$ product was not observed in the forward or reverse direction of the reaction $^{14}N_2H^+ + {}^{15}N_2 \rightleftharpoons {}^{15}N_2H^+ + {}^{14}N_2$ [1]. The equilibrium constant $K = 0.98 \exp(10/T)$ for this reaction was calculated using standard statistical mechanics, and the fractionation via this reaction was predicted to be significant at the lowest temperatures of interstellar clouds (efficiency $\eta = K/(K+1) = 0.73$ at 10 K) [3]. The temperature dependence observed for the forward and reverse rate constants of the deuteration reaction $N_2H^+ + D \rightleftharpoons N_2D^+ + H$ at 120 K was also used to predict significant fractionation of deuterium in interstellar media [2]. Indeed the ratio N_2D^+/N_2H^+ in interstellar media was observed to be far greater than that which cosmic deuterium abundance suggests [4].

References:

[1] Adams, N. G.; Smith, D. (Astrophys. J. **247** [1981] L123/L125).
[2] Adams, N. G.; Smith, D. (Astrophys. J. **294** [1985] L63/L65).

[3] Henchman, M.; Paulson, J. F. (J. Chem. Soc. Faraday Trans. II **285** [1989] 1673/84).
[4] Woods, R. C. (Ann. Isr. Phys. Soc. **4** [1981] 221/7).

2.2.2.8.5 Proton-Transfer Reactions

The rate constants for gas-phase proton transfer reactions of N_2H^+ are summarized in Table 6. The rate constants generally refer to thermal or near-thermal measurements at room temperature. Further information on the tabulated reactions and on other proton transfer reactions is given in the text. For some comments regarding experimental techniques used in studying gas-phase ion molecule reactions, see p. 6.

Predictions of collision rate constants for systems in which a reactive collision of N_2H^+ with its partner would result in proton transfer have not been treated in the text. Such collision rate constants obtained using classical theories, such as the Langevin ion-induced dipole theory, the locked-dipole theory, and the average dipole orientation theory, are given, for example, in [1 to 11]. Langevin rate constants for the reactions of N_2H^+ with many species, including those for which there are no laboratory data (for example C, S, NH, OH, CH_2, NH_2, HCO, C_2H), are given in [12].

Table 6
Rate Constants k (in $cm^3 \cdot molecule^{-1} \cdot s^{-1}$) for Proton Transfer Reactions of N_2H^+.

reaction	10^9 k	experimental technique	Ref.
$N_2H^+ + Kr \rightarrow KrH^+ + N_2$	0.01	selected-ion drift tube	[13]
$N_2H^+ + Xe \rightarrow XeH^+ + N_2$	0.66 ± 0.20	flowing afterglow	[14]
$N_2H^+ + O \rightarrow OH^+ + N_2$	0.14 ± 0.03	flowing afterglow	[15]
$N_2H^+ + H_2 \rightarrow H_3^+ + N_2$	5.1 ± 2.1	flowing afterglow	[16]
$N_2H^+ + O_2 \rightarrow HO_2^+ + N_2$	≤0.0008	flowing afterglow	[3]
$N_2H^+ + O_2(a\ ^1\Delta_g) \rightarrow HO_2^+ + N_2$	0.08	flowing afterglow	[3]
$N_2H^+ + H_2O \rightarrow H_3O^+ + N_2$	2.6 ± 1.0	selected-ion drift chamber	[2]
	2.5 ± 0.7	flowing afterglow	[17]
	2.77	flowing afterglow	[18]
	2.6 ± 0.65	flowing afterglow	[8]
	2.9	corona discharge	[19]
$N_2H^+ + NH_3 \rightarrow NH_4^+ + N_2$	1.9	selected-ion flow tube	[4]
	2.3 ± 0.5	flowing afterglow	[1]
	2.0 ± 0.4	mass spectrometer ion source	[11]
$N_2H^+ + N_2O \rightarrow N_2OH^+ + N_2$	1.7 ± 0.7	selected-ion drift chamber	[2]
	0.79	flowing afterglow	[5]
	1.2*)	selected-ion flow tube	[4]
$N_2H^+ + NO \rightarrow NOH^+ + N_2$	0.34 ± 0.14	selected-ion drift chamber	[2]
	<0.1	flowing afterglow	[20]
	0.83	selected-ion flow tube	[4]
$N_2H^+ + CO \rightarrow COH^+ + N_2$	0.88 ± 0.22	flowing afterglow	[21]
$N_2H^+ + CO_2 \rightarrow CO_2H^+ + N_2$	1.4 ± 0.6	selected-ion drift chamber	[2]
	0.92	flowing afterglow	[5]
	0.98 ± 0.20	flowing afterglow	[14]
	0.89	flowing afterglow	[22]
	<0.1	flowing afterglow	[20]
	1.1*)	selected-ion flow tube	[4]

Table 6 (continued)

reaction	10^9 k	experimental technique	Ref.
$N_2H^+ + SO_2 \rightarrow SO_2H^+ + N_2$	1.7 ± 0.7	selected-ion drift chamber	[2]
$N_2H^+ + CS_2 \rightarrow CS_2H^+ + N_2$	0.6 ± 0.2	selected-ion drift chamber	[2]
$N_2H^+ + COS \rightarrow COSH^+ + N_2$	1.3	selected-ion flow tube	[4]
$N_2H^+ + HCN \rightarrow HCNH^+ + N_2$	3.2 ± 0.2	flowing afterglow	[7]
$N_2H^+ + HCOOH \rightarrow (HCOOH)H^+ + N_2$	1.7	flowing afterglow	[23]
$N_2H^+ + CH_3Cl \rightarrow CH_3ClH^+ + N_2$	2.4 ± 1.0	selected-ion drift chamber	[2]
	1.9	selected-ion flow tube	[4]
$N_2H^+ + CH_4 \rightarrow CH_5^+ + N_2$	0.89	flowing afterglow	[5]
	1.3 ± 0.3	mass spectrometer ion source	[11]
$N_2H^+ + CF_4 \rightarrow CF_4H^+ + N_2$	<0.1	flowing afterglow	[20]
$N_2H^+ + CH_3CHO \rightarrow CH_3CHOH^+ + N_2$	5.8 ± 1.2	mass spectrometer ion source	[11]
$N_2D^+ + CH_3CHO \rightarrow CH_3CHOD^+ + N_2$	6.2 ± 1.2	mass spectrometer ion source	[11]
$N_2H^+ + CH_2O \rightarrow CH_2OH^+ + N_2$	3.3 ± 0.8	flowing afterglow	[24]
$N_2H^+ + CH_3NO_2 \rightarrow CH_3NO_2H^+ + N_2$	3.29 ± 0.12	flowing afterglow	[25]
$N_2H^+ + CH_3CN \rightarrow CH_3CNH^+ + N_2$	4.1 ± 0.1	flowing afterglow	[7]
$N_2H^+ + C_2H_2 \rightarrow C_2H_3^+ + N_2$	1.41 ± 0.35	flowing afterglow	[9]
$N_2H^+ + C_2H_6 \rightarrow C_2H_7^+ + N_2$	0.17 ± 0.07	selected-ion flow tube	[26]
$N_2H^+ + C_2N_2 \rightarrow C_2N_2H^+ + N_2$	1.2 ± 0.4	selected-ion flow tube	[27]
$N_2H^+ + HC_3N \rightarrow HC_3NH^+ + N_2$	4.2 ± 1.3	selected-ion flow tube	[27]
	4.2	flowing afterglow	[28]
	4.3 ± 0.9	selected-ion flow tube	[29]
	4.2 ± 0.8	selected-ion flow tube	[30]
$N_2H^+ + C_4H_2 \rightarrow C_4H_3^+ + N_2$	1.1 ± 0.3	selected-ion flow tube	[31]

*) The analysis of the N_2H^+ decay yielded the second rate constants $k = 2.2 \times 10^{-9}$ (CO_2) and 1.7×10^{-9} $cm^3 \cdot molecule^{-1} \cdot s^{-1}$ (N_2O) which are attributed to the proton transfer reaction of N_2H^+ in excited states (45% of the total N_2H^+ reacting).

Kr. In addition to the tabulated rate constant, the rate constants $k = 1.1 \times 10^{-9}$ and 0.27×10^{-9} $cm^3 \cdot molecule^{-1} \cdot s^{-1}$ were obtained in the selected-ion drift tube experiment and were assigned to the proton transfer reactions of N_2H^+ in two vibrationally excited states. This assignment was corroborated by observations of the dependence of the rate constants on the center-of-mass collision energy as well as by observations of the collisional relaxation of N_2H^+ ion by added N_2. (There was no state-selective observation.) The reaction of N_2H^+ in the higher vibrationally excited state was predicted to be exothermic by 27 kJ/mol and the reactions of N_2H^+ in the lower vibrationally excited state and in the ground state were predicted to be endothermic by 12 and 50 kJ/mol, respectively. Activation energies for the ground (44 kJ/mol), lower (19 kJ/mol), and higher excited states (0 kJ/mol) were derived from the dependence of the rate constants on the center-of-mass kinetic energy (0.5 to 3 eV) [13].

Ar. Proton transfer to Ar was observed in a flow-drift tube study [32]. The dependence of the absolute cross sections for the $N_2D^+ + Ar \rightarrow ArD^+ + N_2$ reaction in the forward and reverse directions on the center-of-mass kinetic energy of the colliding particles (0 to 15 eV) was studied using a twin mass spectrometer apparatus [33].

Xe. The proton transfer reaction $N_2H^+ + Xe \rightarrow XeH^+ + N_2$ in the forward and back directions was investigated between 300 to 800 K. The equilibrium constant $K = 58 \pm 8$ at 297

K was measured. The entropy change $\Delta S^\circ_{298} = 24.3 \pm 7.9$ J·mol^{-1}·K^{-1} and the enthalpy change $\Delta H^\circ_{298} = -2.63 \pm 0.79$ kJ/mol were derived from a van't Hoff plot [14]. The Gibb's free energy change $\Delta G^\circ_{298} = -10.0 \pm 0.4$ kJ/mol was obtained [15] from the measured equilibrium constant [14].

O_2. The endothermic proton transfer reaction ($\Delta H = 53$ kJ/mol) between N_2H^+ and O_2 in its electronic ground state (X $^3\Sigma_g^-$) was observed in a flowing afterglow study to be highly inefficient compared to the exothermic transfer ($\Delta H = -43$ kJ/mol) between N_2H^+ and electronically excited O_2 (a $^1\Delta_g$) [3].

N_2. The rate constant $k = 0.3 \times 10^{-9}$ cm^3·molecule^{-1}·s^{-1} for the reaction $N_2H^+ + N_2 \rightarrow N_2H + N_2^+$ was deduced presuming that the collisional relaxation of vibrationally excited N_2H^+ by N_2 proceeds via a proton transfer reaction [13]. For isotope exchange reactions in the $N_2 + N_2H^+$ system, see p. 30.

H_2O. The proton transfer to H_2O was predicted to be exothermic: $\Delta H = -328$ kJ/mol [19], -222 kJ/mol [18]. The rate constant $k = (5.5 \pm 2) \times 10^{-9}$ cm^3·molecule^{-1}·s^{-1} was determined using a hollow cathode discharge technique [34]. The cross sections $\sigma = 1170$ [35], 440 [36], and 410 Å^2 [19] were measured using hollow cathode [35] and corona discharge techniques [19, 36]. The higher value (1170 Å^2) was measured at a lower ion energy (0.3 vs. 0.6 eV) and was suggested to reflect an expected E^{-n} ($n = 0.6$ to 0.8) energy dependence of the cross section [35]. The proton transfer from N_2H^+ to H_2O was suggested to yield the first member of the series of $(H_2O)_nH^+$ ion clusters, formed in corona discharges in air [37].

NH_3. The rate constant, determined using a mass spectrometer ion source technique, decreased slightly with increasing temperature (k(320 K) $= 2.0 \times 10^{-9}$, k(640 K) $= 1.7 \times 10^{-9}$ cm^3·molecule^{-1}·s^{-1}). This effect is attributed to an ion-dipole interaction [11]. $\Delta H = -401$ kJ/mol was reported [1].

CO. This reaction was proposed to be the principal depletion reaction for N_2H^+ in dense interstellar clouds [21].

CO_2. The rate constants $k = 1.05 \times 10^{-9}$ at 150 K [22] and $(0.82 \pm 0.25) \times 10^{-9}$ cm^3·molecule^{-1}·s^{-1} at 700 K [14] were determined using flowing afterglow techniques [14, 22]. An equilibrium constant of $K \geq 4 \times 10^5$ at room temperature was determined [14].

CS. The proton transfer reaction $N_2H^+ + CS \rightarrow HCS^+ + N_2$ is suggested to be one of the reactions responsible for the depletion of N_2H^+ in interstellar dark clouds [38].

HCN. The enthalpy of reaction $\Delta H = -222 \pm 19$ kJ/mol was derived using data available in the literature [7].

CH_3CN. $\Delta H = -289 \pm 12$ kJ/mol [7] and -305 kJ/mol [39] were estimated.

CH_2O. $\Delta H = -218 \pm 8$ kJ/mol was reported [24].

CH_4. The rate constant, determined in a mass spectrometer ion source study, was observed to be independent of temperature between 130 and 650 K [11].

CH_3CHO. The rate constants, determined for the reactions with N_2H^+ and N_2D^+ in a mass spectrometer ion source study, were observed to decrease slightly from $k = 5.8 \times 10^{-9}$ (N_2H^+) and 6.2×10^{-9} (N_2D^+) at 320 K to $k = 4.2 \times 10^{-9}$ cm^3·molecule^{-1}·s^{-1} at 640 K [11].

CH_3OH, CD_3OH. The principle channels for the reaction of CH_3OH with N_2H^+ are proton transfer ($\Delta H \approx -259$ kJ/mol), hydride ion abstraction ($\rightarrow CH_2OH^+ + H_2 + N_2$, $\Delta H = -130$ kJ/mol), and H_2O elimination ($\rightarrow CH_3^+ + H_2O + N_2$, $\Delta H = 9$ kJ/mol). Products from two further feasible channels ($\rightarrow CH_3OH^+ + H + N_2$, $\Delta H = 226$ kJ/mol and $\rightarrow CHO^+ + 2\,H_2 + N_2$, $\Delta H =$

−15 kJ/mol) were not observed. The total rate constant, $k=(1.7\pm0.3)\times10^{-9}$ $cm^3\cdot molecule^{-1}\cdot s^{-1}$, was observed to decrease slightly on progressing from excited to collisionally relaxed N_2H^+ reactant ions. The proton transfer channel accounted for 20% of the products in the reaction of excited N_2H^+ and 80% in the reaction of relaxed N_2H^+. This channnel did not show an isotope effect for the reactions with CH_3OH and CD_3OH [40].

CH_3NO_2. Small branchings of 0.5% into the $N_2H^+ + CH_3NO_2 \rightarrow NO^+ + CH_3OH + N_2$ channel and about 0.01% into $N_2H^+ + CH_3NO_2 \rightarrow CH_3NO^+ + OH + N_2$ were observed in addition to the proton transfer channnel ($\Delta H = -268\pm17$ kJ/mol) [25].

C_2H_2. A reaction enthalpy of −163 kJ/mol was estimated [9].

$C_2H_6(C_2D_6)$. The product distribution from the reaction of N_2H^+ with C_2H_6, obtained using the selected-ion flow tube technique, indicates that 87% of the reactive collisions lead to proton transfer via $N_2H^+ + C_2H_6 \rightarrow [C_2H_7^+] + N_2$, followed by $[C_2H_7^+] \rightarrow C_2H_5^+ + H_2$ [26]. A tandem ion cyclotron resonance mass spectrometer study of the reaction of excited N_2H^+ ions with C_2D_6 revealed no branching into the proton transfer channel to give $C_2D_6H^+$ (branching ratio $\Phi_1=0$), but into the hydride abstraction channel to give $C_2D_5^+$ ($\Phi_2=0.65$) and $C_2D_4H^+$ ($\Phi_3=0.35$). Relaxation of N_2H^+ opens the proton transfer channel ($\Phi_1=0.09$) and effects a decrease in the $C_2D_5^+$ ($\Phi_2=0.40$) and an increase in the $C_2D_4H^+$ ($\Phi_3=0.51$) productions [41].

HC_3N. $\Delta H = -251$ kJ/mol was estimated [29].

References:

[1] Hemsworth, R. S.; Payzant, J. D.; Schiff, H. I.; Bohme, D. K. (Chem. Phys. Lett. **26** [1974] 417/21).
[2] Rakshit, A. B. (Int. J. Mass Spectrom. Ion Phys. **41** [1982] 185/97).
[3] Bohme, D. K. (NATO ASI Ser. B **6** [1975] 489/504; rate constants according to Albritton, D. L., At. Data Nucl. Data Tables **22** [1978] 1/101).
[4] Raouf, A. S. M.; Jones, T. T. C.; Lister, D. G.; Birkinshaw, K.; Twiddy, N. D. (Contrib.-Symp. At. Surf. Phys., Maria Alm, Salzburg, Austria 1982, pp. 218/22; C.A. **94** [1981] No. 37096).
[5] Burt, J. A.; Dunn, J. L.; McEwan, M. J.; Sutton, M. M.; Roche, A. E.; Schiff, H. I. (J. Chem. Phys. **52** [1970] 6062/75).
[6] Stiller, W.; Schmidt, R.; Schuster, R. (Radiat. Phys. Chem. **26** [1985] 571/3).
[7] Mackay, G. I.; Betowski, L. D.; Payzant, J. D.; Schiff, H. I.; Bohme, D. K. (J. Phys. Chem. **80** [1976] 2919/22).
[8] Betowski, D.; Payzant, J. D.; Mackay, G. I.; Bohme, D. K. (Chem. Phys. Lett. **31** [1975] 321/4).
[9] Mackay, G. I.; Tanaka, K.; Bohme, D. K. (Int. J. Mass Spectrom. Ion Phys. **24** [1977] 125/36).
[10] Stiller, W.; Loeser, U.; Scherzer, K. (Z. Phys. Chem. [Munich] **149** [1986] 125/8).

[11] Meot-Ner, M.; Field, F. H. (J. Am. Chem. Soc. **97** [1975] 2014/7).
[12] Prasad, S. S.; Huntress, W. T., Jr. (Astrophys. J. Suppl. Ser. **43** [1980] 1/35).
[13] Villinger, H.; Futrell, J. H.; Saxer, A.; Richter, R.; Lindinger, W. (J. Chem. Phys. **80** [1984] 2543/7).
[14] Fehsenfeld, F. C.; Lindinger, W.; Schiff, H. I.; Hemsworth, R. S.; Bohme, D. K. S. (J. Chem. Phys. **64** [1976] 4887/91).
[15] Bohme, D. K.; Mackay, G. I.; Schiff, H. I. (J. Chem. Phys. **73** [1980] 4976/86).
[16] Schiff, H. I.; Bohme, D. K. (Int. J. Mass Spectrom. Ion Phys. **16** [1975] 167/89).
[17] Bolden, R. C.; Jeffs, S. P.; Twiddy, N. D. (Chem. Phys. Lett. **23** [1973] 73/4).

[18] Bierbaum, V. M.; Kaufman, F. (J. Chem. Phys. **61** [1974] 3804/9).
[19] Shahin, M. (J. Chem. Phys. **47** [1967] 4392/8).
[20] Roche, M.; Sutton, M. M.; Bohme, D. K.; Schiff, H. I. (J. Chem. Phys. **55** [1971] 5480/4).

[21] Herbst, E.; Bohme, D. K.; Payzant, J. D.; Schiff, H. I. (Astrophys. J. **201** [1975] 603/6).
[22] Rakshit, A. B.; Stock, H. M. P.; Wareing, D.; Twiddy, N. D. (J. Phys. B **11** [1978] 4237/47).
[23] Freeman, C. G.; Harland, P. W.; McEwan, M. J. (Austral. J. Chem. **31** [1978] 2157/60).
[24] Tanner, S. D.; Mackay, G. I.; Bohme, D. K. (Can. J. Chem. **57** [1979] 2350/4).
[25] Mackay, G. I.; Bohme, D. K. (Int. J. Mass Spectrom. Ion Phys. **26** [1978] 327/43).
[26] Mackay, G. I.; Schiff, H. I.; Bohme, D. K. (Can. J. Chem. **59** [1981] 1771/8).
[27] Raksit, A. B.; Bohme, D. K. (Int. J. Mass Spectrom. Ion Processes **57** [1984] 211/24).
[28] Freeman, C. G.; Harland, P. W.; McEwan, M. J. (Mon. Not. R. Astron. Soc. **187** [1979] 441/4).
[29] Knight, J. S.; Freeman, C. G.; McEwan, M. J.; Adams, N. G.; Smith, D. (Int. J. Mass Spectrom. Ion Processes **67** [1985] 317/30).
[30] Raksit, A. B.; Bohme, D. K. (Can. J. Chem. **63** [1985] 854/61).

[31] Dheandhanoo, S.; Forte, L.; Fox, A.; Bohme, D. K. (Can. J. Chem. **64** [1986] 641/8).
[32] Jones, T. T. C.; Jones, J. D. C.; Birkinshaw, K.; Twiddy, N. D. (Chem. Phys. Lett. **89** [1982] 443/5).
[33] Malkhasyan, R. T.; Zhurkin, E. S.; Tunitskii, N. N. (Dokl. Akad. Nauk Arm. SSR **59** [1974] 281/5; C.A. **83** [1975] No. 36498).
[34] Howorka, F.; Lindinger, W.; Varney, R. N. (J. Chem. Phys. **61** [1974] 1180/8).
[35] Helm, H.; Howorka, F.; Handle, F.; Egger, F.; Lindinger, W. (J. Phys. B **7** [1974] 170/7).
[36] Shahin, M. M. (Adv. Chem. Ser. **58** [1966] 315/32).
[37] Shahin, M. M. (J. Chem. Phys. **45** [1966] 2600/5).
[38] Swade, D. A. (Astrophys. J. **345** [1989] 828/52).
[39] Gray, G. A. (J. Am. Chem. Soc. **90** [1968] 6002/8).
[40] Smith, R. D.; Futrell, J. H. (J. Phys. Chem. **81** [1977] 195/9).

[41] Smith, R. D.; Futrell, J. H. (Int. J. Mass Spectrom. Ion Phys. **20** [1976] 347/78).

2.2.2.8.6 Association Reactions

Reactions of N_2H^+ with H_2 and with N_2 to form the ion clusters $N_2H^+ \cdot H_2$ and $(N_2)_2H^+$, respectively, were observed to proceed via a three-body association [1 to 4].

The association reaction $N_2H^+ + 2\ H_2 \rightarrow N_2H^+ \cdot H_2 + H_2$ was studied between 44 to 192 K using a selected-ion drift tube technique. The experimental rate constants were fitted to $k = 2.6 \times 10^{-30}\ (100/T)^{2.2 \pm 0.5}\ cm^6 \cdot molecule^{-2} \cdot s^{-1}$ [2]. Pulsed, high-pressure mass spectrometry was used to determine the rate constants at 160 K ($k = 5.5 \times 10^{-30}\ cm^6 \cdot molecule^{-2} \cdot s^{-1}$) and 300 K ($k = 0.33 \times 10^{-30}\ cm^6 \cdot molecule^{-2} \cdot s^{-1}$) [1].

Formation of the $(N_2)_2H^+$ cluster ion in the association reaction $N_2H^+ + N_2 + H_2 \rightarrow (N_2)_2H^+ + H_2$ in H_2-N_2 mixtures at about 4 Torr (N_2 about 0.1 Torr) was studied using pulsed, high-pressure mass spectrometry. The rate constants at 270 K ($k = 113 \times 10^{-30}\ cm^6 \cdot molecule^{-2} \cdot s^{-1}$) and at 325 K ($k = 5.6 \times 10^{-30}\ cm^6 \cdot molecule^{-2} \cdot s^{-1}$) were determined. From 160 K up to room temperature, the reaction was found to proceed via an $N_2H^+ \cdot H_2$ intermediate [1]. In a similar study, the rate constant $k = 5.4 \times 10^{-30}\ cm^6 \cdot molecule^{-2} \cdot s^{-1}$ at 328 K for the reaction $N_2H^+ + 2\ N_2 \rightarrow (N_2)_2H^+ + N_2$ was determined [3]. In a selected-ion flow tube study, the rate constant $k = 28 \times 10^{-30}\ cm^6 \cdot molecule^{-2} \cdot s^{-1}$ at 80 K for the reaction $N_2H^+ + N_2 + He \rightarrow (N_2)_2H^+ + He$ was obtained [4].

Thermochemical data ($\Delta H°$ and $\Delta G°$ in kJ/mol, ΔS in $J \cdot mol^{-1} \cdot K^{-1}$) were derived from pulsed, high-pressure mass spectrometric studies of the association reactions $N_2H^+ + X_2$ where $X = H_2$ or N_2:

X_2	cluster	$-\Delta H°_{298}$	$-\Delta S_{298}$	$-\Delta G°_{298}$	comment	Ref.
H_2	$N_2H^+ \cdot H_2$	30.1	94.6	1.7	1 to 6 Torr H_2 with trace N_2 229, 281, and 303 K	[5]
N_2	$(N_2)_2H^+$	60.7	85.4	35.1	~1 to 4 Torr N_2 with 10% H_2 474 to 571 K	[3]
N_2	$(N_2)_2H^+$	66.9	100	36.8	4 Torr H_2 with 3 to 300 mTorr N_2 340 to 450 K	[6]

Ab initio techniques were used to predict the $N_2H^+ \cdot H_2$ [7, 8] and $(N_2)_2H^+$ [9, 10] stabilization energies, which correspond to the enthalpy of the $N_2H^+ + H_2$ and $N_2H^+ + N_2$ association reactions. The potential energy curve for the approach of H_2 to the protonated end of N_2H^+ was calculated at the CI-SDQ level. The well depth, excluding zero-point corrections, was found to be 28.5 kJ/mol at R = 1.53 Å, where R is the internuclear distance between N_2H^+ and H_2. The interaction at the nitrogen end produces a very shallow well depth of about 2.9 kJ/mol [8].

The radiative association $N_2H^+ + H_2 \rightarrow N_2H^+ \cdot H_2 + h\nu$ was estimated to proceed with a rate constant of the order of 10^{-17} $cm^3 \cdot molecule^{-1} \cdot s^{-1}$ at temperatures around 20 to 70 K (this estimate is based on the rate constant for the three-body association $N_2H^+ + 2\,H_2$) [2].

References:

[1] Blades, A. T.; Kebarle, P. (J. Chem. Phys. **78** [1983] 783/9).
[2] Bohringer, H.; Arnold, F. (NATO ASI Ser. C **157** [1985] 639/47).
[3] Meot-Ner, M.; Field, F. H. (J. Chem. Phys. **61** [1974] 3742/9).
[4] Adams, N. G.; Smith, D.; Alge, E. (J. Chem. Phys. **81** [1984] 1778/84).
[5] Hiraoka, K. (Bull. Chem. Soc. Jpn. **52** [1979] 1578/82).
[6] Hiraoka, K.; Saluja, P. P. S.; Kebarle, P. (Can. J. Chem. **57** [1979] 2159/66).
[7] Hirao, K.; Yamabe, S. (Chem. Phys. Lett. **79** [1981] 279/83).
[8] Kraemer, W. P.; Komornicki, A.; Dixon, D. A. (Chem. Phys. **105** [1986] 87/96).
[9] Yamabe, S.; Hirao, K. (J. Am. Chem. Soc. **103** [1981] 2176/9).
[10] Ikuta, S. (Chem. Phys. Lett. **77** [1981] 369/72).

2.2.2.8.7 Protonation

$N_2H^+ + H^+$. The minimum energy reaction path for the protonation of N_2H^+ ($H^+ + N_2H^+ \rightarrow HN_2H^{2+}$) was calculated using an ab initio SCF method. An energy barrier of 371.5 kJ/mol for the protonation of N_2H^+ was predicted.

Reference:

Summers, N. L.; Tyrrell, J. (Theor. Chim. Acta **47** [1978] 223/31).

2.2.3 Adducts of N_2H^+, $N_2H^+ \cdot H_2$ and $N_2H^+ \cdot n\,NH_3$

$N_2H^+ \cdot H_2$

CAS Registry Number: *[71691-32-2]*

The formation of this adduct is described in Section 2.2.2.8.6.

$N_2H^+ \cdot n\,NH_3$

The ion intensity of the adduct $N_2H^+ \cdot n\,NH_3$ with $n = 1$ to 4 was found to be low relative to the main product $NH_4^+ \cdot n\,NH_3$ in high-pressure mass spectrometry of NH_3 at $p \geq 0.04$ Torr and disappeared at 1 Torr.

Reference:

Long, J. W.; Franklin, J. L. (Int. J. Mass Spectrom. Ion Phys. **12** [1973] 403/10).

2.2.4 The Diazenyl Anion, N_2H^-

Systematic name: Diazenide

CAS Registry Number: *[71004-29-0]*

There is apparently no evidence that this anion exists.

An enthalpy of formation (-173 kJ/mol) for the anion with C_s symmetry with an NNH angle of 114.1° and the N_2 bond distance lengthened by 0.079 Å was calculated using a semiempirical (MNDO) method to study the interaction of molecular nitrogen with the hydride ion [1]. An optimum structure with C_s symmetry with an angle of 113°, $r(NN) = 1.24$ Å and $r(NH) = 1.09$ Å was obtained using an ab initio (SCF 4-31G) method. A reaction enthalpy of 306 kJ/mol for the hydride transfer from CH_3O^- to N_2 via $CH_3O^- + N_2 \rightarrow H_2CO + N_2H^-$ was calculated with the same method [2].

References:

[1] Chadha, R.; Ray, N. K. (Theor. Chim. Acta **60** [1982] 579/87).
[2] Sheldon, J. C.; Currie, G. J.; Lahnstein, J.; Hayes, R. N.; Bowie, J. H. (Nouv. J. Chim. **9** [1985] 205/9).

2.2.5 Diazene, N_2H_2

Other names: Diimide, diimine, diamide

CAS Registry Numbers: N_2H_2 *[3618-05-1]*, *trans*-N_2H_2 *[15626-43-4]*, *cis*-N_2H_2 *[15626-42-3]*, N_2D_2 *[14989-24-3]*, *trans*-N_2D_2 *[40712-39-8]*, *cis*-N_2D_2 *[66511-78-2]*, N_2HD *[14989-15-2]*, *trans*-N_2HD *[40712-38-7]*, N_2T_2 *[24525-35-7]*

General References:

Back, R. A.; The Preparation, Properties and Reactions of Diimide, Rev. Chem. Intermed. **5** [1984] 293/323.

Abdul Hai, S. M.; Qureshi, A. W.; Begum, A.; Diimide. Novel Intermediate, Pak. J. Sci. Ind. Res. **17** [1974] 76/81.

Willis, C.; Back, R. A.; Di-imide. Some Physical and Chemical Properties and the Kinetics and Stoichiometry of the Gas-phase Decomposition, Can. J. Chem. **51** [1973] 3605/19.

Sellmann, D.; Diimin und seine Derivate, Chem. Unserer Zeit **7** [1973] 163/70.
Hünig, S.; Müller, H. R.; Thier, W.; Zur Chemie des Diimins, Angew. Chem. **77** [1965] 368/77.
Pasto, D. J.; Reduction with Diimide, Org. React. [N.Y.] **40** [1991] 92/155.
Stedman, G.; Reaction Mechanisms of Inorganic Nitrogen Compounds, Adv. Inorg. Chem. Radiochem. **22** [1979] 113/70,121.
Miller, C. E.; Hydrogenation with Diimide, J. Chem. Educ. **42** [1965] 254/9.

At normal conditions diazene is a moderately stable, yellow compound with a lifetime of several minutes. Inconsistencies between the results of early work (see "Stickstoff" 2, 1935, p. 306) had led to the assumption that it may exist as an intermediate. It was first detected in 1958 when the products of a discharge through hydrazine were analyzed in a mass spectrometer. Aside of generating it by electrical decomposition of hydrazine, N_2H_2 can also be prepared by thermal decomposition of several tosylhydrazides. The planar molecule can form a trans and a cis isomer, but only *trans*-N_2H_2 has unambiguously been identified so far. The third structural isomer, 1,1-diazene, is discussed in Chapter 2.2.9, p. 67. N_2H_2 is used as a reagent for stereospecific hydrogenations. It can be stabilized as ligand in transition metal complexes.

2.2.5.1 Preparation. Formation

Preparation and Formation in the Gas Phase

Pure diazene is readily obtained by thermolysis of alkali metal tosylhydrazides in high vacuum (pressure $<10^{-4}$ Torr) via

$$CH_3C_6H_4SO_2(M)NNH_2 \rightarrow N_2H_2 + CH_3C_6H_4SO_2M \ (M = Li, Na, K)$$

The reaction is clean and, because both hydrazide and the metal tosylate by-product are nonvolatile, yields N_2H_2 vapor contaminated with variable amounts of N_2H_4, N_2, and some NH_3, HN_3, and H_2. The portion of N_2H_2 increases from 60 to 90% on going from lithium to potassium, and the optimum thermolysis temperatures are 353, 333, and 318 K for the three tosylhydrazides, respectively. Fractional condensation of the gas mixture in 10 m-long tubings yields brilliant yellow, solid N_2H_2 which can be isolated at 77 K; if the pressure does not exceed 10^{-4} Torr, about 1/10 mmol N_2H_2 per hour are condensed. Owing to possible photolytic dissociation of solid N_2H_2, visible and UV light must be excluded. Solid N_2H_2 collected at 77 K decomposes upon warming, before a vapor pressure of more than a few mTorr is attained [1, 2]. However, rapid warming of the condensate generates N_2H_2 pressures of a few Torr despite some decomposition [3]. Raising the thermolysis temperature to about 370 K and using faster pumping increases the ratio N_2H_2 to N_2 severalfold [5]. In the earliest studies on the decomposition of alkali metal tosylhydrazides, two constitutional isomers were thought to form depending on the alkali metal: Li, Na, K, and altered Cs tosylhydrazides give mainly yellow HN=NH (diazene), while fresh Cs tosylhydrazide gives colorless H_2N=N (1,1-diazene) (see Chapter 2.2.9, p. 67). Rb tosylhydrazide yields a mixture of diazene and 1,1-diazene. Diazene has two geometric isomers, *cis*- and *trans*-diazene. It was reported that Li, Na, and K tosylhydrazides yield mainly the cis isomer which isomerizes to *trans*-N_2H_2 during passage through a coil condenser. At lower (higher) temperatures one obtains mainly *cis*-diazene (*trans*-diazene). These conclusions for the formation of *cis*-N_2H_2 and H_2N=N, drawn from changes in the IR and mass spectra [6 to 8], were questioned by Back [4], who established on the basis of all evidences available up to 1982 that the detection and isolation of these species have to be regarded unproven.

The decomposition of N_2H_4, HN_3, or an N_2-H_2 mixture in a microwave discharge and trapping the reaction mixture at 77 K yields *trans*-N_2H_2, but it can not be separated from simultaneously in a tenfold excess formed NH_3 (aside of N_2 and H_2 and small amounts of nitrogen hydrides) [9 to 11]. By varying the hydrazine flow rate and the discharge power it is possible to increase the percentage of N_2H_2 from <1 to 20%. The optimal N_2H_2 to NH_3 ratio is obtained at a fairly high N_2H_2 flow rate and a weak discharge power [12, 13]. Trapping of N_2H_2 and NH_3 at 77 K from the discharge gas and subsequent sudden warming yield a gas mixture which contains typically about 15% N_2H_2, estimated from the gases evolved by decomposition. In this way as much as 0.5 g N_2H_2 were collected and after vaporization partial pressures of 100 Torr were attained. On the other hand, ammonia seems to have a stabilizing effect on diazene either as a diluent or by complex formation at low temperatures [14, 15]. Later, it was reported that NH_3 can be precipitated as NH_4Cl by titrating the gas phase products with HCl after condensing them in a trap at 195 K [5]. In contrast to earlier investigations, e.g. [10], and following a suggestion by Mock [16], N_2H_2 has a lifetime of several minutes at room temperature in the gas phase [14, 15].

N_2H_2 formation was observed in the gas phase during decomposition of N_2H_4 and NH_3 on a Rh surface in the temperature range 180 to 500 K [17].

N_2H_2 can also be generated by reacting oxygen atoms with N_2H_4 [18, 19], by decomposing anthracene-9,10-biimine at 373 K [20], and by thermolysis of triazanium sulfate [21].

Formation in situ in Solution

N_2H_2 formed in situ in solution is generally used as a reducing agent for unsaturated compounds. There are four general methods for generating it in situ: oxidation of hydrazine, decarboxylation of azodicarboxylates, dissociation of the diazene – anthracene adduct, and elimination of HX from an acid hydrazide. N_2H_2 has never been detected directly and it can not be decided unambiguously whether the cis or trans isomer is mainly formed. The stereospecific hydration of the multiple bonds and the formation of the self-reduction products N_2 and N_2H_4 serve as proof for the intermediate formation of *cis*-N_2H_2 [4, 22].

Hydrazine is typically oxidized with oxygen, air, or hydrogen peroxide in basic media with or without a catalytic amount of copper(II) ions [23 to 28]. Other oxidants used are mercuric oxide [24], iron(III) cyanide [24, 29], iodine [30], iodate [26], dichromate [26], or selenium [31].

The decarboxylation of azodicarboxylates, e.g. KOOCN=NCOOK, (dating back to earlier assumptions [32, 33]) is carried out in acid media, normally in acetic acid, and it is probably the most useful source of N_2H_2 formed in situ [16, 23, 24, 34 to 36]. A similar reagent which yields N_2H_2 is 1,1′-dihydroxyazocyclohexane [16, 37].

The thermal decomposition of anthracene-9,10-biimine at 353 K is a straightforward way to get N_2H_2 [16, 20]. The similar 1,4 Diels-Alder adduct with cyclopentadiene may be a precursor of N_2H_2 [38]. 1-amino-2,2-diphenylaziridine decomposes at room temperature to give N_2H_2, perhaps as a result of an internal rearrangement of the primarily formed aminonitrene [39].

The elimination of HX from an acid hydrazide via $H_2N\text{-}NHX \rightarrow N_2H_2 + HX$ is a thermal or base-catalyzed reaction [24, 40 to 44]. Tosylhydrazide groups bonded to polymers also yield N_2H_2 [45]. The base-catalyzed dissociations of chloroacetylhydrazine hydrochloride, $ClCH_2CONHNH_2 \cdot HCl + 2\ NaOH \rightarrow N_2H_2 + 2\ NaCl + 2\ H_2O + CH_2CO$ [46], of hydroxylamine-O-sulfonic acid, $2\ NH_2OSO_3H \rightarrow N_2H_2 + 2\ H_2SO_4$ [47 to 50], and of chloramine, $2\ NH_2Cl \rightarrow N_2H_2 + 2\ HCl$ [47, 48], may proceed similarly.

Formation as Intermediate

N_2H_2 is thought to be involved in many reactions as an intermediate. The most important reactions are listed below together with selected references.

Reduction of N_2 to NH_3. A great variety of metallic and organometallic complexes with N_2H_2 were prepared by reduction of the corresponding N_2 complexes (or by oxidation of the corresponding N_2H_4 complexes); compare, e.g., the pentacarbonyl complexes discussed in [51, 52] or the iron complex discussed in [53]. In the biological nitrogen fixation process, N_2 complexed with Mo is stepwise reduced to NH_3, whereby N_2H_2 seems to play a key role in the only partly understood reaction. For general information, see the following reviews [54 to 60]. N_2H_2 also forms intermediately during the reduction of N_2 with $V(OH)_2$ in $Mg(OH)_2$ or $ZrO_2 \cdot H_2O$ matrices [61], catalytic reduction with $TiCl_4$ or Li naphthalide [62], or photoreduction in the presence of 2,5-dihydrofuran and undoped or metal-doped (M = Pd, Pt, Zn) CdS powder [63].

N_2H_2 forms intermediately during the **reduction of HN_3 (N_3^-) to NH_3**, for example catalytically with $[Fe_4S_4L_4]^{2-}$, $[Mo_2Fe_6S_8L_9]^{3-}$ ($L = SCH_2CH_2OH$), or $[Fe_4S_4(SC_6H_5)_4]^{2-}$ [64] and photolytically in an N_2 matrix [65], in an Ar, N_2, or CO matrix [66], or in aqueous solution [67]. The photochemically, thermally, or electrical-discharge-induced **decomposition of HN_3** in the gas phase proceeds probably via intermediate NH radical and N_2H_2 formation [68].

The oxidation of N_2H_4 by $NaIO_4$ in an aqueous CH_3SO-$CuSO_4$-CH_3COOH mixture [69], by Tl^{III} as a two-electron-transfer agent in aqueous solution, by the OH radical as a one-electron-transfer agent [70], by CCl_4 [71] probably proceeds via N_2H_2 as does the electrooxidation on a Pt electrode in CH_3CN [72] or a $[NiFe(CN)_6]^{2-/-}$-derivatized Ni electrode [73]. Intermediate formation of N_2H_2 was also found to occur at low pressures during the thermal [74 to 76] and photochemically induced [77, 78] **decomposition of N_2H_4** in the gas phase.

Decomposition of NH_3. Photodecomposition by $Hg(6^3P_1)$ atoms [79] and decomposition by ionizing radiation (100 eV) [80] give N_2H_2 via intermediately formed N_2H_4. Irradiation of NH_3-CO_2 mixtures with He^+ at 30 keV at 77 K led to a rich variety of compounds, among which N_2H_2 could be identified [81]. N_2H_2 was detected in the front region of a NH_3 flame by measuring the NH_3 decay via laser absorption [82]. Solidified NH_3-H_2O mixtures released, besides N_2H_4 and NH_2OH, diazene when irradiating the surface with a 193-nm laser [83].

Intermediate formation of N_2H_2 was also found during a study of the flash photolysis of HNCO [84] and of the reaction of bis(trimethylsilyl)diazene with H_2SO_4 or HCl [85].

Preparation of Deuterated Diazenes

N_2HD and N_2D_2 can be prepared analogously to N_2H_2 by thermal decomposition of N,N′-deuterotosylhydrazines [1, 86] and by the hydrazine discharge method; see e.g. [87].

References:

[1] Wiberg, N.; Bachhuber, H.; Fischer, G. (Angew. Chem. **84** [1972] 889/90; Angew. Chem. Int. Ed. Engl. **11** [1972] 829/30).

[2] Wiberg, N.; Fischer, G.; Bachhuber, H. (Chem. Ber. **107** [1974] 1456/71).

[3] Back, R. A.; Neudorfl, P. (unpublished results, cited as ref. 72 in [4]).

[4] Back, R. A. (Rev. Chem. Intermed. **5** [1984] 293/323).

[5] Frost, D. C.; Lee, S. T.; McDowell, C. A.; Westwood, N. P. C. (J. Chem. Phys. **64** [1976] 4719/29).

[6] Wiberg, N.; Fischer, G.; Bachhuber, H. (Angew. Chem. **89** [1977] 828/9; Angew. Chem. Int. Ed. Engl. **16** [1977] 780).
[7] Wiberg, N.; Fischer, G.; Bachhuber, H. (Angew. Chem. **88** [1976] 386/7; Angew. Chem. Int. Ed. Engl. **15** [1976] 385).
[8] Wiberg, N.; Fischer, G.; Bachhuber, H. (Z. Naturforsch. **34b** [1979] 1385/90).
[9] Foner, S. N.; Hudson, R. L. (J. Chem. Phys. **29** [1958] 442/3).
[10] Foner, S. N.; Hudson, R. L. (J. Chem. Phys. **28** [1958] 719/20).

[11] Foner, S. N.; Hudson, R. L. (Adv. Chem. Ser. No. 36 [1962] 34/49).
[12] Blau, E. J.; Hochheimer, B. F.; Unger, H. J. (J. Chem. Phys. **34** [1961] 1060/1).
[13] Blau, E. J.; Hochheimer, B. F. (J. Chem. Phys. **41** [1964] 1174/82).
[14] Willis, C.; Back, R. A. (Can. J. Chem. **51** [1973] 3605/19).
[15] Willis, C.; Back, R. A. (Nature **241** [1973] 43).
[16] Mock, W. L. (Diss. Harvard Univ. 1965, pp. 1/176, 1/68; Diss. Abstr. **26** [1965/66] 6374).
[17] Prasad, J.; Gland, J. L. (J. Am. Chem. Soc. **113** [1991] 1577/9).
[18] Foner, S. N.; Hudson, R. L. (J. Chem. Phys. **49** [1968] 3724/5).
[19] Foner, S. N.; Hudson, R. L. (J. Chem. Phys. **53** [1970] 4377/86).
[20] Corey, E. J.; Mock, W. L. (J. Am. Chem. Soc. **84** [1961] 685/6).

[21] Wiberg, N.; Wanninger, P. (unpublished results, cited as ref. 4 in [7]).
[22] Hünig, S.; Müller, H. R.; Thier, W. (Angew. Chem. **77** [1965] 368/77; Angew. Chem. Int. Ed. Engl. **4** [1965] 271).
[23] Corey, E. J.; Mock, W. L.; Pasto, D. J. (Tetrahedron Lett. **1961** 347/52).
[24] Hünig, S.; Müller, H. R.; Thier, W. (Tetrahedron Lett. **1961** 353/7).
[25] Nagendrappa, G.; Moorthy, S. N.; Devaprabhakara, D. (Indian J. Chem. B **14** [1976] 81/3).
[26] Aylward, F.; Sawistowska, M. (Chem. Ind. [London] **1962** 484/91).
[27] Aylward, F.; Sawistowska, M. (J. Chem. Soc. **1964** 1435/41).
[28] Corey, E. J.; Pasto, D. J.; Mock, W. L. (J. Am. Chem. Soc. **83** [1961] 2957/8).
[29] Hünig, S.; Müller, H. R. (Angew. Chem. **74** [1962] 215/6; Angew. Chem. Int. Ed. Engl. **1** [1962] 213).
[30] Nozaki, H.; Simokawa, Y.; Mori, T.; Noyori, R. (Can. J. Chem. **44** [1966] 2921/5).

[31] Kondo, K.; Murai, S.; Sonoda, N. (Tetrahedron Lett. **1977** 3727/30).
[32] Thiele, J. (Liebigs Ann. Chem. **271** [1892] 127/36).
[33] King, C. V. (J. Am. Chem. Soc. **62** [1940] 379/85).
[34] van Tamelen, E. E.; Dewey, R. S.; Timmons, R. J. (J. Am. Chem. Soc. **83** [1961] 3725/6).
[35] Hamersma, J. W.; Snyder, E. I. (J. Org. Chem. **30** [1965] 3985/8).
[36] Stanbury, D. M. (Inorg. Chem. **30** [1991] 1293/6).
[37] Schmitz, E.; Ohme, R.; Schram, S. (Angew. Chem. **75** [1963] 208; Angew. Chem. Int. Ed. Engl. **2** [1963] 157).
[38] Cohen, S. G.; Zand, R.; Seel, C. (J. Am. Chem. Soc. **83** [1961] 2895/900).
[39] Annunziata, R.; Fornasier, R.; Monanari, F. (J. Org. Chem. **39** [1974] 3195/7).
[40] Hünig, S.; Müller, H. R.; Thier, W. (Angew. Chem. **75** [1963] 298; Angew. Chem. Int. Ed. Engl. **2** [1963] 214/5).

[41] Dewey, R. S.; van Tamelen, E. E. (J. Am. Chem. Soc. **83** [1961] 3729).
[42] Smushkevich, Y. I.; Usorov, M. I.; Surorov, N. N. (Zh. Org. Khim. **13** [1977] 893; J. Org. Chem. [USSR] **13** [1977] 816/7).
[43] Steinmetz, W. E.; Robinson, D. H.; Ackermann, M. N. (Inorg. Chem. **14** [1975] 421/5).
[44] Cusack, N. J.; Reese, C. B.; Risius, A. C.; Roozpeikar, B. (Tetrahedron **32** [1976] 2157/62).
[45] Gavina, F.; Gil, P.; Palazon, B. (Tetrahedron Lett. **1979** 1333/6).

[46] Buyle, R.; van Overstraeten, A.; Eloy, F. (Chem. Ind. [London] **1964** 839).
[47] Schmitz, E.; Ohme, R. (Angew. Chem. **73** [1961] 807).
[48] Schmitz, E.; Ohme, R.; Kozakiewicz, G. (Z. Anorg. Allg. Chem. **339** [1965] 44/51).
[49] Appel, R.; Büchner, W. (Angew. Chem. **73** [1961] 807).
[50] Appel, R.; Büchner, W. (Liebigs Ann. Chem. **654** [1962] 1/8).

[51] Sellmann, D.; Brandl, A.; Endell, R. (Z. Naturforsch. **33b** [1978] 542/53).
[52] Wuerminghausen, T.; Sellmann, D. (J. Organomet. Chem. **199** [1980] 77/85).
[53] Sellmann, D.; Soglowek, W.; Knoch, F.; Moll, M. (Angew. Chem. **101** [1989] 1244/5; Angew. Chem. Int. Ed. Engl. **28** [1989] 1271).
[54] Sellmann, D. (Chem. Unserer Zeit **7** [1973] 163/70).
[55] Chatt, J.; Dilworth, J. R.; Richards, R. L. (Chem. Rev. **78** [1978] 589/625).
[56] Skinner, K. J. (Chem. Eng. News **1976** 22/35).
[57] Henderson, R. A.; Leigh, G. J.; Pickett, C. J. (Adv. Inorg. Chem. Radiochem. **27** [1983] 197/292).
[58] Pratt, J. M. (Inorg. Perspect. Biol. Med. **2** [1979] 357/68).
[59] Leigh, G. J. (in: Newton, W.; Postgate, J. R.; Rodrigue-Barrueco, C.; Recent Developments in Nitrogen Fixation, Academic, London 1977, pp. 1/24).
[60] Sellmann, D. (in: Newton, W.; Postgate, J. R.; Rodrigue-Barrueco, C.; Recent Developments in Nitrogen Fixation, Academic, London 1977, pp. 53/67).

[61] Schrauzer, G. N.; Strampach, N.; Hughes, L. A. (Inorg. Chem. **21** [1982] 2184/8).
[62] Rummel, S. (Z. Chem. **16** [1976] 288/9).
[63] Hetterich, W.; Kisch, H. (Chem. Ber. **122** [1989] 621/7).
[64] Imasaka, Y.; Tanaka, K.; Tanaka, T. (Chem. Lett. **1983** 1477/80).
[65] van Thiel, M.; Pimentel, G. C. (J. Chem. Phys. **32** [1960] 133/40).
[66] Milligan, D. E.; Jacox, M. E. (J. Chem. Phys. **41** [1964] 2838/41).
[67] Burak, I.; Treinin, A. (J. Am. Chem. Soc. **87** [1965] 4031/6).
[68] Rice, F. O.; Grelecki, C. (J. Am. Chem. Soc. **79** [1957] 1880/1).
[69] Hoffman, J. M., Jr.; Schlessinger, R. H. (J. Chem. Soc. D **1971** 1245/6).
[70] Higginson, W. C. E.; Sutton, D.; Wright, P. (J. Chem. Soc. **1953** 1380/6).

[71] Wolinsky, J.; Schultz, T. (J. Org. Chem. **30** [1965] 3980/1).
[72] Jannakoudakis, A. D.; Kokkinidis, G. (J. Electroanal. Chem. Interfacial Electrochem. **134** [1982] 311/24).
[73] Lin, C.; Bocarsly, A. B. (J. Electroanal. Chem. Interfacial Electrochem. **300** [1991] 325/45).
[74] Diesen, R. W. (J. Chem. Phys. **39** [1963] 2121/8).
[75] Homann, K. H.; MacLean, D. I.; Wagner, H. G. (Naturwissenschaften **52** [1965] 12).
[76] Willhoft, E. M. A.; Robertson, A. J. B. (Chem. Commun. **1967** 385/7).
[77] Stief, L. J.; DeCarlo, V. J. (J. Chem. Phys. **44** [1966] 4638/9).
[78] Arvis, M.; Gillois, M.; Curtat, M. (J. Phys. Chem. **78** [1974] 1356/60).
[79] McDonald, C. C.; Gunning, H. E. (J. Chem. Phys. **23** [1955] 532/41).
[80] Melton, C. E. (J. Chem. Phys. **45** [1966] 4414/24).

[81] Benit, J.; Bibring, J.-P.; Rocard, F. (NATO ASI Ser. E No. 155 [1989] 123/38).
[82] Dean, A. M.; Chou, M. S.; Stern, D. (Int. J. Chem. Kinet. **16** [1984] 633/53).
[83] Nishi, N.; Shinohara, H.; Okuyama, T. (J. Chem. Phys. **80** [1984] 3898/910).
[84] Back, R. A. (J. Chem. Phys. **40** [1964] 3493/6).
[85] Wiberg, N.; Haering, H. W.; Vasisht, S. K. (Z. Naturforsch. **34b** [1979] 356/7).
[86] Holzmann, G.; Minkwitz, R. (Z. Anorg. Allg. Chem. **413** [1975] 72/6).
[87] Bondybey, V. E.; Nibler, J. W. (J. Chem. Phys. **58** [1973] 2125/34).

2.2.5.2 Molecular Properties and Spectra

The isomer *trans*-N_2H_2 has been detected and identified experimentally, specifically through its IR and UV spectra in the gas phase. The existence of the cis isomer has been sometimes suggested, but it could not be unambiguously identified. The cis isomer is regarded to be a transient intermediate in many reactions.

2.2.5.2.1 Electron Configurations. Ionization Potentials

The diazene molecule has a planar, bent, ground-state structure which was already predicted from the number of the valence electrons by Walsh [1] and later confirmed by experimental and theoretical studies. Two configurational isomers, *trans*-N_2H_2 and *cis*-N_2H_2, with C_{2h} and C_{2v} symmetry are possible. MO calculations gave the following electron configurations:

trans-N_2H_2 [2 to 4]: $(1a_g)^2\ (1b_u)^2\ (2a_g)^2\ (2b_u)^2\ (3a_g)^2\ (3b_u)^2\ (1a_u)^2\ (4a_g)^2\ 1b_g\ 4b_u,\ ^1A_g$
cis-N_2H_2 [2, 3]: $(1a_1)^2\ (1b_2)^2\ (2a_1)^2\ (2b_2)^2\ (3a_1)^2\ (1b_1)^2\ (4a_1)^2\ (3b_2)^2\ 1a_2\ 5a_1,\ ^1A_1$

With respect to the three highest occupied orbitals, the electronic structure of both molecules is quite different as shown by the ordering of the orbitals and their approximate chemical description: For *trans*-N_2H_2 (*cis*-N_2H_2) the $4a_g(4a_1)$ and $3b_u(3b_2)$ MOs are symmetric (n_+) and antisymmetric (n_-) combinations of the nitrogen lone pairs. The $1a_u(1b_1)$ orbital is the NN π-bonding orbital. The MOs $3a_g(3a_1)$ and $2b_u(2b_2)$ are symmetric and antisymmetric combinations of the NH σ bonds, while $2a_g(2a_1)$ describes the NN σ bond [2, 3].

For excited states, see p. 55.

The following ionization potentials were obtained for *trans*-N_2H_2 and *trans*-N_2D_2 from the He I photoelectron spectrum and assigned to molecular orbitals by analyzing the observed vibrational structures and by comparing them with other N=N compounds and theoretical calculations [5, 6]:

trans-N_2H_2:	E_i(vertical) in eV*⁾	10.02	14.39	15.03	16.9
	E_i(adiabatic) in eV*⁾	9.59	14.10	14.71	16.19
trans-N_2D_2:	E_i(vertical) in eV*⁾	10.10	14.39	15.05	–
	E_i(adiabatic) in eV*⁾	9.61	14.11	14.69	–
	orbital assignment	$4a_g(n_+)$	$1a_u(\pi)$	$3b_u(n_-)$	$3a_g(\sigma)$

*⁾ Uncertainties are ±0.01 eV on the first three E_i's.

The adiabatic ionization potential of 9.589±0.007 eV, determined by photoionization mass spectrometry [7], is in excellent agreement with one obtained by photoelectron spectroscopy (see above). Other values for the first ionization potential obtained from various electron impact experiments range from about 9.6 to 9.9 eV [8 to 14], with the most recent measurements giving 9.8±0.05 [11] and 9.65±0.08 eV [8]. A value of 9.62 eV was derived from two Rydberg transitions in the UV absorption spectrum (see p. 54) [15].

For *cis*-N_2H_2, only calculated ionization energies are known. Quoted here are the results of a many-body Green's function calculation: 9.94($3b_2$), 13.52($4a_1$), 14.14($1b_1$), 18.90($3a_1$), and 22.67($2b_2$) eV. The corresponding values calculated for *trans*-N_2H_2 are reproduced in the correct order and are within 0.3 eV of the measured values [3]. A similar calculation yielding comparable results was reported earlier [2].

Other ab initio and semiempirical SCF MO calculations of the ionization energies of *trans*-N_2H_2 and partly also of *cis*-N_2H_2 are available at different levels of theory [16 to 23].

References:

[1] Walsh, A. D. (J. Chem. Soc. **1953** 2288/960).

[2] Von Niessen, W.; Domcke, W.; Cederbaum, L. S.; Kraemer, W. P. (J. Chem. Phys. **67** [1977] 44/51).

[3] Galasso, V. (Chem. Phys. **83** [1984] 407/13).

[4] Winter, N. W.; Pitzer, R. M. (J. Chem. Phys. **62** [1975] 1269/75).

[5] Frost, D. C.; Lee, S. T.; McDowell, C. A.; Westwood, N. P. C. (J. Chem. Phys. **64** [1976] 4719/29).

[6] Frost, D. C.; Lee, S. T.; McDowell, C. A.; Westwood, N. P. C. (Chem. Phys. Lett. **30** [1975] 26/7).

[7] Ruscic, B.; Berkowitz, J. (J. Chem. Phys. **95** [1991] 4378/84).

[8] Foner, S. N.; Hudson, R. L. (J. Chem. Phys. **68** [1978] 3162/8).

[9] Foner, S. N.; Hudson, R. L. (J. Chem. Phys. **29** [1958] 442/3).

[10] Foner, S. N.; Hudson, R. L. (J. Chem. Phys. **28** [1958] 719/20).

[11] Wiberg, N.; Fischer, G.; Bachhuber, H. (Z. Naturforsch. **34b** [1979] 1385/90).

[12] Wiberg, N.; Bachhuber, H.; Fischer, G. (Angew. Chem. **84** [1972] 889/90; Angew. Chem. Int. Ed. Engl. **11** [1972] 829/30).

[13] Holzmann, G.; Minkwitz, R. (Z. Anorg. Allg. Chem. **413** [1975] 72/6).

[14] Willis, C.; Lossing, F. P.; Back, R. A. (Can. J. Chem. **54** [1976] 1/3).

[15] Neudorfl, P. S.; Back, R. A.; Douglas, A. E. (Can. J. Chem. **59** [1981] 506/17).

[16] Pople, J. A.; Curtiss, L. A. (J. Chem. Phys. **95** [1991] 4385/8).

[17] Casida, M. E.; Chong, D. P. (Phys. Rev. [3] A **40** [1989] 4837/48).

[18] Baird, N. C.; Wernette, D. A. (Can. J. Chem. **55** [1977] 350/4).

[19] Chong, D. P.; Herring, F. G.; McWilliams, D. (J. Electron Spectrosc. Relat. Phenom. **7** [1975] 445/55).

[20] Frost, D. C.; Lau, W. M.; McDowell, C. A.; Westwood, N. P. C. (J. Mol. Struct. **40** [1982] 283/95 [THEOCHEM **7**]).

[21] Decleva, P.; Lisini, A. (Chem. Phys. **106** [1986] 39/49).

[22] Decleva, P.; Lisini, A. (Chem. Phys. **97** [1985] 95/102).

[23] De Alti, G.; Decleva, P.; Lisini, A. (Chem. Phys. **76** [1983] 185/93).

2.2.5.2.2 Dipole Moment. Polarizability

The dipole moment μ of N_2H_2 has not yet been experimentally determined. For *trans*-N_2H_2, $\mu=0$ for reasons of symmetry.

For *cis*-N_2H_2, reliable quantum-chemical calculations gave dipole moments between 3.0 and 3.2 D: 3.1 (contracted CI) [1], 3.17 (CEPA-PNO) [2], 3.18 (HF/6-31+G(2d,p)) [3], 3.0 (HF/3-21G(N*)) [4], 3.06 (HF/triple-ζ basis) [5], and 3.20 (HF/6-31G**) [6]. Results of previous ab initio calculations were given in [7 to 9]. Dipole moments calculated with semiempirical methods (CNDO, MNDO) were reported in [10 to 13].

Dipole moment derivatives were calculated (ab initio SCF) in order to obtain complementary spectral assignment data: $\partial\mu/\partial S_4 = -1.778$ D/rad, $\partial\mu/\partial S_5 = -0.427$ D/Å, $\partial\mu/\partial S_6 = 1.857$ D/rad (the normal coordinates for τ, ν_{as}(NH) and δ_{as}(NNH) were reduced to the symmetry coordinates S_4, S_5, and S_6) [14].

Isotropic dipole polarizabilities for *trans*-N_2H_2 and *cis*-N_2H_2 were obtained by ab initio SCF calculations to be $\alpha = 18.18$ and 18.53 a_0^3. Hyperpolarizabilities were also calculated [5].

References:

[1] Brandemark, U.; Siegbahn, P. E. M. (Theor. Chim. Acta **66** [1984] 217/32).
[2] Burton, P. G. (Mol. Phys. **34** [1977] 51/63).
[3] McKee, M. L.; Squillacote, M. E.; Stanmbury, D. M. (J. Phys. Chem. **96** [1992] 3266/72).
[4] Riggs, N. V.; Radom, L. (Int. J. Quant. Chem. **31** [1987] 393/403).
[5] Liu, S.; Dykstra, C. E. (J. Phys. Chem. **91** [1987] 1749/54).
[6] Ritter, G.; Haefelinger, G.; Lueddecke, E.; Rau, H. (J. Am. Chem. Soc. **111** [1989] 627/35).
[7] Kao, J.; Huang, T. N. (J. Am. Chem. Soc. **101** [1979] 5546/57).
[8] Wong, D. P.; Fink, W. H.; Allen, L. C. (J. Chem. Phys. **52** [1970] 6291/8).
[9] Robin, M. B.; Hart, R. R.; Kuebler, N. A. (J. Am. Chem. Soc. **89** [1967] 1564/72).
[10] Pilipenko, A. T.; Zaets, V. A.; Falendysh, E. R.; Gorlov, Y. I. (Teor. Eksp. Khim. **24** [1988] 713/7; Theor. Exp. Chem. [USSR] **24** [1988] 682/6).

[11] Chantranupong, L. (J. Sci. Soc. Thailand **9** [1983] 187/90).
[12] Kharabaev, N. N.; Kogan, V. A.; Osipov, O. A. (Zh. Fiz. Khim. **51** [1977] 1775/6; Russ. J. Phys. Chem. **51** [1977] 1035/6).
[13] Tinland, B. (Spectrosc. Lett. **3** [1970] 51/3).
[14] Pouchan, C.; Dargelos, A.; Chaillet, M. (J. Mol. Spectrosc. **76** [1979] 118/30).

2.2.5.2.3 Nuclear Quadrupole Coupling Constants

Experimental results are not available. Ab initio calculations at the SCF level, using a basis set of double-zeta quality augmented by bond functions, yielded the component q_{zz} (maximum absolute value of all tensor elements) of the electric field gradients and the asymmetry parameters η at the ^{14}N and ^2H nuclei [1]:

trans-N_2H_2: $q_{zz}(N) = -1.366$, $\eta = 0.643$, $q_{zz}(H) = 0.319$, $\eta = 0.022$
cis-N_2H_2: $q_{zz}(N) = -1.429$, $\eta = 0.542$, $q_{zz}(H) = 0.325$, $\eta = 0.014$

The same calculations carried out for ammonia gave coupling constants in good agreement with experimental values [1].

Previous theoretical studies at the ab initio SCF level were reported in [2 to 4].

References:

[1] Prasad, G.; Lal, A.; Chandra, P. (Theor. Chim. Acta **75** [1989] 475/80).
[2] Snyder, C. L. (J. Chem. Phys. **68** [1978] 291/4).
[3] Winter, N. W.; Pitzer, R. M. (J. Chem. Phys. **62** [1975] 1269/75).
[4] Kochanski, E.; Lehn, J. M.; Levy, B. (Theor. Chim. Acta **22** [1971] 111/29).

2.2.5.2.4 Magnetic Susceptibility. NMR Parameters. Nuclear Shielding

Only results of theoretical studies are known.

Magnetic Susceptibility χ

Magnetic susceptibility tensors were calculated by the ab initio IGLO (individual gauge for localized molecular orbitals) method with a large basis set. The calculations showed both isomers of N_2H_2 to be nearly paramagnetic. The following table lists the principal tensor elements and the diamagnetic, paramagnetic, and nonlocal contributions in ppm cgs/mol (sign convention: diamagnetic contributions are positive and paramagnetic ones negative) [1]:

molecule	χ_{11}	χ_{22}	χ_{33}	χ^d	χ^p	χ^{nl}	χ
trans-N_2H_2	17.1	6.6	−15.0	20.8	−13.2	−4.7	2.9
cis-N_2H_2	15.1	4.0	−8.0	20.8	−12.3	−4.8	3.7

Nuclear Spin-Spin Coupling Constants

Ab initio calculations with the EOM (equations-of-motion) method gave $^1J(^{15}N^{15}N) = -9.03$ Hz for *trans*-N_2H_2 and −11.81 Hz for *cis*-N_2H_2 [2]. Previous calculations by the same author with the SOS CI method yielded $^1J(^{15}N^{15}N) = -16.78$ Hz and $^1J(^{15}NH) = -44.58$ Hz for *trans*-N_2H_2 and $^1J(^{15}N^{15}N) = -21.71$ Hz and $^1J(^{15}NH) = -36.10$ Hz for *cis*-N_2H_2 [3].

The contribution of the Fermi contact term to J(NN) in both *trans*- and *cis*-N_2H_2 was computed using the scanning molecular orbital method, a special approach within the Hartree-Fock framework [4]. The diamagnetic spin-orbital (DSO) contribution to J(HH) in N_2H_2 was calculated at the ab initio SCF level of theory [5].

Chemical Shifts δ. Nuclear Magnetic Shielding Constants σ

Nitrogen NMR shifts and nitrogen shielding tensors were calculated by means of the ab initio SOS CI (sum-over-states configuration interaction) [3] and IGLO [1] schemes using large or moderately large basis sets. The results (given in the following table) are only preliminary. Both authors agree that for correctly describing the nitrogen NMR shielding it is essential to include electron correlation (neglected in [1]) and to use very large basis sets (insufficient in [3]).

$\delta = 660$ [3] and 700.4 [1] ppm for *trans*-N_2H_2 and 578 [3] and 646.2 [1] ppm for *cis*-N_2H_2 were obtained; the shifts are relative to NH_3 having r_z geometry.

The following table gives the diamagnetic and paramagnetic shielding constants in ppm:

molecule	atom	σ^d [3]	σ^p [3]	σ [3]	σ [1]
trans-N_2H_2	N	366.35	−783.22	−416.22	−464
cis-N_2H_2	N	366.64	−700.46	−333.82	−390
trans-N_2H_2	H	19.74	−11.59	8.15	–
cis-N_2H_2	H	15.72	−4.52	11.20	–

The diamagnetic shielding of nitrogen and hydrogen in N_2H_2 was also estimated from a relation containing its electronegativity, equilibrium structure, and total energy [6].

References:

[1] Schindler, M. (J. Am. Chem. Soc. **109** [1987] 5950/5).
[2] Galasso, V. (Chem. Phys. Lett. **145** [1988] 259/61).
[3] Galasso, V. (Chem. Phys. **83** [1984] 407/13).

[4] Jansen, H. B.; Meeuwis, A.; Pyykkö, P. (Chem. Phys. **38** [1979] 173/9).
[5] Scuseria, G. E. (Chem. Phys. **107** [1986] 417/27).
[6] Ray, N. K.; Parr, R. G. (J. Chem. Phys. **73** [1980] 1334/9).

2.2.5.2.5 Rotational Constants. Bond Distances and Angles

The rotational and centrifugal distortion constants A, B, C, D_K, D_{JK}, D_J, D_1, and D_2 of the ground and the vibrational states $v_4=1$, $v_5=1$, and $v_6=1$ were obtained by analyzing the corresponding vibration-rotation bands. The constants (in cm^{-1}) of the ground state are listed in the following table:

constant	*trans*-N_2H_2	*trans*-N_2H_2	*trans*-N_2D_2
A	10.001002(52)	10.00021(23)	6.02490(21)
B	1.304248(17)	1.304194(47)	1.089385(63)
C	1.150096(15)	1.149861(42)	0.919525(54)
$D_K\cdot10^4$	6.5307(70)	6.325(42)	2.869(35)
$D_{JK}\cdot10^5$	3.934(30)	4.001(72)	1.46(12)
$D_J\cdot10^6$	2.845(26)	2.870(58)	1.71(10)
$D_1\cdot10^7$	−2.59(15)	2.89(26)	2.18(58)
$D_2\cdot10^5$	−5.80(90)	−1.86(24)	−0.84(31)
Ref.	[1]	[2]	[2]

Earlier values of rotational constants were based on low-resolution spectra and on the assumption that *trans*-N_2H_2 and *cis*-N_2H_2 are both present [3, 4]. Constants for the $v_4=1$, $v_5=1$, $v_6=1$ states are given in [1] and for the $v_5=1$ state (also for *trans*-N_2D_2) in [2]. Calculated centrifugal distortion constants are reported in [5].

Bond distances and angles for planar *trans*-N_2H_2 were determined from the rotational constants of *trans*-N_2H_2 and *trans*-N_2D_2 quoted above [2]:

$$r(NN)=1.252\pm0.002\ Å,\ r(NH)=1.028\pm0.005\ Å,\ \angle NNH=106.9\pm0.5°$$

Earlier experimental data are either incomplete [3] or incorrect [4]. The following table compares equilibrium-structural data determined for *trans*-N_2H_2 and *cis*-N_2H_2 by the most recent quantum-chemical calculations at a high level of theory.

molecule	r(NN) in Å	r(NH) in Å	∠NNH	method	Ref.
trans-N_2H_2	1.24	1.03	106.3°	CASSCF-CI/[4s3p2d1f/3s2p1d]	[6]
	1.265	1.031	105.2°	MP2/6-31G**	[7]
	1.266	1.036	105.4°	MP2/6-31G*	[8]
cis-N_2H_2	1.25	1.04	112.8°	CASSCF-CI/[4s3p2d1f/3s2p1d]	[6]
	1.260	1.036	112.0°	MP2/6-31G**	[7]
	1.260	1.042	112.3°	MP2/6-31G*	[8]

Results of comparable studies are given in [9 to 12]. Theoretical studies on the structure of diazene done before experimental data were available are described in [13 to 17].

For geometry data of *trans*-N_2H_2 in electronically excited states, see p. 55.

References:

[1] Hallin, K. E. J.; Johns, J. W. C.; Trombetti, A. (Can. J. Phys. **59** [1981] 663/72).
[2] Carlotti, M.; Johns, J. W. C.; Trombetti, A. (Can. J. Phys. **52** [1974] 340/4).
[3] Trombetti, A. (Can. J. Phys. **46** [1968] 1005/11).
[4] Blau, E. J.; Hochheimer, B. F. (J. Chem. Phys. **41** [1964] 1174/82).
[5] Namasivayam, R.; Viswanathan, S. (Indian J. Pure Appl. Phys. **19** [1981] 40/3).
[6] Walch, S. P. (J. Chem. Phys. **91** [1989] 389/94).
[7] Whitelegg, D.; Woolley, R. G. (J. Mol. Struct. **209** [1990] 23/31 [THEOCHEM **68**]).
[8] Pople, J. A.; Curtiss, L. A. (J. Chem. Phys. **95** [1991] 4385/8).
[9] McKee, M. L.; Squillacote, M. E.; Stanbury, D. M. (J. Phys. Chem. **96** [1992] 3266/72).
[10] Jensen, H. J. A.; Joergensen, P.; Helgaker, T. (J. Am. Chem. Soc. **109** [1987] 2895/901).

[11] Brandemark, U.; Siegbahn, P. E. M. (Theor. Chim. Acta **66** [1984] 217/32).
[12] Casewit, C. J.; Goddard, W. A., III (J. Am. Chem. Soc. **102** [1980] 4057/62).
[13] Winter, N. W.; Pitzer, R. M. (J. Chem. Phys. **62** [1975] 1269/75).
[14] Baird, N. C.; Swenson, J. R. (Can. J. Chem. **51** [1973] 3097/101).
[15] Radom, L.; Hehre, W. J.; Pople, J. A. (J. Am. Chem. Soc. **93** [1971] 289/300).
[16] Wong, D. P.; Fink, W. H.; Allen, L. C. (J. Chem. Phys. **52** [1970] 6291/8).
[17] Schaad, L. J.; Kinser, H. B. (J. Phys. Chem. **73** [1969] 1901/11).

2.2.5.2.6 Constants of Molecular Vibrations

Fundamental Vibrations

trans- and *cis*-N_2H_2 (point groups C_{2h} and C_{2v}) as well as *trans*- and *cis*-N_2HD (point group C_s) have six normal modes of vibration. Their symmetry species, selection rules (IR- or Raman-active), and approximate mode descriptions (only the leading terms of the calculated potential energy distributions [1]) are given in the following table (for the C_{2v} point group, the molecule is in the xy plane with $z = C_2$ axis):

trans-N_2H_2			*cis*-N_2H_2			N_2HD		
$\nu_1(A_g)$	Ra	ν_s(NH)	$\nu_1(A_1)$	IR, Ra	ν_s(NH)	$\nu_1(A')$	IR, Ra	ν(NH)
$\nu_2(A_g)$	Ra	δ_s(NNH)	$\nu_2(A_1)$	IR, Ra	ν_s(NN)	$\nu_2(A')$	IR, Ra	ν(ND)
$\nu_3(A_g)$	Ra	ν_s(NN)	$\nu_3(A_1)$	IR, Ra	δ_s(NNH)	$\nu_3(A')$	IR, Ra	ν(NN)
$\nu_4(A_u)$	IR	τ	$\nu_4(A_2)$	Ra	τ	$\nu_4(A')$	IR, Ra	δ(NNH)
$\nu_5(B_u)$	IR	ν_a(NH)	$\nu_5(B_2)$	IR, Ra	ν_a(NH)	$\nu_5(A')$	IR, Ra	δ(NND)
$\nu_6(B_u)$	IR	δ_a(NNH)	$\nu_6(B_2)$	IR, Ra	δ_a(NNH)	$\nu_6(A'')$	IR, Ra	τ

Fundamental vibration frequencies are known only for *trans*-N_2H_2 and its isotopomers. Previous assignments to *cis*-H_2H_2 [2 to 5] are apparently incorrect (cf. p. 52). Table 7 (p. 50) lists fundamental vibration frequencies observed for *trans*-N_2H_2 and its deuterated modifications, calculated with a potential function for *cis*-N_2H_2. Also included are the "latest" assignments for all fundamentals of *trans*-N_2H_2, -N_2D_2, and -N_2HD, assigned after reviewing the experimental results and supported by potential-function calculations [1].

Frequencies of ^{15}N-substituted *trans*-N_2H_2 modifications were also reported [1, 12]. Frequencies calculated in a normal coordinate analysis are given in [1, 12 to 15]. Quantum-chemical ab initio calculations (MP2 [16 to 18], MCSCF [19], CI [20, 21], SCF [22]) yielded fundamental vibration frequencies in the harmonic approximation.

For fundamental vibration frequencies in electronically excited states, see p. 55.

Force Constants

A general harmonic force field for *trans*- or *cis*-N_2H_2 contains ten independent potential constants. In terms of internal coordinates, there are two stretching constants, f_R and f_r, with R = r(NN) and r = r(NH), two angle deformation constants, f_α and f_γ, with α = in-plane deformation and γ = out-of-plane torsion, and six interaction constants, f_{Rr}, $f_{rr'}$, $f_{R\alpha}$, $f_{r\alpha}$, $f_{r\alpha'}$ (the latter two refer to interactions between the HNN angle and an adjacent and nonadjacent NH bond, respectively), and $f_{\alpha\alpha}$. The values for an empirical force field [1] and a scaled quantum-mechanical force field [19] are compared in the table below. The empirical force field [1] reproduces the experimental frequencies of *trans*-N_2H_2, -N_2HD, -N_2D_2 [1] with an average deviation of 6.6 cm^{-1}. The scaled quantum-mechanical force field, obtained by scaling the calculated ab initio force constants (MCSCF method) to the observed frequencies, reproduces the experimental frequencies [1] with an average deviation of 10.0 cm^{-1} (scaled to *trans*-N_2H_2 frequencies) and 8.2 cm^{-1} (scaled to *trans*-N_2D_2 frequencies) [19]. The force fields for *cis*-N_2H_2 were obtained by transferring force constants from *trans*-diazene and *trans*- and *cis*-methyldiazene [1] and by ab initio calculations [19]. Units are mdyn/Å for stretching, mdyn·Å for bending, and mdyn for stretch-bend interactions.

molecule	f_R	f_r	f_α	f_γ	$f_{R\alpha}$	f_{Rr}
trans-N_2H_2	10.59(14)	5.418(21)	1.144(10)	0.446(6)	0.675(39)	0.0
	10.36(17)	5.424(65)	1.177(14)	0.4699(76)	0.657	0.330
trans-N_2D_2	10.52(20)	5.585(78)	1.193(16)	0.4740(83)	0.666	0.338
cis-N_2H_2	10.75	4.89	1.10	0.394	0.669	0.0
	10.42	5.366	1.296	0.389	0.712	0.222

molecule	$f_{rr'}$	$f_{r\alpha}$	$f_{r\alpha'}$	$f_{\alpha\alpha}$	Ref.
trans-N_2H_2	−0.027(26)	0.0	0.0	0.115(11)	[1]
	−0.054	0.094	0.095	0.136	[19]
trans-N_2D_2	−0.056	0.096	0.097	0.138	[19]
cis-N_2H_2	−0.027	0.0	0.0	0.115	[1]
	0.115	0.023	−0.117	0.026	[19]

Previous empirical force constants for *trans*-N_2H_2 based on a valence force field model [12, 14, 23, 24] and a Urey-Bradley model [13] used partly different frequencies. Based on frequencies originally assigned to *cis*-N_2H_2, a force field for *cis*-N_2H_2 was derived [15]. Ab initio calculations of the force field were also made for *trans*-N_2H_2 [21, 22, 25] and for *cis*-N_2H_2 [22, 25].

Mean Amplitudes of Vibration

The following values for *trans*-N_2H_2 were calculated: u(N=N) = 0.0397, u(N-H) = 0.0788, u(NNH) = 0.0991, u(N···H) = 0.1035, and u(H···H) = 0.1326 Å [24].

Coriolis Coupling Constants

For *trans*-N_2H_2, $|\zeta^a_{46}| = 0.4602$ and $|\zeta^b_{46}| = 0.9095$ were obtained from an analysis of the overlapping ν_4 (1288 cm^{-1}) and ν_6 (1317 cm^{-1}) gas-phase bands. These values are in reasonable agreement with the calculated values $|\zeta^a_{46}| = 0.3413$ and $|\zeta^b_{46}| = 0.9399$, for which

Table 7

Observed and Calculated Fundamental Vibrational Frequencies (in cm^{-1}) of N_2H_2, N_2D_2, and N_2HD.

molecule	method, medium, temperature	ν_1	ν_2	ν_3	ν_4	ν_5	ν_6	Ref.
trans-N_2H_2	Raman, IR, N_2 matrix, 12 K	3128	1583	1529	1285.8[a]	3131	–	[6]
	IR, N_2 matrix, 5 K	–	–	–	1288	3137	1322	[7]
	IR, Ar matrix, 5 K	–	–	–	1283	3118	1313	[7]
	IR, gas phase, room temperature	–	–	–	1288.64	3120.28	1316.41	[8, 9]
	IR, gas phase, room temperature	–	–	–	–	3120.1	–	[10]
	"latest" assignment	3128	1583	1529	1286	3120	1322	[1]
trans-N_2D_2	Raman, IR, N_2 matrix, 12 K	2320[b]	1215	1539	946.2[a]	2321	–	[6]
	IR, N_2 matrix, 5 K	–	–	–	947	2308[c]	972	[7]
	IR, gas phase, room temperature	–	–	–	–	2315	–	[9]
	"latest" assignment	2320	1215	1539	946	2315	972	[1]
trans-N_2HD	Raman, IR, N_2 matrix, 12 K	3124	2311	1536	1480.5	1058.0[a]	–	[6]
	"latest" assignment	3124	2310	1536	1481	1058	1131	[1]
cis-N_2H_2	potential function	2966	1558	1390	1259	2984	1439	[1]
cis-N_2D_2	potential function	2178	1543	988	949	2188	1124	[1]
cis-N_2HD	potential function	2975	2183	1552	1414	1056	1115	[1]

[a] Originally assigned to ν_6. — [b] Estimated. — [c] Assignment according to [11].

the force field of [1] was used. Additionally, two second-order terms, which allow ν_4 to interact with ν_6 mainly through ν_5, were estimated, $|\eta^{bc}_{46}|=0.0014$ and $|\eta^{ac}_{46}|=0.029$ [8]. Calculated values are: $\zeta_{12}=0.3421$, $\zeta_{13}=0.3656$, $\zeta_{23}=-0.8656$, $\zeta_{56}=0.9727$ [24].

References:

[1] Craig, N. C.; Levin, I. W. (J. Chem. Phys. **71** [1979] 400/7).
[2] Blau, E. J.; Hochheimer, B. F.; Unger, H. J. (J. Chem. Phys. **34** [1961] 1060/1).
[3] Blau, E. J.; Hochheimer, B. F. (J. Chem. Phys. **41** [1964] 1174/82).
[4] Rosengren, K.; Pimentel, G. C. (J. Chem. Phys. **43** [1965] 507/16).
[5] Wiberg, N.; Fischer, G.; Bachhuber, H. (Angew. Chem. **89** [1977] 828/9; Angew. Chem. Int. Ed. Engl. **16** [1977] 780/1).
[6] Bondybey, V. E.; Nibler, J. W. (J. Chem. Phys. **58** [1973] 2125/34).
[7] Minkwitz, R. (Z. Anorg. Allg. Chem. **411** [1975] 1/14).
[8] Hallin, K. E. J.; Johns, J. W. C.; Trombetti, A. (Can. J. Phys. **59** [1981] 663/72).
[9] Carlotti, M.; Johns, J. W. C.; Trombetti, A. (Can. J. Phys. **52** [1974] 340/4).
[10] Trombetti, A. (Can. J. Phys. **46** [1968] 1005/11).

[11] Jacox, M. E. (J. Phys. Chem. Ref. Data **17** [1988] 269/511, 366).
[12] Nibler, J. W.; Bondybey, V. E. (J. Chem. Phys. **60** [1974] 1307/12).
[13] Ackermann, M. N.; Burdge, J. J.; Craig, N. C. (J. Chem. Phys. **58** [1973] 203/15).
[14] Nibler, J. W.; Barnhart, D. M. (J. Mol. Spectrosc. **44** [1972] 236/50).
[15] Afifi, M. S.; El Sharabasy, S. (Egypt. J. Chem. **20** [1977] 347/52).
[16] McKee, M. L.; Squillacote, M. E.; Stanbury, D. M. (J. Phys. Chem. **96** [1992] 3266/72).
[17] Whitelegg, D.; Woolley, R. G. (J. Mol. Struct. **209** [1990] 23/31 [THEOCHEM **66**]).
[18] Harrison, R. J.; Fitzgerald, G. B.; Laidig, W. D.; Bartlett, R. J. (Chem. Phys. Lett. **124** [1986] 291/4).
[19] Jensen, H. J. A.; Joergensen, P.; Helgaker, T. (J. Am. Chem. Soc. **109** [1987] 2895/901).
[20] Peric, M.; Buenker, R. J.; Peyerimhoff, S. D. (Can. J. Chem. **55** [1977] 1533/45).

[21] Peric, M.; Buenker, R. J.; Peyerimhoff, S. D. (Mol. Phys. **35** [1978] 1495/8).
[22] Pouchan, C.; Dargelos, A.; Chaillet, M. (J. Mol. Spectrosc. **76** [1979] 118/30).
[23] Mielke, Z.; Ratajczak, H. (J. Mol. Struct. **19** [1973] 751/9).
[24] Namasivayam, R.; Viswanathan, S. (Indian J. Pure Appl. Phys. **19** [1981] 40/3).
[25] Wong, D. P.; Fink, W. H.; Allen, L. C. (J. Chem. Phys. **52** [1970] 6291/8).

2.2.5.2.7 Bond Dissociation Energies. π-Bond Strength

Experimental bond dissociation energies were derived from the enthalpy of formation of N_2H_2 together with auxiliary data.

D_0(HN=NH). Based on $\Delta_fH^\circ_0(N_2H_2)\geq 195.0$ and 219.2 kJ/mol from mass-spectrometric experiments (see p. 56), $D^\circ_0\leq 518.0\pm 4.6$ [1] and 536 ± 38 kJ/mol [2] were obtained. Another experimental value is 510 kJ/mol [3]. Ab initio MO calculations at the G2 level yielded $D_0=513.8$ kJ/mol [4]. A semiempirical delta-function model of chemical binding predicted $D=477$ kJ/mol [5].

D_0(HN_2-H). Two quite different experimental values were reported; the more reliable one seems to be $D_0=250.2\pm 8.4$ kJ/mol [2], the second one is $D_0=339$ kJ/mol [3]. With the G2 procedure $D_0=268.2$ kJ/mol was computed [4]. Another extensive calculation (CASSCF+CI) yielded $D_0=234$ kJ/mol [6]. $D_0=293$ kJ/mol was calculated with the GVB/CI method [7]. HF calculations gave 222.6 [8] and 209.2 kJ/mol [9] (apparently without a vibrational correction).

E_π. The π-bond energy is equated with the N_2H_2 trans-cis rotation barrier. Values for this barrier, calculated at various levels of theory, are in the range 230 to 351 kJ/mol (see p. 58). Publications comparing the π-bond strengths for HN=NH, HP=NH, and HP=PH reported 251 kJ/mol as a result of second-order CI calculations [10, 11]. Estimates based on the heats of formation of N_2H_2 and N_2H_4 and on bond energies of both molecules gave 268 ± 46 and 230 ± 25 kJ/mol, respectively [10]. In analogy to C_2H_4 and CH_2NH, a value of 196 ± 42 kJ/mol was estimated [12].

References:

[1] Ruscic, B.; Berkowitz, J. (J. Chem. Phys. **95** [1991] 4378/84).
[2] Foner, S. N.; Hudson, R. L. (J. Chem. Phys. **68** [1978] 3162/8).
[3] Wiberg, N.; Fischer, G.; Bachhuber, H. (Z. Naturforsch. **34b** [1979] 1385/90).
[4] Pople, J. A.; Curtiss, L. A. (J. Chem. Phys. **95** [1991] 4385/8).
[5] Lippincott, E. R.; Dayhoff, M. O. (Spectrochim. Acta **16** [1960] 807/34).
[6] Brandemark, U.; Siegbahn, P. E. M. (Theor. Chim. Acta **66** [1984] 217/32).
[7] Casewit, C. J.; Goddard, W. A., III (J. Am. Chem. Soc. **102** [1980] 4057/62).
[8] Baird, N. C.; Kathpal, H. B. (Can. J. Chem. **55** [1977] 863/8).
[9] Pasto, D. J.; Chipman, D. M. (J. Am. Chem. Soc. **101** [1979] 2290/6).
[10] Schmidt, M. W.; Gordon, M. S. (Inorg. Chem. **25** [1986] 248/54).

[11] Schmidt, M. W.; Truong, P. N.; Gordon, M. S. (J. Am. Chem. Soc. **109** [1987] 5217/27).
[12] Grela, M. A.; Colussi, A. J. (Intern. J. Chem. Kinet. **20** [1988] 713/8).

2.2.5.2.8 Infrared and Raman Spectra

For fundamental vibrational frequencies, see p. 50.

Gas Phase. The first exploratory paper on the gas-phase IR spectrum was published in 1964 [1]. A moderately high-resolution IR spectrum was later recorded between 3000 and 3250 cm^{-1} (region of ν_5) [2]. Another measurement of ν_5 on N_2H_2 and N_2D_2 at a higher resolution with complete rotational analysis showed that the molecule exists in the trans configuration with a totally symmetric ground state [3]. More recently, a high-resolution IR study identified the fundamentals ν_4 and ν_6 [4]. In all these studies, N_2H_2 was generated by microwave discharge through hydrazine.

Condensed Phases. The interpretation of solid-phase and matrix spectra at low temperatures has been controversial for a long time. It is additionally complicated by the presence of ammonia which is simultaneously formed together with N_2H_2 during the discharge decomposition of HN_3 or N_2H_4. The spectra are obscured by bands due to NH_3 and hydrogen-bonded complexes of N_2H_2 with N_2H_2 and NH_3 [5, 6].

The presence of N_2H_2 was thought to be responsible for bands observed in early IR studies where condensed decomposition products of HN_3 were investigated [7 to 10]. The first interpretations of IR spectra of decomposition products of HN_3 and N_2H_4 favored the existence of *cis*-N_2H_2 [1, 11] or assigned some bands to *cis*-N_2H_2 [12]. Later, the IR and Raman spectra of condensates from the discharge decomposition of N_2H_4 [6, 13, 14] and HN_3 [6] and from the thermolysis of metal tosylhydrazides [5, 13, 15, 16] were mostly interpreted in terms of a trans configuration. Based on all experimental facts and supported by a potential-function calculation, all six fundamentals of *trans*-N_2H_2, -N_2D_2, and -N_2HD were successfully assigned [17] (see p. 50). The spectral identification of *cis*-N_2H_2 in several IR spectra [1, 11, 12, 16] is questionable. Fundamental vibrational frequencies calculated with a potential function [17] and a comparison with an IR study of *cis*-methyldiazene [18] suggest a misinterpretation. However, a more recent ab initio force field calculation suggests certain assignments in [12] and in [16] to be in favor of *cis*-N_2H_2 [19].

References:

[1] Blau, E. J.; Hochheimer, B. F. (J. Chem. Phys. **41** [1964] 1174/82).
[2] Trombetti, A. (Can. J. Phys. **46** [1968] 1005/11).
[3] Carlotti, M.; Johns, J. W. C.; Trombetti, A. (Can. J. Phys. **52** [1974] 340/4).
[4] Hallin, K. E. J.; Johns, J. W. C.; Trombetti, A. (Can. J. Phys. **59** [1981] 663/72).
[5] Minkwitz, R. (Z. Anorg. Allg. Chem. **411** [1975] 1/14).
[6] Bondybey, V. E.; Nibler, J. W. (J. Chem. Phys. **58** [1973] 2125/34).
[7] Dows, D. A.; Primentel, G. C.; Whittle, E. (J. Chem. Phys. **23** [1955] 1606/9).
[8] Becker, E. D.; Pimentel, G. C.; Van Thiel, M. (J. Chem. Phys. **26** [1957] 145/50).
[9] Van Thiel, M.; Pimentel, G. C. (J. Chem. Phys. **32** [1960] 133/40).
[10] Milligan, D. E.; Jacox, M. E. (J. Chem. Phys. **41** [1964] 2838/41).

[11] Blau, E. J.; Hochheimer, B. F.; Unger, H. J. (J. Chem. Phys. **34** [1961] 1060/1).
[12] Rosengren, K.; Pimentel, G. C. (J. Chem. Phys. **43** [1965] 507/16).
[13] Wiberg, N.; Fischer, G.; Bachhuber, H. (Angew. Chem. **88** [1976] 386/7; Angew. Chem. Int. Ed. Engl. **15** [1976] 385).
[14] Trombetti, A. (J. Chem. Soc. A **1971** 1086/8).
[15] Wiberg, N.; Fischer, G.; Bachhuber, H. (Chem. Ber. **107** [1974] 1456/71).
[16] Wiberg, N.; Fischer, G.; Bachhuber, H. (Angew. Chem. **89** [1977] 828/9; Angew. Chem. Int. Ed. Engl. **16** [1977] 780/1).
[17] Craig, N. C.; Levin, I. W. (J. Chem. Phys. **71** [1979] 400/7).
[18] Craig, N. C.; Kliewer, M. A.; Shih, N. C. (J. Am. Chem. Soc. **101** [1979] 2480/2).
[19] Jensen, H. J. A.; Joergensen, P.; Helgaker, T. (J. Am. Chem. Soc. **109** [1987] 2895/901).

2.2.5.2.9 UV Absorption Spectra

Two regions in the UV absorption spectrum, one in the near-ultraviolet at 300 to 430 nm and the other in the vacuum ultraviolet at 130 to 180 nm, were observed in N_2H_2 in the gas phase. The near-ultraviolet spectrum of N_2H_2 in ammonia was also studied.

The near-ultraviolet spectrum, earlier characterized having a weak and broad continuum centered at 350 nm [1], shows a well-resolved vibrational structure under better experimental conditions [2] (see **Fig. 1**). The spectra of both N_2H_2 and N_2D_2, prepared by passing hydrazine through a microwave discharge, consist of about 30 diffuse bands. Analysis showed long progressions in ν_2', the symmetric NNH bending vibration of the upper state, and shorter progressions in the NN stretching vibration ν_3'. The absorption is attributed to the symmetry-forbidden $\pi^* \leftarrow n_+$, $\tilde{A}\,{}^1B_g \leftarrow \tilde{X}\,{}^1A_g$ transition of *trans*-diazene, made vibronically allowed by the antisymmetric NH stretching vibration ν_5'. Weaker progressions are also induced by the torsional vibration ν_4' and the antisymmetric NNH bending vibration ν_6' [3, 4]. This interpretation is in satisfactory agreement with an ab initio CI study on the vibrational structure of the ${}^1B_g(\pi^*,n_+)$ transition; a renumbering of the ν_2' progression was also given [5]. An alternative interpretation of the long progression (ν_2') on the basis of ab initio calculations [6] was later refuted [4]. In another ab initio CI study, all six vibrational frequencies in this state were calculated [7].

The absorption in liquid ammonia at 223 K is shifted about 50 nm to longer wavelengths ($\lambda_{max} \approx 400$ nm) compared with the gas-phase absorption. The spectrum is considerably broadened, and the vibrational structure is almost completely lost. Hydrogen bonding is thought to be responsible for these changes [8].

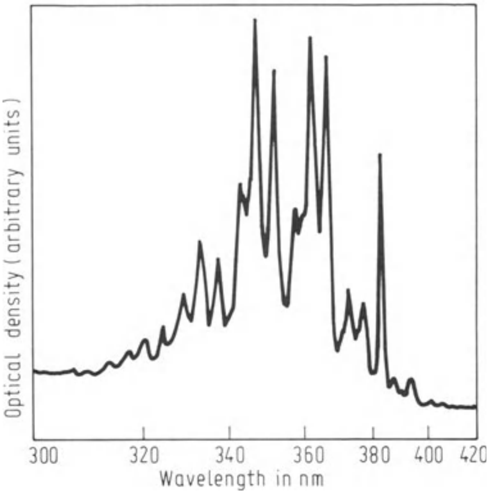

Fig. 1 Near-ultraviolet spectrum of gaseous N_2H_2 (from [2]).

The vacuum UV spectrum of diazene prepared by thermolysis of sodium tosylhydrazide between 130 and 180 nm shows at least two band systems, one at 173 to 152 nm ($\tilde{B} \leftarrow \tilde{X}$), the other below 147 nm ($\tilde{C} \leftarrow \tilde{X}$) (**Fig. 2**) [9]. The region around 170 nm in the spectrum of N_2H_2 and N_2D_2 generated by microwave discharge through hydrazine had been investigated earlier [1]. Both band systems with origins at 172.7 and 147.3 nm were assigned to the Rydberg transitions $3p_\pi(b_u) \leftarrow n_+$ and $4p_\pi(b_u) \leftarrow n_+$ in *trans*-N_2H_2, respectively. Long progressions in ν'_2 and short progressions in ν'_3 were analyzed in both systems, and a rotational analysis was performed for the $\tilde{B} \leftarrow \tilde{X}$ system [9]. Ab initio CI calculations for the $\tilde{B}\,^1B_u$ Rydberg state gave vibrational frequencies and geometry data [10].

Ab initio CI calculations [6], the appearance of unassignable, diffuse bands between the $\tilde{B} \leftarrow \tilde{X}$ and $\tilde{C} \leftarrow \tilde{X}$ systems (cf. Fig. 2), and many unresolved bands below 136 nm suggest

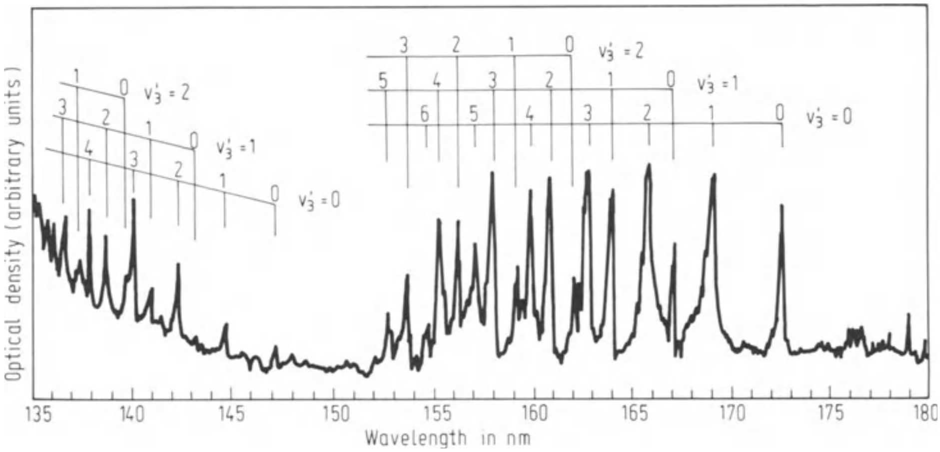

Fig. 2 Vacuum-ultraviolet spectrum of gaseous N_2H_2. Vibrational assignments show progressions in ν'_2 and ν'_3. Long progressions belong to ν'_2 (from [9]).

that some transitions may be hidden under the stronger $\tilde{B} \leftarrow \tilde{X}$ and $\tilde{C} \leftarrow \tilde{X}$ systems. A tentative assignment was performed in [9].

The following table summarizes the experimental data on the vertical excitation energies and on the geometry and frequencies of the symmetric vibrations in the ground and known excited $\tilde{A}$, $\tilde{B}$, and $\tilde{C}$ states of *trans*-N_2H_2:

state	excitation	transition energy in eV	frequencies in cm^{-1} ν_1	ν_2	ν_3	bond length in Å r(NN)	r(NH)	∠NNH	Ref.
$\tilde{X}\,{}^1A_g$		0.0	3128	1583	1529	1.252	1.028	106.9°	[11, 12]
$\tilde{A}\,{}^1B_g$	$\pi^* \leftarrow n_+$	3.6 (345 nm)	–	1184	1579	1.340[a]	1.010[a]	123°[a]	[4, 5]
$\tilde{B}\,{}^1B_u$	$3p_\pi \leftarrow n_+$	7.6 (163 nm)	3092	1180	1875	1.167	1.028[b]	127.6°	[9]
$\tilde{C}\,{}^1B_u$	$4p_\pi \leftarrow n_+$	8.8 (140 nm)	–	1180	1849	–	–	–	[9]

[a] Calculated data [5]; empirical values originally given for r(NN) and ∠NNH in [3] were not quoted in later studies [4, 9]. — [b] A planar trans structure with the same NH bond length as in the ground state was assumed.

The lowest predicted, but not observed transition ${}^3B_g(\pi^* \leftarrow n_+)$ was calculated several times by using ab initio SCF [13, 14] and CI methods [6, 15]. Ab initio CI calculations were carried out for a large number of other excited states [6]. Calculations of the lowest excited states at lower levels of theory are reported in [13 to 19].

References:

[1] Trombetti, A. (Can. J. Phys. **46** [1968] 1005/11).
[2] Willis, C.; Back, R. A. (Can. J. Chem. **51** [1973] 3605/19).
[3] Back, R. A.; Willis, C.; Ramsay, D. A. (Can. J. Chem. **52** [1974] 1006/12).
[4] Back, R. A.; Willis, C.; Ramsay, D. A. (Can. J. Chem. **56** [1978] 1575/8).
[5] Peric, M.; Buenker, R. J.; Peyerimhoff, S. D. (Can. J. Chem. **55** [1977] 1533/45).
[6] Vasudevan, K.; Peyerimhoff, S. D.; Buenker, R. J.; Kammer, W. E.; Hsu, H. L. (Chem. Phys. **7** [1975] 187/209).
[7] Peric, M.; Buenker, R. J.; Peyerimhoff, S. D. (Mol. Phys. **35** [1978] 1495/8).
[8] Back, R. A.; Willis, C. (Can. J. Chem. **52** [1974] 2513/5).
[9] Neudorfl, P. S.; Back, R. A.; Douglas, A. E. (Can. J. Chem. **59** [1981] 506/17).
[10] Groenenboom, G. C.; Van Lenthe, J. H.; Buck, H. M. (J. Chem. Phys. **91** [1989] 3027/35).

[11] Craig, N. C.; Levin, I. W. (J. Chem. Phys. **71** [1979] 400/7).
[12] Carlotti, M.; Johns, J. W. C.; Trombetti, A. (Can. J. Phys. **52** [1974] 340/4).
[13] Wagnière, G. (Theor. Chim. Acta **31** [1973] 269/74).
[14] Winter, N. W.; Pitzer, R. M. (J. Chem. Phys. **62** [1975] 1269/75).
[15] Robin, M. B.; Hart, R. R.; Kuebler, N. A. (J. Am. Chem. Soc. **89** [1967] 1564/72).
[16] Ditchfield, R.; Del Bene, J. E.; Pople, J. A. (J. Am. Chem. Soc. **94** [1972] 703/7).
[17] Baird, N. C.; Swenson, J. R. (Can. J. Chem. **51** [1973] 3097/101).
[18] Camp, R. N.; Epstein, I. R.; Steel, C. (J. Am. Chem. Soc. **99** [1977] 2453/9).
[19] Ertl, P.; Leska, J. (J. Mol. Struct. **165** [1988] 1/8 [THEOCHEM **42**]).

2.2.5.2.10 Intramolecular Relaxation

Theoretical studies were performed to describe the transfer of energy between various modes of vibration in N_2H_2 [1 to 4]. The interaction of the torsion with NNH bending and

NH stretching modes was investigated, and the consequences for the trans-cis isomerization were demonstrated [3, 4].

References:

[1] Sumpter, B. G.; Thompson, P. L. (J. Chem. Phys. **82** [1985] 4557/65).
[2] Sumpter, B. G.; Thompson, P. L. (J. Chem. Phys. **86** [1987] 2805/17).
[3] Spears, L. G., Jr.; Hutchinson, J. S. (J. Chem. Phys. **88** [1988] 240/9).
[4] Spears, L. G., Jr.; Hutchinson, J. S. (J. Chem. Phys. **88** [1988] 250/9).

2.2.5.2.11 Quantum-Chemical Calculations

The N_2H_2 molecule has been the subject of many quantum-chemical studies. Most of them are referenced in this chapter which also gives the results of all important calculations. For a more complete list of quantum-chemical studies (method, basis set, parameters calculated), consult the bibliography of ab initio calculations given on pp. 16/7.

2.2.5.3 Enthalpy of Formation. Thermodynamic Functions

The enthalpy of formation was experimentally determined from the appearance potentials (AP) of the fragments of N_2H_2 or N_2H_4. The values show considerable variation, mainly because of the difficulty of accurately measuring these appearance potentials.

In the most recent study, the appearance potential measured for H_2^+ via $N_2H_2 + e^- \rightarrow H_2^+ + N_2 + 2\ e^-$ together with the known ionization energy of H_2 gave $\Delta_fH^\circ_{298}$ values of $>176.1 \pm 2.9$ and, more probable, $\geq 188.3 \pm 3.3$ kJ/mol ($\Delta_fH^\circ_0 > 183.3 \pm 2.9$ or $\geq 195.0 \pm 3.3$). The two Δ_fH° values result from two different AP(H_2^+) values obtained by analyzing the photoion yield curve of H_2^+ [1].

By combining the mass-spectrometrically measured ionization energy of N_2H_2 with the appearance potential of $N_2H_2^+$ in the reaction $N_2H_4 + e^- \rightarrow N_2H_2^+ + H_2 + 2\ e^-$ and the known heat of formation of N_2H_4, $\Delta_fH^\circ_{298} = 212.1 \pm 8.4$ and $\Delta_fH^\circ_0 = 219.2 \pm 8.4$ kJ/mol were obtained [2]. An older, less accurate AP($N_2H_2^+$) value of the same authors yielded $\Delta_fH^\circ_{298} = 204 \pm 21$ kJ/mol [3]. The data adopted by the JANAF tables, $\Delta_fH^\circ_{298}(N_2H_2) = 212.97 \pm 10.9$ and $\Delta_fH^\circ_{298}(N_2D_2) = 207.1 \pm 2.1$ kJ/mol, are based on the latter AP value [4].

Based on the appearance potential of N_2^+ via $N_2H_2 + e^- \rightarrow N_2^+ + H_2 + 2\ e^-$ and the ionization energy of N_2, the values $\Delta_fH^\circ_{298} = 151 \pm 9$ [5] and 134 kJ/mol [6] were derived.

The following table lists the results of quantum-chemical ab initio calculations on *trans*-N_2H_2 at high levels of theory:

method (basis set)	$\Delta_fH^\circ_0$ in kJ/mol	$\Delta_fH^\circ_{298}$	Ref.
G2 theory (6-311+G(3df, 2p))	207.5	200.4	[7]
CASSCF/CI ([4s3p2d1f/3s2p1d] ANO basis)	206.3	212.5	[8]*)
CASSCF/CI + Davidson correction (triple zeta + polarization functions)	247.3	240.2	[9]
CISD + Davidson correction (6-31G**)	219.8	214.9	[10]
GVB CI (double zeta + polarization functions)	245.2	238.1	[11]
EPA (extended + polarization functions)	223.8	216.7	[12]
MCSCF (extended + polarization functions)	302.9	295.8	[13]

*) There is an inconsistency, since $\Delta_fH^\circ_0 < \Delta_fH^\circ_{298}$.

Results of computations on a smaller scale (e.g. SCF level, small basis sets) are given in [14 to 20].

The heat capacity C_p°, thermodynamic functions S°, $-(G^\circ-H_{298}^\circ)/T$ (all in $J \cdot K^{-1} \cdot mol^{-1}$), and $H^\circ-H_{298}^\circ$ (in kJ/mol), and the equilibrium constant K_f of *cis*-N_2H_2 in the ideal gas state at a standard pressure of 0.1 MPa for temperatures up to 6000 K are compiled in the JANAF tables [4] based on 1965 calculations and uncertain frequency and geometry data. Selected values are as follows:

T in K	C_p°	S°	$-(G^\circ-H_{298}^\circ)/T$	$H^\circ-H_{298}^\circ$	log K_f
298.15	36.554	218.603	218.603	0	−42.727
500	45.508	239.565	223.040	8.263	−27.777
800	56.683	263.541	233.919	23.698	−19.623
1000	62.049	276.792	241.198	35.594	−16.925
1500	70.655	303.767	257.765	69.004	−13.327

The JANAF tables [4] also give values for *cis*-N_2D_2, but not for *trans*-N_2H_2.

References:

[1] Ruscic, B.; Berkowitz, J. (J. Chem. Phys. **95** [1991] 4378/84).
[2] Foner, S. N.; Hudson, R. L. (J. Chem. Phys. **68** [1978] 3162/8).
[3] Foner, S. N.; Hudson, R. L. (J. Chem. Phys. **28** [1958] 719/20).
[4] Chase, M. W., Jr.; Davis, C. A.; Downey, I. R., Jr.; Frurip, D. J.; McDonald, R. A.; Syverud, A. N. (JANAF Thermochemical Tables, 3rd Ed., 1985; J. Phys. Chem. Ref. Data Suppl. **14** No. 1 [1985] 1006,1271).
[5] Willis, C.; Lossing, F. P.; Back, R. A. (Can. J. Chem. **54** [1976] 1/3).
[6] Wiberg, N.; Fischer, G.; Bachhuber, H. (Z. Naturforsch. **34b** [1979] 1385/90).
[7] Pople, J. A.; Curtiss, L. A. (J. Chem. Phys. **95** [1991] 4385/8).
[8] Walch, S. P. (J. Chem. Phys. **91** [1989] 389/94).
[9] Brandemark, U.; Siegbahn, P. E. M. (Theor. Chim. Acta **66** [1984] 217/32).
[10] Whitelegg, D.; Woolley, R. G. (J. Mol. Struct. **209** [1990] 23/31 [THEOCHEM **68**]).

[11] Casewit, C. J.; Goddard, W. A., III (J. Am. Chem. Soc. **102** [1980] 4057/62).
[12] Ahlrichs, R.; Staemmler, V. (Chem. Phys. Letters **37** [1976] 77/81).
[13] Jensen, H. J. A.; Joergensen, P.; Helgaker, T. (J. Am. Chem. Soc. **109** [1987] 2895/901).
[14] Baird, N. C.; Wernette, D. A. (Can. J. Chem. **55** [1977] 350/4).
[15] Winter, N. W.; Pitzer, R. M. (J. Chem. Phys. **62** [1975] 1269/75).
[16] Schaad, L. J.; Kinser, H. B. (J. Phys. Chem. **73** [1969] 1901/11).
[17] Radom, L.; Hehre, W. J.; Pople, J. A. (J. Am. Chem. Soc. **93** [1971] 289/300).
[18] Ibrahim, M. R.; Schleyer, P. v. R. (J. Comp. Chem. **6** [1985] 157/67).
[19] Kao, J.; Huang, T. N. (J. Am. Chem. Soc. **101** [1979] 5546/57).
[20] Kao, J.; Leister, D. (J. Am. Chem. Soc. **110** [1988] 7286/91).

2.2.5.4 Chemical Behavior

2.2.5.4.1 Isomerization

Trans-Cis Isomerization

Only *trans*-diazene has been unambiguously identified; it also seems to be the predominant isomer in the gas phase. However, there is evidence that *cis*-diazene is the reactive species in many reactions. The isomerization process, involving a change of configuration at the N=N bond, therefore is of great interest and was the subject of numerous ab initio studies at various levels of theory and of a few semiempirical investigations [1 to 20]. In the literature cited *cis*-N_2H_2 is always placed higher in energy than *trans*-N_2H_2. The most relevant results for the energy difference tend to be between 21 and 30 kJ/mol; compare the literature above cited and [21 to 29]. However, two older semiempirical calculations [30, 31] predicted in contrast *cis*-N_2H_2 to be the more stable isomer (by about 19 to 33 kJ/mol). Four main isomerization pathways are discussed: (1) inversion at one end through an in-plane asymmetric bending motion, (2) rotation around the N=N bond, (3) dissociation and recombination of one N-H bond, and (4) a radical chain mechanism. For these four pathways nearly all calculations show a considerably high barrier for the isomerization reaction and even the best estimates are not in agreement with experimental results, specifically the temperature dependence of N_2H_2 decomposition (activation energy of 17.6 kJ/mol; see below) or isomerization reactions which readily proceed at room temperature. Calculations show that the inversion (1) is usually favored over rotation (2), as the reaction barriers were found to be between 193 to 213 kJ/mol for inversion [3, 5, 6, 8 to 11, 14, 17, 18, 32] and between 230 to 351 kJ/mol for rotation [4, 8, 10, 11, 13, 14, 18]. Orbital symmetry reflections in agreement with ab initio MO calculations predict that isomerization via (2) is forbidden for N_2H_2 in the ground and excited $^3(\pi^*,\pi)$ states and only allowed in the excited states $^1(\pi^*,n)$ and $^3(\pi^*,n)$ [14]. The activation energy for the dissociation-recombination mechanism (3) was calculated to be 276 to 318 kJ/mol [6]. Assuming the barrier of the NH bond rupture to be approximately equal to ΔH for this process, the activation energy for pathway (3) was found to be 299 kJ/mol [4]. The radical chain mechanism (4) via hydrazyl radical formation, on the other hand, was found to be consistent [4] with the experimental activation energy of 17.6 kJ/mol for the *trans*-N_2H_2 decomposition observed by [33]. However, this mechanism is questioned [34] because it is incompatible with the observed kinetics for the thermal and photochemical reactions [33, 35]. Besides the four main isomerization pathways discussed above isomerization by a surface reaction, by quantum mechanical tunneling, or by a concerted hydrogen exchange, for example with NH_3 (the four-centered hydrogen structure was detected in low-temperature matrices [36]), was proposed, but these mechanisms are not in satisfactory agreement with the kinetics observed or the deuterium effect expected [33].

A theoretical investigation found that the solvent effect, mainly related to the hybridization state of the nitrogens and to the relative orientation of their lone pairs, lowers the barrier of pathways (1) and (2) and stabilizes *cis*-N_2H_2 with respect to *trans*-N_2H_2 [2].

A study of the classical dynamics for the isomerization of vibrationally excited *trans*-N_2H_2 showed that the Coriolis coupling of the NH stretches and NNH bends to torsion is responsible for the energy transfer to and from the torsion and that isomerization via a planar bending mechanism does not take place [37] (see also [38]).

From studies of the thermal decomposition of N_2H_2 in the gas phase (see p. 60), the Arrhenius expressions $k(N_2H_2)=1.8\ \exp(-17.6\ \text{kJ}\cdot\text{mol}^{-1}/RT)\ \text{s}^{-1}$ and $k(N_2D_2)=\exp(-18.4\ \text{kJ}\cdot\text{mol}^{-1}/RT)\ \text{s}^{-1}$ for the homogeneous isomerization were deduced (T = 320 to 430 K) assuming that the rate-determining step is the isomerization of *trans*-N_2H_2 [33]. In [39] $k(N_2H_2)=1\times10^{-2}\ \text{s}^{-1}$ at 373 K was estimated.

trans-Diazene$\rightleftharpoons$1,1-Diazene Isomerization

An example for a structural isomerism is the *trans*-diazene$\rightleftharpoons$1,1-diazene isomerization reaction. The most relevant ab initio calculations show that *trans*-N_2H_2 is more stable than 1,1-diazene by 85 to 145 kJ/mol [5, 21 to 24, 26, 40 to 42]. Two possible pathways for the rearrangement, a unimolecular 1,2-hydrogen shift assumed to proceed via a planar transition state and a dissociation-recombination reaction, were extensively studied. SCF calculations including electron correlation yielded energy barriers of 300 to 367 kJ/mol for the hydrogen-shift pathway [3, 5, 6, 26, 41]. The Hartree-Fock model is unable to give even a qualitatively correct description of the unimolecular hydrogen shift. The out-of-plane transition state, which is obtained at the Hartree-Fock level [3, 41], becomes planar as electron correlation is considered in the structure optimization [22]. Several authors found the dissociation-recombination pathway to have a significantly lower energy barrier [4, 6, 22, 43]. But it has to be kept in mind that the recombination is unlikely to proceed, as the diazenyl radical was found to be unstable [22]. Since the activation energy for a bimolecular hydrogen exchange reaction was found to be quite low (17.9 kJ/mol, SCF), the isomerization is expected to proceed via a bimolecular hydrogen rather than a unimolecular 1,2-hydrogen shift or a dissociation-recombination mechanism [44].

The energy barrier for the isomerization in the triplet states (triplet *trans*-N_2H_2 lies 175 kJ/mol above singlet *trans*-N_2H_2) was calculated to be 148.1 kJ/mol. The height of the energy barriers for both the singlet and triplet states suggests that the isomerization is unlikely to proceed at room temperature [41].

References:

[1] McKnee, M. L.; Squillacote, M. E.; Stanbury, D. M. (J. Phys. Chem. **96** [1992] 3266/72).
[2] Persico, M.; Tomasi, J. (Croat. Chem. Acta **57** [1984] 1395/409).
[3] Pople, J. A.; Raghavachari, K.; Frisch, M. J.; Binkley, J. S.; Schleyer, P. v. R. (J. Am. Chem. Soc. **105** [1983] 6389/99).
[4] Casewit, C. J.; Goddard, William A., III (J. Am. Chem. Soc. **102** [1980] 4057/62).
[5] Parsons, C. A.; Dykstra, C. E. (J. Chem. Phys. **71** [1979] 3025/33).
[6] Pasto, D. J.; Chipman, D. M. (J. Am. Chem. Soc. **101** [1979] 2290/6).
[7] Flood, E.; Skancke, P. N. (Chem. Phys. Lett. **54** [1978] 53/6).
[8] Cimiraglia, R.; Riera, J. M.; Tomasi, J. (Theor. Chim. Acta **46** [1977] 223/35).
[9] Howell, J. M.; Kirschenbaum, L. J. (J. Am. Chem. Soc. **98** [1976] 877/85).
[10] Ahlrichs, R.; Staemmler, V. (Chem. Phys. Lett. **37** [1976] 77/81).

[11] Winter, N. W.; Pitzer, R. M. (J. Chem. Phys. **62** [1975] 1269/75).
[12] Wagnière, G. (Theor. Chim. Acta **31** [1973] 269/74).
[13] Merenyi, G.; Wettermark, G.; Roos, B. (Chem. Phys. **1** [1973] 340/7).
[14] Baird, N. C.; Swenson, J. R. (Can. J. Chem. **51** [1973] 3097/101).
[15] Radom, L.; Hehre, W. J.; Pople, J. A. (J. Am. Chem. Soc. **93** [1971] 289/300).
[16] Wong, D. P.; Fink, W. H.; Allen, L. C. (J. Chem. Phys. **52** [1970] 6291/8).
[17] Schaad, L. J.; Kinser, H. B. (J. Phys. Chem. **73** [1969] 1901/11).
[18] Lehn, J. M.; Munsch, B. (Theor. Chim. Acta **12** [1968] 91/4).
[19] Chantranupong, L. (J. Sci. Soc. Thailand **9** [1983] 187/90).
[20] Li, X.; Sun, C. (Gaodeng Xuexiao Huaxue Xuebao **10** [1989] 1238/41).

[21] Whitelegg, D.; Woolley, R. G. (J. Mol. Struct. **209** [1990] 23/31 [THEOCHEM **68**]).
[22] Jensen, H. J. A.; Joergensen, P.; Helgakaer, T. (J. Am. Chem. Soc. **109** [1987] 2895/901).
[23] Walch, S. P. (J. Chem. Phys. **91** [1989] 389/94).
[24] Walch, S. P. (J. Chem. Phys. **94** [1991] 6937).
[25] Brandemark, U.; Siegbahn, P. E. M. (Theor. Chim. Acta **66** [1984] 217/32).
[26] Pople, J. A.; Krishan, R.; Schlegel, H. B.; Binkley, J. S. (Int. J. Quantum Chem. **14** [1978] 565/60).
[27] Bigot, B.; Sevin, A.; Devaquet, A. (J. Am. Chem. Soc. **100** [1978] 2639/42).

[28] Vasudevan, K.; Peyerimhoff, S. D.; Buenker, R. J.; Kammer, W. E.; Hsu, H. L. (Chem. Phys. **7** [1975] 187/209).
[29] Robin, M. B.; Hart, R. R.; Kuebler, N. A. (J. Am. Chem. Soc. **89** [1967] 1564/72).
[30] Alster, J.; Burnelle, L. (J. Am. Chem. Soc. **89** [1967] 1261/3).

[31] Gordon, M. S.; Fischer, H. (J. Am. Chem. Soc. **90** [1968] 2471/6).
[32] Skancke, P. N. (Chem. Phys. Lett. **47** [1977] 259/64).
[33] Willis, C.; Back, R. A.; Purdon, J. G. (Int. J. Chem. Kinet. **9** [1977] 787/809).
[34] Back, R. A. (Rev. Chem. Intermed. **5** [1984] 293/323).
[35] Willis, C.; Back, R. A.; Parsons, J. M. (J. Photochem. **6** [1977] 253/64).
[36] Bondybey, V. E.; Nibler, J. W. (J. Chem. Phys. **58** [1973] 2125/34).
[37] Spears, L. G., Jr.; Hutchinson, J. S. (J. Chem. Phys. **88** [1988] 250/9).
[38] Spears, L. G., Jr.; Hutchinson, J. S. (J. Chem. Phys. **88** [1988] 240/9).
[39] Vidyarthi, S. K.; Willis, C.; Back, R. A.; McKitrick, R. M. (J. Am. Chem. Soc. **96** [1974] 7647/50).
[40] Baird, N. C.; Wernette, D. A. (Can. J. Chem. **55** [1977] 350/4).

[41] Ito, K.; Nagase, S. (Chem. Phys. Lett. **126** [1986] 531/6).
[42] Pople, J. A.; Curtiss, L. A. (J. Chem. Phys. **95** [1991] 4385/8).
[43] Pasto, D. J. (J. Am. Chem. Soc. **101** [1979] 6852/7).
[44] Kemper, M. J. H.; Buck, H. M. (Can. J. Chem. **59** [1981] 3044/8).

2.2.5.4.2 Decomposition

In the Gas Phase

N_2H_2, prepared by microwave discharge through N_2H_4 vapor and collected at 77 K, is always accompanied by a manifold excess of NH_3; it shows no sign of decomposition below 208 K. The major decomposition products are H_2, N_2, and N_2H_4. N_2D_2 dissociates almost completely into N_2 and N_2D_4. No azide formation was detected, neither for N_2H_2 nor for N_2D_2. The **thermal** decomposition, studied as a function of sample size, pressure, and temperature, shows essentially a first-order kinetics between 320 and 433 K (between 320 and 575 K, see [1]) if the effects of self-heating and surface catalysis are taken into account. The Arrhenius expressions $k_1(N_2H_2)=1.8\ \exp(-17.6\ kJ\cdot mol^{-1}/RT)\ s^{-1}$ and $k_1(N_2D_2)=1.0\ \exp(-18.4\ kJ\cdot mol^{-1}/RT)\ s^{-1}$ were derived. The first step in the decomposition process is probably the rapid trans-cis isomerization which is followed by reactions of the more reactive *cis*-N_2H_2 isomer

$$cis\text{-}N_2H_2+trans\text{-}N_2H_2\rightarrow N_2+N_2H_4\ (1)$$

$$cis\text{-}N_2H_2+trans\text{-}N_2H_2\rightarrow N_2+H_2+trans\text{-}N_2H_2\ (2)$$

[2]. The results of the preceding kinetic investigations [3 to 5] showed that reactions (1),

$$cis\text{-}N_2H_2\rightarrow N_2+H_2\ (3),$$

and a competitive reaction between reactions (1) and (3) are insufficient to describe the diazene decomposition, following the more comprehensive investigations of [2]. Possible pathways for the decomposition into N_2H_4 and N_2 were investigated by ab initio SCF calculations; a mechanism where reactions (1) and (2) are preceded by trans-cis isomerization is supported by calculation, but the estimated overall activation energy is much higher than the observed one [6]. Decomposition only into N_2 and H_2 was observed at low pressures (0.1 Torr) [7] and is believed to arise from the concerted decomposition of *cis*-N_2H_2. However, this unimolecular reaction is symmetry-forbidden for *cis*-N_2H_2 and symmetry-allowed for the trans isomer. Ab initio CAS SCF and CI studies [8] on the question whether diazene dissociates stepwise or by a simultaneous fission showed that the stepwise dissociation is preferred, even though the concerted dissociation is very close in energy.

Gaseous N_2H_2, prepared by pyrolysis of alkali metal tosylhydrazides followed by rapid trapping at 77 K, is almost free of NH_3; compared to the N_2H_2 used above, it shows a different decomposition behavior. Thermolysis via disproportionation to N_2 and N_2H_4 is the predominant reaction path at 393 K, but also simple decomposition into N_2 and H_2, dimerization via tetrazene to $NH_4^+N_3^-$, and cleavage to N_2 and NH_3 take place [9].

An empirical relation, which relates the activation parameters for the homolysis of various *trans*-azo compounds with thermodynamic quantities, allows one to estimate the activation energy for the stepwise homolysis of *trans*-N_2H_2: Activation energies between 223 to 240 kJ/mol were given [10]. Based on GVB CI calculations, a significantly higher value for the NH bond energy in *trans*-N_2H_2, 299 kJ/mol, was estimated [11].

Photolytic decomposition of *trans*-N_2H_2, produced by the hydrazine discharge method, into N_2 and H_2 was examined at room temperature at wavelengths between 310 and 405 nm. A radical chain mechanism was proposed:

$$N_2H_2 + h\nu \rightarrow N_2 + 2\,H \text{ or } H + N_2H \quad (4)$$

$$H + N_2H_2 \rightarrow H_2 + N_2H \qquad\qquad N_2H \rightarrow N_2 + H$$

The primary photodissociation probably occurs from high vibrational levels of the electronic ground state reached by rapid intersystem crossing directly from the originally excited ^1B_g state. No evidence was found for collisional deexcitation, and the dissociation via reaction (4) occurred with a quantum yield close to unity. Some molecular dissociation into N_2 and H_2 can not be excluded, because this process is symmetry-allowed for *cis*-N_2H_2 [1, 12]. The successive fission of the NH bonds is predicted from ab initio SCF CI studies to be the preferred pathway in the photolysis of *cis*-N_2H_2 [13, 14]. The photolytic decomposition into N_2 and H_2 was already observed earlier in a few qualitative experiments at very low pressures ($<$ 0.1 Torr) [9].

In Solution

The rapid decomposition of N_2H_2, generated in situ in solution (e.g. in ether) into N_2 and N_2H_4 in the absence of a reactive substrate, can be interpreted as self-reduction via a cyclic intermediate complex. Only under extremely basic conditions nearly complete decomposition into N_2 and H_2 is observed, probably via $N_2H_2 + OH^- \rightarrow H_2O + N_2H^-$, $N_2H^- \rightarrow N_2 + H^-$, and $H^- + HB \rightarrow H_2 + B^-$ [15, 16]. The acid-catalyzed decomposition in ethereal solution at low temperatures leads to dimerization via tetrazene to NH_4N_3 [17].

The decomposition of N_2H_2 in liquid NH_3 at temperatures from 208 to 235 K was observed spectrophotometrically. N_2H_2 was found to be much more stable in NH_3 than in the gas phase at room temperature. A rapid initial disappearance with a reaction order greater than one was observed, followed by a first-order decay with $k = 1.9 \times 10^3 \exp(-27.6\ kJ \cdot mol^{-1}/RT)\ s^{-1}$ [18].

In the Solid State

N_2H_2 (NH_3-free) decomposes quite rapidly at temperatures as low as 113 K into N_2 and N_2H_4 with small yields of NH_4N_3 and H_2 [9]; see also [19].

References:

[1] Back, R. A. (Rev. Chem. Intermed. **5** [1984] 293/323).
[2] Willis, C.; Back, R. A.; Purdon, J. G. (Int. J. Chem. Kinet. **9** [1977] 787/809).
[3] Willis, C.; Back, R. A. (Can. J. Chem. **51** [1973] 3605/19).
[4] Willis, C.; Back, R. A. (Nature **241** [1973] 43).
[5] Vidyarthi, S. K.; Willis, C.; Back, R. A.; McKitrick, R. M. (J. Am. Chem. Soc. **96** [1974] 7647/50).
[6] Pasto, D. J. (J. Am. Chem. Soc. **101** [1979] 6852/7).
[7] Mock, W. L. (Diss. Harvard Univ. 1965, pp. 1/176, 1/68; Diss. Abstr. **26** [1965/66] 6374).
[8] Brandemark, U.; Siegbahn, P. E. M. (Theor. Chim. Acta **66** [1984] 217/32).
[9] Wiberg, N.; Fischer, G.; Bachhuber, H. (Chem. Ber. **107** [1974] 1456/71).
[10] Mendenhall, G. D.; Chen, H.-T. E. (J. Phys. Chem. **89** [1985] 2849/51).

[11] Casewit, C. J.; Goddard, W. A., III (J. Am. Chem. Soc. **102** [1980] 4057/62).
[12] Willis, C.; Back, R. A.; Parsons, J. M. (J. Photochem. **6** [1977] 253/64).
[13] Bigot, B.; Sevin, A.; Devaquet, A. (J. Am. Chem. Soc. **100** [1978] 2639/42).
[14] Sevin, A.; Bigot, B.; Devaquet, A. (Tetrahedron **34** [1978] 3275/80).
[15] Hünig, S.; Müller, H. R.; Thier, W. (Angew. Chem. **75** [1963] 298; Angew. Chem. Int. Ed. Engl. **2** [1963] 214/5).
[16] Hünig, S.; Müller, H. R.; Thier, W. (Angew. Chem. **77** [1965] 368/77; Angew. Chem. Int. Ed. Engl. **4** [1965] 271).
[17] Wiberg, N.; Häring, H. W.; Vasisht, S. K. (Z. Naturforsch. **34b** [1979] 356/7).
[18] Back, R. A.; Willis, C. (Can. J. Chem. **52** [1974] 2513/5).
[19] Wiberg, N.; Bachhuber, H.; Fischer, G. (Angew. Chem. **84** [1972] 889/90; Angew. Chem. Int. Ed. Engl. **11** [1972] 829/30).

2.2.5.4.3 Hydrogenation Reactions

Unsaturated organic compounds can be hydrogenated with N_2H_2 in the gas and the liquid phase. Due to the highly functional selectivity and stereoselectivity, hydrogenation with N_2H_2 in the **liquid phase** is a useful alternative to catalytic hydrogenation. N_2H_2 reduces nonpolar carbon-carbon and nitrogen-nitrogen bonds. Polar functional groups such as NO_2, C≡N, C=N, S=O, and C=O are usually inert towards N_2H_2 under conditions in which the nonpolar multiple bonds are reduced. The hydrogenation is carried out with in situ prepared N_2H_2 in a variety of solvents or solvent mixtures in the temperature range from 258 to 423 K. The yields increase occasionally above 90%; they decrease with increasing substitution at the multiple bond. Trans double bonds are more rapidly attacked than cis double bonds. *cis*-N_2H_2 appears to be the most favorable structure for the concerted transfer of two hydrogen atoms to an unsaturated compound. Aside of simple and sterically hindered alkenes and alkines, alkyl- or aryl allenes, and conjugated dienes, cyclic compounds (e.g. norbornadienes or endoperoxides), azobenzenes, and phenanthrenes are reduced by N_2H_2. A recently published review [1] surveys the literature up to mid-1988 and tabulates the reduction processes with diazene; in addition to the procedure and the reaction conditions, the yields are also given. For older, less informative reviews on the hydrogenation with N_2H_2 in solution, see [2 to 5].

In the **gas phase** the reaction of N_2H_2 (produced by the hydrazine discharge method) with a great number of unsaturates, e.g. ethylene, propene, 2-butene, 1,3-cyclohexadiene, azomethane, and acetylene, was examined, and relative reaction rates were determined. At room temperature only little reaction was observed, but at 372 K hydrogenation prevailed with a reasonable efficiency over self-reduction [6, 7]. An earlier proposal for the mechanism

[6], i.e. a simple bimolecular reaction with *cis*-N_2H_2 via a six-membered cyclic transition state, was later revised by the same group [7]. Inconsistencies between the kinetic data suggested a competition between the reaction of N_2H_2 with the unsaturated compound and the normal decay process according to

$$trans\text{-}N_2H_2 \rightarrow cis\text{-}N_2H_2$$

$$cis\text{-}N_2H_2 \rightarrow N_2 + H_2 \qquad trans\text{-}N_2H_2 + cis\text{-}N_2H_2 \rightarrow N_2 + N_2H_4$$

$$\text{alkene} + cis\text{-}N_2H_2 \rightarrow N_2 + \text{alkane}$$

Isomerization is the rate-determining process. In addition to direct hydrogenation, adduct formation, probably a π complex between *cis*-N_2H_2 and the unsaturate, was suggested. The complex then either undergoes a rearrangement to yield the hydrogenation products or it can hydrogenate *trans*-N_2H_2 or another unsaturated compound [7]. The reaction of N_2H_2 (prepared by thermolysis of alkali metal tosylhydrazides) with CCl_4 is mentioned in [8]; only 3% of N_2H_2 reacted with CCl_4.

The reaction of *cis*-N_2H_2 with unsaturates, mainly ethylene, via a six-membered cyclic activated complex was treated theoretically assuming that the dihydrogen transfer proceeds in a concerted way [9 to 15]. Two recent semiempirical SCF MO studies (AM1 and MINDO) took a look at the hydrogenation not only via the concerted, but also examined a stepwise mechanism. Whereas the AM1 method favors the concerted hydrogen transfer, the MINDO method favors the stepwise pathway [16, 17].

References:

[1] Pasto, D. J. (Org. React. [N.Y.] **40** [1991] 91/155).
[2] Back, R. A. (Rev. Chem. Intermed. **5** [1984] 293/323).
[3] Veefkind, A. (Chem. Tech. [Amsterdam] **23** [1968] 69/72).
[4] Hünig, S.; Müller, H. R.; Thier, W. (Angew. Chem. **77** [1965] 368/77; Angew. Chem. Int. Ed. Engl. **4** [1965] 271).
[5] Miller, C. E. (J. Chem. Educ. **42** [1965] 254/9).
[6] Vidyarthi, S. K.; Willis, C.; Back, R. A.; McKitrick, R. M. (J. Am. Chem. Soc. **96** [1974] 7647/50).
[7] Willis, C.; Back, R. A.; Parsons, J. M.; Purdon, J. G. (J. Am. Chem. Soc. **99** [1977] 4451/6).
[8] Wiberg, N.; Fischer, G.; Bachhuber, H. (Chem. Ber. **107** [1974] 1456/71).
[9] McKnee, M. L.; Squillacote, M. E.; Stanbury, D. M. (J. Phys. Chem. **96** [1992] 3266/72).
[10] Pasto, D. J. (J. Am. Chem. Soc. **101** [1979] 6852/7).

[11] Pasto, D. J.; Chipman, D. M. (J. Am. Chem. Soc. **101** [1979] 2290/6).
[12] Flood, E.; Skancke, P. N. (Chem. Phys. Lett. **54** [1978] 53/6).
[13] Skancke, P. N. (Chem. Phys. Lett. **47** [1977] 259/64).
[14] Zhuravlev, V. I.; Krivoshei, I. V.; Sleta, L. A. (Zh. Strukt. Khim. **16** [1975] 951/5; J. Struct. Chem. [USSR] **16** [1975] 876/9).
[15] Sana, M.; Leroy, G. (J. Mol. Struct. **109** [1984] 251/69 [THEOCHEM **18**]).
[16] Agrafiotis, D. K.; Rzepa, H. S. (J. Chem. Soc. Perkin Trans. II **1989** 475/88).
[17] Agrafiotis, D. K.; Rzepa, H. S. (J. Chem. Soc. Chem. Commun. **1987** 902/4).

2.2.5.4.4 Miscellaneous Reactions

Electrons. The mass spectrum of gaseous N_2H_2 (at 70 eV) shows, aside of the peaks for the molecular ions $N_2H_2^+$ and $N_2H_2^{2+}$, mainly peaks for ions with an intact nitrogen chain, such as N_2H^+ and N_2^+. Ions formed by rupture of the N=N bond, i.e. NH_2^+, NH^+, and N^+, notably have low intensity (<10%) [1 to 3]. The spectrum at 20 eV shows only peaks for $N_2H_2^+$ and N_2H^+ [3, 4]. The mass spectra of the mono- and dideutero diazene show the same characteristic features as the spectrum of N_2H_2 [2]. Appearance potentials AP (given in eV) were determined to be $AP(N_2H_2^+) = 9.7 \pm 0.1$, $AP(N_2H^+) = 10.98 \pm 0.05$, and $AP(N_2^+) = 14.00 \pm 0.05$ [5]. Deuteration seems to have not much influence on the value of the appearance potentials; compare $AP(N_2HD^+) = 9.84 \pm 0.3$ and $AP(N_2D_2^+) = 9.42 \pm 0.3$ [2].

F. Using an arrested-relaxation infrared-chemiluminescence technique, the reaction with N_2H_2 generated by thermolysis of Na tosylhydrazide was studied between 353 and 397 K. The reaction is very fast and yields vibrationally excited HF via $F + N_2H_2 \rightarrow HF(v \leq 5) + N_2H$ ($\Delta H_0^\circ = -305$ kJ/mol). The initial vibrational energy distribution of HF is inverted, peaking at HF(v=2). It was assumed that the reaction occurs without the formation of a long-lived intermediate species and that perhaps the excess energy (the maximum vibrational excitation possible is v=7) partly remains in the N_2H fragment which then may dissociate [6].

H_2. Ab initio SCF calculations (using various basis sets) of the hydrogenation energy for the reaction $N_2H_2 + 2\,H_2 \rightarrow 2\,NH_3$ gave values between −340.6 and −379.5 kJ/mol (the experimental value at 0 K, corrected for zero-point vibrations, from thermodynamic and spectroscopic data is −349.4 kJ/mol) [7, 8].

N_2. Ab initio SCF calculations at various levels were performed on the symmetric dihydrogen transfer reaction *cis*-$N_2H_2 + N_2$; a pericyclic transition structure with synchronous motion of the transferring hydrogen atoms was derived [9].

O_2. N_2H_2 (from metal tosylhydrazides) causes a slow reduction of O_2 to H_2O_2 at 77 K [3].

HF. A semiempirical calculation on the structure of the hydrogen-bonded $N_2H_2 \cdot HF$ complex shows that the nitrogen-bonded complex is more stable than the fluorine-bonded complex [10].

N_2H_2. The acid-catalyzed decomposition leads by dimerization via tetrazene to ammonium azide [11]. Spectrophotometrically, the absolute rate constant for the reaction of N_2H_2 with itself in aqueous solution (at pH≈6) was determined to be 2.0×10^4 $L \cdot mol^{-1} \cdot s^{-1}$ at 298 K [12]. The reactions of *cis*-N_2H_2 with *trans*-N_2H_2 and with *cis*-N_2H_2 were investigated by ab initio methods at various levels [13, 14]. In all cases hydrogen-bonded complexes were found. Calculations of the reaction barriers revealed that it is necessary to include electron correlation which was not done earlier [14]. The formation of tetrazetidine by the reaction of two *trans*-N_2H_2 molecules was investigated by ab initio calculations (see p. 171) [15].

N_2H_4. Ab initio calculations at various levels showed the reaction *trans*-N_2H_2 with N_2H_4 to proceed probably via a pericyclic transition structure, although the exact transition structure could not be located [9].

Complexes. The structures and some properties of complexes, such as $HN{=}NH \cdot BeF_2$ [16], $N_2H_2 \cdot H_3O^+$ [17], $N_2H_2 \cdot Li^+$ [18], $Ni(PH_3)_2 \cdot$*trans*-N_2H_2 [19], and of $Ni(HNC)_2 \cdot$*trans*-N_2H_2 [20], were investigated by ab initio and semiempirical calculations.

References:

[1] Wiberg, N.; Bachhuber, H.; Fischer, G. (Angew. Chem. **84** [1972] 889/90; Angew. Chem. Int. Ed. Engl. **11** [1972] 829/30).

[2] Holzmann, G.; Minkwitz, R. (Z. Anorg. Allg. Chem. **413** [1975] 72/6).

[3] Wiberg, N.; Fischer, G.; Bachhuber, H. (Chem. Ber. **107** [1974] 1456/71).

[4] Wiberg, N.; Fischer, G.; Bachhuber, H. (Angew. Chem. **88** [1976] 386/7; Angew. Chem. Int. Ed. Engl. **15** [1976] 385).
[5] Willis, C.; Lossing, F. P.; Back, R. A. (Can. J. Chem. **54** [1976] 1/3).
[6] Back, R. A.; Neudorfl, P. S.; Sloan, J. J.; Wassell, P. T. (Can. J. Chem. **65** [1987] 451/5).
[7] Radom, L.; Hehre, W. J.; Pople, J. A. (J. Am. Chem. Soc. **93** [1971] 289/300).
[8] Hariharan, P. C.; Pople, J. A. (Theor. Chim. Acta **28** [1973] 213/22).
[9] McKnee, M. L.; Stanbury, D. M. (J. Am. Chem. Soc. **114** [1992] 3214/9).
[10] Sabin, J. R. (Theor. Chim. Acta **27** [1972] 69/74).

[11] Wiberg, N.; Haering, H. W.; Vasisht, S. K. (Z. Naturforsch. **34b** [1979] 356/7).
[12] Stanbury, D. M. (Inorg. Chem. **30** [1991] 1293/6).
[13] McKnee, M. L.; Squillacote, M. E.; Stanbury, D. M. (J. Phys. Chem. **96** [1992] 3266/72).
[14] Pasto, D. J. (J. Am. Chem. Soc. **101** [1979] 6852/7).
[15] Ritter, G.; Häfelinger, G.; Lüddecke, E.; Rau, H. (J. Am. Chem. Soc. **111** [1989] 4627/35).
[16] Kogan, V. A.; Kharabaev, N. N.; Osipov, O. A.; Polunin, A. A.; Egorov, A. S.; Ivanova, N. A. (3rd Int. Symp. Specific Interact. Mol. Ions Proc., Wroclaw-Karpacz, Pol., 1976, Vol. 2, pp. 330/5).
[17] Jones, W. H.; Mariani, R. D.; Lively, M. L. (Chem. Phys. Lett. **108** [1984] 602/8).
[18] Del Bene, J. E.; Frisch, M. J.; Raghavachari, K.; Pople, J. A.; Schleyer, P. R. (J. Phys. Chem. **87** [1983] 73/8).
[19] Rosi, M.; Sgamellotti, A.; Tarantelli, A.; Floriani, C.; Cederbaum, L. S. (J. Chem. Soc. Dalton Trans. **1989** 33/8).
[20] Tatsumi, K.; Fueno, T.; Nakamura, A.; Otsuka, S. (Bull. Chem. Soc. Jpn. **49** [1976] 2170/7).

2.2.6 The Diazene Cation, $N_2H_2^+$

Systematic name: Diazenylium(1+)

CAS Registry Numbers: $N_2H_2^+$ *[76986-17-9]*, *trans*-$N_2H_2^+$ *[59952-06-6]*, *cis*-$N_2H_2^+$ *[86631-37-0]*, *trans*-$N_2D_2^+$ *[59952-07-7]*

$N_2H_2^+$ (together with other products) is formed in collisions of N_2H_4 with O^+, Ar^+, and Kr^+ ions at center-of-mass collision energies between 1 and 30 eV according to the scheme $O^+(Ar^+, Kr^+) + N_2H_4 \rightarrow O(Ar, Kr) + N_2H_2^+ + H_2$. The reactions of O^+ with N_2H_4 and its derivatives are important chemical processes in the plasma environment surrounding spacecraft in low earth orbit [1]. The formation of $HNNH^+$ as an intermediate in the reaction $N_2^+ + H_2 \rightarrow N_2H^+ + H$ was discussed [2].

The appearance potential for $N_2H_2^+$ from N_2H_4 is 10.75 ± 0.08 eV ($N_2H_4 + e^- \rightarrow N_2H_2^+ + H_2 + 2\ e^-$) [3] replacing an older value of 10.98 ± 0.2 eV [4]. Other authors [5 to 7] obtained (partly not reproducible) values in the range 9.7 to 11.9 eV. A second appearance potential of 16.6 ± 0.1 eV ($N_2H_4 + e^- \rightarrow N_2H_2^+ + 2\ H + 2\ e^-$) was also reported [7].

The enthalpy of formation of $N_2H_2^+$ was obtained by combining the enthalpy of formation of N_2H_2 (determined with the appearance potential given above; see p. 56) with the ionization energy of N_2H_2 yielding for *trans*-$N_2H_2^+$ $\Delta_fH^\circ_{298} = 1137$ kJ/mol. For *cis*-$N_2H_2^+$ $\Delta_fH^\circ_{298} = 1150$ kJ/mol was derived [9] from an ionization energy, which was apparently estimated, and by considering a 20 kJ/mol higher energy for *cis*-N_2H_2 based on calculations by [8].

From the photoelectron spectrum (PES) of gaseous *trans*-N_2H_2 and *trans*-N_2D_2 [10, 11], the following term energies T_0 and vibrational frequencies ν for various electronic states (all of C_{2h} symmetry) of the ion are known [12]:

	$\tilde{X}\ ^2A_g$		$\tilde{A}\ ^2A_u$	$\tilde{B}\ ^2B_u$	$\tilde{C}\ ^2A_g$
trans-N_2H_2					
T_0 in cm^{-1}	0		36390(160)	41310(160)	53250(160)
ν in cm^{-1}	~1850	1180(30)	1110(30)	1170(30)	940(30)
appr. type of mode	NN stretch	NNH bend	NN stretch	NNH bend	NNH bend
trans-N_2D_2					
T_0 in cm^{-1}	0		36310(160)	40990(160)	
ν in cm^{-1}	1020(30)		1110(30)	960(30)	
appr. type of mode	NND bend		NN stretch	NND bend	

The geometry of the ground-state ion was deduced from the vibrational structure of the corresponding band in the PES. Compared to the neutral species, the angle is widened by about 20° and the NN bond is slightly shortened; cf. p. 47. The following table compares these data with the results of ab initio calculations:

molecule	r(N-N) in Å	r(N-H(D)) in Å	∠H(D)NN	method	Ref.
trans-$N_2H_2^+$	1.222	1.045	127°	PES	[10]
trans-$N_2D_2^+$	1.232	1.051	127°	PES	[10]
trans-$N_2H_2^+$	1.186	1.045	123.5°	MP2/6-31G*	[13]
trans-$N_2H_2^+$	1.19	1.02	128°	CI/4-31G	[14]
cis-$N_2H_2^+$	1.173	1.047	132.5°	MP2/6-31G*	[13]
cis-$N_2H_2^+$	1.17	1.02	138°	CI/4-31G	[14]

trans-$N_2H_2^+$ was calculated to be more stable than *cis*-$N_2H_2^+$ by 27.5 (MP2/6-31G*) [13] and 28.9 kJ/mol (CI/4-31G), respectively [14]. Ab initio calculations on *cis*-$N_2H_2^+$ as a function of the angle HNN were reported in [15].

References:

[1] Gardner, J. A.; Dressler, R. A.; Salter, R. H.; Murad, E. (J. Phys. Chem. **96** [1992] 4210/7).

[2] Schultz, R. H.; Armentrout, P. B. (J. Chem. Phys. **96** [1992] 1036/45, 1039).

[3] Foner, S. N.; Hudson, R. L. (J. Chem. Phys. **68** [1978] 3162/8).

[4] Foner, S. N.; Hudson, R. L. (J. Chem. Phys. **28** [1958] 719/20).

[5] Wiberg, N.; Fischer, G.; Bachhuber, H. (Z. Naturforsch. **34b** [1979] 1385/90).

[6] Willis, C.; Lossing, F. P.; Back, R. A. (Can. J. Chem. **54** [1976] 1/3).

[7] Dibeler, V. H.; Franklin, J. L.; Reese, R. M. (J. Am. Chem. Soc. **81** [1959] 68/73).

[8] Casewit, C. J.; Goddard, W. A., III (J. Am. Chem. Soc. **102** [1980] 4057/62).

[9] Lias, S. G.; Bartmess, J. E.; Liebman, J. F.; Holmes, J. E.; Levin, R. D.; Mallard, W. G. (J. Phys. Chem. Ref. Data Suppl. **17** No. 1 [1988] 1/861, 620).

[10] Frost, D. C.; Lee, S. T.; McDowell, C. A.; Westwood, N. P. C. (J. Chem. Phys. **64** [1976] 4719/29).

[11] Frost, D. C.; Lee, S. T.; McDowell, C. A.; Westwood, N. P. C. (Chem. Phys. Lett. **30** [1975] 26/7).

[12] Jacox, M. E. (J. Phys. Chem. Ref. Data **17** [1988] 269/511, 362).

[13] Pople, J. A.; Curtiss, L. A. (J. Chem. Phys. **95** [1991] 4385/8).

[14] Baird, N. C.; Wernette, D. A. (Can. J. Chem. **55** [1977] 350/4).

[15] Baird, N. C. (Can. J. Chem. **57** [1979] 98/103).

2.2.7 The Diazene Dication, $N_2H_2^{2+}$

Systematic name: Diazenylium(2+)

CAS Registry Number: *[63559-79-5]*

The $N_2H_2^{2+}$ ion is linear with the valence electron configuration $...(2\sigma_g)^2\ (2\sigma_u)^2\ (3\sigma_g)^2\ (1\pi)^4$ [1]. The NN bond length is noticeably shortened compared to that in N_2H_2 as was concurringly shown by ab initio HF and semiempirical calculations [1 to 4]. An HF/6-31G calculation gave an equilibrium structure with r(NN) = 1.067 and r(NH) = 1.080 Å [2]. The barrier to form $HNNH^{2+}$ from N_2H^+ and H^+ was calculated to be higher than the barrier to remove a proton to form N_2H^+ (371 and 125 kJ/mol; HF/4-31G) [1].

References:

[1] Summers, N. L.; Tyrrell, J. (J. Am. Chem. Soc. **99** [1977] 3960/5; Theor. Chim. Acta **47** [1978] 223/31).
[2] Sana, M.; Leroy, G. (J. Mol. Struct. **109** [1984] 251/69, 266 [THEOCHEM **18**]).
[3] Maksic, Z. B.; Eckert-Maksic, M.; Skancke, P. N.; Skancke, A. (J. Mol. Struct. **169** [1988] 447/57 [THEOCHEM **46**]).
[4] Oles, A. M.; Pfirsch, F.; Böhm, M. C. (Chem. Phys. **120** [1988] 65/77).

2.2.8 The Diazene Anion, $N_2H_2^-$

Systematic name: Diazylide

Other name: Hydrazylide

CAS Registry Number: *[100429-75-2]*

Ab initio calculations at the UHF level predicted a planar trans structure (^2B_g) with the geometrical data r(NN) = 1.353, r(NH) = 1.012 Å, and ∠HNN = 104.7°. The 1,2-H shift to pyramidal H_2NN^- was calculated to be endothermic by 126 kJ/mol with an energy barrier of 246 kJ/mol [1]. Ab initio calculations on *cis*-$N_2H_2^-$ as a function of the angle HNN were reported in [2].

References:

[1] Nguyen, M. T. (J. Phys. Chem. **91** [1987] 2679/81).
[2] Baird, N. C. (Can. J. Chem. **57** [1979] 98/103).

2.2.9 1,1-Diazene, H_2NN

Other names: Isodiazene, aminonitrene, 1,1-diazine, 1,1-dihydrodiazine
CAS Registry Numbers: H_2NN *[28647-38-3]*, D_2NN *[91210-61-6]*, $H_2{}^{15}N^{15}N$ *[91210-62-7]*, $D_2{}^{15}N^{15}N$ *[91210-63-8]*

This chapter deals with 1,1-diazene, H_2NN, the third of three possible N_2H_2 isomers; *cis*- and *trans*-N_2H_2 are discussed in Chapter 2.2.5, p. 37; for a review, see [1]. Ab initio studies predict H_2NN to lie about 85 to 145 kJ/mol above *trans*-N_2H_2 (cf. *trans*-$N_2H_2 \leftrightarrow H_2NN$ isomerization reaction, p. 58) [2].

Formation

H_2NN (HDNN and D_2NN) is produced by irradiating the corresponding aminoisocyanate isolated in an Ar matrix at 12 K with 313- or 254-nm light [3]. Accordingly prepared H_2NN

has better optical quality and yield than H_2NN prepared by irradiation of carbamoyl azide in a glass matrix at 80 K or in an Ar matrix at 10 K [4]. The blue-violet species was characterized by IR and UV spectroscopy. Due to its photolability visible light has to be excluded. Mass-spectrometric results had earlier led to the assumption that H_2NN forms during the thermolysis of Cs tosylhydrazide or by microwave discharge through hydrazine; the thermolysis of Rb tosylhydrazide was said to give a mixture of H_2NN and *cis*-N_2H_2 [5, 6]. The mass-spectrometric evidence was later questioned, and H_2NN formation in this way could not be confirmed [1].

Molecular Properties and Spectra

The **electronic states** of 1,1-diazene were examined at various levels of ab initio theory. There is some disagreement as to the nature of the electronic ground state. Early theoretical work suggested the possibility of a nonplanar triplet ground state with C_s symmetry ($^3A''$) [7 to 10], but this question now seems to be firmly resolved in favor of a planar singlet ground state with C_{2v} symmetry ($^1A_1$) [2, 11 to 13]. Using larger basis sets and, even more importantly, the inclusion of electron correlation lower the singlet state with respect to the triplet state [7, 8]. For the first time, a CI calculation placed the singlet state lower in energy than the triplet state, though only by 6.7 kJ/mol [11, 12]. In more extended ab initio calculations, the adiabatic singlet-triplet energy separation for H_2NN was predicted to range from 58 to 65 kJ/mol [13] and to be 62 kJ/mol [11], 50 kJ/mol [14], and 44 kJ/mol [2]. The stabilization of the singlet ground state with respect to the triplet state is due to the large double-bond character of the NN bond ($H_2N^+{=}N^-$), as reflected by the short bond length and large dipole moment (see below) [2, 11]. A vibrational frequency calculation showed that planar triplet H_2NN with C_{2v} symmetry ($^3A_2$), proposed by Davis and Goddard [11] to be the stable triplet species, has an imaginary frequency and hence is a transition state on the triplet surface [14].

From SCF calculations the electronic configuration for the singlet state ($^1A_1$) was deduced as follows: $(1a_1)^2$ $(2a_1)^2$ $(3a_1)^2$ $(4a_1)^2$ $(1b_2)^2$ $(1b_1)^2$ $(5a_1)^2$ $(2b_2)^2$ $2b_1$ $6a_1$ [14, 15]. Using the approximate chemical description, the three highest occupied orbitals can be written in agreement with N_2H_2 (cf. p. 43) to be π, n_+, n_-. But in contrast to N_2H_2, the two lone-pair orbitals in H_2NN are on the same N atom [15].

The first excited state of singlet H_2NN is pyramidal with C_s symmetry ($^1A''$) and was calculated to lie 175 to 177 kJ/mol above the $^1A_1$ state [13].

Values for the calculated **bond distances and bond angles** of H_2NN in the singlet and triplet states are listed in the table below. Additionally, bond distances and angles of H_2NN, derived from ab initio calculations at the HF level, are given in [2, 7, 10, 11, 17 to 19, 28, 29]. The geometry was also calculated with semiempirical methods [9, 20 to 24]. Calculations predict the singlet state to be planar and the triplet state to be pyramidal. Surprisingly, a slight distortion from the C_{2v} symmetry in singlet H_2NN was found in an MCSCF calculation [25]. The equilibrium geometry of the first excited singlet H_2NN ($^1A''$) was calculated using a CASSCF wave function with a DZ+P basis: $r(NN)=1.356$ Å, $r(NH)=1.000$ Å, $\angle HNN=115.5°$, and $\phi=35.5°$ (angle between the plane defined by the H atoms and the central N atom and the NN bond) [13].

The **ionization potentials** for H_2NN in its $^1A_1$ state were obtained by ab initio calculations. The value for the first ionization potential varies between 7.23 and 9.4 eV [11, 12, 15, 30]. An ionization potential was also calculated for the $^3A_2$ state, assumed to be planar [11].

Fundamental vibrational frequencies were obtained from IR spectra of matrix-isolated H_2NN [3, 4]. The values are also compiled in [31]. The fundamentals observed for 1,1-diazene

r(NN) in Å	r(NH) in Å	$\angle$HNH in degree	$\angle$HNN in degree	method of calculation	electronic state	Ref.
1.248	1.012	115.6	122.2	GVB(DZ+P)	$^1A_1$	[13]
1.389	1.002	111.8	$\phi=50.7°$	GVB(DZ+P)	$^3A''$	[13]
1.26	1.02	112	124	CI(4-31G)	$^1A_1$	[12]
1.39	1.00	115	115	CI(4-31G)	$^3A''$	[12]
1.23	1.03		123.3	CI(ANO)	$^1A_1$	[26]
1.221	1.044		124.2	MP2(6-31G*)	$^1A_1$	[27]
1.221	1.0371		124.1	MP2(6-31G**)	$^1A_1$	[3, 14]
1.224	1.038		124.4	MCSCF(DZ+P)	$^1A_1$	[25]

and its mono- and dideutero compounds in an Ar matrix are listed below [3]. Only the NN stretching frequency of 1574 cm^{-1} was assigned in [4]. Good agreement was found between the observed [3] and calculated (MP2 [3] and CASCF [13]) spectra of singlet H_2NN, HDNN, and D_2NN. The normal modes, being more sensitive to the hydrogen basis, were overestimated in both calculations [13]. The same holds for the results of an SCF calculation [32]. Frequencies for $H_2NN(^1A_1)$, estimated from the experimental results on hydrazine, are given in [11]. Values calculated for the vibrational frequencies of the nonplanar $^1A''$ and $^3A''$ states are given in [13], and those for the planar $^3A_2$ state, estimated on the basis of the frequencies of diazene and hydrazine, in [11].

ν_i	X_2NN (C_{2v}) type of mode	H_2NN ν in cm^{-1}	D_2NN ν in cm^{-1}	ν_i	HDNN (C_s) type of mode	ν in cm^{-1}
$\nu_1(A_1)$	$\nu_s(NX_2)$	2862.0 s	2140.2 vs	$\nu_1(A')$	ν(NH)	
$\nu_2(A_1)$	$\delta(NX_2)$	1644.7 w		$\nu_2(A')$	ν(ND)	
$\nu_3(A_1)$	ν(NN)	1574.2 m	1599.0 mw	$\nu_3(A')$	ν(NN)	1587.2 mw
$\nu_4(B_1)$	γ	1002.7 vs	793.5 ms	$\nu_4(A')$	δ(NHD)	1507.6*⁾ mw
						1498.9*⁾ mw
$\nu_5(B_2)$	$\nu_{as}(NX_2)$	2804.6 m	2107.0 s	$\nu_5(A')$	ρ(NHD)	
$\nu_6(B_2)$	$\rho(NX_2)$	1287.5 vw		$\nu_6(A'')$	γ	913.5*⁾ m
						899.5*⁾ s

*⁾ Splitting is caused by complexation with CO.

Three quantum-chemical studies on H_2NN include the calculation of the **dipole moment** μ. An SCEP calculation gave for the ground state $\mu=3.64$ D [28], whereas a GVB calculation gave $\mu=4.04$ D for the $^1A_1$ state and $\mu=2.35$ D for the $^3A_2$ state [11]. A value of $\mu=3.19$ was obtained from a semiempirical calculation [22].

The **indirect nuclear spin-spin coupling constant** $^1J(^{15}N^{15}N)=-10.45$ Hz was obtained from an ab initio EOM (equation-of-motion) calculation [33].

The valence **force constants** were obtained by MCSCF calculations. The surprisingly slight distortion from C_{2v} symmetry (see above) found for the molecule effects the force constants. In addition to one NN stretching force constant, $f_R=11.66$ mdyn/Å, and one out-of-plane torsion bending force contant, $f_\gamma=0.912$ mdyn·Å, two NH stretching force constants, f_r and $f_{r'}$, for the tight and loose bonds as well as two force constants for the in-plane deformation, f_α and $f_{\alpha'}$, do exist: $f_r=5.885$ mdyn/Å, $f_{r'}=4.605$ mdyn/Å, $f_\alpha=1.489$ mdyn·Å, and $f_{\alpha'}=1.469$ mdyn·Å [25]. In another study the force constants were calculated (SCF) to be $f_R=11.14$ mdyn/Å and $f_r=8.65$ mdyn/Å [19].

MCSCF CI calculations gave an NH **bond dissociation energy** of 179.9 kJ/mol at 289 K for H_2NN in the singlet ground state [34]. An NN bond dissociation energy of $D_0 = 288.7$ kJ/mol (to ground state products) was derived from extensive CI calculations [11]. A value of $D_0 = 350.2$ kJ/mol was calculated for $H_2NN(^3A_2)$ [11].

1,1-diazene was predicted to have two transitions in the **near ultraviolet and visible region**, a weak symmetry-forbidden one, $S_1(^1A_2) \leftarrow S_0(^1A_1)$, at 558 nm and a strong symmetry-allowed one, $S_2(^1A_1) \leftarrow S_0(^1A_1)$, at 175 nm [3]. The spectrum of H_2NN at 80 K, photochemically prepared in 2-methyltetrahydrofuran, reveals a structured absorption in the visible range between 500 and 720 nm with $\lambda_{max} = 636$ nm [4], which is assigned to the $S_1 \leftarrow S_0$ transition [3]. The $S_2 \leftarrow S_0$ transition was only indirectly identified, and it was concluded that the onset of the absorption lies somewhere between 313 and 254 nm [3].

Ab initio studies at the CISD (energies modified by the Davidson correction) level yielded $\Delta_fH^\circ_0 = 328.3$ ($\Delta_fH^\circ_{298} = 323.2$) kJ/mol for the **enthalpy of formation** of H_2NN ($^1A_1$) [14]. A value of $\Delta_fH^\circ_0 = 308.4$ kJ/mol was predicted from ab initio calculations at the G2 level [27]. Larger values were derived from GVB CI ($\Delta_fH^\circ_0 = 368.2$ [34] and 369.9 kJ/mol [11]) and MCSCF ($\Delta_fH^\circ_0 = 447.8$ kJ/mol [25]) calculations. The **entropy** of H_2NN was calculated at the CISD level (without the Davidson correction) to be 217.8 $J \cdot K^{-1} \cdot mol^{-1}$ at 298 K [14].

Chemical Behavior

Decomposition. Irradiation of H_2NN in a matrix at 80 K with visible light results in decoloration of the blue-violet species and in apparently quantitative formation of H_2 and N_2 [4]. Carrying out the irradiation at 254 nm also produces hydrogen atoms. At wavelengths >570 nm the formation of hydrogen atoms could not be proven. Three different mechanisms were proposed for this photochemical reaction: (a) cleavage into the diazenyl radical and a hydrogen atom, (b) direct cleavage into molecular nitrogen and hydrogen, and (c) concerted cleavage into molecular nitrogen and hydrogen. Taking the isotopic effects measured for HDNN and D_2NN into account, the feasibility of the proposed pathways was discussed, but no final conclusion could be arrived [3]. From ab initio studies, $\Delta_rH_0 = 173.6$ [34] and 145.2 kJ/mol [26] were derived for a decomposition according to pathway (a) [34]. Tentatively, it was proposed that warming the glass to the softening point (90 K) results in the rearrangement $H_2NN \rightarrow$ *trans*-N_2H_2, which is consistent with the observation of *trans*-N_2H_2 in the UV spectrum [4].

The 1,1-diazene$\rightleftharpoons$*trans*-diazene **isomerization reaction** is discussed in Section 2.2.5.4.1, p. 58.

Ab initio calculations were performed on the **proton affinity** of H_2NN in comparison to other double-bond systems [16], on the concerted **hydrogen transfer** from H_2NN to *cis*- and *trans*-N_2H_2 with respect to the energy barrier of the coplanar intermediate σ-complex, and the **dimerization reaction** of H_2NN [32, 35]. Ab initio [18, 35, 36] and semiempirical [24] calculations were performed on the potential surface of the cycloaddition reaction of H_2NN with $H_2C{=}CH_2$. The calculations on one hand indicate the existence of a stable complex, but on the other hand a high reaction barrier.

References:

[1] Back, R. A. (Rev. Chem. Intermed. **5** [1984] 293/323).

[2] Pople, J. A.; Raghavachari, K.; Frisch, M. J.; Binkley, J. S.; Schleyer, P. v. R. (J. Am. Chem. Soc. **105** [1983] 6389/99).

[3] Teles, J. H.; Maier, G.; Hess, B. A., Jr.; Schaad, L. J. (Chem. Ber. **122** [1989] 749/52; erratum: Chem. Ber. **122** [1989] 1219).

[4] Sylwester, A. P.; Dervan, P. B. (J. Am. Chem. Soc. **106** [1984] 4648/50).
[5] Wiberg, N.; Fischer, G.; Bachhuber, H. (Angew. Chem. **88** [1976] 386/7; Angew. Chem. Int. Ed. Engl. **88** [1976] 385).
[6] Wiberg, N.; Fischer, G.; Bachhuber, H. (Z. Naturforsch. **34b** [1979] 1385/90).
[7] Baird, N. C.; Barr, R. F. (Can. J. Chem. **51** [1973] 3303/8).
[8] Wagniere, G. (Theor. Chim. Acta **31** [1973] 269/74).
[9] Lathan, W. A.; Curtiss, L. A.; Hehre, W. J.; Lisle, J. B.; Pople, J. A. (Prog. Phys. Org. Chem. **11** [1974] 175/261).
[10] Ahlrichs, R.; Staemmler, V. (Chem. Phys. Lett. **37** [1976] 77/81).

[11] Davis, J. H.; Goddard, W. A., III (J. Am. Chem. Soc. **99** [1977] 7111/21).
[12] Baird, N. C.; Wernette, D. A. (Can. J. Chem. **55** [1977] 350/4).
[13] Hoffmann, M. R.; Kuhler, K. (J. Chem. Phys. **94** [1991] 8029/39).
[14] Whitelegg, D.; Woolley, R. G. (J. Mol. Struct. **209** [1990] 23/31 [THEOCHEM **68**]).
[15] Von Niessen, W.; Domcke, W.; Cederbaum, L. S.; Kraemer, W. P. (J. Chem. Phys. **67** [1977] 44/51).
[16] Ito, K.; Nagase, S. (Chem. Phys. Lett. **126** [1986] 531/6).
[17] Pople, J. A.; Krishnan, R.; Schlegel, H. B.; Binkley, J. S. (Int. J. Quantum Chem. **14** [1978] 545/60).
[18] Pasto, D. J.; Chipman, D. M. (J. Am. Chem. Soc. **101** [1979] 2290/6).
[19] Wong, D. P.; Fink, W. H.; Allen, L. C. (J. Chem. Phys. **52** [1970] 6291/8).
[20] Chantranupong, L. (J. Sci. Soc. Thailand **9** [1983] 187/90).

[21] Talaty, E. R.; Schwartz, A. K.; Simons, G. (J. Am. Chem. Soc. **97** [1975] 972/8).
[22] Hayes, L. J.; Billingsley, F. P., II; Trindle, C. (J. Org. Chem. **37** [1972] 3924/9).
[23] Bespalov, V. Y.; Kartsova, L. A.; Baranovskii, V. I.; Ioffe, B. V. (Dokl. Akad. Nauk SSSR **200** [1971] 99/102; Dokl. Chem. Proc. Acad. Sci. USSR **196/201** [1971] 725/7).
[24] Bespalov, V. Y. (Zh. Org. Khim. **18** [1982] 2241/3; J. Org. Chem. [USSR] **18** [1982] 1977/8).
[25] Jensen, H. J. A.; Joergensen, P.; Helgaker, T. (J. Am. Chem. Soc. **109** [1987] 2895/901).
[26] Walch, S. P. (J. Chem. Phys. **91** [1989] 389/94; erratum: J. Chem. Phys. **94** [1991] 6937).
[27] Pople, J. A.; Curtiss, L. A. (J. Chem. Phys. **95** [1991] 4385/8).
[28] Parsons, C. A.; Dykstra, C. E. (J. Chem. Phys. **71** [1979] 3025/33).
[29] Benard, M.; Kraemer, W. P.; Diercksen, G. H. F. (private communication; given as ref. 5 in [10]).
[30] Decleva, P.; Lisini, A. (Chem. Phys. **106** [1986] 39/49).

[31] Jacox, M. E. (J. Phys. Chem. Ref. Data **19** [1990] 1387/546).
[32] Kemper, M. J. H.; Buck, H. M. (Can. J. Chem. **59** [1981] 3044/8).
[33] Galasso, V. (Chem. Phys. Lett. **145** [1988] 259/61).
[34] Casewit, C. J.; Goddard, William A., III (J. Am. Chem. Soc. **102** [1980] 4057/62).
[35] Pasto, D. J. (J. Am. Chem. Soc. **101** [1979] 6852/7).
[36] Lazareva, M. (Teor. Eksp. Khim. **22** [1986] 477/81; Theor. Exp. Chem. [USSR] **22** [1986] 456/60).

2.2.10 The 1,1-Diazene Cation, H_2NN^+

CAS Registry Number: *[63986-30-1]*

The planar H_2NN^+ cation has C_{2v} symmetry in its ground state $^2B_2$. The following geometries were obtained from ab initio calculations (bond lengths in Å, bond angles in degree):

r(NN)	r(NH)	∠HNN	method of calculation	Ref.
1.178	1.044	120.7	MP2(FULL 6-31G)	[1]
1.24	1.02	121	CI(4-31G)	[2]

References:

[1] Pople, J. A.; Curtiss, L. A. (J. Chem. Phys. **95** [1991] 4385/8).

[2] Baird, N. C.; Wernette, D. A. (Can. J. Chem. **55** [1977] 350/4).

2.2.11 The 1,1-Diazene Dication, H_2NN^{2+}

CAS Registry Number: *[123641-79-2]*

In its ground state $^1A_1$, H_2NN^{2+} has C_{2v} symmetry. In the course of theoretical investigations on multiply charged isoelectronic analogues of $C_3H_3^+$, the species $NH_2NCH_3^{3+}$ and its fragmentation products $H_2NN^{2+}+CH_3^+$ were studied with various ab initio methods. Total and zero-point vibrational energies of H_2NN^{2+} and relative energies of the fragmentation products of $NH_2NCH_3^{3+}$ were calculated.

Reference:

Wong, M. W.; Radom, L. (J. Am. Chem. Soc. **111** [1989] 6976/83).

2.2.12 The Hydrazyl Radical, N_2H_3

Other names: Hydrazinyl, diazyl

CAS Registry Number: *[13598-46-4]*

2.2.12.1 Formation

From Hydrazine

Decomposition of Hydrazine. N_2H_3 radicals were generated by a MW discharge [1, 2] and by photoionization [3, 4] of hydrazine as shown by mass spectrometry.

N_2H_3 radicals were detected spectroscopically (EPR, UV) during electron pulse radiolysis of aqueous N_2H_4 solutions [5] and liquid N_2H_4 [6], during electron irradiation of liquid N_2H_4 adsorbed on a zeolite matrix [7], and during radiolysis of frozen N_2H_4 [8, 9], frozen aqueous N_2H_4 solutions [10], and $Mg(ClO_4)_2\cdot 2\,N_2H_4$ and hydrazinates of other ionic salts, such as $Ca(ClO_4)_2$ or MCl_2 (M = Ca, Zn, Ba, Mg) [11].

The formation of N_2H_3 radicals during the low-pressure $Hg(^3P_1)$-photosensitized decomposition of gaseous hydrazine was demonstrated by adding dimethyl mercury to give monomethylhydrazine [12].

N_2H_3 radicals were UV-spectroscopically observed during flash photolysis of gaseous N_2H_4 [13]. The primary step in the photolysis of gaseous N_2H_4 was discussed to be the formation of N_2H_3 radicals via $N_2H_4 + h\nu \rightarrow N_2H_3 + H$; for details, see e.g. [14 to 21].

N_2H_3 radicals were mass-spectrometrically detected during the decomposition of hydrazine on a heated platinum surface between 773 and 973 K [22]. The formation of N_2H_3 via a secondary reaction (N_2H_4+H, see below) during the thermolytic decomposition of gaseous hydrazine at 1123 K [23], at 1273 K [24], between 750 and 1000 K [25], between 1200 to 2500 K [26], and during flash heating of gaseous hydrazine in the presence of NO [27] was discussed.

Reactions of Hydrazine. N_2H_3 radicals were obtained by the hydrogen abstraction reaction $N_2H_4 + M \rightarrow N_2H_3 + MH$. The reaction with H atoms (M = H) is an important secondary reaction in the decomposition of N_2H_4 (see above). The generation of N_2H_3 by photolysis of CH_3SH ($\lambda = 253.7$ nm) in the presence of N_2H_4 is described in [28]. Several studies of the $N_2H_4 + H$ reaction were performed in flow systems by recording the concentration profiles mass-spectrometrically [29 to 31] and by EPR [30 to 32]. The results were fitted to the following Arrhenius equations (rate constant k in $cm^3 \cdot mol^{-1} \cdot s^{-1}$, activation energy E in kJ/mol):

$k = A \cdot \exp(-E/RT)$	temperature range	Ref.
$3.5 \times 10^{11} \exp(-8.4/RT)$	298 to 423 K	[29]
$(1.5 \pm 0.3) \times 10^{12} \exp[-(5.4 \pm 0.8)/RT]$	300 to 540 K	[32]
$(1.3 \pm 0.3) \times 10^{13} \exp[-(10.5 \pm 0.8)/RT]$	213 to 473 K	[31]

The rate law given in [31] was recommended in a critical evaluation of kinetic data on high-temperature reactions [33]. A reevaluation led to a 50% higher rate constant at room temperature, $k = 3 \times 10^{11}$ $cm^3 \cdot mol^{-1} \cdot s^{-1}$ [34]. The rate constant for the reaction $N_2H_4 + D \rightarrow N_2H_3 + DH$ at 295 K was determined to be $k = 1.6 \times 10^{11}$ $cm^3 \cdot mol^{-1} \cdot s^{-1}$ [30].

The formation of N_2H_3 radicals during the reaction of O atoms with hydrazine in a flow system was investigated. A rate constant of $k = 3.2 \times 10^{12}$ $cm^3 \cdot mol^{-1} \cdot s^{-1}$ for the reaction channel $N_2H_4 + O \rightarrow N_2H_3 + OH$ was determined at room temperature [34]; for further investigations, see [30, 35].

The abstraction of H atoms from N_2H_4 by F atoms in a flow system was used to produce N_2H_3 radicals [34].

Hydrazyl radicals were spectroscopically detected during pulse radiolysis of aqueous hydrazine solutions in the presence of N_2O. The radicals were formed by the reaction of N_2H_4 with OH radicals produced via $N_2O + e^-_{aq} + H_2O \rightarrow OH + OH^- + N_2$ [36]; for a similar investigation, see [37]. The reaction $N_2H_4 + OH \rightarrow N_2H_3 + H_2O$ was also discussed as one of the steps in the chain mechanism of the manganese-catalyzed autoxidation of aqueous hydrazine [38] and of the γ-radiation-induced, N_2H_4-inhibited oxidation of Fe^{2+} in sulfuric acid in the presence of oxygen [39].

For the formation of N_2H_3 radicals by the reaction of N_2H_4 with NH_2 radicals, see "Nitrogen" Suppl. Vol. B 1.

N_2H_3 radicals were generated by abstracting H atoms from hydrazine in benzene solution with *tert*-butoxy radicals (formed by photolysis of di-*tert*-butyl peroxide) [40].

N_2H_3 radicals were formed in aqueous hydrazine solutions containing one-electron-oxidants like Fe^{3+} [41 to 43] and Tl^{3+} [44].

From Ammonia

N_2H_3 radicals were detected (by EPR) during the γ radiolysis of NH_3 adsorbed on zeolites [45] or trapped in solid nitrogen [46], and in the mass spectrum of NH_3 [47].

N_2H_3 radicals are believed to be intermediates in the radiolytic [48 to 50] and Hg($^3P_1$)-photosensitized [51] decomposition of gaseous NH_3 and in NH_3 flames [52].

References:

[1] Foner, S. N.; Hudson, R. L. (J. Chem. Phys. **29** [1958] 442/3).
[2] Wiberg, N.; Fischer, G.; Bachhuber, H. (Z. Naturforsch. **34b** [1979] 1385/90).
[3] Gibson, S. T.; Greene, J. P.; Berkowitz, J. (J. Chem. Phys. **83** [1985] 4319/28).
[4] Ruscic, B.; Berkowitz, J. (J. Chem. Phys. **95** [1991] 4378/84).
[5] Ershov, B. G.; Mikhailova, T. L. (Izv. Akad. Nauk SSSR Ser. Khim. **1991** 341/5; Bull. Acad. Sci. USSR Div. Chem. Sci. [Engl. Transl.] **40** [1991] 288/92).
[6] Delaire, J.; Cordier, P.; Belloni, J.; Billiau, F.; Delcourt, M. O. (J. Phys. Chem. **80** [1976] 1687/90).
[7] Fantechi, R.; Helcke, G. A. (J. Chem. Soc. Faraday Trans. II **68** [1972] 924/33).
[8] Tupikov, V. I.; Tsivenko, V. I.; Pshezhetskii, S. Ya.; Kotov, A. G.; Milinchuk, V. K. (Zh. Fiz. Khim. **37** [1963] 138; Russ. J. Phys. Chem. [Engl. Transl.] **37** [1963] 65/7).
[9] Pshezhetskii, S. Y.; Slavinskaya, N. A.; Trakhtenberg, L. I. (Khim. Vys. Energ. **18** [1984] 225/31; High Energy Chem. [Engl. Transl.] **18** [1984] 182/8).
[10] Tupikov, V. I.; Pshezhetskii, S. Ya. (Zh. Fiz. Khim. **38** [1964] 2511/3; Russ. J. Phys. Chem. [Engl. Transl.] **38** [1964] 1364/5).

[11] Khusidman, M. B.; Vyatkin, V. P.; Grigor'eva, N. V.; Posadov, I. A. (Zh. Prikl. Khim. [Leningrad] **55** [1982] 1475/80; J. Appl. Chem. USSR [Engl. Transl.] **55** [1982] 1345/9).
[12] Jones, A.; Lossing, F. P. (Can. J. Chem. **47** [1969] 1391/3).
[13] Arvis, M.; Devillers, C.; Gillois, M.; Curtat, M. (J. Phys. Chem. **78** [1974] 1356/60).
[14] Haak, H. K.; Stuhl, F. (J. Phys. Chem. **88** [1984] 3627/33).
[15] Kenner, R. D.; Rohrer, F.; Stuhl, F. (Chem. Phys. Lett. **116** [1985] 374/9).
[16] Hawkins, W. G.; Houston, P. L. (J. Phys. Chem. **86** [1982] 704/9).
[17] Schurath, U.; Ralph, N. (Ber. Bunsen-Ges. Phys. Chem. **72** [1968] 1027/9).
[18] Stief, J. L.; DeCarlo, V. J. (J. Chem. Phys. **44** [1966] 4638/9).
[19] Stief, J. L.; DeCarlo, V. J.; Mataloni, R. J. (J. Chem. Phys. **46** [1967] 592/8).
[20] Stief, J. L.; DeCarlo, V. J. (J. Chem. Phys. **49** [1968] 100/5).

[21] Schurath, U.; Schindler, R. N. (J. Phys. Chem. **74** [1970] 3188/94).
[22] Foner, S. N.; Hudson, R. L. (J. Vac. Sci. Technol. [2] A **1** [1983] 1261/4; C.A. **99** [1983] No. 13477).
[23] Rice, F. O.; Scherber, F. (J. Am. Chem. Soc. **77** [1955] 291/3).
[24] Lavrovskaya, G. K.; Markin, M. I.; Tal'roze, V. L. (Tr. Kom. Anal. Khim. Akad. Nauk SSSR **13** [1963] 474/82).
[25] Eberstein, I. J.; Glassman, I. (Symp. Int. Combust. Proc. **10** [1965] 365/74).
[26] Diesen, R. W. (J. Chem. Phys. **39** [1963] 2121/8).
[27] Husain, D.; Norrish, R. G. W. (Proc. R. Soc. London A **273** [1963] 145/64).
[28] Stief, L. J. (J. Chem. Phys. **52** [1970] 4841/5).
[29] Schiavello, M.; Volpi, G.G. (J. Chem. Phys. **37** [1962] 1510/3).
[30] Gehring, M.; Hoyermann, K.; Wagner, H. G.; Wolfrum, J. (Ber. Bunsen-Ges. Phys. Chem. **73** [1969] 956/61).

[31] Gehring, M.; Hoyermann, K.; Wagner, H. G.; Wolfrum, J. (Ber. Bunsen-Ges. Phys. Chem. **75** [1971] 1287/94).
[32] Francis, P. D.; Jones, A. R. (J. Chem. Phys. **54** [1971] 5085/8).
[33] Baulch, D. L.; Drysdale, D. D.; Horne, D. G. (Evaluated Kinetic Data for High Temperature Reactions, Vol. 2, Butterworth, London 1973, pp. 519/26).
[34] Dransfeld, P. (Diss. Univ. Göttingen 1986, pp. 1/153).

[35] Foner, S. N.; Hudson, R. L. (J. Chem. Phys. **49** [1968] 3724/5).

[36] Hayon, E.; Simic, M. (J. Am. Chem. Soc. **94** [1972] 42/7).

[37] Ershov, B. G.; Mikhailova, T. L.; Emel'yanova, A. Yu. (Izv. Akad. Nauk SSSR Ser. Khim. **1988** 1192; Bull. Acad. Sci. USSR Div. Chem. Sci. [Engl. Transl.] **37** [1988] 1051).

[38] Lim, P. K.; Fagg, B. S. (J. Phys. Chem. **88** [1984] 1136/40).

[39] Ahrens, R. W. (J. Phys. Chem. **66** [1962] 2108/11).

[40] Malatesta, V.; Lindsay, D.; Horswill, E. C.; Ingold, K. U. (Can. J. Chem. **52** [1974] 864/6).

[41] Higginson, W. C. E.; Wright, P. (J. Chem. Soc. **1955** 1551/6).

[42] Cahn, J. W.; Powell, R. E. (J. Am. Chem. Soc. **76** [1954] 2568/72).

[43] Higginson, W. C. E.; Sutton, D. (J. Chem. Soc. **1953** 1402/6).

[44] Higginson, W. C. E.; Sutton, D.; Wright, P. (J. Chem. Soc. **1953** [1953] 1380/6).

[45] Kotov, A. G.; Sorokin, Yu. A.; Pshezhetskii, S. Ya. (Dokl. Akad. Nauk SSSR **166** [1966] 1386/9; C.A. **64** [1966] 16880).

[46] Tupikov, V. I.; Pshezhetskii, V. S.; Pshezhetskii, S. Ya. (Elem. Protsessy Khim. Vys. Energ. Tr. Simp., Moscow 1963 [1965], pp. 215/20; C.A. **65** [1966] 9990).

[47] Melton, C. E. (Int. J. Mass Spectrom. Ion Phys. **1** [1968] 353/75).

[48] Dzantiev, B. G.; Nichipor, G. V. (Khim. Vys. Energ. **3** [1969] 368; High Energy Chem. [Engl. Transl.] **3** [1969] 335).

[49] Pagsberg, P. B.; Eriksen, J.; Christensen, H. C. (J. Phys. Chem. **83** [1979] 582/90).

[50] Sorokin, Yu. A.; Pshezhetskii, S. Ya. (Zh. Fiz. Khim. **39** [1965] 1955/9; Russ. J. Phys. Chem. [Engl. Transl.] **39** [1965] 1037/40).

[51] McDonald, C. C.; Gunning, H. E. (J. Chem. Phys. **23** [1955] 532/41).

[52] Dean, A. M.; Chou, M. S.; Stern, D. (Int. J. Chem. Kinet. **16** [1984] 633/53).

2.2.12.2 Molecular Properties and Spectra

Electron Configuration and Geometrical Structure

The structure of the N_2H_3 radical has not yet been determined by experimental means. Several ab initio calculations on the radical were performed, but the results differ with respect to the spatial arrangement of the atoms. The most extensive ab initio studies, a CI calculation [1], a second-order Møller-Plesset perturbation (MP2) calculation [2], and several ab initio SCF MO calculations (STO-3G basis) [3 to 6], all yield a nonplanar structure (C_1 symmetry). A nonplanar form was also deduced from semiempirical calculations which roughly reproduced the results of the EPR spectra [7, 8]. A planar geometry resulted from ab initio SCF MO studies (4-31G basis) [4 to 6, 9, 10]. The electron configuration in the **ground state** is ....$(7a)^2(8a)^2(9a)^1\ ^2A''$. The 9a orbital is slightly antibonding and predominantly localized on N^2 (see figure below), while the 8a orbital is mainly localized on N^1. The σ orbital 7a is almost a pure sp^2 hybrid [1]. The electronic structure of free nitrogen-centered radicals, among them N_2H_3, was analyzed in terms of Linnett structures [11].

Bond distances r (in Å) and angles α are listed below according to the following numbering:

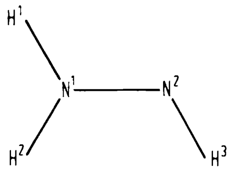

$r(N^1\text{-}N^2)$	$r(N^1\text{-}H^1)$	$r(N^1\text{-}H^2)$	$r(N^2\text{-}H^3)$	Ref.
1.346	0.999	0.996	1.008	[1]
1.352	1.017	1.012	1.026	[2]

$\alpha(NNH^1)$	$\alpha(NNH^2)$	$\alpha(NNH^3)$	$\alpha(H^1N^1H^2)$	Ref.
121.5°	114.3°	106.2°	116.1°	[1]
119.7°	112.3°	105.2°	–	[2]

According to [1] the NH_2 group is depressed from the $N^1\text{-}N^2\text{-}H^3$ plane by about 28° (i.e., both hydrogen atoms are on the same side of the plane), whereas according to [2] the NH_2 group is twisted around the N-N bond by the dihedral angle $\alpha(H^2N^1N^2H^3) = 29.8°$ (dihedral angle $\alpha(H^1N^1N^2H^3) = 166.5°$).

Ab initio calculations yielded a low inversion barrier of about 2 kJ/mol for the motion of the NH_2 group through the planar conformation [1]. Rotation around the N-N bond is shown to be the lowest energy path for interconversion between equivalent ground state structures (cis-trans isomerization). Rotation barriers of 104 [1] and 123 kJ/mol [10] were calculated; for a detailed discussion, see [1, 10].

The lowest **excited** doublet state has the configuration.... $(7a)\ (8a)^2\ (9a)^2\ {}^2A''$. The geometry in this state is characterized by the $N\text{-}N\text{-}H^3$ plane bisecting the plane of the NH_2 group. The vertical and adiabatic excitation energies of 4.32 and 1.37 eV, respectively, were obtained by SCF + CI calculations [1].

Other Molecular Properties. Spectra

CI calculations gave a dipole moment of $\mu = 2.95$ D [1]. The proton affinity was determined to be −7.65 eV [12], and the electron affinity estimated to be 23.8 kJ/mol [13].

A photoionization mass-spectrometric study of N_2H_3 yielded the adiabatic ionization potential $E_i = 7.61 \pm 0.01$ eV [14]; for a preliminary result, see [15]. From mass-spectrometric investigations of N_2H_4, the ionization potentials $E_i = 7.88 \pm 0.2$ eV [16] and 7.85 ± 0.05 eV [12] were obtained. Similarly, $E_i = 7.6$ [17] and 8.2 eV [18] were determined from the mass spectrum of NH_3 and N_2H_2, respectively. Quantum-chemically calculated ionization potentials [2, 17] agree well with the experimental values.

The bond dissociation energies $D_0(HNNH\text{-}H) = 183 \pm 4.6$ [14] and 184 kJ/mol [12] were derived from the ionization potential of N_2H_3. A well-agreeing value of $D_0(HNNH\text{-}H) = 182$ kJ/mol was obtained by a MP2 calculation [2]. A mean N-H bond dissociation energy of 223 ± 13 kJ/mol was derived from the formation enthalpies of diazene and hydrazine [19].

EPR spectra of the N_2H_3 radical were produced by fast-electron irradiation of liquid hydrazine adsorbed on zeolite [7], by γ irradiation of hydrazinates of $X(ClO_4)_2$ (X = Mg, Ca) and YCl_2 (Y = Ca, Zn, Ba, Mg) [8], and by photolysis of hydrazine in a benzene solution containing di-*tert*-butyl peroxide [20].

The EPR spectrum of N_2H_3 from hydrazine adsorbed on zeolite, recorded between 233 and 363 K, was best resolved at 363 K. It showed a doublet assigned to the H^3 atom, two triplets assigned to the nitrogen atoms, and one triplet assigned to the H^1 and H^2 atoms. The assignments followed from the temperature dependence of the spectrum. The following isotropic hyperfine splitting constants (in 10^{-4} T) were determined:

T in K	a(N^1)	a(N^2)	a(H^1)	a(H^2)	a(H^3)	Ref.
363	8.8	11.7	2.3*)	2.3*)	18.8	[7]
273	8.8	11.7	4.3	1.6	16.3	[20]

*)Average value.

Anisotropic hyperfine (HF) coupling constants were derived from the EPR spectra of N_2H_3 in dehydrated magnesium perchlorate hydrazinate. The parallel HF components (in 10^{-4} T) were: $A_{\parallel}(N^1)=18$, $A_{\parallel}(N^2)=40$, $A_{\parallel}(H^1)=6$, $A_{\parallel}(H^2)=3$, $A_{\parallel}(H^3)=18$. Perpendicular HF constants (in 10^{-4} T) could only be determined for the nitrogen atoms: $A_{\perp}(N^1)=4.2$, $A_{\perp}(N^2)=-2.4$ [8].

Less resolved spectra were recorded from γ-irradiated, pure, frozen hydrazine [21, 22], frozen alcoholic [23], and aqueous hydrazine solutions [24].

Semiempirically (INDO) calculated isotropic splitting constants [4, 5] are in agreement with the experimental values. Spin densities of 0.79 at the N^2 atom and 0.21 at the N^1 atom were derived [4].

In flash-photolyzed gaseous hydrazine a continuous **optical absorption** (half-life ca. 10 µs) between 400 and 290 nm was assigned to the N_2H_3 radical [25]. The absorption increased in intensity towards the UV region. In pulse-radiolyzed, aqueous, alkaline (pH 9.2 to 13.4) solutions of hydrazine, an absorption maximum at $\lambda_{max}=230$ nm (extinction coefficient $\varepsilon_{max}=3.5\times10^3$ $L\cdot mol^{-1}\cdot cm^{-1}$) was observed [26]. A similar absorption band around about 230 nm was found in photolyzed [27] and electron-irradiated [28] aqueous N_2H_4 solutions. The optical absorption in γ-irradiated amorphous hydrazine at about 400 nm was assigned to N_2H_3 ($\varepsilon=10^3$ $L\cdot mol^{-1}\cdot cm^{-1}$) [22].

References:

[1] Chandler, G. S.; McLean, A. D. (J. Chem. Phys. **71** [1979] 2175/81).

[2] Pople, J. A.; Curtiss, L. A. (J. Chem. Phys. **95** [1991] 4385/8).

[3] Pasto, D. J. (J. Am. Chem. Soc. **101** [1979] 6852/7).

[4] Wood, D. E.; Wood, C. A.; Lathan, W. A. (J. Am. Chem. Soc. **94** [1972] 9278/80).

[5] Smith, P.; Donovan, W. H. (J. Mol. Struct. **204** [1990] 21/32 [THEOCHEM **63**]).

[6] Lathan, W. A.; Curtiss, L. A.; Hehre, W. J.; Lisle, J. B.; Pople, J. A. (Prog. Phys. Org. Chem. **11** [1974] 175/261).

[7] Fantechi, R.; Helcke, G. A. (J. Chem. Soc. Faraday Trans. II **68** [1972] 924/33).

[8] Khusidman, M. B.; Vyatkin, V. P.; Grigor'eva, N. V.; Posadov, I. A. (Zh. Prikl. Khim. [Leningrad] **55** [1982] 1475/80; J. Appl. Chem. USSR [Engl. Transl.] **55** [1982] 1345/9).

[9] Raban, M.; Aviram, K.; Kost, D. (Tetrahedron Lett. **26** [1985] 3591/4).

[10] Kost, D.; Aviram, K.; Raban, M. (J. Org. Chem. **54** [1989] 4903/8).

[11] Leroy, G.; Sana, M.; Wilante, C.; Peeters, D.; Dogimont, C. (J. Mol. Struct. **153** [1987] 249/67 [THEOCHEM **38**]).

[12] Wiberg, N.; Fischer, G.; Bachhuber, H. (Z. Naturforsch. **34b** [1979] 1385/90).

[13] Bauer, N. (J. Phys. Chem. **64** [1960] 833/7).

[14] Ruscic, B.; Berkowitz, J. (J. Chem. Phys. **95** [1991] 4378/84).

[15] Gibson, S. T.; Greene, J. P.; Berkowitz, J. (J. Chem. Phys. **83** [1985] 4319/28).

[16] Foner, S. N.; Hudson, R. L. (J. Chem. Phys. **29** [1958] 442/3).

[17] Melton, C. E. (Int. J. Mass Spectrom. Ion Phys. **1** [1968] 353/75).

[18] Holzmann, G.; Minkwitz, R. (Z. Anorg. Allg. Chem. **413** [1975] 72/6).

[19] Foner, S. N.; Hudson, R. L. (J. Chem. Phys. **68** [1978] 3162/8).

[20] Malatesta, V.; Lindsay, D.; Horswill, E. C.; Ingold, K. U. (Can. J. Chem. **52** [1974] 864/6).

[21] Tupikov, V. I.; Tsivenko, V. I.; Pshezhetskii, S. Ya.; Kotov, A. G.; Milinchuk, V. K. (Zh. Fiz. Khim. **37** [1963] 138; Russ. J. Phys. Chem. [Engl. Transl.] **37** [1963] 65/7).

[22] Pshezhetskii, S. Y.; Slavinskaya, N. A.; Trakhtenberg, L. I. (Khim. Vys. Energ. **18** [1984] 225/31; High Energy Chem. [Engl. Transl.] **18** [1984] 182/8).

[23] Roginskii, V. A.; Kotov, A. G.; Pshezhetskii, S. Ya. (Zh. Fiz. Khim. **40** [1966] 51; Russ. J. Phys. Chem. [Engl. Transl.] **40** [1966] 25/8).

[24] Tupikov, V. I.; Pshezhetskii, S. Ya. (Zh. Fiz. Khim. **38** [1964] 2511/3; Russ. J. Phys. Chem. [Engl. Transl.] **38** [1964] 1364/5).

[25] Arvis, M.; Devillers, C.; Gillois, M.; Curtat, M. (J. Phys. Chem. **78** [1974] 1356/60).

[26] Hayon, E.; Simic, M. (J. Am. Chem. Soc. **94** [1972] 42/7).

[27] Curtat, M.; Souil, F.; Devillers, C. (Propr. Hydrazine Ses Appl. Source Energ. Colloq. Int., Poitiers, Fr., 1974 [1975], pp. 41/5; C.A. **85** [1976] No. 80479).

[28] Ershov, B. G.; Mikhailova, T. L. (Izv. Akad. Nauk SSSR Ser. Khim. **1991** 341/5; Bull. Acad. Sci. USSR Div. Chem. Sci. [Engl. Transl.] **40** [1991] 288/92).

2.2.12.3 Thermochemical Values

The enthalpy of formation, $\Delta_fH_0^\circ = 231 \pm 1.3$ kJ/mol, was derived from the adiabatic ionization potential of N_2H_3 and the enthalpies of formation of N_2H_4 and H [1]. Ab initio calculations gave $\Delta_fH = 238.5$ [2], 226.0 [3], 222.6 [4], and 227.7 kJ/mol [5]. A much higher value of 364 kJ/mol [6] was based on the erroneous assumption that the radical has the same planar structure as the $N_2H_3^+$ ion.

The enthalpy $H_{298} - H_0 = 110.784$ kJ/mol, heat capacity $C_p = 48.476$ $J \cdot mol^{-1} \cdot K^{-1}$, and entropy $S = 248.873$ $J \cdot mol^{-1} \cdot K^{-1}$ at 298.15 K were obtained by ab initio calculations [3].

References:

[1] Ruscic, B.; Berkowitz, J. (J. Chem. Phys. **95** [1991] 4378/84).

[2] Melius, C. F.; Binkley, J. S. (Chem. Phys. Processes Combust. **1983** Paper 39, 4 pp.; C.A. **100** [1984] No. 216703).

[3] Sana, M.; Leroy, G.; Peeters, D.; Younang, E. (J. Mol. Struct. **151** [1987] 325/30).

[4] Leroy, G.; Sana, M.; Wilante, C. (J. Mol. Struct. **207** [1990] 85/94 [THEOCHEM **66**]).

[5] Leroy, G.; Sana, M.; Wilante, C.; Peeters, D.; Dogimont, C. (J. Mol. Struct. **153** [1987] 249/67 [THEOCHEM **38**]).

[6] Dibeler, V. H.; Franklin, J. L.; Reese, R. M. (Adv. Mass Spectrom. **1** [1959] 443/57).

2.2.12.4 Chemical Behavior

2.2.12.4.1 Decomposition

The decay of N_2H_3 radicals in the bimolecular reaction (1) 2 $N_2H_3 \rightarrow$ products occurs via two channels: (1a) dimerization followed by decomposition of the dimer and (1b) disproportionation

$$\text{(1a)}\ 2\,N_2H_3 \rightarrow N_4H_6 \rightarrow N_2 + 2\,NH_3 \qquad \text{(1b)}\ 2\,N_2H_3 \rightarrow N_2H_4 + N_2H_2$$

The rate constant $k_1 = 3.5 \times 10^{10}$ $L \cdot mol^{-1} \cdot s^{-1}$ (at room temperature) was determined for the decay of N_2H_3 radicals in isothermally flash-photolyzed, gaseous N_2H_4 [1]. An investigation of the gas-phase reaction of N_2H_4 with H atoms by mass spectrometry [2] and of the thermolysis of N_2H_4 at 750 to 1000 K [3] led to the estimated values $k_{1a} \geq 3 \times 10^9$ (at 423 K) [2] and $k_{1a} = 10^9$ $L \cdot mol^{-1} \cdot s^{-1}$ [3]. In a computer simulation of the decomposition of ammonia-oxygen mixtures by pulse radiolysis at 349 K, a value of $k_{1a} = 10^{11}$ $L \cdot mol^{-1} \cdot s^{-1}$ was used [4]. The decomposition of the radicals presumably occurs via reaction (1a) during the thermolysis of N_2H_4 at about 1100 K [5] and during the adiabatic flash photolysis of N_2H_4 [6]. The isotope effect observed in another adiabatic flash heating study of ^{15}N-marked hydrazine suggested reaction (1b) to be more important than reaction (1a) [7].

Reactions (1a) and (1b) are assumed to account for the decomposition of the N_2H_3 radical in gaseous hydrazine photolyzed at 1062 Å [8]. Investigations of the gas-phase photolysis of isotopically marked hydrazine gave a ratio of $k_{1b}/k_{1a} = 2.8$ [9], 3.7 ± 0.9 [10], and 5 [11].

The rate constant for the decay of N_2H_3 radicals in aqueous solutions according to reaction (1a) was determined to be $k_{1a} = 1.2 \times 10^9$ $L \cdot mol^{-1} \cdot s^{-1}$ (at room temperature) [12, 13]. Reaction (1b) is of minor importance. In γ-irradiated aqueous Fe^{II} solutions containing hydrazine as an oxidation inhibitor, about 90% of the N_2H_3 radicals formed react to give NH_3 via reaction (1a) [2]. Similarly, decomposition with dimerization as the first step was assumed to account for the disappearance of N_2H_3 in oxidized aqueous hydrazine solutions [14 to 16]. Studies of the oxidation of acidic hydrazine solutions by Fe^{3+} ions led to $k_{1b}/k_{1a} = 0.015$ in chloride-containing solutions at 333 K [15] and $k_{1b}/k_{1a} = 0.15$ in sulfate-containing solutions at 323 K [14]. The decay of N_2H_3 in frozen alcoholic solutions has been investigated [17].

In order to fit the reaction kinetics of ammonia combustion, the Arrhenius equation $k = 1.2 \times 10^{13}$ $\exp(-243\ kJ \cdot mol^{-1}/RT)$ $cm^3 \cdot mol^{-1} \cdot s^{-1}$ [18] ($k = 3.5 \times 10^{13}$ $\exp(-192\ kJ \cdot mol^{-1}/RT)$ $cm^3 \cdot mol^{-1} \cdot s^{-1}$ [19]) was used for the reaction $N_2H_3 + M \rightarrow N_2H_2 + H + M$ [18]. A reaction enthalpy of about 226 kJ/mol was estimated [20].

N_2H_3 radicals in crystalline N_2H_4 were decomposed by photolysis ($\lambda = 280$ to 400 nm) with the primary step $N_2H_3 + h\nu \rightarrow N_2H_3^* \rightarrow N_2H_2 + H$ to give N_2 and H_2 as final products. The kinetic parameters of the photoradical chain reaction were determined in the range 77 to 194 K and interpreted in terms of a diffusion-controlled process [21].

In the photochemistry of hydrazine induced by an ArF laser, strong two-photon-induced fluorescence from excited radicals NH(A $^3\Pi$) was observed and attributed to secondary absorption by the N_2H_3 primary photoproduct according to $N_2H_3 + h\nu \rightarrow NH_2 + NH^*$ [22]; for critical remarks, see [23, 24].

The reaction $N_2H_3 + M \rightarrow NH_2 + NH + M$ was considered to interprete the mechanism of the pyrolysis of ammonia [20] and of hydrazine [3]. The Arrhenius equation was calculated to be $k = 6.31 \times 10^{12}$ $\exp(-42\ kJ \cdot mol^{-1}/RT)$ [20] and $k = 7.9 \times 10^{12}$ $\exp(-75\ kJ \cdot mol^{-1}/RT)$ $cm^3 \cdot mol^{-1} \cdot s^{-1}$ [3]. A reaction enthalpy of about 301 kJ/mol was estimated [20]. Similarly, the equation $k = 10^{13}$ $\exp(-84\ kJ \cdot mol^{-1}/RT)$ $cm^3 \cdot mol^{-1} \cdot s^{-1}$ was derived for the reaction $N_2H_3 + M \rightarrow N_2 + H_2 + H + M$ [3].

References:

[1] Arvis, M.; Devillers, C.; Gillois, M.; Curtat, M. (J. Phys. Chem. **78** [1974] 1356/60).
[2] Ahrens, R. W. (J. Phys. Chem. **66** [1962] 2108/11).
[3] Eberstein, I. J.; Glassman, I. (Symp. Int. Combust. Proc. **10** [1965] 365/74).
[4] Pagsberg, P. B.; Eriksen, J.; Christensen, H. C. (J. Phys. Chem. **83** [1979] 582/90).
[5] Rice, F. O.; Scherber, F. (J. Am. Chem. Soc. **77** [1955] 291/3).
[6] Husain, D.; Norrish, R. G. W. (Proc. R. Soc. London A **273** [1963] 145/64).
[7] Stief, L. J.; DeCarlo, V. J. (J. Phys. Chem. **71** [1967] 2350/1).

[8] Schurath, U.; Schindler, R. N. (J. Phys. Chem. **74** [1970] 3188/94).
[9] Stief, J. L.; DeCarlo, V. J. (J. Chem. Phys. **44** [1966] 4638/9).
[10] Stief, L. J. (J. Chem. Phys. **52** [1970] 4841/5).

[11] Stief, J. L.; DeCarlo, V. J. (J. Chem. Phys. **49** [1968] 100/5).
[12] Curtat, M.; Souil, F.; Devillers, C. (Propr. Hydrazine Ses Appl. Source Energ. Colloq. Int., Poitiers, Fr., 1974 [1975], pp. 41/5; C.A. **85** [1976] No. 80479).
[13] Hayon, E.; Simic, M. (J. Am. Chem. Soc. **94** [1972] 42/7).
[14] Cahn, J. W.; Powell, R. E. (J. Am. Chem. Soc. **76** [1954] 2568/72).
[15] Higginson, W. C. E.; Wright, P. (J. Chem. Soc. **1955** 1551/6).
[16] Higginson, W. C. E.; Sutton, D.; Wright, P. (J. Chem. Soc. **1953** [1953] 1380/6).
[17] Roginskii, V. A.; Kotov, A. G.; Pshezhetskii, S. Ya. (Zh. Fiz. Khim. **40** [1966] 51; Russ. J. Phys. Chem. [Engl. Transl.] **40** [1966] 25/8).
[18] Dean, A. M.; Chou, M. S.; Stern, D. (Int. J. Chem. Kinet. **16** [1984] 633/53).
[19] Roose, T. R. (Diss. Stanford Univ. 1981 from Miller, J. A.; Smooke, M. D.; Green, R. M.; Kee, R. J.; Combust. Sci. Technol. **34** [1983] 149/76, 151).
[20] Dove, J. E.; Nip, W. S. (Can. J. Chem. **57** [1979] 689/701).

[21] Pshezhetskii, S. Y.; Slavinskaya, N. A.; Trakhtenberg, L. I. (Khim. Vys. Energ. **18** [1984] 225/31; High Energy Chem. [Engl. Transl.] **18** [1984] 182/8).
[22] Hawkins, W. G.; Houston, P. L. (J. Phys. Chem. **86** [1982] 704/9).
[23] Haak, H. K.; Stuhl, F. (J. Phys. Chem. **88** [1984] 3627/33).
[24] Kenner, R. D.; Rohrer, F.; Stuhl, F. (Chem. Phys. Lett. **116** [1985] 374/9).

2.2.12.4.2 Reactions with Elements and Compounds

Hydrogen. The rate constant $k=(1.6\pm0.8)\times10^{12}$ $cm^3\cdot mol^{-1}\cdot s^{-1}$ at 300 K for the reaction (1) $N_2H_3+H\rightarrow2\ NH_2$ was derived by EPR and mass-spectrometric investigations of the reaction of N_2H_4 with H atoms in a flow system [1]. A revised mechanism for the N_2H_4+H reaction did not appreciably change the rate constant $k(N_2H_3+H)$ [2]; for a discussion of reaction (1) in earlier work on the N_2H_4+H reaction system, see [3, 4]. Reaction (1) was considered to occur in the gas-phase photolysis of hydrazine [5, 6].

In a simulation of atmospheric-pressure ammonia flames, the Arrhenius expression $k=1\times10^{12}\cdot T^{0.5}\cdot\exp(-8.4\ kJ\cdot mol^{-1}/RT)$ $cm^3\cdot mol^{-1}\cdot s^{-1}$ was used for reaction (2) $N_2H_3+H\rightarrow N_2H_2+H_2$ [7]. Reaction (2) was mentioned as one step in the photolytic decomposition of hydrazine [8].

Enthalpies were estimated for the following reactions:

reaction	Δ_rH in kJ/mol	Ref.
$N_2H_3+H+M\rightarrow N_2H_4+M$	−(377 to 397)	[9]
$N_2H_3+5\ H\rightarrow2\ N+4\ H_2$	−368.99	[10]
$N_2H_3+H\rightarrow\ N_2+2\ H_2$	−464	[11]
	−(473 to 494)	[9]

A rate constant of 10^{-10} $cm^3\cdot mol^{-1}\cdot s^{-1}$ for the reaction $N_2H_3+H_2\rightarrow N_2H_4+H$ at room temperature was derived based on the rate constant of the reverse reaction [12].

A pK_a value of 7.1 ± 0.1 was derived for the acid-base equilibrium $N_2H_4^+\rightleftharpoons N_2H_3+H^+$ by monitoring radiolyzed aqueous hydrazine solutions with an UV absorption spectrometer [13].

Oxygen. A lower limit for the rate constant, $k \geq 3 \times 10^9\ L \cdot mol^{-1} \cdot s^{-1}$, was derived for the reaction $N_2H_3 + O_2 + OH^- \rightarrow O_2^- + N_2H_2 + H_2O$ in radiolyzed aqueous alkaline solutions of hydrazine containing oxygen [14].

The reaction $N_2H_3 + O_2 \rightarrow O_2^- + H^+ + N_2H_2$ is considered part of the reaction mechanism of the Mn^{II}-catalyzed autoxidation of hydrazine in aqueous alkaline solutions [15]. A chain mechanism, including the reaction $N_2H_3 + O_2 \rightarrow N_2H_3O_2$, was proposed for the decay of N_2H_3 radicals in radiolyzed, oxygen-containing, aqueous hydrazine solutions [16].

In a simulation of atmospheric-pressure ammonia flames, the Arrhenius equation $k_3 = 2 \times 10^{13} \exp(-4.2\ kJ \cdot mol^{-1}/RT)$ was used for the reaction (3) $N_2H_3 + O \rightarrow N_2H_2 + OH$ [7]. An upper limit of $k_3 \leq 5 \times 10^{12}\ cm^3 \cdot mol^{-1} \cdot s^{-1}$ was determined in an investigation of the gas-phase reaction system $N_2H_4 + O$ at room temperature. For the reaction path (4) $N_2H_3 + O \rightarrow NH_2 + HNO$, a rate constant of $k_4 = 4 \times 10^{13}\ cm^3 \cdot mol^{-1} \cdot s^{-1}$ was derived [2]. A theoretical study of the kinetics of NH_3-O_2 flames yielded the rate constant $k_4 = 10^{13}\ cm^3 \cdot mol^{-1} \cdot s^{-1}$ which was used in a simulation of the reaction mechanism [17].

Miscellaneous. The oxidation of N_2H_3 by Fe^{III} and Cu^{II} in aqueous solutions gives N_2H_2 which in turn decomposes to give N_2. The oxidation by Cu^{II} at pH 0.6 and 323 K is about 1200 times faster than the oxidation by Fe^{III} [18].

An upper limit of $k_5 \leq 5 \times 10^{13}\ cm^3 \cdot mol^{-1} \cdot s^{-1}$ was determined for the reaction (5) $N_2H_3 + OH \rightarrow N_2H_2 + H_2O$ from an investigation of the gas-phase reaction system $N_2H_4 + O$ at room temperature [2]. The Arrhenius expression $k_5 = 3 \times 10^{10} \cdot T^{0.68} \cdot \exp(-5.40\ kJ \cdot mol^{-1}/RT)\ cm^3 \cdot mol^{-1} \cdot s^{-1}$ was derived to simulate the kinetics in ammonia flames [7]. Another simulation of the ammonia-oxygen flames used $k_5 = 10^{13} \exp(-4.2\ kJ \cdot mol^{-1}/RT)\ cm^3 \cdot mol^{-1} \cdot s^{-1}$ [17].

A free enthalpy of hydration of $\Delta G^\circ = 18.8$ kJ/mol was estimated for the process $N_2H_3(aq) \rightarrow N_2H_3(g)$ [19].

UV-spectroscopic studies of the autoxidation of alkaline aqueous hydrazine solutions gave for the reaction $N_2H_3 + HO_2^- \rightarrow N_2H_2 + OH + OH^-$ an estimate for the rate constant of $95\ L \cdot mol^{-1} \cdot s^{-1}$ [15].

The reaction enthalpy for $N_2H_3 + N_2H \rightarrow N_2 + N_2H_4$ was calculated in a SCF MO study to be -276.6 (STO-3G basis) and -297.9 kJ/mol (4-31G basis) [20].

A rate constant of $k = 2 \times 10^{13}\ cm^3 \cdot mol^{-1} \cdot s^{-1}$ was estimated for the reaction $N_2H_3 + NH \rightarrow N_2H_2 + NH_2$ and used to model the kinetics of a 98-reaction mechanism for ammonia-oxygen flames [17].

The reaction $N_2H_3 + NH_2 \rightarrow NH_3 + H_2 + N_2$ is considered part of the mechanism of the thermolysis of hydrazine (at 1123 K) [21]. The reaction enthalpy was estimated to be $\Delta_rH = -(489$ to $510)$ kJ/mol [9] and -469 kJ/mol [11]. For the reaction system $NH_2 + N_2H_4$ (at 2.3 mbar) a rate constant of $k(298\ K) = 5 \times 10^{13}\ cm^3 \cdot mol^{-1} \cdot s^{-1}$ was estimated for the reaction $N_2H_3 + NH_2 \rightarrow NH_3 + N_2H_2$ [2].

N_2H_3 radicals are scavenged by NO via $N_2H_3 + NO \rightarrow N_2O + NH_3$ [22, 23]; $\Delta_rH = 502$ kJ/mol [24].

In the $Hg(^3P_1)$-photosensitized decomposition of N_2H_4, the intermediate N_2H_3 reacts with CH_3 radicals (from added dimethyl mercury) to give CH_3NHNH_2. A second reaction channel discussed is a fast reaction yielding CH_4 and N_2H_2 [25]. The enthalpy of this hydrogen transfer reaction is $\Delta_rH = -218 \pm 25$ [25] and -88 kJ/mol (ab initio calculation) [26].

References:

[1] Gehring, M.; Hoyermann, K.; Wagner, H. G.; Wolfrum, J. (Ber. Bunsen-Ges. Phys. Chem. **75** [1971] 1287/94).
[2] Dransfeld, P. (Diss. Univ. Göttingen 1986, pp. 1/153).
[3] Gibson, S. T.; Greene, J. P.; Berkowitz, J. (J. Chem. Phys. **83** [1985] 4319/28).
[4] Ghosh, P. K.; Bair, E. J. (J. Chem. Phys. **45** [1966] 4738/41).
[5] Arvis, M.; Devillers, C.; Gillois, M.; Curtat, M. (J. Phys. Chem. **78** [1974] 1356/60).
[6] Hawkins, W. G.; Houston, P. L. (J. Phys. Chem. **86** [1982] 704/9).
[7] Dean, A. M.; Chou, M. S.; Stern, D. (Int. J. Chem. Kinet. **16** [1984] 633/53).
[8] McDonald, C. C.; Gunning, H. E. (J. Chem. Phys. **23** [1955] 532/41).
[9] Freeman, G. R.; Winkler, C. A. (Can. J. Chem. **33** [1955] 692/8).
[10] Sana, M.; Leroy, G.; Peeters, D.; Younang, E. (J. Mol. Struct. **151** [1987] 325/30).

[11] Moberly, W. H. (J. Phys. Chem. **66** [1962] 366/8).
[12] Baulch, D. L.; Drysdale, D. D.; Horne, D. G. (Evaluated Kinetic Data for High Temperature Reactions, Vol. 2, Butterworth, London 1973, pp. 519/26).
[13] Hayon, E.; Simic, M. (J. Am. Chem. Soc. **94** [1972] 42/7).
[14] Ershov, B. G.; Mikhailova, T. L. (Izv. Akad. Nauk SSSR Ser. Khim. **1991** 341/5; Bull. Acad. Sci. USSR Div. Chem. Sci. [Engl. Transl.] **40** [1991] 288/92).
[15] Lim, P. K.; Fagg, B. S. (J. Phys. Chem. **88** [1984] 1136/40).
[16] Ershov, B. G.; Mikhailova, T. L.; Emel'yanova, A. Yu. (Izv. Akad. Nauk SSSR Ser. Khim. **1988** 1192; Bull. Acad. Sci. USSR Div. Chem. Sci. [Engl. Transl.] **37** [1988] 1051).
[17] Miller, J. A.; Smooke, M. D.; Green, R. M.; Kee, R. J. (Combust. Sci. Technol. **34** [1983] 149/76).
[18] Cahn, J. W.; Powell, R. E. (J. Am. Chem. Soc. **76** [1954] 2568/72).
[19] Bauer, N. (J. Phys. Chem. **64** [1960] 833/7).
[20] Pasto, D. J. (J. Am. Chem. Soc. **101** [1979] 6852/7).

[21] Rice, F. O.; Scherber, F. (J. Am. Chem. Soc. **77** [1955] 291/3).
[22] Stief, J. L.; DeCarlo, V. J. (J. Chem. Phys. **49** [1968] 100/5).
[23] Bamford, C. H. (Trans. Faraday Soc. **35** [1939] 568/76).
[24] Husain, D.; Norrish, R. G. W. (Proc. R. Soc. London A **273** [1963] 145/64).
[25] Jones, A.; Lossing, F. P. (Can. J. Chem. **47** [1969] 1391/3).
[26] Leroy, G.; Sana, M.; Wilante, C. (J. Mol. Struct. **207** [1990] 85/94 [THEOCHEM **66**]).

2.2.13 The Hydrazyl Cation, $N_2H_3^+$

Systematic name: Diazenium

CAS Registry Number: *[37369-93-0]*

Formation. $N_2H_3^+$ ions were observed as secondary ions in the mass spectrum of gaseous ammonia (electron energies up to 80 V, NH_3 pressures of 2.5×10^{-3} to 65×10^{-3} Torr). The ions were presumably formed by the reactions $NH^+ + NH_3 \rightarrow N_2H_3^+ + H$ and $NH_2^+ + NH_3 \rightarrow N_2H_3^+ + H_2$ (cross sections $\sigma = 35\times10^{-18}$ and 5.3×10^{-18} $cm^2\cdot molecule^{-1}$, respectively) [1].

$N_2H_3^+$ ions were mass-spectrometrically detected in electron-impact experiments on N_2H_4 [2 to 5] and methyl hydrazines [3], photoionization studies on N_2H_4 [6, 7] and $CH_3N_2H_3$ [6], and in a microwave discharge through N_2H_4 [8, 9]. The following appearance potentials AP of the cation in the process $N_2H_4 \rightarrow N_2H_3^+ + H + e^-$ and enthalpies of formation Δ_fH_{298} (in kJ/mol) were reported:

AP (eV)	11.1 ± 0.1	11.18 ± 0.1	11.3 ± 0.1	11.1	10.86 ± 0.05	11.10[a]
Δ_fH_{298}	946	–	962	–	–	971[b]
Ref.	[6]	[8]	[2, 3]	[7]	[9]	[10, 11]

[a] Calculated with ab initio methods (G2 procedure) [10]. – [b] Semiempirically (MNDO) calculated value [11].

$N_2H_3^+$ ions were formed by interaction of N_2H_4 with a platinum surface. The yield of $N_2H_3^+$ ions was monitored with a field ion mass spectrometer in the range of 298 to 448 K, passing through a maximum at ~335 K [12].

The formation of $N_2H_3^+$ ions was observed mass-spectrometrically in collision reactions of N_2H_4 (at pressures of 0.133 Pa) with beams of O^+, Ar^+, Kr^+, CO^+, and CO_2^+. For the reaction path $O^+ + N_2H_4 \rightarrow OH + N_2H_3^+$, a reaction energy of $\Delta E = -637$ kJ/mol was determined. For the reactions $O^+(Ar^+, Kr^+) + N_2H_4 \rightarrow O$ (Ar, Kr) $+ N_2H_3^+ + H$, the energies $\Delta E = -212$ (-425, -251) kJ/mol were determined, respectively [13].

The formation of $N_2H_3^+$ ions was assumed to be the rate-determining first step in the electrooxidation of hydrazine at a dropping mercury electrode according to $N_2H_4 + OH^- \rightarrow N_2H_3^+ + H_2O + 2\,e^-$ [14].

Structure and Properties. Ab initio [10, 11, 15 to 17] and semiempirical [11, 18] calculations predicted a planar structure (C_s symmetry) for the $N_2H_3^+$ ion in its electronic ground state $^1A'$. An ab initio SCF MO calculation at the 4-31G level [16] and SCF MO [11] and MP2 [10] calculations at the 6-31G** level gave the following optimized geometry (bond distance r in Å, angles α; for atom numbering, see p. 75):

$r(N^1\text{-}N^2)$	$r(N^1\text{-}H^1)$	$r(N^1\text{-}H^2)$	$r(N^2\text{-}H^3)$	$\alpha(NNH^1)$	$\alpha(NNH^2)$	$\alpha(NNH^3)$	Ref.
1.240	1.032	1.035	1.035	125.2°	116.7°	110.4°	[10]
1.213	1.008	1.008	1.016	121.3°	121.3°	116.0°	[16]
1.204	1.013	1.013	1.016	124.1°	117.5°	112.5°	[11]

The bond distance r(N-N) = 1.271 Å was obtained in a MP2/3-21G calculation [19].

Ab initio and semiempirical (MNDO) calculations were performed on the ion in the electronically excited doublet and triplet states [11].

Further ab initio and semiempirical studies on $N_2H_3^+$ were reported in [19 to 22].

Ab initio SCF MO calculations and frontier molecular orbital analysis (FMO) reveal a preference for an inversion mechanism for the topomerization of the cation over a torsional process. The calculations gave for planar inversion (i.e. H^3 changes from trans position to cis position towards H^1 without rotation around the N-N bond) a considerably lower barrier (123 kJ/mol) than for rotation around the N-N bond (309.8 kJ/mol) [16, 23]; for earlier studies, see [24, 25].

Ab initio calculations yielded a high barrier of 264.8 kJ/mol for the 1,2-hydrogen atom shift (i.e. H^1 changes its position from N^1 to N^2) passing through a C_{2v} transition structure [17].

An N-N stretching frequency of 1570 ± 80 cm^{-1} was derived from the vibrational structure in the photoion-yield curve obtained by N_2H_3 photoionization mass spectrometry [26]. From the SCF MO equilibrium geometry the vibrational frequencies 1177, 1296, 1373, 1605, 1780, 1974, 3603, 3648, and 3744 cm^{-1} were calculated [11].

A force constant of 13.1 mdyn/Å was calculated for the N-N bond with the MNDO procedure [19].

Calculated bond dissociation energies $D(H_2^+N\text{-}NH) = 674$ kJ/mol and $D(HNN^+H\text{-}H) = 372$ kJ/mol were reported in [9].

Reactions. A cross section of 8.9×10^{-15} $cm^2 \cdot molecule^{-1}$ was determined for the decay of $N_2H_3^+$ ions formed as secondary ions in the mass spectrum of gaseous NH_3 [1].

In the mechanism of the electrooxidation of hydrazine in aqueous hydrochloric acid solutions, the reaction $N_2H_3^+ + Cl^- \rightarrow N_2H_3Cl$ was discussed in order to explain the significant lowering of the nitrogen yield [14].

The reaction $N_2H_3^+ + N_2H_4 \rightarrow N_2H_5^+ + N_2H_2$ probably occurs in the high-pressure mass spectra of hydrazine. Rate constants of 1.0×10^{-10} and 3.8×10^{-10} $cm^3 \cdot molecule^{-1} \cdot s^{-1}$ were measured at zero field strength using pulse techniques and at a constant repeller voltage of 10.5 V/cm, respectively [5].

References:

[1] Derwish, G. A. W.; Galli, A.; Gardini-Guidoni, A.; Volpi, G. G. (J. Chem. Phys. **39** [1963] 1599/605).
[2] Fisher, I. P.; Heath, G. A. (Nature **208** [1965] 1199/200).
[3] Dibeler, V. H.; Franklin, J. L.; Reese, R. M. (J. Am. Chem. Soc. **81** [1959] 68/73).
[4] Dibeler, V. H.; Franklin, J. L.; Reese, R. M. (Adv. Mass Spectrom. **1** [1959] 443/57).
[5] Harrison, A. G.; Thynne, J. C. J. (Trans. Faraday Soc. **62** [1966] 2804/14).
[6] Akopyan, M. E.; Vilesov, F. I. (Kinet. Katal. **4** [1963] 39/52; Kinet. Catal. [Engl. Transl.] **4** [1963] 32/43).
[7] Gibson, S. T.; Greene, J. P.; Berkowitz, J. (J. Chem. Phys. **83** [1985] 4319/28).
[8] Foner, S. N.; Hudson, R. L. (J. Chem. Phys. **29** [1958] 442/3).
[9] Wiberg, N.; Fischer, G.; Bachhuber, H. (Z. Naturforsch. **34b** [1979] 1385/90).
[10] Pople, J. A.; Curtiss, L. A. (J. Chem. Phys. **95** [1991] 4385/8).

[11] Glover, S. A.; Scott, A. P. (Tetrahedron **45** [1989] 1763/76).
[12] Block, J. (Z. Phys. Chem. [Munich] **82** [1972] 1/10).
[13] Gardner, J. A.; Dressler, R. A.; Salter, R. H.; Murad, E. (J. Phys. Chem. **96** [1992] 4210/7).
[14] Karp, S.; Meites, L. (J. Am. Chem. Soc. **84** [1962] 906/12).
[15] Lathan, W. A.; Curtiss, L. A.; Hehre, W. J.; Lisle, J. B.; Pople, J. A. (Prog. Phys. Org. Chem. **11** [1974] 175/261).
[16] Kost, D.; Aviram, K.; Raban, M. (Isr. J. Chem. **23** [1983] 124/8).
[17] Del Bene, J. E.; Frisch, M. J.; Raghavachari, K.; Pople, J. A. (J. Phys. Chem. **86** [1982] 1529/35).
[18] Fabian, J.; Suehnel, J. (J. Prakt. Chem. **315** [1973] 307/12).
[19] Maksic, Z. B.; Eckert-Maksic, M.; Skancke, P. N.; Skancke, A. (J. Mol. Struct. **169** [1988] 447/57 [THEOCHEM **46**]).
[20] Dilworth, J. R.; Garcia-Rodriguez, A.; Leigh, G. J.; Murrell, J. N. (J. Chem. Soc. Dalton Trans. **1983** 455/61).

[21] Nelsen, S. F.; Blackstock, S. C. (J. Org. Chem. **49** [1984] 1134/5).
[22] Bespalov, V. Y.; Kuznetsov, M. A. (Zh. Strukt. Khim. **15** [1974] 740/3; J. Struct. Chem. [Engl. Transl.] **15** [1974] 648/50).
[23] Kost, D.; Aviram, K.; Raban, M. (J. Org. Chem. **54** [1989] 4903/8).
[24] Bespalov, V. Y.; Kuznetsov, M. A. (Teor. Eksp. Khim. **15** [1979] 557/9; Theor. Exp. Chem. [Engl. Transl.] **15** [1979] 434/5).

[25] Merenyi, G.; Wettermark, G.; Roos, B. (Chem. Phys. **1** [1973] 340/7).
[26] Ruscic, B.; Berkowitz, J. (J. Chem. Phys. **95** [1991] 4378/84).

2.2.14 The Hydrazyl Anion, $N_2H_3^-$

Other names: Diazanide, hydrazide, hydrazinide

CAS Registry Number: *[25415-88-7]*

Formation. The only known hydrazides isolated are the probably ionic compound NaN_2H_3 (see "Natrium" 1928, pp. 260/1 and "Natrium" Erg.-Bd. 3, 1966, pp. 928/9) and the more covalent compound $Zn(N_2H_3)_2$. The hydrazides are formed by the reaction of anhydrous N_2H_4 with metallic Na and $Zn(C_2H_5O)_2$, respectively. NaN_2H_3 is extremely unstable and explosive; $Zn(N_2H_3)_2$ is more stable, but hydrolyzes within a few seconds [1].

Structure and Properties. From ab initio calculations [2 to 4] a nonplanar structure with C_s symmetry, i.e., a staggered configuration of the NH_2 group to the NNH plane, was predicted to be the most stable form of the anion. This structure also followed from an analysis of the vibrational spectrum of the anion [5]. Bond distances (in Å) and angles (in °) were obtained by ab initio calculations at the 4-31G level (for atom numbering, see p. 75):

$r(N^1-N^2)$	$r(N^1-H^1)$	$r(N^1-H^2)$	$r(N^2-H^3)$	$\alpha(NNH^1)$	$\alpha(NNH^2)$	$\alpha(NNH^3)$	Ref.
1.538	1.004	1.004	1.032	106.9	100.8	107.9	[2]
1.540	1.009	1.009	1.031	106.5	100.0	120.7	[3]
1.540	1.009	1.009	1.031	107.8	100.1	107.8	[4]

The dihedral angle $\alpha(H^1N^1N^2H^3)$ was determined to be 122.7° [4].

Theoretical studies were performed on the topomerization of the anion [2, 4, 6]. A complete topomerization of the anion requires both planar inversion and rotation around the N-N bond. The sum of the barriers of the consecutive processes, rotation (33.9 kJ/mol [2, 4]) and inversion (31.4 kJ/mol [4]), is lower than the barrier for the simultaneous interconversion (72.05 kJ/mol); for details, see [4, 6].

A proton affinity for $N_2H_3^-$ of 1820 kJ/mol was obtained from ab initio calculations [2].

The following wavenumbers of the nine fundamentals of the anion were reported in a revised analysis [5] of the vibrational spectra of NaN_2H_3 in Nujol and between NaCl plates [1]; see "Natrium" Suppl. Vol. 3, 1966, p. 929 (ν denotes stretching, δ bending, γ twisting, τ torsional vibrations, sciss scissoring and wag wagging modes):

assignment	$\nu_1(A')$	$\nu_2(A')$	$\nu_3(A')$	$\nu_4(A')$
approx. description	$\nu(N^2-H)$	$\nu_s(NH_2)$	$\delta_{sciss}(NH_2)$	$\delta(NNH^3)$
frequency (in cm^{-1})	3202	3100	1599	1330

assignment	$\nu_5(A')$	$\nu_6(A')$	$\nu_7(A'')$	$\nu_8(A'')$	$\nu_9(A'')$
approx. description	$\delta_{wag}(NH_2)$	$\nu(N-N)$	$\nu_{as}(NH_2)$	$\gamma(NH_2)$	$\tau(N-N)$
frequency (in cm^{-1})	1103	847	3155	1232	386*)

*) Estimated value.

Based on these frequencies and on the estimated geometrical parameters r(N-N) = 1.47, r(N-H) = 1.03 Å, α(H^1NH^2) = 107°, α(NNH^3) = 101°, and α(H^1NN) = 103°, a normal coordinate analysis was performed yielding the stretching force constants (in mdyn/Å) f(N^2-H^3) = 5.675, f(N-N) = 3.15, and f(N^1-H) = 5.41 [5]. A force constant of f(N-N) = 3.35 mdyn/Å was calculated earlier [1].

The energy for the reaction $N_2H_3^- + H_2 \rightarrow NH_3 + NH_2^-$ was calculated with ab initio methods to be −177.0 [7] and −154 kJ/mol [3].

The free enthalpy of hydration for the gaseous $N_2H_3^-$ ion was estimated to be −333.5 kJ/mol [8].

An acid constant of $10^{-30.5}$ for $N_2H_4 \rightleftharpoons N_2H_3^- + H^+$ in aqueous solutions was predicted from a linear relationship between the acidities of a series of nitrogen acids and (ab initio) calculated average local ionization energies of the conjugate bases [9]. A free enthalpy of 181.2 kJ/mol was derived for this process [8].

References:

[1] Goubeau, J.; Kull, U. (Z. Anorg. Allg. Chem. **316** [1962] 182/9).
[2] Hopkinson, A. C.; Lien, M. H. (Int. J. Quantum Chem. **13** [1978] 349/66).
[3] Hinde, A. L.; Pross, A.; Radom, L. (J. Comput. Chem. **1** [1980] 118/28).
[4] Kost, D.; Aviram, K.; Raban, M. (J. Org. Chem. **54** [1989] 4903/8).
[5] Christe, K. O.; Wilson, W. W.; Curtis, E. C. (Inorg. Chem. **18** [1979] 2578/86).
[6] Kost, D.; Aviram, K.; Raban, M. (Isr. J. Chem. **23** [1983] 124/8).
[7] Magnusson, E. (Tetrahedron **41** [1985] 5235/40).
[8] Bauer, N. (J. Phys. Chem. **64** [1960] 833/7).
[9] Brinck, T.; Murray, J. S.; Politzer, P. (J. Org. Chem. **56** [1991] 5012/5).

2.3 Trinitrogen Compounds

2.3.1 Hydrogen Azide, HN_3

Other common name: Hydrazoic acid

Systematic name: Hydrogen trinitride

Other names: Azoimide, hydronitric acid, triazadiene

CAS Registry Numbers: HN_3 *[7782-79-8]*, DN_3 *[14989-19-6]*, $H^{15}NNN$ *[14706-85-5]*, $HN^{15}NN$ *[15608-46-5]*, $HNN^{15}N$ *[14706-90-2]*, $D^{15}NNN$ *[101059-18-1]*, $DN^{15}NN$ *[15608-43-2]*, $DNN^{15}N$ *[101059-17-0]*, DN_3 (labeled with ^{15}N) *[14989-20-9]*

General References:

Jones, K.; Hydrogen Azide and Azides, in: Bailar, J. C.; Emeléus, H. J.; Nyholm, R.; Trotman-Dickensen, A. F.; Comprehensive Inorganic Chemistry, Vol. 2, Pergamon, Oxford 1973, pp. 276/93.

Mason, K. G.; Hydrogen Azide, in: Mellor's Comprehensive Treatise on Inorganic and Theoretical Chemistry, Vol. 8, Suppl. 2, Longmans, London 1967, pp. 1/15.

Rosenwasser, H.; Hydrazoic Acid and the Metal Azides, AD-208892 [1958] 72 pp., 1/9; C.A. **1961** 15203.

Pure hydrogen azide is a highly explosive, colorless liquid of unbearably acrid odor at ambient temperature. Explosions seem to be triggered by shocks. Aqueous solutions of less than about 20 wt% of HN_3 do not detonate. Inhalation of the highly toxic vapors in small quantities causes the blood pressure to drop and irritates the mucous membranes. Contact with the aqueous solution damages the skin.

HN_3 is prepared by acidification of alkali azides, which can substitute it in many reactions. The acid strength of HN_3 is similar to that of acetic acid. HN_3 is used in organic reactions, either as a reactant, for example in additions to unsaturated bonds, or as an inhibitor of side reactions, for example by liberating nitrite. The application of HN_3 for generating lasing species was also tested. Early work on HN_3 is described in "Stickstoff" 2, 1935, pp. 285/303.

Some relevant properties are:

molecular weight	43.03
melting point	193 K
boiling point	308.9 K (extrapolated)
triple point	~193 K, 1 Torr
vapor pressure	498 Torr (298 K)
standard enthalpy of formation (l)	267 kJ/mol (298 K, 1 bar)
density (l)	1.127 g/cm^3 (290 K)
dipole moment (g)	HN_3: 1.70 D, DN_3: 1.76 D
solubility in water	completely miscible
enthalpy of solution	−34 kJ/mol (1 M solution, 298 K)
dissociation constant pK_a	4.64 (298 K, $\mu \to 0$)

2.3.1.1 Preparation and Formation

All recent preparations of HN_3 use the well known reaction of NaN_3 with a stronger or less volatile acid. Mineral acids like HCl or H_2SO_4 are used for its large-scale production.

Laboratory preparations involve H_2SO_4, H_3PO_4, or stearic acid. Other synthetic methods described in "Stickstoff" 2, 1935, pp. 285/90, are not used any more.

2.3.1.1.1 Hydrolysis of Azides

Gaseous HN_3 is conveniently prepared on a laboratory scale by adding concentrated H_3PO_4 to dry solid NaN_3 while kept at 320 to 330 K under vacuum [1 to 3]. The reaction can be controlled by gentle warming or cooling [2]. A stable flow of gas results from using several independent reactors simultaneously [4]. The synthesis of HN_3 from a saturated solution of NaN_3 and concentrated H_3PO_4 under vacuum at 363 K was described in [5]. Addition of concentrated H_2SO_4 to NaN_3 at 77 K under vacuum and slow warming to ~350 K also yields HN_3 upon condensation at 77 K [6]. The thus isolated products contain moisture.

Small amounts of dry HN_3 are commonly prepared from NaN_3 and a slight excess of stearic acid under vacuum. The reaction of the solid mixture starts upon melting and proceeds smoothly at 350 to 360 K. The simultaneously formed HN_3 is removed, for example by condensation at ~230 K [7]. Moisture-free, gaseous HN_3 is also obtained by passing HCl in an inert gas through a column packed with finely powdered NaN_3 [8]. An apparatus for preparing relatively large amounts of gaseous HN_3 was described in a report [9].

An aqueous solution with ~3% of HN_3 results by slowly acidifying a boiling, aqueous solution of NaN_3 with 40% H_2SO_4 and collecting the distillate in a flask containing water [10]. Sulfate contamination in the HN_3 solution can be prevented by acidifying the cold solution and slowly heating it to the boiling point. The resulting distillate contains up to 80% HN_3 [11]. An inherently safer method for the preparation of aqueous solutions with up to 20% of HN_3 involves passing a solution of technical-grade NaN_3 through a column filled with the hydrogen form of a sulfonic acid-type cationic exchange resin. The concentration of HN_3 in the eluate is essentially the same as that of the NaN_3 solution used, cation impurities are effectively removed [12]. Contact of HN_3 with the resin should be as short as possible. A more concentrated solution with 30 to 60% HN_3 can be obtained by bubbling N_2 through the eluate and condensing the volatiles at 273 K [13]. A diethyl ether solution of HN_3 distills upon adding 40% H_2SO_4 to the aqueous NaN_3 solution covered with a layer of ether. The distillation is completed by heating. The ether solution is dried over $CaCl_2$ and redistilled [10, 14].

A gaseous mixture of HN_3 in N_2 for industrial purposes results from the reaction of crude NaN_3 with aqueous HCl at ~350 K and stripping the HN_3 thus formed from the solution with a stream of N_2 [15 to 17]. The yield of this process is maximized by separating the solid salts formed in the process from the mother liquor which then is reacted with additional azide [18].

Formation of HN_3 from N_3^- and $CH_2(CN)_2$, $CH_2(COCH_3)_2$, and HCO_2H, but not with $C_2H_5CO_2H$, was observed during ion cyclotron resonance-spectrometric measurements of the proton affinity of N_3^- [19]. The liberation of HN_3 from MN_3 (M = Na, Cs, $N(CH_3)_4$) by less than one equivalent of gaseous HF at ambient temperature leaves a residue of $MF \cdot nHF$ in MN_3 which is attributed to the formation of the more acidic HF_2^- replacing the weaker acid HN_3 [20]. Hydrolysis of $Pb(N_3)_2$ yields HN_3 via $Pb(N_3)_2(s) + H_2O(l) \rightleftharpoons HN_3(g) + Pb(N_3)OH(s)$ with an equilibrium constant of $K = 4.5 \times 10^{-2}$ Torr at 298 K. Hydrolysis in the presence of CO_2 leads to HN_3 and $Pb_3(OH)_2(CO_3)_2$ [21]. A solution containing the 1:1 complex of N_3^- and Sm^{3+} decomposes with formation of HN_3 at pH values below 5.5 and temperatures above 298 K [22].

References:

[1] Amble, E.; Dailey, B. P. (J. Chem. Phys. **18** [1950] 1422).
[2] Pannetier, G. (C. R. Hebd. Seances Acad. Sci. **232** [1951] 817/8).
[3] Pannetier, G.; Gaydon, A. G. (J. Chim. Phys. Phys.-Chim. Biol. **48** [1951] 221/4).
[4] Guenebaut, H. (Bull. Soc. Chim. Fr. **1959** 962/1018).
[5] Welge, K. H. (J. Chem. Phys. **45** [1966] 4373/4).
[6] Gholivand, K.; Schatte, G.; Willner, H. (Inorg. Chem. **26** [1987] 2137/40).
[7] Günther, P.; Meyer, R.; Müller-Skjold, F. (Z. Phys. Chem. A **175** [1935] 154/69).
[8] Milligan, D. E.; Jacox, M. E. (J. Chem. Phys. **47** [1967] 5157/68).
[9] Reitzner, B.; Manno, R. P. (NASA Doc. N63-16521 [1963] 13 pp. from C.A. **60** [1964] 6462).
[10] Audrieth, L. F.; Gibbs, C. F. (Inorg. Synth. **1** [1939] 77/9).

[11] Kemp, M. D. (J. Chem. Educ. **37** [1960] 142).
[12] Bryant, J. I.; Rosenwasser, H. (J. Chem. Educ. **39** [1962] 296/7).
[13] Pannetier, G.; Margineanu, F.; Dereigne, A.; Bonnaire, R. (Bull. Soc. Chim. Fr. **1972** 2617/22).
[14] Steudel, R.; Schenk, P. W. (in: Brauer, G.; Handbuch der Präparativen Anorganischen Chemie, 3rd Ed., Vol. 1, Enke, Stuttgart 1975, pp. 455/6).
[15] Snead, W. K.; PPG Industries, Inc. (U.S. 3752881 [1973] 4 pp.; C.A. **80** [1974] No. 5394).
[16] Snead, W. K.; Knoop, J. F.; PPG Industries, Inc. (U.S. 3705008 [1972] 6 pp.; C.A. **78** [1973] No. 74251).
[17] Pieser, L. W.; PPG Industries, Inc. (U.S. 3734998 [1973] 4 pp.; C.A. **79** [1973] No. 33206).
[18] Rowan, C. M., Jr.; PPG Industries, Inc. (U.S. 3781411 [1973] 4 pp.; C.A. **80** [1974] No. 85241).
[19] Pellerite, M. J.; Jackson, R. L.; Brauman, J. I. (J. Phys. Chem. **85** [1981] 1624/6).
[20] Christe, K. O.; Wilson, W. W.; Bau, R.; Bunte, S. W. (J. Am. Chem. Soc. **114** [1992] 3411/4).

[21] Lamnevik, S. (Symp. Chem. Probl. Connected Stab. Explos., 1967 [1968], pp. 21/33; C.A. **70** [1969] No. 98403).
[22] Abdel-Aziz, I. E. (Indian J. Chem. A **16** [1978] 218/20).

2.3.1.1.2 Oxidation of Hydrazine and Its Salts

The formation of HN_3 by oxidation of N_2H_4 in aqueous HNO_3 can be formulated by the equation $17\ N_2H_4 + 16\ HNO_3 \rightarrow 4\ HN_3 + 4\ NH_4NO_3 + 4\ N_2O + 11\ N_2 + 32\ H_2O$. A kinetic investigation suggests N_2H_2 to be an intermediate [1]. The reaction is accelerated by γ radiation; the yield of HN_3 passes through a maximum of ~35% in 2 M HNO_3 at 310 K and decreases with increasing concentration of HNO_3 [2].

The oxidation of N_2H_4 to HN_3 by HNO_3 in aqueous solution is catalyzed by Tc ions [3, 4] and is also responsible for the degradation of N_2H_4 with formation of HN_3 and NH_4^+ in aqueous, Tc-bearing process solutions during the U-Pu separation in the PUREX process [5]. The presence of TcO_4^- ions catalyzes the formation of HN_3, reaching a maximum yield of ~50% in 5.3 M HNO_3 at 313 K [2, 6]. The oxidation of N_2H_4 leads to $N_2H_5NO_3$ and HN_3 at a molar ratio of 1.5 to 2 which remains constant as the oxidation of N_2H_4 and HN_3 continues [4]. Addition of NO_2^- ions decreases the HN_3 yield [2]. The yield of HN_3 is hardly influenced by U^{IV} and depressed by Pu^{IV} ions [6]. The formation of HN_3 in diluted HNO_3 containing Fe^{2+} is attributed to intermediately formed HNO_2 [7]. The reaction was also observed in solutions containing additional Cu^{2+} ions [8]. A minor amount of gaseous HN_3 forms during fast thermolysis of $N_2H_5NO_3$ [9].

The formation of HN_3 via the well known reaction $N_2H_5^+ + HNO_2 \rightarrow HN_3 + 2\ H_2O + H^+$ is nearly quantitative with excess N_2H_4 in aqueous HNO_3 [7] or $HClO_4$ [10] at $[H^+] > 0.2$ mol/L. Lowering $[H^+]$ decreases the yield of HN_3 in favor of NH_3 [10]. Experiments with $^{15}N_2H_4$ and HNO_2 yield exclusively HN_3 with ^{14}N in one of the molecule's terminal positions and eliminate cyclic azide to be an intermediate during the formation of the product [11]. The reaction in $HClO_4$ is catalyzed weakly by Cl^- and Br^- and much stronger by SCN^-. A reaction mechanism was proposed involving nitrosation of $N_2H_5^+$ by NOX (X = Cl, Br, SCN) and decomposition of the thus formed adduct to HN_3 and H_2O or NH_3 and N_2O, with the relative contribution of either reaction depending on the pH [10]. The reaction in aqueous 0.05 to 0.5 M HNO_3 is given by $7\ N_2H_4 + 12\ HNO_2 + H^+ \rightarrow HN_3 + NH_4^+ + 5\ N_2 + 6\ N_2O + 18\ H_2O$ [12].

The formation of HN_3 in a mixture of NH_3 and other nitrogen-hydrogen compounds was established mass-spectrometrically upon exposing gaseous N_2H_4 at 233 K to a microwave discharge [13]. A gaseous mixture of HN_3, N_2, N_2O, NO, and H_2O resulted when N_2O_4 was passed over condensed N_2H_4 [14]. Oxidation of N_2H_4 by primary aliphatic nitrate esters yielded a trace of HN_3 besides N_2, NH_3, and NO [15]. Mixtures of HN_3 and NH_3 form during the oxidation of N_2H_4 by the 2-equivalent oxidizers H_2O_2, $S_2O_8^{2-}$, ClO_3^-, ClO_4^-, BrO_3^-, MnO_4^-, Tl^{III}, Pb^{IV}, V^V, Sb^V, Cr^{VI}, Mo^{VI}, and Se^{VI} in acidic solution. The yield of HN_3 increases with the temperature of the solutions [16]. Formation of HN_3 by the overall reaction $3\ N_2H_5N_3 + 2\ KIO_3 \rightarrow 3\ HN_3 + 3\ N_2 + 2\ KI + 6\ H_2O$ was observed in aqueous solution [17].

References:

[1] Koltunov, V. S.; Nikol'skii, V. A.; Agureev, Yu. P. (Kinet. Katal. **3** [1962] 877/81; Kinet. Catal. [Engl. Transl.] **3** [1962] 764/8).

[2] Zil'berman, B. Ya.; Lelyuk, G. A.; Mashkin, A. N.; Yasnovitskaya, A. L. (Radiokhimiya **30** [1988] 833/7; Sov. Radiochem. [Engl. Transl.] **30** [1988] 788/92).

[3] Brodda, B. G.; Lammertz, H.; Merz, E. (Radiochim. Acta **37** [1984] 213/6).

[4] Mashkin, A. N.; Zil'berman, B. Y. (Radiokhimia **33** No. 2 [1991] 43/51; Sov. Radiochem. [Engl. Transl.] **33** [1991] 143/9).

[5] Schoen, J.; Schmieder, H.; Kanellakopulos, B. (Sep. Sci. Technol. **25** [1990] 1737/50 from C.A. **114** [1991] No. 216310).

[6] Zil'berman, B. Ya.; Lelyuk, G. A.; Mashkin, A. N.; Fedorov, Yu. S. (Radiokhimiya **30** [1988] 837/40; Sov. Radiochem. [Engl. Transl.] **30** [1988] 792/4).

[7] Dukes, E. K.; Wallace, R. M. (DP-728 [1962] 13 pp.; C.A. **60** [1964] 15404).

[8] Karraker, D. G. (Ger. 82010815 [1981] 16 pp.; C.A. **97** [1982] No. 173938).

[9] Russell, T. P.; Brill, T. B. (Combust. Flame **76** [1989] 393/401).

[10] Perrott, J. R.; Stedman, G.; Uysal, N. (J. Chem. Soc. Dalton Trans. **1976** 2058/64).

[11] Gowland, R. J.; Howes, K. R.; Stedman, G. (J. Chem. Soc. Dalton Trans. **1992** 797/9).

[12] Koltunov, V. S.; Marchenko, V. I. (Kinet. Katal. **7** [1966] 224/9; Kinet. Catal. [Engl. Transl.] **7** [1966] 202/7).

[13] Wiberg, N.; Fischer, G.; Bachhuber, H. (unpublished, ref. 1 in Wiberg, N.; Chimia **30** [1976] 426).

[14] Ray, A. B.; Koehler, G.; Salser, G. E.; Dauerman, L. (AIAA J. **6** [1968] 2186/7).

[15] Merrow, R. T.; Van Dolah, R. W. (J. Am. Chem. Soc. **76** [1954] 4522/5).

[16] Higginson, W. C. E. (J. Chem. Soc. Spec. Pub. **10** [1957] 95/111).

[17] Pannetier, G.; Margineanu, F.; Dereigne, A.; Bonnaire, R. (Bull. Soc. Chim. Fr. **1972** 2617/22).

2.3.1.1.3 Other Reactions

The formation of HN_3 during decomposition of organic azides, usually by thermolysis, was reviewed in [1]. A γ-radiolyzed solution of H_2 in liquid N_2 at 77 K yielded HN_3 as a by-product of NH_3. G values of 0.02 and 0.7 extrapolated to an infinite concentration of H_2 were obtained [2]. A very small yield of HN_3 in addition to some NH_3 resulted from the reaction of H_2 with N_2, when activated by glow and condensed discharges [3]. The admixture of N_2 and NH_3 in a ratio of 1:4 to an Ar plasma yielded a condensable product which contained HN_3 and N_2H_4 after evaporation of NH_3 and other volatiles [4]. Formation of HN_3 was observed during γ radiolysis of liquid NH_3 at doses exceeding 4×10^4 rad [5]. Thermal decomposition of $(CH_3NH_3)NO_3$ yielded a trace of HN_3 besides CH_3NH_2, N_2, NO, and H_2O in the temperature range 400 to 770 K [6]. Reactions of benzenesulfinyl azide with thiols or primary and secondary amines liberated HN_3 [7]. A mixture of NH_2^- and N_2O in a selected-ion flow tube yielded HN_3 and OH^- (28%) and the conjugated base pair N_3^- and H_2O (72%) in a rapid reaction with an enthalpy calculated to be -38 kJ/mol [8]. Frequently, HN_3 forms during the decomposition of compounds containing chains of three or more N atoms; see the corresponding chapters in the present volume.

References:

[1] Abramovitch, R. A.; Kyba, E. P. (in: Patai, S.; The Chemistry of the Azido Group, Interscience, London 1971, pp. 221/329).

[2] Horigome, K.; Hirokami, S.; Sato, S. (Bull. Chem. Soc. Jpn. **51** [1978] 725/8).

[3] Stewart, K. (Nature **157** [1946] 191/2).

[4] Koehne, R.; Lindner, F. (Dtsch. Luft-Raumfahrt Forschungsber. DLR-FB 75-27 [1975] 1/43, 27/8; C.A. **83** [1975] No. 100191).

[5] Sutherland, J. W.; Kramer, H. (J. Phys. Chem. **71** [1967] 4161/2).

[6] Miron, Y. (J. Hazard. Mater. **3** [1980] 301/21).

[7] Maricich, T. J.; Angeletakis, C. N. (J. Org. Chem. **49** [1984] 1931/4).

[8] Bierbaum, V. M.; Grabowski, J. J.; DePuy, C. H. (J. Phys. Chem. **88** [1984] 1389/93).

2.3.1.1.4 Preparation of HN_3 Isotopomers

Methods used for the preparation of DN_3 and ^{15}N-labeled molecules are basically the same used in HN_3 syntheses. DN_3 was prepared by reacting NaN_3 with D_3PO_4 [1, 2]. This gave a much better yield than the reaction of NaN_3 with monodeuterated stearic acid [3] as described in [4]. Formation of DN_3 by exchange between HN_3 and excess liquid D_2O was described in [5].

Mixtures of $H^{15}NNN$ and $HNN^{15}N$ were obtained from $NaNN^{15}N$ and stearic acid [6] and from $KNN^{15}N$ and H_2SO_4 [7]. A mixture of all ^{15}N-labeled isotopomers of HN_3 resulted from end- and central-labeled NaN_3 and H_3PO_4 [1]. A mixture of $D^{15}NNN$ and $DNN^{15}N$ was obtained by gas-phase hydrogen exchange of labeled HN_3 and excess D_2O [8].

References:

[1] Amble, E.; Dailey, B. P. (J. Chem. Phys. **18** [1950] 1422).

[2] Guenebaut, H. (Bull. Soc. Chim. Fr. **1959** 962/1018).

[3] Kewley, R.; Sastry, K. V. L. N.; Winnewisser, M. (J. Mol. Spectrosc. **12** [1964] 387/401).

[4] Dows, D. A.; Pimentel, G. C. (J. Chem. Phys. **23** [1955] 1258/63).

[5] Thrush, B. A. (Proc. R. Soc. London A **235** [1956] 143/7).

[6] Gerry, M. C. L.; Heineking, N.; Maeder, H.; Dreizler, H. (Z. Naturforsch. **44a** [1989] 1079/86).

[7] Winnewisser, M.; Cook, R. L. (J. Chem. Phys. **41** [1964] 999/1004).
[8] Moore, C. B.; Rosengren, K. (J. Chem. Phys. **44** [1966] 4108/15).

2.3.1.2 Purification

Crude HN_3 can be purified by fractionation under vacuum in traps cooled to 223, 173, and 77 K; HN_3 collects at 173 K [1]. Distillation at ambient pressure can also be used, because HN_3 and H_2O do not form an azeotrope [2]. Double distillation through a dephlegmator and drying the condensate with $MgSO_4$ or $CaCl_2$ yielded HN_3 with less than 0.2% of impurities [3]. Residual moisture was removed from gaseous HN_3 by passing it through drying towers filled with P_4O_{10} [4, 5], $CaCl_2$ [6], or $Mg(ClO_4)_2$ [7] with loss of HN_3 by absorption. Purification of HN_3 by pumping on the condensate at $\sim$210 K followed by slow distillation in the temperature range 200 to 230 K was used in [8]. The purity of gaseous HN_3 can be checked by the doubling of the pressure after exploding a sample [9].

References:

[1] Gholivand, K.; Schatte, G.; Willner, H. (Inorg. Chem. **26** [1987] 2137/40).
[2] Kurbangalina, R. Kh.; Yakovleva, G. S. (Zh. Fiz. Khim. **43** [1969] 2649/50; Russ. J. Phys. Chem. [Engl. Transl.] **43** [1969] 1490/1).
[3] Kurbangalina, R. Kh.; Patskov, E. A.; Stesik, L. N.; Yakovleva, G. S. (PMTF Zh. Prikl. Mekh. Tekh. Fiz. **1970** 160/5; J. Appl. Mech. Tech. Phys. [Engl. Transl.] **1970** 672/7).
[4] Pannetier, G. (C. R. Hebd. Seances Acad. Sci. **232** [1951] 817/8).
[5] Pannetier, G.; Gaydon, A. G. (J. Chim. Phys. Phys.-Chim. Biol. **48** [1951] 221/4).
[6] Amble, E.; Dailey, B. P. (J. Chem. Phys. **18** [1950] 1422).
[7] Guenebaut, H. (Bull. Soc. Chim. Fr. **1959** 962/1018, 964/5).
[8] Günther, P.; Meyer, R.; Müller-Skjold, F. (Z. Phys. Chem. A **175** [1935] 154/69).
[9] Dupré, G.; Paillard, C. (Dyn. Mass Spectrom. **4** [1976] 233/45).

2.3.1.3 Toxicity

Hydrogen azide has an unbearingly pungent odor. The substance is classified supertoxic, the lethal dose for oral ingestion by humans being probably <5 mg/kg. The poisoning action of HN_3 is similar to that of the azide ion [1]. Hydrogen azide solutions damage the skin. Inhalation of the gas causes dizziness, headache, and strong irritation of the mucous membranes; see "Stickstoff" 2, 1935, p. 290 for earlier results. Other symptoms are a rapid and severe drop of the blood pressure [2] and an increase in the pulse rate. Hypersensitivity to HN_3 may develop [3]; a concentration as low as 0.5 ppm was sufficient to cause irritation to some workmen [4]. Bronchitis and pulmonary edema were mentioned to result from heavy exposure [1]. However, regular exposure to HN_3 fumes at concentrations between 0.3 and 3.9 ppm over years did not lead to any pathological symptoms. Toxic effects of higher HN_3 doses on animals are described in [2].

The maximum concentration at the workplace (MAK value) of HN_3 in the Federal Republic of Germany is 0.1 ppm (0.27 mg/m^3); occasional exposure to twice that concentration is tolerable for short periods of time [5]. A limit of 1 ppm to exposure is given in [6].

The recovery from moderate HN_3 poisoning is fast upon ceasing the exposure [2] and admitting fresh air. In case of heavy poisoning, blood circulation analeptics may be useful in order to counteract paralysis of the vasomotor nerves [3].

The HN_3 concentration in air can be determined colorimetrically via the reddish compound which forms with Fe^{3+} in diluted HNO_3 [7] after absorbing HN_3 either in an $AgNO_3$

solution and liberating it with diluted H_2SO_4 [8] or in sample tubes filled with solid diatomaceous earth impregnated with Na_2CO_3 and desorption with water [9]. Determining HN_3 in soils by the HPLC method requires derivatization to 3,5-dinitrobenzoyl azide [10].

References:

[1] Gosselin, R. E.; Smith, R. P.; Hodge, H. C.; Braddock, J. E. (Clinical Toxicology of Commercial Products, 5th Ed., Williams and Wilkins, Baltimore 1984, pp. II-114/II-115).

[2] Graham, J. D. P.; Rogan, J. M.; Robertson, D. G. (J. Ind. Hyg. Toxicol. **30** [1948] 98/102).

[3] Rentsch, G. (Angew. Chem. **68** [1956] 439/40).

[4] Haas, J. M.; Marsh, W. W., Jr. (Am. Ind. Hyg. Assoc. J. **31** [1970] 318/21).

[5] Deutsche Forschungsgemeinschaft (Maximale Arbeitsplatzkonzentrationen und Biologische Arbeitsstofftoleranzwerte, VCH Verlagsgesellschaft, Weinheim 1992, p. 68).

[6] Steere, N. V. (Handbook of Laboratory Safety, 2nd Ed., The Chemical Rubber Co., Cleveland 1971, p. 776).

[7] Aratone Sugar, E.; Bittera, E. (Munkavedelem **18** [1972] 33).

[8] Strnad, J.; Pesata, V.; Richter, Z. (Czech. 247689 [1988] 5 pp. from C.A. **109** [1988] No. 60700).

[9] Williams, K. E.; Esposito, G. G.; Rinehart, D. S. (Am. Ind. Hyg. Assoc. J. **42** [1981] 476/8).

[10] Van Wambeke, E.; Decoster, P.; Van Assche, C.; Vanachter, A. (Meded. Fac. Landbouwwet. Rijksuniv. Gent **56** [1991] 961/7 from C.A. **116** [1992] No. 168255).

2.3.1.4 Handling. Storage. Disposal

Pure HN_3 in any physical state and solutions is noxious and potentially explosive. Appropriate precautions are required during work. Plastics are the preferable container materials, but nonsparking metals may also be used [1, 2]. Materials not corroded by HN_3 include glass, stainless steel, Al, Sn, Pb, Ti, Ag, and Au [2]. Other heavy metals are frequently attacked with formation of explosive azides [3]. While polyethene is inert to HN_3, polyurethane, cellulose products, and plexiglass do react [4].

Explosions of HN_3 seem to be triggered by shocks; if they are avoided, gaseous and also liquid HN_3 can be relatively safely handled. Accordingly, the liquid should not be decanted, rather be transferred by slow evaporation and condensation. Conventional distillation should be avoided because of delayed boiling, possibly resulting in explosions [5]. Explosions may also result from HN_3 trapped in crevices of joints and corners of experimental equipment [6] or absorbed in drying towers. These residues have to be removed thoroughly after terminating the experiment [7]. The phase transition between solid and liquid HN_3 is accompanied by a large volume change, thus increasing the risk of explosion. This risk is diminished in the presence of water in the vessel when cooled below the melting point ($\sim$193 K) of HN_3 [5].

The condensate of the vapor over a 0.05 M aqueous solution of HN_3 can reach the potentially explosive concentration of 17% (4.7 M). A solution with a concentration $\leq$0.05 M cannot evolve HN_3 in quantities sufficient to cause an explosion damaging to an ordinary steel tank [8]. The safety aspects of HN_3 formed in solutions during the PUREX process are discussed in [9].

Moderate quantities of gaseous HN_3 can conveniently be stored several months in glass containers at pressures below 300 Torr and ambient temperature without decomposition [10, 11]. Gaseous HN_3 at less than 100 Torr did not decompose on contact with Hg or silicon vacuum grease [12]. Storage of liquid HN_3 in suspended glass vessels was also described [5]. Exclusion of light was recommended [13]; the same holds for aqueous solutions in sealed containers [11]. The HN_3 loss from open vessels is relatively fast for solutions with ~45 g/L of HN_3 and slows down with decreasing initial concentration, becoming negligible below 10 g/L HN_3 [14].

Addition of ceric ammonium nitrate decomposes HN_3 in aqueous solution [15]. Slowly forming HN_3, for example from hydrolysis of $Pb(N_3)_2$, is destroyed on contact with elemental Zn or Mg, thereby generating N_2, NH_3, and the metal oxides. The metals can be used in bulk form or as pressed and sintered powders [16].

References:

[1] Jobelius, H. H.; Scharff, H.-D. (Ullman's Encycl. Ind. Chem. 5th Ed. A **13** [1989] 193/7).

[2] Lamnevik, S. (Symp. Chem. Probl. Connected Stabil. Explos., 1967 [1968], pp. 21/33; C.A. **70** [1969] No. 98403).

[3] Cowley, B. R.; Oughton, J. F. (Chem. Ind. [London] **1973** 444).

[4] Yakovleva, G. S.; Kurbangalina, R. Kh. (Detonatsiya Mater. 6th Vses. Simp. Goreniyu Vrzyvu, Alma-Ata 1980, pp. 56/60).

[5] Günther, P.; Meyer, R.; Müller-Skjold, F. (Z. Phys. Chem. A **175** [1935] 154/69).

[6] Sood, R. K.; Nya, A. E. (J. Therm. Anal. **20** [1981] 491/3).

[7] Sloan, J. J.; Watson, D. G.; Wright, J. S. (Chem. Phys. **43** [1979] 1/8).

[8] Dukes, E. K.; Wallace, R. M. (DP-728 [1962] 1/13; C.A. **60** [1964] 15404).

[9] Ertel, D.; Schmieder, H.; Stollenwerk, A. H. (Nukl. Entsorgung **4** [1989] 107/19 from C.A. **113** [1990] No. 67098).

[10] Bendtsen, J. (J. Raman Spectrosc. **9** [1980] 162/5).

[11] McDonald, J. R.; Rabalais, J. W.; McGlynn, S. P. (J. Chem. Phys. **52** [1970] 1332/40).

[12] Guenebaut, H. (Bull. Soc. Chim. Fr. **1959** 962/1018, 966).

[13] Gerry, M. C. L.; Heineking, N.; Mäder, H.; Dreizler, H. (Z. Naturforsch. **44a** [1989] 1079/86).

[14] Pannetier, G.; Margineanu, F.; Dereigne, A.; Bonnaire, R. (Bull. Soc. Chim. Fr. **1972** 2617/22).

[15] Bryant, J. I.; Rosenwasser, H. (J. Chem. Educ. **39** [1962] 296/7).

[16] Eldh, J. A. D.; Gustafsson, G. V.; Bjorklund, J. O. (Ger. 1163211 [1964] 3 pp.; C.A. **60** [1964] 15676).

2.3.1.5 Applications

Hydrazoic acid itself has little industrial significance [1]; however, its industrial use to prepare heavy-metal azides for shell detonators was mentioned [2]. A mixture of HN_3 in N_2 can be used to prepare azides from the appropriate bases [3 to 5]. A detonation-transferring copper azide coating on an inert support was prepared by reacting gaseous HN_3 with a $CuCl_2$ layer [6].

Photo- and spark-induced explosions of HN_3-containing gas mixtures were investigated for the construction of lasers. Excited N_2 thus formed leads to population inversion of CO_2 levels, but the gain is low due to the high rotational and vibrational temperature of CO_2 [7]. Chemical pumping of the IF(B $^3\Pi_0^+$) state in HN_3-CF_3I-F mixtures results from collisions with intermediately formed N_3 radicals [8]; the system is theoretically treated in [9]. Chemical pumping of IF in HN_3-F-H_2 supersonic flames is discussed in [10, 11]. Excited XeF in HN_3-XeF_2-He mixtures is a potentially useful excimer lasant for a short-wavelength chemical laser [12, 13].

HN_3 effectively scavenges intermediately formed HNO_2 [14], for example in organic reactions like the Fischer-Hepp rearrangement [15], the photolysis of nitrosamines [16], or oxidations by HNO_3 [17]. Patents describe the effective, reductive removal of nitrogen oxides from exhaust and flue gases upon sparging the gas through aqueous HN_3 at ambient temperature [18, 19]. The formation of a greenish blue V^V complex in acetic acid with HN_3 and a benzamidine can be used for the determination of V, for example in steel [20]. The feasibility of aqueous HN_3 for chromatographically separating metal ions was investigated; see [21, 22] for details.

Semiconducting gallium nitride films can be grown from HN_3 and $Ga(CH_3)_3$ by chemical vapor deposition at very low pressures. A silicon nitride film could be obtained similarly [23]. The thermal behavior of HN_3 adsorbed on Si is described on p. 137; chemical vapor deposition of HN_3 on silicon at elevated temperature yields hydrogen-containing silicon nitride suitable for transistors [24]. The patent literature also describes the surface treatment of semiconductors with a HN_3 plasma [25] and the gas phase reaction of HN_3 with silicon compounds for the deposition of photoconducting films; see for example [26]. Gaseous HN_3-H_2O mixtures poison the autocatalytic decomposition of $Pb(N_3)_2$ by reacting with the metallic nuclei which are necessary for the catalytic acceleration of the reaction [27, 28]. The inhibiting effect of HN_3 on bacterial growth [29] and yeast activity was noted [30].

References:

[1] Jobelius, H. H.; Scharff, H.-D. (Ullman's Encycl. Ind. Chem. 5th Ed. A **13** [1989] 193/7).

[2] Gosselin, R. E.; Smith, R. P.; Hodge, H. C.; Braddock, J. E. (Clinical Toxicology of Commercial Products, 5th Ed., Williams and Wilkins, Baltimore 1984, pp. II-114/II-115).

[3] Snead, W. K.; PPG Industries, Inc. (U.S. 3752881 [1973] 4 pp.; C.A. **80** [1974] No. 5394).

[4] Snead, W. K.; Knoop, J. F.; PPG Industries, Inc. (U.S. 3705008 [1972] 6 pp.; C.A. **78** [1973] No. 74251).

[5] Pieser, L. W.; PPG Industries, Inc. (U.S. 3734998 [1973] 4 pp.; C.A. **79** [1973] No. 33206).

[6] Heinzelmann, W.; Schnapp, H.; Dynamit Nobel A.-G. (Ger. 3843883 [1988/92] 4 pp. from C.A. **116** [1992] No. 238462).

[7] Dzhidzhoev, M. S.; Pimenov, M. I.; Platonenko, V. G.; Filippov, Yu. V.; Khokhlov, R. V. (Zh. Eksp. Teor. Fiz. **57** [1969] 411/20; Sov. Phys.-JETP [Engl. Transl.] **30** [1970] 225/9).

[8] David, S. J.; Ongstad, A. P.; MacDonald, M. A.; Coombe, R. D. (Chem. Phys. Lett. **136** [1987] 352/7).

[9] Dvoryankin, A. N.; Shcheglov, V. A. (Kratk. Soobshch. Fiz. **1988** 31/3; Sov. Phys.-Lebedev Inst. Rep. [Engl. Transl.] **1988** 39/43).

[10] Dvoryankin, A. N.; Makarov, V. N.; Shcheglov, V. A. (Kratk. Soobshch. Fiz. **1990** 6/8 from C.A. **113** [1990] No. 220718).

[11] Dvoryankin, A. N. (Proc. SPIE Int. Soc. Opt. Eng. **1397** [1991] 145/52 from C.A. **115** [1991] No. 18087).

[12] Mead, R. D.; Baughcum, S. L.; Fisher, C. H.; Kushner, M. J.; Ewing, J. J. (Proc. SPIE Int. Soc. Opt. Eng. **875** [1988] 149/62).

[13] Ewing, J. J. (NATO ASI Ser. C **245** [1988] 481/95).

[14] Fitzpatrick, J.; Meyer, T. A.; O'Neill, M. E.; Williams, D. L. H. (J. Chem. Soc. Perkin Trans. II **1984** 927/32).

[15] Williams, D. L. H. (J. Chem. Soc. Perkin Trans. II **1975** 655/9).

[16] Polo, J.; Chow, Y. L. (IARC Sci. Publ. No. 14 [1975/76] 473/86; C.A. **86** [1977] No. 188789).

[17] Stedman, G.; Thomas, N. (J. Inorg. Nucl. Chem. **39** [1977] 1015/8).

[18] Syouzi, F.; Ishizaka, Y.; Haba, M.; Asano, Y.; Yamashita, S.; Syougi, Y.; Meidensha Corp. (PCT Int. Appl. 9112070 [1991] 43 pp. from C.A. **115** [1991] No. 238789).
[19] Asano, Y.; Haba, H.; Shoji, F.; Meidensha K. K. (Jpn. Kokkai Tokkyo Koho 04-71618 [1992] 4 pp. from C.A. **117** [1992] No. 13691).
[20] Kharsan, R. S.; Patel, K. S.; Mishra, R. K. (Talanta **26** [1979] 254/6).

[21] Kuroda, R.; Kojima, N. (Bull. Chem. Soc. Jpn. **45** [1972] 3211/3).
[22] Oguma, K.; Maruyama, T.; Kuroda, R. (Anal. Chim. Acta **74** [1975] 339/45).
[23] Flowers, M. C.; Jonathan, N. B. H.; Laurie, A. B.; Morris, A.; Parker, G. J. (J. Mater. Chem. **2** [1992] 365/6).
[24] Ishihara, R.; Kanoh, H.; Sugiura, O.; Matsumura, M. (Jpn. J. Appl. Phys. Pt. 2 **31** [1992] L74/L77 from C.A. **116** [1992] No. 140406).
[25] Lu, S.; Ruan, B.; Guo, Y.; Cai, Y.; Lu, M. (Faming Zhuanli Shenqing Gongkai Shuomingshu CN 87-105937 [1988] 4 pp. from C.A. **110** [1989] No. 126964).
[26] Toshiba Corp. (Jpn. Kokai Tokkyo Koho 58-124224 [1983] 5 pp. from C.A. **100** [1984] No. 129854).
[27] Reitzner, B. (J. Phys. Chem. **65** [1961] 948/52).
[28] Reitzner, B.; Kaufman, J. V. R.; Bartell, E. F. (J. Phys. Chem. **66** [1962] 421/6).
[29] Wong, J. M.; Envirodyne, Inc. (U.S. 4673505 [1987] 4 pp.; C.A. **107** [1987] No. 120517).
[30] Eeckhaut, R. G. (Fermentatio **2** [1960] 37/43 from C.A. **1960** 18875).

2.3.1.6 Molecular Properties and Spectra

2.3.1.6.1 Molecular Structure of HN_3

The substitution structure of HN_3 was determined from the rotational constants; it approximates the equilibrium structure. The planar HN_3 has an angular N_3 group and a trans configuration at the central bond; the internuclear distances in Å and angles in degree are as follows [1]:

$r_s(H\text{-}N_\alpha)$	$r_s(N_\alpha\text{-}N_\beta)$	$r_s(N_\beta\text{-}N_\gamma)$	$\angle$HNN	$\angle$NNN
1.015(15)	1.243(5)	1.134(2)	108.8(40)	171.3(50)

Values estimated for the rotational constants A_0 of $H^{15}NNN$ and $HNN^{15}N$ were used in determining the structural parameters; a later evaluation of microwave spectra confirmed these constants and the structure deduced therefrom [2]. The structure is consistent with the vibrational data, chemical reactivity [1], and the geometry predicted by earlier ab initio calculations [3, 4]. A planar HN_3 is indicated by very small inertial defects of HN_3 and the ^{15}N end-labeled isotopomers [5]. The results of ab initio calculations on the geometries and energies of HN_3 in the ground state until 1988 are summarized in [6] and more recently reviewed in [7].

All earlier structural determinations are based on the assumption of a linear N_3 group. Other structural data from earlier microwave spectra [5, 8, 9] and an electron diffraction study [10] are similar to the values listed above.

The experimentally unknown cyclic isomer of HN_3 is described in Chapter 2.3.3 on pp. 154/5.

A CNDO/2 calculation predicts an HN_3 dimeric adduct with a hydrogen bond from one molecule to the terminal N atom of the second to be most stable with a dissociation energy of 31.8 kJ/mol. A second, linear structure and two cyclic ones are less stable [11]. These results agree qualitatively with the conclusions drawn from the IR spectra which are described on p. 111. The possible formation of an $(HN_3)_3$ molecule with a hexaazabenzene skeleton is discussed on p. 185.

References:

[1] Winnewisser, B. P. (J. Mol. Spectrosc. **82** [1980] 220/3).
[2] Gerry, M. C. L.; Heineking, N.; Mäder, H.; Dreizler, H. (Z. Naturforsch. **44a** [1989] 1079/86).
[3] Harrison, S. W.; Fischer, C. R.; Kemmey, P. J. (Chem. Phys. Lett. **36** [1975] 229/31).
[4] Lievin, J.; Breulet, J.; Verhaegen, G. (Theor. Chim. Acta **52** [1979] 75/88).
[5] Winnewisser, M.; Cook, R. L. (J. Chem. Phys. **41** [1964] 999/1004).
[6] Alexander, M. H.; Werner, H. J.; Dagdigian, P. J. (J. Chem. Phys. **89** [1988] 1388/400).
[7] Palmer, M. H. (J. Mol. Struct. **246** [1991] 321/38).
[8] Amble, E.; Dailey, B. P. (J. Chem. Phys. **18** [1950] 1422).
[9] Kewley, R.; Sastry, K. V. L. N.; Winnewisser, M. (J. Mol. Spectrosc. **12** [1964] 387/401).
[10] Schomaker, V.; Spurr, R. (J. Am. Chem. Soc. **64** [1942] 1184/7).

[11] Murthy, A. S. N. (Indian J. Chem. **9** [1971] 1297/9).

2.3.1.6.2 Electronic Structure

The electron configuration of ground-state $HN_3(^1A')$ is $(1a')^2$ $(2a')^2$ $(3a')^2$ $(4a')^2$ $(5a')^2$ $(6a')^2$ $(1a'')^2$ $(7a')^2$ $(8a')^2$ $(9a')^2$ $(2a'')^2$ [1]. The electron configuration of the first excited state $^3A''$ is $\ldots(9a')^2$ 10a′ 2a″ [2] or $\ldots(9a')^2$ 2a″ 10a′. Other low-lying valence states are two $^3A'$ states with $\ldots(9a')^2$ 2a″ 3a″ and ...9a′ $(2a'')^2$ 10a′ and a $^3A''$ state with ...9a′ $(2a'')^2$ 3a″ [3]. Slightly different electron configurations were used in earlier assignments of the photoelectron spectra; see below.

The bonding in HN_3 is usually described in terms of equal contributions of the resonance structures $HN_\alpha{=}N_\beta^+{=}N_\gamma^-$ and $HN_\alpha^-{-}N_\beta^+{\equiv}N_\gamma$. The σ framework of HN_3 approximately results from an sp hybrid at N_β which is bonded to a pδs orbital of N_α and a p or pδs orbital of N_γ. A second pδs orbital of N_α is used for the σ bond to H. A supplemental, localized π bond connects N_β and N_γ. The bonding of the N_3 group is completed by a delocalized π bond which links N_β with N_α and N_γ [4, 5]. The calculation of the bond orders at the MP2/6-31G(d, p) level predicts less than a single bond for $H{-}N_\alpha$, an intermediate between a single and a double bond for $N_\alpha{-}N_\beta$, and nearly a triple bond for $N_\beta{-}N_\gamma$ [6].

References:

[1] Alexander, M. H.; Werner, H. J.; Dagdigian, P. J. (J. Chem. Phys. **89** [1988] 1388/400).
[2] Yarkony, D. R. (J. Chem. Phys. **92** [1990] 320/3).
[3] Meier, U.; Staemmler, V. (J. Phys. Chem. **95** [1991] 6111/7).
[4] Treinin, A. (in: Patai, S.; The Chemistry of the Azido Group, Wiley-Interscience, London 1971, pp. 1/55, 4/8).
[5] Murgich, J.; Aray, Y. (J. Chem. Phys. **87** [1987] 3580/6).
[6] Otto, M.; Lotz, S. D.; Frenking, G. (Inorg. Chem. **31** [1992] 3647/55).

2.3.1.6.3 Ionization Potentials

Six photoelectron bands, expected for nonlinear HN_3 analogous to the spectrum of the isoelectronic linear N_2O, were observed in the most recent studies of He I and He II photoelectron (PE) spectra. The first three bands exhibit vibrational splitting; see p. 154 for details.

Vertical ionization potentials E_i in eV are as follows:

E_i [1]	10.74(2)	12.25(2)[a]	15.45(2)	16.8(1)	20.3(1)	21.6(1)
E_i [2]	10.72	12.24	15.47	16.8	20.6	21.9
E_i [3]	10.70	12.2[b]	15.47	16.7	17.4	20.1[c]
assignment[d]	2a″	9a′	8a′	7a′	1a″	6a′

[a] Adiabatic $E_i = 11.70$ eV. — [b] Adiabatic $E_i = 11.6$ eV. — [c] Additional peaks at 24.0 eV (5a′) and 26.4 eV (4a′) in the X-ray PE spectrum of frozen HN_3. — [d] From STO-3G and MINDO calculations [1] and INDO and ab initio literature data [3].

The interpretation of the PE spectra depends on whether to assign one or two ionization potentials to the fourth band and consequently on the designation of the higher bands [4, 5]. Energies and assignments of the first four bands from earlier He I PE spectra [6, 7] are similar to the more recent results, whereas the earlier published ionization potentials, 11.5 and 12.6 eV from Rydberg series [8] and 10.3 eV from the mass spectrum [9], disagree with the PE values [1 to 3]. The energy gaps between the three peaks of lowest energy in the PE spectrum of HN_3 adsorbed on an Si(110) surface agree reasonably well with those of gaseous HN_3 [10].

The N 1s core binding energies were taken from X-ray PE spectra of frozen HN_3 relative to the Au 4f spin doublet. The spectrum at 150 K consists of two bands with a 1:2 intensity ratio. The weaker, narrower band at 403.6 eV is assigned to the central N atom, and the stronger, broader band at 399.7 eV can be devoluted into two bands of the terminal N atoms differing by 0.9 eV. This energy splitting confirms the largely covalent HN_3 structure [3, 11] and agrees with a splitting of 1.0 eV reported earlier, where ionization energies for HNNN of 401.5, 405.6, and 402.5 eV were assigned by comparing them with values calculated by the SCF method [12].

References:

[1] Bastide, J.; Maier, J. P. (Chem. Phys. **12** [1976] 177/90).
[2] Cvitas, T.; Klasinc, L. (J. Chem. Soc. Faraday Trans. II **72** [1976] 1240/4).
[3] Lee, T. H.; Colton, R. J.; White, M. G.; Rabalais, J. W. (J. Am. Chem. Soc. **97** [1975] 4845/51).
[4] Frost, D. C.; Macdonald, C. B.; McDowell, C. A.; Westwood, N. P. C. (Chem. Phys. **47** [1980] 111/24).
[5] Zeiss, G. D.; Chong, D. P. (J. Electron Spectrosc. Relat. Phenom. **18** [1980] 279/94).
[6] Cradock, S.; Ebsworth, E. A. V.; Murdoch, J. D. (J. Chem. Soc. Faraday Trans. II **68** [1972] 86/100).
[7] Eland, J. H. D. (Philos. Trans. R. Soc. London A **268** [1970] 87/96).
[8] McDonald, J. R.; Rabalais, J. W.; McGlynn, S. P. (J. Chem. Phys. **52** [1970] 1332/40).
[9] Franklin, J. L.; Dibeler, V. H.; Reese, R. M.; Krauss, M. (J. Am. Chem. Soc. **80** [1958] 298/302).
[10] Bu, Y.; Chu, J. C. S.; Lin, M. C. (Surf. Sci. **264** [1992] L151/L156).

[11] Colton, R. J.; Rabalais, J. W. (J. Chem. Phys. **64** [1976] 3481/6).
[12] Wyatt, J. F.; Hillier, I. H.; Saunders, V. R.; Connor, J. A.; Barber, M. (J. Chem. Phys. **54** [1971] 5311/5).

2.3.1.6.4 Proton Affinity

The proton affinity of HN_3 is 738.9 ± 4.2 kJ/mol; the value was calculated from the experimental equilibrium constant of proton transfer between $N_3H_2^+$ and methyl nitrate and agrees with the result of an MP2 calculation. Tandem mass spectrometry indicated that the aminodiazonium ion, H_2NNN^+, forms preferentially. A calculation at the MP2 level gave proton affinities of 636.0 kJ/mol and 168.2 kJ/mol for the formation of the isomers $HNNNH^+$ and $HNN(H)N^+$ [1]; see pp. 157/8 for additional results. A proton affinity of 749 ± 29 kJ/mol for the formation of the H_2NNN^+ isomer was estimated from the experimental core binding energy of isoelectronic H_2NCN and the heat of formation of HN_3 (equivalent-cores approximation) [2].

References:

[1] Cacace, F.; Attinà, M.; De Petris, G.; Grandinetti, F.; Speranza, M. (Gazz. Chim. Ital. **120** [1990] 691/700).

[2] Beach, D. B.; Eyermann, C. J.; Smit, S. P.; Xiang, S. F.; Jolly, W. L. (J. Am. Chem. Soc. **106** [1984] 536/9).

2.3.1.6.5 Dipole Moment

The electric dipole moments μ of $H^{14}N_3$ and $D^{14}N_3$ were obtained by vector addition of the components $|\mu_a|$ ($\sim$ along the N_3 axis) and $|\mu_b|$ (perpendicular to μ_a in the plane of the molecule). These were determined from the results of Stark effect measurements in microwave spectra as follows (values in D):

molecule	μ	$\lvert\mu_a\rvert$	used transition	$\lvert\mu_b\rvert$	used transition	Ref.
$H^{14}N_3$	1.70(5)	0.8369(20)*)	$J=4 \leftarrow 3, K=1$	1.48(5)	$25_{0,25} \leftarrow 24_{1,24}$	[1]
$D^{14}N_3$	1.76(5)	0.894(10)	$1_{0,1} \leftarrow 0_{0,0}$	1.51(5)	$16_{0,16} \leftarrow 15_{1,15}$	[2]

*) From [3]. An earlier value of $|\mu_a|$ in [4] was less precise.

The μ values of both isotopomers agree satisfactorily with each other [2]. Theoretical calculations show that μ is essentially parallel to the N-H bond [1, 2], the positive end being the H atom [2].

The dipole moment of HN_3 can be calculated without too much difficulty with an accuracy of 0.1 to 0.2 D. Experimental dipole moments are compared with values from own and previous ab initio calculations at different levels [5].

References:

[1] Bendtsen, J.; Winnewisser, M. (Chem. Phys. Lett. **33** [1975] 141/5).

[2] Bendtsen, J.; Winnewisser, M. (Chem. Phys. **40** [1979] 359/65).

[3] White, K. J.; Cook, R. L. (J. Chem. Phys. **46** [1967] 143/51).

[4] Amble, E.; Dailey, B. P. (J. Chem. Phys. **18** [1950] 1422).

[5] Chong, D. P. (Chem. Phys. Lett. **175** [1990] 525/30).

2.3.1.6.6 Nuclear Quadrupole Coupling Constants

The resolution of the hyperfine structure in microwave Fourier transform spectra yielded precise values of the N coupling constants. The assignment of the bands was facilitated by comparing them with the simpler spectrum obtained with the mixed isotopomers $H^{15}NNN$ and $HNN^{15}N$. The $1_{01} \leftarrow 0_{00}$ transition was used for the determination of $eq_{aa}Q$; the other constants resulted from a-type Q-branch transitions. Values for $HN_\alpha N_\beta N_\gamma$ in MHz are [1]:

$eq_{aa}Q_\alpha = 4.727(5)$ $eq_{bb}Q_\alpha = -1.228(3)$ $eq_{cc}Q_\alpha = -3.499(3)$
$eq_{aa}Q_\beta = -0.84(3)$ $eq_{bb}Q_\beta = 0.52(2)$ $eq_{cc}Q_\beta = 0.32(2)$
$eq_{aa}Q_\gamma = -1.224(14)$ $eq_{bb}Q_\gamma = 2.611(7)$ $eq_{cc}Q_\gamma = -1.387(7)$

Earlier values of $eq_{aa}Q_\alpha$ [2, 3] and $eq_{aa}Q_\gamma$ [2] from microwave spectra are in excellent agreement with the more recent results, but are less precise [1]. The quadrupole coupling constant given in [4] is incorrect [2, 3]. Experimental ^{14}N quadrupole coupling constants are compared with the values from own and previous ab initio calculations in [5] which also gives calculated eq_{ab} values.

References:

[1] Gerry, M. C. L.; Heineking, N.; Maeder, H.; Dreizler, H. (Z. Naturforsch. **44a** [1989] 1079/86).
[2] Forman, R. A.; Lide, D. R., Jr. (J. Chem. Phys. **39** [1963] 1133/4).
[3] Kewley, R.; Sastry, K. V. L. N.; Winnewisser, M. (J. Mol. Spectrosc. **12** [1964] 387/401).
[4] Rogers, J. D.; Williams, D. (Phys. Rev. [2] **86** [1952] 654).
[5] Chong, D. P. (Chem. Phys. Lett. **175** [1990] 525/30).

2.3.1.6.7 Rotational Constants. Centrifugal Distortion Constants

HN_3 and DN_3 are semirigid, slightly asymmetric rotors: HN_3 with $\kappa = -0.99916$ [1] and DN_3 with $\kappa = -0.99769$ [2]. The asymmetry suffices to lift the degeneracy of the transitions starting from levels with the rotational pseudoquantum numbers $K_a'' = 1$ and 2 (lower state) [3, 4]. The large value of A_0 means that even for moderate numbers of K_a the rotational levels of the ground vibrational state have energies comparable to the rotational levels in the ν_5 state; perturbations result [5]. Therefore, an analysis of the spectra has to include sextic terms for larger values of K [4]. Simultaneous analyses of several vibrational bands were used in recent papers in order to eliminate difficulties arising from interactions [5, 6].

The most exact rotational constants were derived from Fourier transform IR (FT-IR) [7] and FT-MW spectra [8] for HN_3 and from FT-IR [6] and MW spectra for DN_3 [2]. The results were evaluated within the Watson representation of the Hamiltonian for the near-symmetric asymmetric top and are listed in Table 8. The only rotational parameter published for $HN^{15}NN$ is $(B_0 + C_0) = 23.814$ MHz [9].

Table 8
Effective Ground State Rotational Constants of Hydrogen Azide in MHz.

molecule	A_0	B_0	C_0	analysis includes	Ref.
HN_3	611036.95(78)	12034.1734(42)	11781.4759(36)	dodecaïc terms	[7]
$H^{15}NNN$	605583.30(15)	11667.5433(15)$^{a)}$	11427.8558(15)$^{a)}$	sextic terms	[8]
$HNN^{15}N$	610979.7(2)	11641.7764(14)$^{a)}$	11405.0788(14)$^{a)}$	sextic terms	[8]
DN_3	344746.849(90)	11350.832(21)	10964.999(21)	octic terms$^{b)}$	[6]
DN_3	344746.589(64)	11350.983(16)	10964.755(15)	sextic terms	[2]

$^{a)}$ The values were refined from the results in [4]. — $^{b)}$ Interaction with ν_5 was included.

The Watson representation of the Hamiltonian for the near-symmetric asymmetric top was also used in order to obtain centrifugal distortion constants from FT-IR spectra [5 to 7], FT-MW spectra [8], and a continuous MW spectrum [2]. The resulting quartic constants are given in Table 9; see the cited papers for the values of the sextic and higher terms.

Table 9
Quartic Centrifugal Distortion Constants of Hydrogen Azide in kHz.

molecule	Δ_J	Δ_K	Δ_{JK}	δ_J	δ_K
HN_3 [a]	4.8770(42)	270479(249)	790.46(2.28)	−0.0916(20)	−0.0176(43)
HN_3 [b]	5.52(18)	270560(12)	605.6(3.0)	0.096(15)	435(66)
$H^{15}NNN$ [c]	4.627(5)	270480.0 [f]	769.0(8)	−0.0836(15)	−0.023(14)
$HNN^{15}N$ [c]	4.540(5)	270480.0 [f]	752.3(8)	−0.0827(15)	−0.027(13)
DN_3 [d]	4.329(18)	92588(33)	335.2(4.2)	0.1745(33)	281(12)
DN_3 [e]	4.281(16)	92242(33)	444.51(44)	0.1864(41)	365.1(7.7)

Terms included in the analysis are [a] dodecaïc [7], — [b] octic [5], — [c] sextic [8], — [d] octic [6], — [e] sextic [2]. — [f] Fixed value from [7].

Less complete or earlier sets of rotational and centrifugal distortion constants for hydrazoic acid in the ground state were given in a number of papers which are listed in Table 10. Very early microwave investigations of HN_3 and DN_3 are described in [9, 10].

Table 10
Additional Rotational Parameters of Hydrazoic Acid in the Ground State.

molecule	determined parameters	source	Ref.
HN_3	B_0, C_0, Δ_J	FT-IR of ν_4	[11]
	A_0, B_0, C_0, Δ_J, Δ_K, Δ_{JK}, δ_J, δ_K, four sextic terms	far FT-IR	[3]
	A_0, (B_0+C_0), Δ_J, Δ_K, Δ_{JK}, δ_J, δ_K, four sextic terms	FT-IR of ν_5, ν_6	[12]
	B_0, Δ_K	laser-IR of ν_3	[13]
	A_0, (B_0+C_0), Δ_J, Δ_K, Δ_{JK}, one sextic term	far Raman	[14]
	$A_0-(B_0+C_0)/2$, Δ_J, Δ_K, Δ_{JK}, one sextic term	far Raman	[15]
	A_0, B_0, C_0, Δ_J, Δ_K, Δ_{JK}, δ_J, three sextic terms	MW	[16]
	$A_0-(B_0+C_0)/2$, Δ_K, three sextic terms	far IR	[17]
	Δ_J, Δ_K, Δ_{JK}, δ_J	valence force field	[18]
	A_0, B_0, C_0, Δ_J, Δ_{JK}, two sextic terms	MW	[19]
	A_0, B_0, C_0, Δ_J, Δ_{JK}, two sextic terms	MW	[4]
$H^{15}NNN$	Δ_J, Δ_K, Δ_{JK}, δ_J	valence force field	[18]
$HNN^{15}N$	A_0, B_0, C_0, Δ_J, Δ_{JK}, two sextic terms	MW	[4]
DN_3	A_0, B_0, C_0, Δ_J, Δ_K, Δ_{JK}, δ_J, δ_K, four sextic terms	far FT-IR	[20]
	A_0, (B_0+C_0), Δ_J, Δ_K, Δ_{JK}, one sextic term	far Raman	[14]
	$A_0-(B_0+C_0)/2$, Δ_K, three sextic terms	far IR	[17]
	Δ_J, Δ_K, Δ_{JK}, δ_J	valence force field	[18]
	A_0, B_0, C_0, Δ_J, Δ_{JK}, two sextic terms	MW	[19]
	A_0, B_0, C_0, Δ_J, Δ_{JK}, two sextic terms	MW	[4]
	B_0+C_0, B_0-C_0, D_J	IR of ν_4	[21]

Rotational and centrifugal distortion constants were also determined for various vibrationally excited states of hydrogen azide. The resulting parameters are listed in Table 11.

Table 11
Rotational Parameters of HN_3 and DN_3 in Vibrationally Excited States.

molecule	state	determined parameters	spectrum	Ref.
HN_3	ν_1, $\nu_2+\nu_4$, $3\nu_1$	B, D, and sometimes H for each K	FT-IR	[7]
	ν_2	(B+C), Δ_J	Raman	[1]
	ν_3	B, Δ_K for each K	laser-IR	[13]
	ν_5, ν_6	A, (B+C), Δ_J, Δ_K, Δ_{JK}, δ_J, δ_K, four sextic terms	FT-IR	[12]
	ν_5, ν_6	(A−B), Δ_K	IR	[22]
	$3\nu_1$, $4\nu_1$	A, B, C, Δ_J, Δ_K, Δ_{JK}	near IR, visible	[23]
	$5\nu_1$, $6\nu_1$	(B+C)	photodissociation	[24]
DN_3	ν_1	A, B, C, Δ_J, Δ_K, Δ_{JK}, δ_J and selected parameters for each K	IR	[25]
	ν_1	A, (B+C), Δ_J, Δ_K, Δ_{JK}, one sextic term	IR, Raman	[26]
	ν_5, ν_6, (ν_4)	A, (B+C), Δ_J, Δ_K, Δ_{JK}, δ_J, δ_K, four sextic terms and an octic one	FT-IR	[6]
	ν_4	B+C, B−C, D_J, δ_J	IR	[21]

References:

[1] Bendtsen, J. (J. Raman Spectrosc. **9** [1980] 162/5).
[2] Bendtsen, J.; Winnewisser, M. (Chem. Phys. **40** [1979] 359/65).
[3] Bendtsen, J.; Nicolaisen, F. M. (J. Mol. Spectrosc. **119** [1986] 456/66).
[4] Winnewisser, M.; Cook, R. L. (J. Chem. Phys. **41** [1964] 999/1004).
[5] Hegelund, F.; Bendtsen, J. (J. Mol. Spectrosc. **124** [1987] 306/16).
[6] Bendtsen, J.; Hegelund, F.; Nicolaisen, F. M. (J. Mol. Spectrosc. **128** [1988] 309/20).
[7] Cheung, A. S.-C.; Merer, A. J. (J. Mol. Spectrosc. **127** [1988] 509/26).
[8] Gerry, M. C. L.; Heineking, N.; Maeder, H.; Dreizler, H. (Z. Naturforsch. **44a** [1989] 1079/86).
[9] Amble, E.; Dailey, B. P. (J. Chem. Phys. **18** [1950] 1422).
[10] Rogers, J. D.; Williams, D. (Phys. Rev. [2] **82** [1951] 131).

[11] Bendtsen, J.; Nicolaisen, F. M. (J. Mol. Spectrosc. **133** [1989] 193/200).
[12] Bendtsen, J.; Hegelund, F.; Nicolaisen, F. M. (J. Mol. Spectrosc. **118** [1986] 121/31).
[13] Yamada, K.; Takami, M. (J. Mol. Spectrosc. **84** [1980] 431/46).
[14] Bendtsen, J. (J. Raman Spectrosc. **6** [1977] 306/13).
[15] Bendtsen, J. (Proc. 5th Int. Conf. Raman Spectrosc., Freiburg i. Br., FRG, 1976, pp. 410/1; C.A. **87** [1977] No. 191470).
[16] Bendtsen, J.; Winnewisser, M. (Chem. Phys. Lett. **33** [1975] 141/5).
[17] Krakow, B.; Lord, R. C.; Neely, G. O. (J. Mol. Spectrosc. **27** [1968] 148/76).
[18] Moore, C. B.; Rosengren, K. (J. Chem. Phys. **44** [1966] 4108/15).
[19] Kewley, R.; Sastry, K. V. L. N.; Winnewisser, M. (J. Mol. Spectrosc. **12** [1964] 387/401).
[20] Bendtsen, J.; Nicolaisen, F. M. (J. Mol. Spectrosc. **125** [1987] 14/23).

[21] Bendtsen, J.; Nicolaisen, F. M. (J. Mol. Spectrosc. **145** [1991] 123/9).
[22] Levine, D. M.; Dows, D. A. (J. Chem. Phys. **46** [1967] 1168/72).

[23] Carlotti, M.; Di Lonardo, G.; Galloni, G.; Trombetti, A. (Trans. Faraday Soc. **67** [1971] 2852/61).

[24] Foy, B. R.; Casassa, M. P.; Stephenson, J. C.; King, D. S. (J. Chem. Phys. **90** [1989] 7037/45).

[25] Bendtsen, J.; Guelachvili, G. (J. Mol. Spectrosc. **107** [1984] 385/94).

[26] Bendtsen, J. (J. Raman Spectrosc. **15** [1984] 113/9).

2.3.1.6.8 Coriolis Coupling. Rovibrational Interactions. Fermi Resonances

Coriolis coupling constants are usually calculated from the fundamental vibrations by the methods of Meal and Polo [1, 2] and Smith and Mills [3]. Only the Coriolis coupling constants $|\zeta^b_{56}| = 0.07755(16)$ for HN_3 [4] and 0.093(8) for DN_3 [5] were obtained from rovibrational spectra. The calculated values are as follows [1]:

constant	HN_3	DN_3	constant	HN_3	DN_3
ζ^a_{16}	-0.0308	-0.0212	ζ^b_{16}	0.2998	0.1028
ζ^a_{26}	-0.0125	-0.0368	ζ^b_{26}	-0.8254	-0.8324
ζ^a_{36}	-0.0010[a]	-0.0662	ζ^b_{36}	0.0335	0.0321
ζ^a_{46}	-0.4027	-0.5330[b]	ζ^b_{46}	0.0013	0.0022
ζ^a_{56}	-0.6863[c]	-0.7266[d]	ζ^b_{56}	0.0099	0.0159

[a] $-0.31(5)$ [3]. — [b] $-0.41(5)$ [3]. — [c] $-0.93(2)$ [3], -0.9227 [2]. — [d] $-0.82(2)$ [3], -0.8308 [2].

Calculated constants ζ^a_{56} are -0.9255 for $H^{15}NNN$ and -0.9224 for $HNN^{15}N$ [2].

Perturbations of the vibrational fundamentals of HN_3 and DN_3 are extensive. The experimental observations are described separately for each isotopomer.

HN_3. Perturbations were observed in the upper levels $K' = 0$ to 2 of ν_1. The interactions take place by anharmonic resonance for $K' = 0$ and $K' = 1$. The vibrational levels ν_5 or ν_6 or both are probably involved in the first case, whereas in the second one, $\nu_2 + 2\nu_6$ is possibly interacting. The small anomaly at the $K' = 2$ level of ν_1 is due to two different perturbations [6].

Substantial mixing of the HNN bending mode ν_3 with the skeletal stretching mode ν_4 is indicated by the change of the rotational constant upon ν_3 excitation and the changes in the IR spectrum upon substitution of the terminal N atom. An a-type Coriolis interaction of ν_3 with ν_5 and ν_6 was also suggested [2]. However, this Coriolis coupling is not compatible with the anomalously small energy difference between the ν_3 subbands for $K = 0$ and $K = 1$ observed in a high-resolution IR spectrum. The small energy difference probably arises from Fermi resonance of ν_3 with $2\nu_6$, which is raised in energy by Fermi resonance with ν_4. Interaction of ν_3 with ν_5 and ν_6 also cannot explain the observed K dependence of the effective B and Δ values of ν_3. A perturbation by energetically close, unidentified states was suggested instead [7].

The fundamental ν_4 of HN_3 is globally disturbed. The perturbation is attributed to Coriolis coupling to nearby levels, the most likely being $\nu_5 + \nu_6$ for symmetry reasons. Additional perturbations are possibly involved. A local interaction involving crossing between the levels $K_a = 3$, 4 of ν_4 and $K_a = 2$, 3 of ν_3 was deduced from anomalies in the rotational constants B [8]. Another crossing at the $K_a = 8$ and 9 levels of the ν_4 state with levels of an unassigned vibrational state was observed in the high-resolution IR spectrum [9].

The main resonance in ν_5 is a strong first-order a-Coriolis perturbation by ν_6 which strongly effects the positions of the K levels in both bands [10]. Fundamentals from a low-resolution IR spectrum yielded ζ_{56}^{a} (see above) [3]. A second-order a-Coriolis interaction between ν_5 and ν_6 for levels with $\Delta K = \pm 2$ was additionally found in a later high-resolution spectrum [11]. The centrifugal distortion parameters $C_5^{ab} = 7.9309(13) \times 10^{-5}$ cm^{-1} and $|\zeta_{56}^{b}|$ (see above) were determined in a simultaneous analysis of the vibrational ground state, ν_5, and ν_6, taking into account the resonance between the ground state and ν_5 via centrifugal distortion and the a- and b-Coriolis-type interactions between ν_5 and ν_6 [4].

DN_3. A perturbation in the K structure of ν_1 became obvious when observed and calculated frequencies were compared. Possible candidates for a Fermi interaction were given [12]. Fermi resonance between ν_2 and $\nu_3 + \nu_4$ and $\nu_3 + 2\nu_5$ was observed in the IR spectrum [2].

The subbands of ν_4 are strongly disturbed for $K_a \geq 8$ by interactions with ν_5 states. Other interacting bands are ν_6, probably ν_3, and overtones and combination bands of ν_5 and ν_6 [13].

The perturbation of the ν_5 band is similar to that of ν_5 in the HN_3 spectrum. An analysis showed that there is a resonance between the ground state and ν_5 due to centrifugal distortion, a- and b-Coriolis type interactions of ν_5 and ν_6, and an a-type Coriolis resonance between ν_4 and ν_6. A centrifugal distortion parameter $C_5^{ab} = 6.29(12) \times 10^{-5}$ cm^{-1} and $|\zeta_{56}^{b}|$ (see above) were determined [5, 14].

An additional, weaker interaction of ν_5 and ν_6 was found with the hydrogen bending mode ν_4 [3]. This local, second-order a-Coriolis interaction between $K_a = 7$ and 8 of ν_6 and $K_a = 5$ and 6 of ν_4 was identified for DN_3 by the perturbation of the ν_6 band. The poor fit of some subbands indicates perturbations in ν_4 due to other levels [5]. A second-order a-Coriolis resonance between ν_5 and ν_6 for levels with $\Delta K = \pm 2$ [11] was observed for DN_3 between the levels $K_a = 3$ and 4 in ν_6 and $K_a = 5$ and 6 in ν_5 [5] as predicted in [4].

References:

[1] Mohan, S.; Gunasekaran, S. (J. Chim. Phys. Phys.-Chim. Biol. **81** [1984] 255/60).
[2] Moore, C. B.; Rosengren, K. (J. Chem. Phys. **44** [1966] 4108/15).
[3] Levine, D. M.; Dows, D. A. (J. Chem. Phys. **46** [1967] 1168/72).
[4] Hegelund, F.; Bendtsen, J. (J. Mol. Spectrosc. **124** [1987] 306/16).
[5] Bendtsen, J.; Hegelund, F.; Nicolaisen, F. M. (J. Mol. Spectrosc. **128** [1988] 309/20).
[6] Cheung, A. S.-C.; Merer, A. J. (J. Mol. Spectrosc. **127** [1988] 509/26).
[7] Yamada, K.; Takami, M. (J. Mol. Spectrosc. **84** [1980] 431/46).
[8] Bendtsen, J.; Nicolaisen, F. M. (J. Mol. Spectrosc. **133** [1989] 193/200).
[9] Bendtsen, J.; Nicolaisen, F. M. (J. Mol. Spectrosc. **152** [1992] 101/8).
[10] Bendtsen, J.; Nicolaisen, F. M. (J. Mol. Spectrosc. **119** [1986] 456/66).

[11] Bendtsen, J.; Hegelund, F.; Nicolaisen, F. M. (J. Mol. Spectrosc. **118** [1986] 121/31).
[12] Bendtsen, J.; Guelachvili, G. (J. Mol. Spectrosc. **107** [1984] 385/94).
[13] Bendtsen, J.; Nicolaisen, F. M. (J. Mol. Spectrosc. **145** [1991] 123/9).
[14] Bendtsen, J.; Nicolaisen, F. M. (J. Mol. Spectrosc. **125** [1987] 14/23).

2.3.1.6.9 Fundamental Vibrations

Ground State. Hydrogen azide has C_s symmetry; the six fundamentals (5A′ + 1A″) are all active in IR and Raman spectra [1, 2]. The vibrational spectra of HN_3 show great complexity despite the small number of fundamental vibrations because of strong Coriolis coupling and Fermi resonances [3] as described above. The fundamental vibrational frequencies of HN_3 and DN_3 are given in Table 12 and those of ^{15}N-substituted isotopomers in Table 13.

Table 12
Fundamental Vibrational Frequencies (Band Origins) of Gaseous HN_3 and DN_3 in cm^{-1}.

ν_i	description	HN_3 IR	 Raman	DN_3 IR	 Raman
ν_1	$\nu(XN)$	3339.8908 [4]	–	2478.443(2) [5]	2478.324(9) [6]
ν_2	$\nu_{as}(NNN)$	2139.8(6) [7]	2140.308(4) [8]	2141 [1]	–
ν_3	$\delta(XNN)$[a]	1266.63223(38) [9] 1266.6327(3) [10]	–	1184.7(2) [7]	–
ν_4	$\nu_s(NNN)$[a]	1147.4075(5) [3] 1147.4042(3) [10]	–	954.769(1) [11]	957.7(3) [12]
ν_5	$\delta(NNN)$[b]	537.2480(17) [13]	–	495.7479(10) [12]	–
ν_6	$\tau(NNN)$[c]	606.3586(15) [13]	–	586.4994(12) [12]	–

[a] A normal-coordinate treatment of hydrazoic acid indicates that the pair ν_3 and ν_4 consists of an H(D)NN bending mode and an NNN stretching mode, respectively. The hydrogen bending mode is ν_3 for HN_3 and ν_4 for DN_3 [14]. — [b] In-plane. — [c] Out-of-plane.

The earlier fundamental frequencies $\nu_1=3336$ (m), $\nu_2=2140$ (vs), $\nu_3=1274$ (m), $\nu_4=1150$ (vs), $\nu_5=522$ (w), and $\nu_6=672$ (w) cm^{-1} of gaseous HN_3 [1] were often used for calculating molecular properties.

The IR band ν_6 in the gas phase spectra depends on ν_5 via Coriolis coupling for most of its intensity [15]. The inherently small intensity of ν_6 becomes evident when comparing spectra of the gases with those of solid samples, where there is no Coriolis coupling [7, 15]. The energy transfer from the very strong a-component of the ν_5 band through first-order a-Coriolis resonance leads to the observed a-type band of ν_6 which is in contrast to the c-type band expected for the molecular symmetry. The absence of the Coriolis interaction for $K_a=0$ results in the missing $K_a=0$ subband in ν_6 [12].

Table 13
Fundamental Vibrational Frequencies of ^{15}N-Substituted, Gaseous Hydrogen Azide in cm^{-1} [7].

molecule	ν_1	ν_2	ν_3	ν_4	ν_5	ν_6[a]
$H^{15}NNN$	3491.1	2133.7(4)	1265.2	1124	525.7	–
$HNN^{15}N$	3497.3	2116.5(4)	1257.5[b]	1146.3	523.7	–
$D^{15}NNN$	2455[c]	2126.5[d]	1164.0(5)	947.6	492.9	–
$DNN^{15}N$	2466[c]	2107.1[d]	1172.1(5)	954.4	490.5	–

[a] Not observed. — [b] Extrapolated from the $^{Q}Q_K$ branches with K=1 to 6. — [c] In an N_2 matrix. — [d] Calculated from the force field; the band is Fermi-resonance-shifted.

Q-branch frequencies of ν_3 and ν_4 for HN_3, $HNN^{15}N$, of ν_1 for DN_3, and of ν_4 for the deuterated ^{15}N isotopomers from gas spectra are listed in [7]. Q-branch frequencies of ν_5 and ν_6 for HN_3 and DN_3 [16] and near 700 cm^{-1} [1] were also reported.

The fundamentals of HN_3 and DN_3 absorbed on an Si(100) surface at 120 K were measured by high-resolution electron energy loss (HREEL) spectroscopy and were found to be similar to those of the gaseous molecules [17].

Electronically Excited States. The fundamentals of excited HN_3 were partly identified in the UV spectrum of the gas. Average values are $\nu'_2 = 1475$ to 1490, $\nu'_3 = 788 \pm 40$, ν'_5 and $\nu'_6 = 428 \pm 26$, and $\nu'_6 \approx 645$ cm^{-1}. A comparison with the ground-state fundamentals demonstrates that the excited species has a considerably bent N_3 group. The vibrational splitting of Rydberg states is also given [2].

References:

[1] Dows, D. A.; Pimentel, G. C. (J. Chem. Phys. **23** [1955] 1258/63).
[2] McDonald, J. R.; Rabalais, J. W.; McGlynn, S. P. (J. Chem. Phys. **52** [1970] 1332/40).
[3] Bendtsen, J.; Nicolaisen, F. M. (J. Mol. Spectrosc. **133** [1989] 193/200).
[4] Cheung, A. S.-C.; Merer, A. J. (J. Mol. Spectrosc. **127** [1988] 509/26).
[5] Bendtsen, J.; Guelachvili, G. (J. Mol. Spectrosc. **107** [1984] 385/94).
[6] Bendtsen, J. (J. Raman Spectrosc. **15** [1984] 113/9).
[7] Moore, C. B.; Rosengren, K. (J. Chem. Phys. **44** [1966] 4108/15).
[8] Bendtsen, J. (J. Raman Spectrosc. **9** [1980] 162/5).
[9] Yamada, K.; Takami, M. (J. Mol. Spectrosc. **84** [1980] 431/46).
[10] Bendtsen, J.; Nicolaisen, F. M. (J. Mol. Spectrosc. **152** [1992] 101/8).

[11] Bendtsen, J.; Nicolaisen, F. M. (J. Mol. Spectrosc. **145** [1991] 123/9).
[12] Bendtsen, J.; Hegelund, F.; Nicolaisen, F. M. (J. Mol. Spectrosc. **128** [1988] 309/20).
[13] Bendtsen, J.; Hegelund, F.; Nicolaisen, F. M. (J. Mol. Spectrosc. **118** [1986] 121/31).
[14] Fletcher, W. H. (unpublished results, ref. 20 in [15]).
[15] Levine, D. M.; Dows, D. A. (J. Chem. Phys. **46** [1967] 1168/72).
[16] Krakow, B.; Lord, R. C.; Neely, G. O. (J. Mol. Spectrosc. **27** [1968] 148/76).
[17] Bu, Y.; Chu, J. C. S.; Lin, M. C. (Surf. Sci. **264** [1992] L151/L156).

2.3.1.6.10 Mean Amplitudes of Vibration. Bastiansen-Morino Shrinkage

The parallel (relative to the molecular axis) mean amplitudes of vibration were calculated from earlier published vibrational frequencies [1] and structural data assuming a linear N_3 group [2]. Results at 300 K in Å are [3]:

molecule	$u(H(D)-N_\alpha)$	$u(N_\alpha-N_\beta)$	$u(N_\beta-N_\gamma)$	$u(H(D)\cdots N_\beta)$	$u(H(D)\cdots N_\gamma)$
HN_3	0.07433	0.03835	0.03558	0.10580	0.12140
DN_3	0.06345	0.03844	0.03567	0.09901	0.11550

The mean amplitudes of the N-N vibrations are the same for HN_3 and DN_3 [3]. Similar results were obtained in a more recent calculation [4]. Perpendicular mean-square amplitudes are given in [5].

The calculated Bastiansen-Morino shrinkage effect in the N_3 group (taken to be linear) was found to be 0.004251 Å for HN_3 and 0.003923 Å for DN_3 [5].

References:

[1] Dows, D. A.; Pimentel, G. C. (J. Chem. Phys. **23** [1955] 1258/63).
[2] Amble, E.; Dailey, B. P. (J. Chem. Phys. **18** [1950] 1422).
[3] Venkateswarlu, K.; Malathy Devi, V. (Proc. Indian Acad. Sci. A **61** [1965] 272/82).
[4] Mohan, S.; Gunasekaran, S. (J. Chim. Phys. Phys.-Chim. Biol. **81** [1984] 255/60).
[5] Venkateswarlu, K.; Malathy Devi, V. (Curr. Sci. **36** [1967] 118/9).

2.3.1.6.11 Force Constants

The most recent calculation of the force constants of hydrogen azide in a general valence force field [1] is based on early vibrational [2] and structural data [3]. In internal coordinates there are three stretching force constants, f_R, f_r, and $f_{r'}$ with $R = r(H\text{-}N)$, $r = r(N_\alpha\text{-}N_\beta)$, and $r' = r(N_\beta\text{-}N_\gamma)$. The angle deformation constants are f_α with $\alpha = \angle HNN$ and f_β and f_τ for the in-plane and out-of-plane deformations of the NNN unit. These values and those of the most important interaction force constants in 10^5 dyn/cm are as follows [1]:

f_R	f_r	$f_{r'}$	f_α	f_β	f_τ	f_{Rr}	$f_{rr'}$	$f_{r\alpha}$
6.1702	13.8971	13.5851	0.5251	0.4089	0.6193	0.3915	1.2590	0.3487

Force constants in a general valence force field in [4] are based on similar molecular parameters; the force constants in a Urey-Bradley force field were less satisfactorily. Force constants from an SCF calculation with a double-zeta basis set are given in [5]. An early calculation [6] using structural parameters from [7] yielded somewhat uncertain force constants because of strong correlation among them. Other early [8] or incomplete [9] sets of force constants were obtained from simple valence force fields. Some force constants were estimated by empirical methods [10 to 12].

References:

[1] Mohan, S.; Gunasekaran, S. (J. Chim. Phys. Phys.-Chim. Biol. **81** [1984] 255/60).
[2] Dows, D. A.; Pimentel, G. C. (J. Chem. Phys. **23** [1955] 1258/63).
[3] Amble, E.; Dailey, B. P. (J. Chem. Phys. **18** [1950] 1422).
[4] Thompson, W. T.; Fletcher, W. H. (Spectrochim. Acta **22** [1966] 1907/21).
[5] Nielsen, C. J.; Sjøgren, C. E. (J. Mol. Struct. **150** [1987] 361/79 [THEOCHEM **35**]).
[6] Moore, C. B.; Rosengren, K. (J. Chem. Phys. **44** [1966] 4108/15).
[7] Winnewisser, M.; Cook, R. L. (J. Chem. Phys. **41** [1964] 999/1004).
[8] Venkateswarlu, K.; Thirugnanasambandam, P. (Z. Phys. Chem. [Leipzig] **218** [1961] 1/12).
[9] Conant, D. R.; Decius, J. C. (Spectrochim. Acta A **23** [1967] 2931/8).
[10] Orville-Thomas, W. J. (Trans. Faraday Soc. **49** [1953] 855/66).
[11] Orville-Thomas, W. J. (J. Chem. Soc. **1952** 2383/9).
[12] Decius, J. C. (J. Chem. Phys. **45** [1966] 1069).

2.3.1.6.12 Gas Phase Acidity. Bond Dissociation Energies

The standard gas phase acidity of HN_3 has an enthalpy of 1439 ± 8 kJ/mol and was measured by ion cyclotron resonance of gas-phase proton transfer reactions. This result disagrees with values calculated from Born-Haber cycles [1]. Thermodynamic data for the dissociation in aqueous solution are given on p. 151.

D(H-N$_3$). Average H-N_3 standard dissociation energies of $D_0^\circ = 385$ to 389 kJ/mol [2] and 384.6 ± 20.9 kJ/mol at 0 K [3] were determined via the reaction of HN_3 with F atoms. An earlier investigation of this reaction yielded ~350 kJ/mol [4]. The thermal emission of N_3^- from a filament heated in gaseous HN_3 was studied in a magnetron cell and yielded $D_0 = 377 \pm 33$ kJ/mol [5]. Values of $D = 386 \pm 19$ [6] and $D_{300}^\circ = 343 \pm 12$ kJ/mol [7] were calculated from the enthalpies of formation of N_3 which in turn were derived from the radical's experimental electron affinity [6] and reaction enthalpy [7]. A dissociation energy of 347 kJ/mol was obtained from a mass-spectrometric investigation of HN_3 [8]. A dissociation energy of 385 ± 20 kJ/mol was calculated from the enthalpy determined for the gas phase acidity of HN_3 [1]. A Born-Haber cycle gave an energy of 406 ± 17 kJ/mol [9]. An ab initio study (second-order Møller-Plesset perturbation theory, various basis sets) yielded $D_0 = 405$ to 415 kJ/mol [13].

D(HN-NN). An HN-NN bond energy of ≤ 42 kJ/mol at 298 K was determined from the reaction of HN_3 with excited Kr atoms [10]. An upper limit of the dissociation energy with formation of NH(X $^3\Sigma^-$) and N_2(X) is 59.3 kJ/mol at 0 K. The value was calculated from the experimentally observed energy of NH(a $^1\Delta$) and spectroscopic constants [11]. A value of 38.5 kJ/mol resulted from mass-spectrometric investigations on HN_3 [8]. Thermodynamic data yielded 73.2 kJ/mol [12]. A value of about 21 kJ/mol at 298 K was calculated from a Born-Haber cycle [9]. An ab initio study (see above) gave $D_0 \approx 63$ kJ/mol [13]. The low HN-NN dissociation energy would require dissociation of HN_3 at ambient temperature; the molecule's actually observed stability stems from an additional energy barrier towards decomposition. It originates from the spin-forbidden character of dissociation into the products in their ground states [8]. The dissociation energy of 224.3 kJ/mol for $HN_3 \rightarrow NH(a\ ^1\Delta) + N_2(X)$ was calculated from thermodynamic data [12].

References:

[1] Pellerite, M. J.; Jackson, R. L.; Brauman, J. I. (J. Phys. Chem. **85** [1981] 1624/6).
[2] Habdas, J.; Wategaonkar, S.; Setser, D. W. (J. Phys. Chem. **91** [1987] 451/8).
[3] Dyke, J. M.; Jonathan, N. B. H.; Lewis, A. E.; Morris, A. (Mol. Phys. **47** [1982] 1231/40).
[4] Sloan, J. J.; Watson, D. G.; Wright, J. S. (Chem. Phys. **43** [1979] 1/8).
[5] Chiang, M.; Wheeler, R. (Can. J. Chem. **46** [1968] 3785/8).
[6] Illenberger, E.; Comita, P. B.; Brauman, J. I.; Fenzlaff, H.-P.; Heni, M.; Heinrich, N.; Koch, W.; Frenking, G. (Ber. Bunsen-Ges. Phys. Chem. **89** [1985] 1026/31).
[7] Clark, T. C.; Clyne, M. A. A. (Trans. Faraday Soc. **66** [1970] 877/85).
[8] Franklin, J. L.; Dibeler, V. H.; Reese, R. M.; Krauss, M. (J. Am. Chem. Soc. **80** [1958] 298/302).
[9] Gray, P.; Waddington, T. C. (Proc. R. Soc. London A **235** [1956] 481/95).
[10] Stedman, D. H. (J. Chem. Phys. **52** [1970] 3966/70).
[11] Casassa, M. P.; Foy, B. R.; Stephenson, J. C.; King, D. S. (J. Chem. Phys. **94** [1991] 250/61).
[12] Kajimoto, O.; Yamamoto, T.; Fueno, T. (J. Phys. Chem. **83** [1979] 429/35).
[13] Otto, M.; Lotz, S. D.; Frenking, G. (Inorg. Chem. **31** [1992] 3647/55).

2.3.1.6.13 Quantum-Chemical Calculations

The HN_3 molecule has been the subject of a series of quantum-chemical studies. The more important ones are referenced in conjunction with the individual properties of HN_3. For a more complete survey of quantum-chemical calculations and especially those covering computational aspects, consult the bibliography of ab initio calculations given on pp. 16/7.

2.3.1.6.14 Spectra

Nuclear Magnetic Resonance

The ^1H NMR shift of HN_3 in CCl_4 at 298 K and infinite dilution is $\delta = 4.10$ ppm; the width of the singlet (half-width 50 Hz) results from the short quadrupole relaxation time [1]. A shift of $\delta = 6.45$ ppm with a coupling constant $^1J(HN) = 69$ Hz was found at 303 K in a 10%

$(C_2H_5)_2O$ solution of triply labeled $H^{15}N_3$ which does not show quadrupole broadening. The value of $^1J(HN)$ is consistent with sp^3 hybridization at the H-bonded N atom; the coupling constant is probably negative [2].

The ^{15}N chemical shifts of 10% of triply labeled $H^{15}N_3$ in $(C_2H_5)_2O$ solution at 303 K [2] agree well with the chemical shifts of $H^{14}N_3$ which were obtained earlier under similar conditions [3], but are less exact due to quadrupole coupling. Spectroscopic data of $HN_\alpha N_\beta N_\gamma$ (negative high-field shifts in ppm) with respect to 1 M $^{15}NO_3^-$ in D_2O are as follows [2]:

	N_α		N_β		N_γ
^{15}N chemical shift (^1H-decoupled)	−321.085		−130.557		−174.816
coupling constant $^1J(NN)$ in Hz		13.95		7.20	
coupling constant J(HN) in Hz	70.18		2.26		2.25

The signals of the terminal N atoms become exchange-averaged in the presence of excess acid; a signal at $\delta = -240$ ppm in the presence of H_2O is the exchange-averaged signal of the terminal N atoms in HN_3 and in N_3^- [3].

Microwave Spectra

The bands in the MW spectra of the HN_3 isotopomers were all assigned to ground state rotational levels. They are identified by the rotational quantum numbers J. Usually the subscripts K_{-1}, K_1 are added, which are the pseudoquantum numbers for the limiting cases of the prolate and oblate symmetrical rotors. The pure rotational spectra of HN_3 and DN_3 are qualitatively similar. They consist of partially overlapping subbands, each subband characterized by the value of K_a'' for the initial state and $\Delta K_a = 1$. The spacing between the subbands of DN_3 is about half the spacing found in the HN_3 spectrum in accordance with the decrease of the constant A_0 upon substitution. The spacing between the rotational lines in the P and R branches of the individual subbands is nearly unaltered after H/D exchange, because the B_0 and C_0 constants remain nearly unchanged [4].

The MW spectra of HN_3 exhibit quadrupole hyperfine splitting for some bands; see for example [5, 6]. Complete resolution of the hyperfine splitting was achieved by Fourier transform spectroscopy [7]. Following are the results of MW measurements:

molecule	spectrum range in GHz	rotational transitions between lowest and highest J levels	band type	Ref.
HN_3	24	$1_{0,1} \leftarrow 0_{0,0}$	a	[7]
	20 to 72	$2_{2,1} \leftarrow 1_{1,0}$ to $55_{5,51} \leftarrow 54_{4,50}$	a	[8]
	9 to 125	$8_{1,7} \leftarrow 8_{1,8}$ to $28_{0,28} \leftarrow 27_{1,27}$	a, b	[6]
	24 to 167	$1_{0,1} \leftarrow 0_{0,0}$ to $7_{5,3} \leftarrow 6_{5,2}$	a	[9]
	213 to 215	$9_{0,9} \leftarrow 8_{0,8}$ to $9_{6,4} \leftarrow 8_{6,3}$	a	[10]
	24	$1_{-1} \leftarrow 0_0$		[11]
$H^{15}NNN$	5 to 37	$1_{0,1} \leftarrow 0_{0,0}$ to $25_{0,25} \leftarrow 24_{1,24}$	a, b	[7]
	92 to 209	$4_{0,4} \leftarrow 3_{0,3}$ to $9_{3,7} \leftarrow 8_{3,6}$	a	[10]
$HNN^{15}N$	5 to 40	$1_{0,1} \leftarrow 0_{0,0}$ to $26_{0,26} \leftarrow 25_{1,25}$	a, b	[7]
	92 to 208	$4_{0,4} \leftarrow 3_{0,3}$ to $9_{3,7} \leftarrow 8_{3,6}$	a	[10]
DN_3	8 to 338	$1_{0,1} \leftarrow 0_{0,0}$ to $46_{1,45} \leftarrow 45_{2,44}$	a, b	[5]
	66 to 180	$3_{0,3} \leftarrow 2_{0,2}$ to $8_{5,4} \leftarrow 7_{5,3}$	a	[9]

Early results on the HN_3 isotopomers were reported in [12] without experimental details.

Infrared and Raman Spectra

Investigations of the vibrational spectra of gaseous and frozen hydrogen azide are listed below. Spectra in CCl_4 [13, 14] and CS_2 solution [14] were also described. The IR spectra of HN_3 and DN_3 measured before 1950 were critically discussed in [13]. Studies on spectra of hydrogen azide are listed in Table 14.

Table 14
IR and Raman Studies of Gaseous Hydrogen Azide at Ambient Temperature.

molecule	spectrum	frequency range in cm^{-1} (resolution in cm^{-1})	investigation of	Ref.
HN_3	FT-IR	1100 to 1200 (0.03)	ν_4, coupling	[15]
	FT-IR	3000 to 3500 (0.007)	ν_1, $\nu_2+\nu_4$, $3\nu_4$, coupling	[16]
	IR	900 to 1900 (0.005)	ν_3, ν_4, coupling	[17]
	FT-IR	190 to 370	rotation, coupling	[18]
	FT-IR	20 to 400 (0.03)	rotation, ν_5, ν_6, coupling	[8]
	FT-IR	300 to 900 (0.03)	ν_5, ν_6, coupling	[19]
	laser-IR	1240 to 1290 (0.007)	ν_3, coupling	[20]
	Raman[a)]	2050 to 2210 (0.25)	ν_2, $\nu_2+\nu_5$, $\nu_2+\nu_6$	[21]
	Raman	2 to 470 (0.5)	rotation	[22]
	Raman	not given (0.3)	rotation	[23]
	IR	20 to 260 (0.5)	rotation	[24]
	IR[b)]	400 to 1300 (1)	ν_3, ν_5, ν_6, coupling	[25]
	IR	170 to 3700	rotation, fundamentals, coupling	[26]
	IR[c)]	450 to 3500	fundamentals, overtones	[13]
	IR[d)]	3000 to 3500	ν_1	[27]
	IR[e)]	290 to 3500	monomer, dimer, polymers	[28]
$H^{15}NNN$	IR	500 to 3500	fundamentals, coupling	[26]
$HNN^{15}N$	IR[e)]	500 to 3500	fundamentals, coupling	[26]
DN_3	FT-IR	400 to 1020 (0.03)	ν_4, ν_5, ν_6, coupling	[29]
	FT-IR	20 to 400 (0.03)	rotation, ν_5, ν_6, coupling	[4]
	IR	2430 to 2520 (0.005)	ν_1, coupling	[30]
	Raman	2200 to 2600 (0.3)	ν_1	[31]
	FT-IR	2200 to 2600 (0.07)	ν_1	[31]
	IR	900 to 1050 (0.03)	ν_4, coupling	[32]
	Raman	2 to 390 (0.5)	rotation	[22]
	IR	20 to 240 (0.5)	rotation	[24]
	IR[b)]	400 to 1300 (1)	ν_4, ν_5, ν_6, coupling	[25]
	IR	350 to 3700	fundamentals, overtones, coupling	[26]
	IR[c)]	450 to 3500	fundamentals, overtones	[13]
$D^{15}NNN$	IR	480 to 1200	fundamentals, coupling	[26]
$DNN^{15}N$	IR[e)]	480 to 2500	fundamentals, coupling	[26]

[a)] Also includes Raman spectrum at 423 K. — [b)] Also of polycrystalline films at ~85 K. — [c)] Also spectra of the solid at 80 K and >120 K. — [d)] In Xe, Ar, N_2 matrix at 20 K. — [e)] In N_2 matrix at 20 K.

Subband origins (K=0) of $3\nu_4$ at 3509 cm^{-1} and of $\nu_2+\nu_4$ at 3251 cm^{-1} were observed in the IR spectrum of HN_3. The value of $\nu_2+\nu_4$ is considerably below the harmonic value of ~3290 cm^{-1}. One reason for this is the intensity transfer from ν_1 by anharmonic resonance which is also responsible for the absence of the expected b-type component of the $\nu_2+\nu_4$ band. The rotational structure of the $\nu_2+\nu_4$ band is disturbed; additional subbands for K=1 to 3 form the K structure of another vibrational level. Both interact by a-Coriolis coupling; the magnitude of the intensities suggests that the other level is $\nu_2+\nu_5+\nu_6$. Additional resonances in both levels are noticeable [16].

The hydrogen bonding in solid HN_3 and DN_3 shifts all bands involving HN vibrations relative to the gas-phase frequencies [13]. An acyclic structure of the hydrazoic acid dimeric adduct in an N_2 matrix was deduced in dilution experiments with HN_3-DN_3 mixtures from the observation that there are only two additional bands irrespective of the D/H ratio. The bands at 387 and 302 cm^{-1} were assigned to the torsional distortions of a hydrogen and deuterium bond. The dimer ν(NH) frequency is shifted 150 cm^{-1} towards lower frequencies in an N_2 matrix and is considerably smaller than the shift of 216 cm^{-1} observed in the pure crystal. The hydrogen bond energy (~9.6 kJ/mol) and the bending force constant (0.089 mdyn/Å) of the hydrogen bridge were estimated for HN_3 in an N_2 matrix [28]. No hydrogen bonding of HN_3 was observed in CCl_4 solution [13].

The Q branches of the hot-band transitions $\nu_5 \rightarrow \nu_2+\nu_5$ and $\nu_6 \rightarrow \nu_2+\nu_6$ were identified at 2129.3(1) cm^{-1} in the Raman spectrum of gaseous HN_3 at ambient temperature [21].

Near-Infrared, Visible, and Ultraviolet Spectra

Overtone and combination bands of gaseous HN_3 were investigated in the near-IR and visible ranges between 1070 and 500 nm. $3\nu_1$, $4\nu_1$, and $5\nu_1$ were excited conventionally [33], whereas $5\nu_1$, $6\nu_1$, $7\nu_1$, and associated combination bands were excited by direct pumping or by IR-visible double-resonance pumping through the ν_1 band [34 to 36]. The band origins in cm^{-1} are:

$3\nu_1$ [33]	$4\nu_1$ [33]	$5\nu_1$ [33, 35]	$6\nu_1$ [35]	$7\nu_1$ [36]
9547.35(2)	12414.03(5)	15121(1)	17671	20070

Earlier observations on the $3\nu_1$ and $4\nu_1$ overtones were discussed in [33] and confirmed qualitatively. The $3\nu_1$ overtone band is an a- and b-type hybrid. The ratio of the individual vibrational transition moments, $\mu_a/\mu_b=0.37\pm0.05$, corresponds to an angle of 160° between the total transition moment and the N_3 group. This value is considerably larger than the angle HNN and inconsistent with a dipole moment transition along the N-H bond as implied by the $3\nu_1$ band's exclusive origin from the N-H stretching mode. Rotational perturbations of the $3\nu_1$ band were observed in the rotational levels with K′=2 and 4; their origin could not be determined [33]. The pure a-type bands of $4\nu_1$ [33], $5\nu_1$ [33, 34], and $6\nu_1$ [34] at ambient temperature show that the transition moment approaches the N_3 axis with increasing excitation of ν_1. Line broadening in $4\nu_1$ and $5\nu_1$ suggests predissociation [33].

The photodissociation spectra of $5\nu_1$, $6\nu_1$ [34, 35] and $7\nu_1$ [36] were measured at a rotational temperature of 8 K after free-jet expansion in Ar and were much better resolved than the room temperature spectra; see also [37]. The activated, rotational levels of the vibrationally excited species and their predissociation lifetimes τ are as follows [34]:

vibrational level	rotational temperature	rotational levels	τ in ns
$5\nu_1$	8 K	J=0 to 7, K=0	$210\pm^{110}_{60}$
	300 K	J=5 to 30, K=0 to 2	$80\pm^{60}_{30}$
$6\nu_1$	8 K	J=0 to 4, K=0	0.95 ± 0.15
	300 K	J=5 to 30, K=0 to 2	1.3 ± 0.2
$7\nu_1$ [36]	~8 K	–	$\geq$ 0.0026

The predissociation lifetime at 8 K does not vary significantly with J for $5\nu_1$ and $6\nu_1$. The energy range between these overtones contains combination bands of $5\nu_1$ which are much weaker; their band origins and predissociation lifetimes are given in [35]. Combination bands of $6\nu_1$ are observed in the wavenumber range $6\nu_1$ to $7\nu_1$; their positions and assignments are given in [36].

An analysis of the observed lines demonstrates that the description of these vibrational eigenstates at high energies by normal- or local-mode motions is inadequate [35, 36]. Deconvolution of the $6\nu_1$ band gives a maximum amount of 35% of $6\nu_1$ character for this eigenstate. The discrete, resolvable spectral features observed for the local mode actually result from anharmonic (Fermi) coupling of the N-H stretching states with background vibrational levels which is facilitated by the high state density of $\geq$10 states/cm^{-1} at the required energy [35]. The C_s symmetry of HN_3 does not severely restrict the vibrational states that couple through anharmonic resonances [34]. Inhomogeneous contributions from rotation and hot bands, and homogeneous (Lorentzian) broadening from the coupling of bound vibrational levels to the dissociation continuum were observed in individual transitions [35].

The UV spectrum of gaseous HN_3 contains the absorptions given below. The experimental extinction coefficients differ slightly; the values in aqueous solution [38] are given in parentheses:

position in nm [38, 39]	extinction coefficient ε in cm^2/mol		absorption coefficient in $(atm\cdot cm)^{-1}$ [40]	assignment [38]
	[39]	[38]		
264 (~260)	24	~20 (~47)	–	$^1A'' (^1\Sigma_u^-) \leftarrow {}^1A' (^1\Sigma_g^+)$
200 (~197)	498	~450 (~600)	–	$^1A'' (^1\Delta_u) \leftarrow {}^1A' (^1\Sigma_g^+)$
190 (~187)	805	~740 (~660)	~78	$^1A' (^1\Delta_u) \leftarrow {}^1A' (^1\Sigma_g^+)$
170, shoulder	–	~500	–	$^1A'' (^1\Pi_{g,u}) \leftarrow {}^1A' (^1\Sigma_g^+)$
156	–	~20000	2200	$^1A' (^1\Pi_{g,u}) \leftarrow {}^1A' (^1\Sigma_g^+)$
140	–	–	1480	$^1A' (^1\Sigma_u^+) \leftarrow {}^1A' (^1\Sigma_g^+)$

The UV spectrum between 210 and 114 nm is displayed in [40], and an additional broad band below 130 nm with a maximum at ~120 nm was mentioned. An absorption coefficient of 1.40×10^{-3} $(Torr\cdot cm)^{-1}$ was measured at 254 nm and 296 K [41]. The absorption coefficient in cm^2/mol at 230 nm can be described by $\varepsilon=35+0.12\times(T-600)$ from 600 to 1200 K and by $\varepsilon=35+0.15\times(1700-T)$ from 1200 to 1700 K [42]. The absorption coefficient of $(2.2\pm0.2)\times10^5$ cm^2/mol at 206 nm changes very little between 1200 and 1350 K [43]. The gas-phase spectra exhibit rather rich vibrational structures [38, 40, 44]; vibrational bands of electronically excited HN_3 are given on p. 106. The spectrum of the solid at 87 K exhibits a weak absorption at ~262 nm and a strong band which begins near 230 nm and cuts off transmission at 210 nm [39].

The absorption of light by aqueous HN_3 at 260 nm falls off with increasing concentrations of acids added at ambient temperature. The decrease is not related directly to the protonation equilibrium [45]. The absorption at 260.3 nm in aqueous solution shifts to 264.3 nm in *i*-octane solution and to 264.4 nm in $HCCl_3$ solution. The insensitivity of the band position to a gross change in solvent polarity was taken to be consistent with a forbidden, perpendicular π^*-π transition [46].

The low-lying Rydberg states $^3A''$ at ~200 nm and $^1A''$ at ~190 nm were calculated [47]. Four Rydberg series were observed in the vacuum UV spectrum. Their onsets are at 153.3, 133.8 (ns ← π), 135.4 (np ← π), and 129.8 nm (nd ← π) and yielded (outdated) ionization potentials [38]; see also p. 98.

The photolytic dissociation of HN_3 is described on pp. 125/32.

References:

[1] Nelson, J.; Spratt, R.; Nelson, S. M. (J. Chem. Soc. A **1970** 583/7).
[2] Müller, J. (Z. Naturforsch. **33b** [1978] 993/6).
[3] Beck, W.; Becker, W.; Chew, K. F.; Derbyshire, W.; Logan, N.; Revitt, D. M.; Sowerby, D. B. (J. Chem. Soc. Dalton Trans. **1972** 245/7).
[4] Bendtsen, J.; Nicolaisen, F. M. (J. Mol. Spectrosc. **125** [1987] 14/23).
[5] Bendtsen, J.; Winnewisser, M. (Chem. Phys. **40** [1979] 359/65).
[6] Bendtsen, J.; Winnewisser, M. (Chem. Phys. Lett. **33** [1975] 141/5).
[7] Gerry, M. C. L.; Heineking, N.; Maeder, H.; Dreizler, H. (Z. Naturforsch. **44a** [1989] 1079/86).
[8] Bendtsen, J.; Nicolaisen, F. M. (J. Mol. Spectrosc. **119** [1986] 456/66).
[9] Kewley, R.; Sastry, K. V. L. N.; Winnewisser, M. (J. Mol. Spectrosc. **12** [1964] 387/401).
[10] Winnewisser, M.; Cook, R. L. (J. Chem. Phys. **41** [1964] 999/1004).

[11] Rogers, J. D.; Williams, D. (Phys. Rev. [2] **82** [1951] 131).
[12] Amble, E.; Dailey, B. P. (J. Chem. Phys. **18** [1950] 1422).
[13] Dows, D. A.; Pimentel, G. C. (J. Chem. Phys. **23** [1955] 1258/63).
[14] Nelson, J. (Spectrochim. Acta A **26** [1970] 235/47).
[15] Bendtsen, J.; Nicolaisen, F. M. (J. Mol. Spectrosc. **133** [1989] 193/200).
[16] Cheung, A. S.-C.; Merer, A. J. (J. Mol. Spectrosc. **127** [1988] 509/26).
[17] Bendtsen, J.; Nicolaisen, F. M. (J. Mol. Spectrosc. **152** [1992] 101/8).
[18] Hegelund, F.; Bendtsen, J. (J. Mol. Spectrosc. **124** [1987] 306/16).
[19] Bendtsen, J.; Hegelund, F.; Nicolaisen, F. M. (J. Mol. Spectrosc. **118** [1986] 121/31).
[20] Yamada, K.; Takami, M. (J. Mol. Spectrosc. **84** [1980] 431/46).

[21] Bendtsen, J. (J. Raman Spectrosc. **9** [1980] 162/5).
[22] Bendtsen, J. (J. Raman Spectrosc. **6** [1977] 306/13).
[23] Bendtsen, J. (Proc. 5th Int. Conf. Raman Spectrosc., Freiburg i. Br., FRG, 1976, pp. 410/1; C.A. **87** [1977] No. 191470).
[24] Krakow, B.; Lord, R. C.; Neely, G. O. (J. Mol. Spectrosc. **27** [1968] 148/76).
[25] Levine, D. M.; Dows, D. A. (J. Chem. Phys. **46** [1967] 1168/72).
[26] Moore, C. B.; Rosengren, K. (J. Chem. Phys. **44** [1966] 4108/15).
[27] Becker, E. D.; Pimentel, G. C. (J. Chem. Phys. **25** [1956] 224/8).
[28] Pimentel, G. C.; Charles, S. W.; Rosengren, K. (J. Chem. Phys. **44** [1966] 3029/33).
[29] Bendtsen, J.; Hegelund, F.; Nicolaisen, F. M. (J. Mol. Spectrosc. **128** [1988] 309/20).
[30] Bendtsen, J.; Guelachvili, G. (J. Mol. Spectrosc. **107** [1984] 385/94).

[31] Bendtsen, J. (J. Raman Spectrosc. **15** [1984] 113/9).
[32] Bendtsen, J.; Nicolaisen, F. M. (J. Mol. Spectrosc. **145** [1991] 123/9).

[33] Carlotti, M.; Di Lonardo, G.; Galloni, G.; Trombetti, A. (Trans. Faraday Soc. **67** [1971] 2852/61).

[34] Foy, B. R.; Casassa, M. P.; Stephenson, J. C.; King, D. S. (J. Chem. Phys. **90** [1989] 7037/45).

[35] Foy, B. R.; Casassa, M. P.; Stephenson, J. C.; King, D. S. (J. Chem. Phys. **92** [1990] 2782/9).

[36] Casassa, M. P.; Foy, B. R.; Stephenson, J. C.; King, D. S. (J. Chem. Phys. **94** [1991] 250/61).

[37] Foy, B. R.; Casassa, M. P.; Stephenson, J. C.; King, D. S. (AIP Conf. Proc. No. 191 [1989] 612/4; C.A. **111** [1989] No. 243197).

[38] McDonald, J. R.; Rabalais, J. W.; McGlynn, S. P. (J. Chem. Phys. **52** [1970] 1332/40).

[39] Papazian, H. A.; Margozzi, A. P. (J. Chem. Phys. **44** [1966] 843/4).

[40] Okabe, H. (J. Chem. Phys. **49** [1968] 2726/33).

[41] Fueno, T.; Fukuda, M.; Yokoyama, K. (Chem. Phys. **124** [1988] 265/72).

[42] Zaslonko, I. S.; Kogarko, S. M.; Mozzhukhin, E. V. (Kinet. Katal. **13** [1972] 829/35; Kinet. Catal. [Engl. Transl.] **13** [1972] 745/50).

[43] Kajimoto, O.; Yamamoto, T.; Fueno, T. (J. Phys. Chem. **83** [1979] 429/35).

[44] Baronavski, A. P.; Miller, R. G.; McDonald, J. R. (Chem. Phys. **30** [1978] 119/31).

[45] Templeton, J. C.; King, E. L. (J. Am. Chem. Soc. **93** [1971] 7160/6).

[46] Closson, W. D.; Gray, H. B. (J. Am. Chem. Soc. **85** [1963] 290/4).

[47] Meier, U.; Staemmler, V. (J. Phys. Chem. **95** [1991] 6111/7).

2.3.1.7 Mechanical and Thermal Properties

Density. Expansion Coefficient. The pycnometric density of pure, liquid HN_3 is 1.127 g/cm^3 at 290 K [1]. The density in the range t = 0 to 21 °C is described by $\varrho = 1.152/(1 + 0.0013\,t)$ [2, 3]. The density of gaseous HN_3 of 1.91 kg/m^3 (temperature not given) was estimated from the experimental densities of other inorganic substances [4].

Sound Velocity. A sound velocity of 1300 m/s in liquid HN_3 is cited in [5]. The sound velocity at 294 K in pure, gaseous HN_3 and HN_3-N_2 mixtures was given in [6] as follows:

speed in m/s.........	266	279	302	323
diluent N_2 in %.....	0	20	50	75

Viscosity. The viscosity of gaseous HN_3 of $\eta_{295} = 109$ µP was calculated from kinetic theory and agrees with the experimental value. The Lennard-Jones parameters $\sigma = 3.98$ Å and $\varepsilon/k = 355$ K were calculated from empirical relations [7].

Triple Point. Boiling Point. The triple point temperature of HN_3 is ~193 K, where the vapor pressure is ~1 Torr. The normal boiling point of 308.9 K was extrapolated from the vapor pressure curve [3].

Heats of Transition. An enthalpy of melting of 6.0 kJ/mol was estimated for HN_3 by comparison with the data of other inorganic substances [4]. The experimental heat of evaporation is 30.5 kJ/mol at 286.6 K and yields a Trouton constant of 92 $J \cdot mol^{-1} \cdot K^{-1}$ indicative of an unassociated liquid [3].

Vapor Pressure. The vapor pressure of HN_3 between 273 and ~195 K is described by $\log(p/Torr) = 6.8426 - 1302.1/T + 0.0567 \log T$. The temperature range between 273 K and the boiling point requires slightly different constants: $\log(p/Torr) = 7.8533 - 1578.3/T + 0.0567 \log T$ [3].

References:

[1] Kurbangalina, R. Kh.; Patskov, E. A.; Stesik, L. N.; Yakovleva, G. S. (PMTF Zh. Prikl. Mekh. Tekh. Fiz. **1970** No. 4, pp. 160/5; J. Appl. Mech. Tech. Phys. [Engl. Transl.] **1970** 672/7).

[2] Kurbangalina, R. Kh.; Yakovleva, G. S. (Zh. Fiz. Khim. **43** [1969] 2649/50; Russ. J. Phys. Chem. [Engl. Transl.] **43** [1969] 1490/1).

[3] Günther, P.; Meyer, R.; Müller-Skjold, F. (Z. Phys. Chem. A **175** [1935] 154/69).

[4] Kafarov, V. V.; Dorokhov, I. N.; Vetokhin, V. N.; Volkov, L. P. (Dokl. Akad. Nauk SSSR **292** [1987] 663/6; Dokl. Phys. Chem. [Engl.Transl.] **292/297** [1987] 97/9).

[5] Yakovleva, G. S.; Kurbangalina, R. Kh. (Detonatsiya Mater. 6th Vses. Simp. Goreniyu Vzryvu, Alma-Ata 1980, pp. 56/60; C.A. **95** [1981] No. 100042).

[6] Hajal, I.; Combourieu, J.; Guenebaut, H. (J. Chim. Phys. Phys.-Chim. Biol. **57** [1960] 941/6).

[7] Hajal, I.; Combourieu, J. (J. Chim. Phys. Phys.-Chim. Biol. **63** [1966] 899/905).

2.3.1.8 Thermodynamic Data of Formation. Heat Capacity. Thermodynamic Functions

The experimental enthalpies of formation are 296.6±2.1 kJ/mol for gaseous HN_3 and 263.6±2.9 kJ/mol for the liquid at or slightly below ambient temperature and at constant pressure. The data were obtained from the heat of explosion [1]. Thermodynamic data of formation of gaseous and liquid HN_3 and of a 1 M aqueous solution are summarized in Table 15.

Table 15
Thermodynamic Data of Formation for HN_3 at 1 bar.

state	temperature	Δ_fG° in kJ/mol	Δ_fH° in kJ/mol	ΔS° in $J\cdot K^{-1}\cdot mol^{-1}$	Ref.
gas	0 K	–	300.290	–	[2]
		–	300.49	–	[3]
	298 K	332.13	299.83	−115.5	[4]
		327.6	292.9	−113.68	[5]
		328.1	294.1	–	[3]
		–	294.000	–	[2]
liquid	298 K	331.12	269.32	−214.35	[4]
		327.3	264.0	–	[3]
aqueous solution	298 K	321.8	260.08	–	[3]
		321.3	259.12	−207.1	[5]

A value of $\Delta_fH^\circ = 259.12 \pm 0.8$ kJ/mol for the formation of undissociated HN_3 in aqueous solution at infinite dilution was also calculated from the measured enthalpy of HN_3 dissociation [4].

Standard entropies of liquid HN_3 at 298 K were calculated from thermodynamic data to be 140.6 [3] and 138.16 $J\cdot K^{-1}\cdot mol^{-1}$ [4]; a value of 146.0 $J\cdot K^{-1}\cdot mol^{-1}$ was given for a 1 M aqueous solution [3]. Values of ΔG° were calculated from vapor pressure measurements of HN_3 over aqueous solutions. Results for HN_3 at 1 atm and in a 1 M solution are [5]:

T in K	273.16	297.58	309.11	322.62
ΔG° in kJ/mol	−8.58(21)	−6.15(13)	−5.02(8)	−3.93(13)

Thermodynamic data of HN_3 in the ideal gas state are given in Table 16. Similar calculations in [6] are based on earlier published vibrational frequencies and structural parameters taken from microwave spectra.

Table 16
Thermodynamic Functions of HN_3 in the Ideal Gas State at 1 atm Pressure [2].

T in K	$-(G^\circ - H^\circ_0)/T$ in $J\cdot K^{-1}\cdot mol^{-1}$	$H^\circ - H^\circ_0$ in kJ/mol	S° in $J\cdot K^{-1}\cdot mol^{-1}$	C°_p in $J\cdot K^{-1}\cdot mol^{-1}$
100	165.001	3.329	198.294	33.608
200	188.340	6.893	222.804	38.338
298.16	202.502	10.948	239.222	44.224
500	222.708	20.927	264.562	54.077
1000	255.033	51.851	306.884	67.825
1500	277.384	87.607	335.789	74.455
2000	294.839	125.794	357.736	77.950
3000	321.520	205.654	390.072	81.2833
4500	350.293	329.443	423.500	83.501
6000	371.759	455.7791	447.724	84.924

The thermodynamic values $H^\circ - H^\circ_0 = 10.874$ kJ/mol, $S^\circ = 238.97\ J\cdot K^{-1}\cdot mol^{-1}$, and $C^\circ_p = 43.68\ J\cdot K^{-1}\cdot mol^{-1}$ were reported for gaseous HN_3 at 298.15 K in [3], $S^\circ = 237.40\ J\cdot K^{-1}\cdot mol^{-1}$ in [4].

References:

[1] Günther, P.; Meyer, R.; Müller-Skjold, F. (Z. Phys. Chem. A **175** [1935] 154/69).

[2] Glushko, V. P.; Gurvich, L. V.; Bergman, G. A.; et al. (Thermodynamic Properties of Individual Substances, Vol. 1, Book 2, Nauka, Moscow 1978, p. 235).

[3] Wagman, D. D.; Evans, W. H.; Parker, V. B.; et al. (J. Phys. Chem. Ref. Data **11** [1982] 2/65; NBS-TN-270-3 [1968] 63).

[4] Gray, P.; Waddington, T. C. (Proc. R. Soc. London A **235** [1956] 106/19).

[5] D'Orazio, L. A.; Wood, R. H. (J. Phys. Chem. **67** [1963] 1435/8).

[6] Dows, D. A.; Pimentel, G. C. (J. Chem. Phys. **23** [1955] 1258/63).

2.3.1.9 Standard Potentials. Electrochemical Behavior

Standard potentials for the following reactions of HN_3 in aqueous solutions at 298 K were calculated from thermodynamic data:

reaction	E° in V	Ref.
$HN_3(g) \rightarrow 3/2\ N_2 + H^+ + e^-$	−3.40	[3]
$HN_3(aq) \rightarrow 3/2\ N_2 + H^+ + e^-$	−3.09	[3]
$HN_3 + 2\ H^+ + 2\ e^- \rightarrow 3\ NH$	0.64	[2]
$HN_3 + 3\ H^+ + 2\ e^- \rightarrow NH_4^+ + N_2$	1.96	[1]
$HN_3 + 5\ H^+ + 2\ e^- + 3\ H_2O \rightarrow 3\ NH_3OH^+$	−1.26	[2]
$HN_3 + 11\ H^+ + 8\ e^- \rightarrow 3\ NH_4^+$	0.69	[1, 2]
$2\ HN_3 + 13\ H^+ + 10\ e^- \rightarrow 3\ N_2H_5^+$	0.34	[2]

The standard potential for the decomposition of HN_3 has temperature coefficients of $dE°/dT = -1.193$ mV/K [3] and $d^2E°/dT^2 = -0.562$ μV/K^2 [4] for gaseous HN_3 and $dE°/dT = -1.57$ mV/K for aquated HN_3 [3]. The first and second temperature coefficients were calculated from the entropy and molal heat capacity, and they can be applied to the design of fuel cells. A standard potential of $E° = -3.334$ V with $dE°/dT = -2.141$ mV/K was calculated for the N_2(g), H^+/HN_3 couple at 298.15 K and pH 0.000 [5].

The electrochemical reduction of HN_3 can be described by $HN_3 + 6\,H^+ + 6\,e^- \rightarrow N_2H_4 + NH_3$ when carried out in an aqueous azide solution with a glassy carbon electrode pretreated with an $[Mo_2Fe_6S_8(SC_6H_5)_9]^{3-}$ solution in CH_3CN. The rate of N_2H_4 formation increases as the pH is lowered from 10 to 5; a mechanism involving the reduction of coordinated HN_3 is proposed [6].

The polarographic reduction of HN_3 in aqueous solution at 298 K is described by $4\,HN_3 + 3\,e^- \rightarrow 3/4\,NH_4^+ + 1/2\,H_2 + 15/4\,N_3^-$ based on the charge transfer to the mercury working cathode and the composition of the products. The stepwise, catalytic reduction in the presence of Co^{II} ions was also investigated, and a mechanism was proposed [7]. In acidified solutions the half-wave potential of HN_3 initially decreased linearly with increasing concentration of H_2SO_4 from -1.2 V in 8 M solution to a limiting value of about -0.75 V which was reached in a 12.8 M solution. The polarographic wave is diffusion-controlled in the experimental concentration range and is suitable for analytical purposes. The single-electron reduction of HN_3 is completely irreversible as N_2 is set free. N_2H_4 is expected to be the second product. The shift of the half-wave potential to positive values in increasingly acidic solutions may indicate initial formation of $H_2N_3^+$ [8]. The polarographic oxidation wave of HN_3 in an acidic solution containing Ru^{IV} ions was observed at -1.00 V [9].

References:

[1] Latimer, W. M. (The Oxidation States of the Elements and Their Potentials in Aqueous Solution, Prentice-Hall, Englewood Cliffs 1961, p. 102).
[2] Gladyshev, V. P.; Syroeshkina, T. V.; Raimzhanova, M. M. (Zh. Fiz. Khim. **55** [1981] 2126/9; Russ. J. Phys. Chem. [Engl. Transl.] **55** [1981] 1205/7).
[3] deBethune, A. J.; Licht, T. S.; Swendeman, N. (J. Electrochem. Soc. **106** [1959] 616/25).
[4] Salvi, G. R.; deBethune, A. J. (J. Electrochem. Soc. **108** [1961] 672/6).
[5] Bratsch, S. G. (J. Phys. Chem. Ref. Data **18** [1989] 1/21).
[6] Tanaka, K.; Kuwabata, S.; Denno, S.; Tanaka, T. (Bull. Chem. Soc. Jpn. **62** [1989] 1561/6).
[7] Tokoro, R.; Neves, E. A. (J. Electroanal. Chem. Interfacial Electrochem. **125** [1981] 115/28).
[8] Masek, J. (Collect. Czech. Chem. Commun. **25** [1960] 3137/42).
[9] Tokoro, R.; de Oliveira Neto, G. (An. 2nd Simp. Bras. Eletroquim. Eletroanal., Sao Paulo 1980, pp. 93/104; C.A. **95** [1981] No. 227952).

2.3.1.10 Chemical Behavior

2.3.1.10.1 Decomposition

The unimolecular decomposition of gaseous HN_3 at low pressures can be expected to start with a scission of either the H-NNN or HN-NN bond. Experiments show that the initial formation of NH and N_2 is favored. The reaction enthalpies are 60 to 75 kJ/mol for the dissociation into N_2(X) and NH(X) and about 385 kJ/mol for the dissociation into N_3 and H; see pp. 107/8. HF calculations of the potential energy surfaces employing a 6-31G** basis set predicted that the reaction yielding N_2 and NH prevails because of its low activation energy. A barrier of dissociation of $E_a = 150$ to 180 kJ/mol was obtained in experimental and theoretical studies; see below and p. 126.

The bimolecular decomposition $2\ HN_3 \rightarrow H_2 + 3\ N_2$ occurs at the high pressures encountered in explosions. An HF/6-31G calculation predicted an activation energy of 192 kJ/mol. The enthalpy of reaction is about −600 kJ/mol; see below. The most favorable potential energy surface of the reaction indicates a mutual approach of two HN_3 molecules by the H-bonded N atoms leading to 2 N_2 and N_2H_2 as initial products.

Reference:

Haskins, P. J.; Cook, M. D. (Proc. Symp. Explos. Pyrotech. **13** [1986] II-1/II-6; C.A. **109** [1988] No. 112938).

2.3.1.10.1.1 Nonphotolytic Decomposition

The nonphotolytic decomposition of gaseous HN_3 can be induced by heat, either applied directly or via a shock wave, by sparking, by Tesla coil discharges, by glow discharges (see the following paragraphs for references), or by high-voltage electric pulses [1]. A microwave discharge leaves HN_3 unchanged [2]. Stable products result from the reactions

$$2\ HN_3(g) \rightarrow H_2 + 3\ N_2 \text{ with } \Delta_rH = -594 \text{ kJ/mol and}$$
$$3\ HN_3(g) \rightarrow NH_3 + 4\ N_2 \text{ with } \Delta_rH = -942 \text{ kJ/mol}$$

The enthalpies were calculated from thermodynamic data [3]; an enthalpy for the first reaction of −603 kJ/mol results from an MP2/6-31G(d, p) calculation [4]. The spark-induced explosion of hydrogen azide does not yield ammonia [5]; the products were identified to be N_2 and H_2 [6, 7]. The decomposition in a flame [8] and the thermolysis of gaseous HN_3 at >1000 K by shock waves mainly follow the first reaction, but the second one becomes more noticeable with increasing concentration of added diluents [5, 9] and with decreasing temperature of decomposition [10]. However, the yield of NH_3 is always less than 33% with respect to the initial quantity of HN_3 in the used gas mixtures [5]. An early mass-spectrometric investigation of the thermolysis of HN_3 at 538 to 598 K showed NH_3 and N_2 to be the exclusive products; intermediates were not found [11]. Small amounts of H_2 were formed during thermolysis at 620 K [12]. Upon passing a Tesla coil discharge through HN_3 at 0.2 Torr or less, the decomposition products N_2, NH_3 [13], and H_2 were identified with a mass spectrometer. The yield of H_2 exceeded that of NH_3 [14].

Thermolysis. Kinetic investigations of the thermolysis require dilution of HN_3 by Ar in order to suppress possible contributions of the rapid and complex subsequent reactions [15]. The decrease of the induction period of the reaction with increasing temperature is more noticeable for mixtures at higher HN_3 concentrations. Above 1250 K the induction period becomes short relative to the half-time of the reaction [10]. The decomposition is first order in both HN_3 and Ar [15]. The results of shock-wave experiments are as follows:

temperature in K	rate constant in $cm^3 \cdot mol^{-1} \cdot s^{-1}$	HN_3 concentration	Ref.
1200 to 1350	$7.6 \times 10^{14} \exp(-18200/T)$	<0.5 mol%	[15]
1250 to 1400	$5.5 \times 10^{13} \exp(-14000/T)$	0.5 mol%	[10]
>1400	$2.2 \times 10^{12} \exp(-9750/T)$	0.5 mol%	[10]

The rate constants at 1250 to 1400 K in [10] agree with the earlier data in [15]. The larger rate constants found for mixtures containing 2% HN_3 can be attributed to the effect of the exothermicity of the reaction on the heated gases, which also explains the differences between the results of [10] and [16]. The activation energy of ~150 kJ/mol indicates a spin-forbidden decomposition to N_2 and $NH(^3\Sigma)$ as does the small preexponential factor which predicts the probability of the singlet-to-triplet transition to be in the range 10^{-2} to 10^{-3} [15]. A larger value of the activation energy was found at higher temperatures; this probably indicates that the decomposition at higher temperatures takes place from a vibrational nonequilibrium state (see also below), because the time intervals required for relaxation and decomposition then become similar [10]. The first-order reaction, determined in early investigations of the decomposition of diluted HN_3 by shock waves [16, 17] and discussed theoretically in [18], is probably due to insufficient dilution [15]. The diluents He, Ar, and N_2 lead to different first-order decomposition rates [19]. Lower activation energies were observed upon decreasing the initial total pressures of mixtures of 5.4 mol% HN_3 in Ar [20].

The thermal decomposition of pure HN_3 at 538 to 598 K is first order with $k(s^{-1}) = 44.5 \times 10^8 \exp(-130\ kJ \cdot mol^{-1}/RT)$; the supposed reaction chain is not interrupted by added NO. The large entropy of activation of $-109\ J \cdot mol^{-1} \cdot K^{-1}$ indicates a decomposition on the glass surface of the reaction vessel [11]. The decomposition of HN_3 after injection into a vessel heated to 820 to 970 K follows first-order kinetics with a rate constant of $k(s^{-1}) = 10^{12} \exp(-172\ kJ \cdot mol^{-1}/RT)$ [21].

The emissions from the intermediates $NH(^1\Pi \rightarrow {}^1\Delta)$, $NH(^3\Pi \rightarrow {}^3\Sigma)$, NH_2, N_3, and $N_2(^1\Pi \rightarrow {}^3\Sigma)$ were observed in the given sequence upon thermolysis in a shock wave. The following mechanism with the most likely reactions and $\Delta_rH^\circ_{298}$ in kJ/mol was deduced [10]:

$HN_3 + Ar \rightarrow NH(^1\Delta) + N_2 + Ar$	224
$HN_3 + NH(^1\Delta) \rightarrow 2\ NH(^3\Sigma^-) + N_2$	−78
$HN_3 + NH(^3\Sigma^-) \rightarrow NH_2 + N_3$	−71
$HN_3 + NH_2 \rightarrow NH_3 + N_3$	−
$2\ N_3 \rightarrow 3\ N_2$	−835

The decomposition is probably accelerated by the transfer of energy to the vibration ν_2 of HN_3 from vibrationally excited $N_2(v)$ which forms via $HN_3 + NH \rightarrow N_2 + N_2(v) + H_2$. This reaction takes the observed excess in the emission of ν_2 of HN_3 from the Boltzmann distribution at temperatures exceeding 1000 K into account [10, 20, 22]. The maximum excess of the vibrational energy of ν_2 over the temperature reaches 500 to 800 K at about the half-conversion point [23]; this was discussed theoretically in [24]. The excitation autoaccelerates the decomposition reaction, whereas due to the nonequilibrium character of the reaction the maximum heat release is found at ~90% HN_3 conversion by observing the density gradient behind the shock wave [25, 26].

The $^3\Pi \rightarrow {}^3\Sigma$ emissions of excited NH [27, 28] and ND [27 to 29] after thermolysis in a shock wave were reported in earlier papers. The emission from NH_2 is weak [27, 28]. The fluorescence of the $^2A_1 \rightarrow {}^2B_1$ transition demonstrates the intermediate formation of electronically excited NH_2 during thermolysis at 620 K [12]; additional experimental results and theoretical considerations are described in [30].

Ionization during decomposition of HN_3 (0.5 to 3.2%) in He by a shock wave reaches a maximum yield of $\sim 7.3 \times 10^{-6}$ electrons per HN_3 molecule at 2060 K. The yield in Ar reaches only ~40% of that in He. The maximum electron concentration is reached earlier than the maximum NH concentration. The activation energy of the ionization process decreases from ~188 kJ/mol at 1200 K to ~134 kJ/mol in the temperature range 1750 to 2100 K for both diluents, but the absolute rate in Ar is about one order of magnitude smaller.

The activation energy for the reaction yielding NH shows a similar decrease from ~100 to ~46 kJ/mol. The ionization is supposed to occur in collisions of the vibrationally excited minor product N_2H_2 with the diluent gas with different rates for He and Ar [31]. Preliminary observations are described in [32].

A mass-spectrometric investigation of laminar flames of HN_3 in noble gases allowed the identification of the intermediates NH and NH_2 [33] and of N_3 [8]. The suspected formation of N_2H_2 in small amounts [14] was confirmed mass-spectrometrically in hf discharge experiments on mixtures of HN_3 and DN_3 [13]. The identification of NH and N_3 did not succeed in this case [14]. The explosion of HN_3 (DN_3) after sparking was accompanied by emissions in the UV-visible range from $^1\Pi$-$^1\Delta$ and $^3\Pi$-$^3\Sigma$ transitions in NH and ND and from electronically excited N_2. The weak emissions from NH_2, NHD, and ND_2 were assumed to result from a chain mechanism [6, 7]; see also [34, 35].

Incomplete Decomposition. Partial decomposition of HN_3 is achieved by passing the gas typically at a pressure of 0.5 Torr or less through a glow discharge, a furnace heated to ~1270 K [36, 37], or a Tesla coil discharge [38]. The reaction proceeds via $6\ HN_3 \rightarrow 7\ N_2 + H_2 + NH_4N_3$ (or $NH_3 + HN_3$) [36]. The yields of N_2, H_2, and NH_3 increase and those of NH_4N_3 decrease with increasing length of the furnace [39]. Cooling the exit gas to 77 K after allowing sufficient time for the reaction yielded colorless NH_4N_3 containing HN_3 [40] and a trace of $N_2H_5N_3$ [41, 42]. Appreciable amounts of $N_2H_5N_3$ were also found in the warm-up product from UV-irradiated, frozen HN_3 [43]. Fast condensation of partly decomposed HN_3 yielded a blue, low-temperature glass [36, 39, 43]. A blue product consisting principally of NH_4N_3 also formed upon UV photolysis of condensed HN_3 [36, 40, 44, 45] with liberation of N_2 [46]. A Tesla coil discharge on glassy, slowly condensed (at 77 K) HN_3 did not produce a colored sample, whereas a blue spot appeared on crystalline HN_3. Two separate spots were obtained when the discharge was applied in a magnetic field. The difference in the intensity of their colors increased with the field strength, indicating that the color results from bombardment with charged particles formed from the residual gas during the discharge [2, 47].

The origin of the blue color of the product resulting from fast condensation is not known and without noticeable influence on the product composition [41]. The UV-visible spectrum of the blue solid contains an absorption at 650 nm (originally assigned to N_2H_2 [36] or to NH_2 [40]), an absorption at 350 nm (assigned to NH [36, 40]), and an unassigned band at 228 nm in UV-irradiated solid HN_3 [48]. Only the first band was found in samples generated by thermolysis [36]. IR bands were assigned tentatively to polyazenes in [46]. The blue solid resulting from a 253.6-nm irradiation of frozen HN_3 or from condensation after subjecting gaseous HN_3 at 0.2 Torr to an electric discharge or to thermolysis at ~1220 K exhibit a single ESR line at $g = 2.003 \pm 0.002$ which could not be assigned [49]. Decomposition of HN_3 in Tesla coil discharges and freezing the products at 77 K in the presence of the matrix gases Xe, CO_2, or H_2O demonstrate that the blue color cannot originate from NH radicals, because it disappears at the same temperature for all matrix materials. Crystal defects in NH_4N_3 can also be excluded, because the color is observed in matrix-isolated, diluted samples [38]. The blue color was also attributed tentatively to N_3H_3 in analogy to the color of O_3; see for example [41].

Warming results in color loss at ~146 [43] to ~150 K for thicker samples and at ~125 K for thin deposits [36] without drastic chemical changes and with crystallization of NH_4N_3 after slow transitions through several solid phases. The crystallization seems closely reminiscent of a devitrification process [43]. Only the liberation of some H_2 and N_2 [46] in less than 0.2% of the total trapped material at the temperature of the color change can be attributed to a reaction and indicates that the products already form nearly all in the gas phase. The composition of the gas before condensation at 77 K and the gas resulting from evaporation of the condensed solid are identical [14]. The product formation in the gas phase is also consistent with the constant composition of the product in spite of the fact that the time elapsed before condensation varied [41].

Detonation. In a 100-cm^3 vessel gaseous HN_3 has a lower explosion limit of 4.5 ± 0.5 Torr at ambient temperature. The explosion is accompanied by a bright yellow flame [50]. An explosion limit of 3.88 ± 0.12 Torr at 295 K was determined in a more recent investigation [51]. The explosion limits of DN_3 and HN_3 are identical. The limiting pressure is hardly influenced by increasing the volume to 500 cm^3, by increasing the temperature to about 330 K, and by the position of the electrodes used for sparking [52]. A continuous decrease of the explosion limit with increasing intensity of the spark pulse was found at low sparking intensities and levels off at higher intensites [53]. The explosion limit in tubes increases with decreasing diameter [54].

The explosion of gaseous HN_3 (25 Torr) upon contact with a heated vessel requires a minimum temperature of 560 K. Even at 570 K the induction period lasts for several minutes and decreases with increasing temperature to fractions of a second. The explosion limit decreases from 23 Torr at 820 K to a minimum of 5 Torr at 1000 K, increases to 14 Torr at 1050 K, and then decreases to 10 Torr at 1100 K. The maximum indicates that the decomposition mechanism of HN_3 changes with temperature and shows the increasing role of a branching reaction [21]. The explosion limit of HN_3 in a heated vessel with different surface to volume ratios drops exponentially from ~40 Torr at 720 K to ~5 Torr at 910 K. The lower decomposition limit with luminescence decreases from ~5 Torr at 720 K to ~3 Torr at 870 K. The decomposition at lower pressures is slow and proceeds without light emission [55]. A kinetic investigation using $p(HN_3) \leq 0.15$ Torr found 538 K to be sufficient for decomposition [11].

The detonation speed of gaseous HN_3 increases from 2550 m/s at 4 Torr about linearly to 2774 m/s at ~10 Torr. The speed levels off at higher pressures [51] and reaches 2802 m/s at 100.0 Torr [56]; see also [57]. The detonation speed in tubes decreases with the tube diameter at constant pressure [58]. Gradients of pressure [54, 59] and temperature [54] behind the detonation wave in tubes were investigated. The spatial speed of deflagration of gaseous HN_3 increases with pressure and was measured after electric sparking in a constant-volume bomb. Experimental values at room temperature are as follows [60]:

pressure in Torr	5.6	8.5	10	11.8	25.0
speed of deflagration in m/s	178	188[a]	196[b]	202	214

[a] From [61]. — [b] From [62].

The flame characteristics of HN_3 in burners were measured. The ratio of the fundamental burning velocities of HN_3 and DN_3 is 1.13 and seems to preclude a decisive role of H and D radicals in the decomposition [57].

Gaseous elements and inorganic compounds (see the next paragraphs for examples) act as inert inhibitors in the explosion of HN_3; organic diluents lead to additional side reactions, which are described on p. 149. The explosion limit of HN_3 shifts to higher pressures when the diluent gas pressure is increased at moderate temperatures. The individual hyperbolic curves at low total pressures become linear at higher total pressures [9]. Changing the temperature between 288 and 373 K had only a small effect on the lower explosion limit [63].

An extrapolation indicated that HN_3 at a partial pressure of 1/7 atm should be stable in H_2 at normal pressures and temperatures [6, 50]. The effects of CO_2 [63] or He [9] are similar to that of H_2. The strong inhibiting effect of H_2 or He was attributed to their high temperature conductivity [5]. Stable mixtures with N_2 [6], HCl, and HBr [62] contain only about half as much HN_3 as a stable HN_3-H_2 mixture. Similar results were found for Ar at ambient temperature [6]. However, adding increasing amounts of Ar to HN_3 at constant temperatures between 768 and 903 K decreases the explosion limit of HN_3 [21]. Experimental explosion limits at ambient temperature were given for mixtures with He [5, 9, 51, 64], Ar [5, 6, 9, 50, 51, 63, 64], H_2 [5, 6, 50, 51, 64], N_2 [5, 6, 9, 50, 51, 63, 64], Cl_2 and Br_2, HF and HCl [5, 9, 64], CO_2 [5, 9, 63, 64], and NF_3 [9]. Hydrocarbons inhibit the decomposition of HN_3 more effectively than inorganic compounds and elements [5, 64]. The stabilizing effect increases with the chain length of alkanes and the length of the side chain of arenes [63]. Experimental results are given in the cited literature and also in [65, 66].

Experimental detonation speeds of mixtures of HN_3 with He, Ar, and N_2 are given in [51]. Equimolar mixtures of HN_3 and H_2 or He detonate with a higher velocity than pure HN_3 at the same pressure, whereas the detonation speed decreases with the amount of N_2 or Ar added [56]. Experimental deflagration velocities in HN_3-N_2 mixtures in tubes [61] and spherical vessels [60] were determined. The inhibiting effect of monohalogenated methanes was measured in [62] and assigned to their reaction with the radicals formed; inhibition by HCl, HBr, CCl_4, and CH_2Br_2 was also investigated. The flame characteristics of HN_3 diluted with N_2 were determined and were used to kinetically estimate the decomposition in [57]. Similar investigations on HN_3-He and HN_3-Ar mixtures are described in [67]. Explosion parameters of HN_3 and its mixtures with gaseous diluents are given in [68, 69].

The detonation speed of pure, liquid HN_3 and its aqueous solutions were measured after initiation by a detonator cap [70]. The resulting shock wave causes a retarded adiabatic, secondary explosion of the compression-heated liquid. The induction period of the explosion decreases with increasing pressure of the initiating shock wave [71]. The brightness and color methods gave a detonation temperature of 4700 K for pure HN_3. The detonation pressure at the (Chapman-Jouget) point of a stable explosion was measured to be 166 kbar. Explosions in the high-velocity range of solutions with less than 80% of HN_3 required an additional detonator. The limit of the high-speed detonation range is appreciably below 54%. Experimental speeds are as follows [70]:

concentration of HN_3 in %	100	88.2	78.4	68.6	58.8	53.9
speed of detonation in m/s	7570(20)	7390(30)	7070(70)	6630(20)	6340(120)	5900(55)

Preliminary detonation speeds are given in [72]. Earlier published detonation velocities in this concentration range [73] are inaccurate [70]. Explosion parameters for liquid HN_3 were calculated in [74, 75].

Deflagration parameters were measured on solutions with less than 80% of HN_3 in the absence of an additional detonator to be:

HN_3 concentration in %	77.4	68.6	63.7	58.8	65	61	54	48	38	16.7
deflagration rate in m/s	2750	2330	2150	1940	1700	630	233	40	2.5	0.14
Ref.	[70]				[73]					

The critical diameter for detonating pure, liquid HN_3 at ambient temperature is 0.08 mm based on experiments in capillary tubes. A further decrease of the diameter first leads to deflagration and then prevents decomposition [76].

References:

[1] Dzhidzhoev, M. S.; Pimenov, M. I.; Platonenko, V. G.; Filippov, Yu. V.; Khokhlov, R. V. (Zh. Eksp. Teor. Fiz. **57** [1969] 411/20; Sov. Phys.-JETP [Engl. Transl.] **30** [1970] 225/9).
[2] Papazian, H. A. (J. Chem. Phys. **27** [1957] 813/4).
[3] Gray, P.; Waddington, T. C. (Proc. Roy. Soc. London A **235** [1956] 106/19).
[4] Otto, M.; Lotz, S. D.; Frenking, G. (Inorg. Chem. **31** [1992] 3647/55).
[5] Rozenberg, A. S.; Arsen'ev, Yu. N.; Voronkov, V. G. (Fiz. Goreniya Vzryva **6** [1970] 302/10; Combust. Explos. Shock Waves [Engl. Transl.] **6** [1970] 271/7).
[6] Guenebaut, H. (Bull. Soc. Chim. Fr. **1959** 962/1018).
[7] Pannetier, G.; Guenebaut, H.; Gaydon, A. G. (C. R. Hebd. Seances Acad. Sci. **240** [1955] 958/60).
[8] Dupré, G.; Paillard, C.; Combourieu, J. (Dyn. Mass Spectrom. **4** [1976] 233/45).
[9] Rozenberg, A. S.; Voronkov, V. G. (Zh. Fiz. Khim. **43** [1969] 2377/9; Russ. J. Phys. Chem. [Engl. Transl.] **43** [1969] 1333/5).
[10] Paillard, C.; Dupré, G.; Combourieu, J. (J. Chim. Phys. Phys.-Chim. Biol. **82** [1985] 489/97).

[11] Franklin, J. L.; Dibeler, V. H.; Morris, P. P., Jr. (J. Res. Natl. Bur. Stand. **61** [1958] 41/6).
[12] Pavlov, A. A.; Rozenberg, A. S. (Dokl. Akad. Nauk SSSR **227** [1976] 394/6; Dokl. Phys. Chem. [Engl. Transl.] **226/231** [1976] 257/9).
[13] Foner, S. N.; Hudson, R. L. (J. Chem. Phys. **28** [1958] 719/20).
[14] Franklin, J. L.; Herron, J. T.; Bradt, P.; Dibeler, V. H. (J. Am. Chem. Soc. **80** [1958] 6188/90).
[15] Kajimoto, O.; Yamamoto, T.; Fueno, T. (J. Phys. Chem. **83** [1979] 429/35).
[16] Zaslonko, I. S.; Kogarko, S. M.; Mozzhukhin, E. V. (Fiz. Goreniya Vzryva **9** [1973] 339/44; Combust. Explos. Shock Waves [Engl. Transl.] **9** [1973] 295/9).
[17] Zaslonko, I. S.; Kogarko, S. M.; Mozzhukhin, E. V. (Kinet. Katal. **13** [1972] 829/35; Kinet. Catal. [Engl. Transl.] **13** [1972] 745/50).
[18] Demin, A. I.; Zaslonko, I. S.; Kogarko, S. M.; Mozzhukhin, E. V. (Kinet. Katal. **14** [1973] 283/8; Kinet. Catal. [Engl. Transl.] **14** [1973] 238/42).
[19] Zaslonko, I. S.; Kogarko, S. M.; Mozzhukhin, E. V. (Fiz. Goreniya Vzryva **12** [1976] 4/8; Combust. Explos. Shock Waves [Engl. Transl.] **12** [1976] 2/5).
[20] Zaslonko, I. S.; Kogarko, S. M.; Mozzhukhin, E. V. (Dokl. Akad. Nauk **210** [1973] 1127/9; Dokl. Phys. Chem. [Engl. Transl.] **208/213** [1973] 478/80).

[21] Voronkov, V. G.; Pavlov, A. A.; Rozenberg, A. S. (Dokl. Akad. Nauk SSSR **210** [1973] 892/4; Dokl. Phys. Chem. [Engl. Transl.] **208/213** [1973] 455/7).
[22] Zaslonko, I. S.; Kogarko, S. M.; Mozzhukhin, E. V.; Demin, A. I. (Kinet. Katal. **14** [1973] 549/56; Kinet. Catal. [Engl. Transl.] **14** [1973] 472/8).
[23] Zaslonko, I. S.; Kogarko, S. M.; Mozzhukhin, E. V.; Demin, A. I. (Dokl. Akad. Nauk SSSR **202** [1972] 1121/4; Dokl. Phys. Chem. [Engl. Transl.] **202/207** [1972] 127/30).
[24] Zaslonko, I. S.; Kogarko, S. M.; Mozzhukhin, E. V. (Kinet. Katal. **13** [1972] 29/32; Kinet. Catal. [Engl. Transl.] **13** [1972] 23/5).
[25] Zaslonko, I. S.; Kogarko, S. M.; Mozzhukhin, E. V.; Mukoseev, Yu. K. (Kinet. Katal. **16** [1975] 1111/7; Kinet. Catal. [Engl. Transl.] **16** [1975] 967/71).
[26] Zaslonko, I. S.; Kogarko, S. M.; Mozzhukhin, E. V.; Mukoseev, Yu. K. (Fiz. Goreniya Vzryva **10** [1974] 623/34; Combust. Explos. Shock Waves [Engl. Transl.] **10** [1974] 541/52).
[27] Guenebaut, H.; Pannetier, G.; Goudmand, P. (Bull. Soc. Chim. Fr. **1962** 80/6).

[28] Guenebaut, H.; Pannetier, G.; Goudmand, P. (C. R. Hebd. Seances Acad. Sci. **251** [1960] 1166/8).

[29] Pannetier, G.; Goudmand, P.; Dessaux, O.; Guenebaut, H. (C. R. Hebd. Seances Acad. Sci. **256** [1963] 3082/5).

[30] Pavlov, A. A.; Rozenberg, A. S. (Dokl. Akad. Nauk SSSR **227** [1976] 1159/62; Dokl. Phys. Chem. [Engl. Transl.] **226/231** [1976] 352/5).

[31] Aravin, G. S.; Karasevich, Yu. K.; Vlasov, P. A. (Khim. Fiz. **1982** 1360/7).

[32] Aravin, G. S.; Karasevich, Yu. K.; Shumeiko, A. N. (Fiz. Goreniya Vzryva **13** [1977] 721/9; Combust. Explos. Shock Waves [Engl. Transl.] **13** [1977] 611/8).

[33] Paillard, C.; Dupré, G.; Combourieu, J. (Adv. Mass Spectrom. B **8** [1980] 1943/52).

[34] Pannetier, G. (C. R. Hebd. Seances Acad. Sci. **232** [1951] 817/8).

[35] Pannetier, G.; Gaydon, A. G. (J. Chim. Phys. Phys.-Chim. Biol. **48** [1951] 221/4).

[36] Rice, F. O.; Grelecki, C. (J. Am. Chem. Soc. **79** [1957] 1880/1).

[37] Rice, F. O.; Freamo, M. (J. Am. Chem. Soc. **75** [1953] 548/9).

[38] Clarke, J. W.; McTurk, G. (Nature **184** [1959] 2014/5).

[39] Rice, F. O.; Luckenbach, T. A. (J. Am. Chem. Soc. **82** [1960] 2681/2).

[40] Mador, I. L.; Williams, M. C. (J. Chem. Phys. **22** [1954] 1627/8).

[41] Wannagat, U.; Kohnen, H. (Z. Anorg. Allg. Chem. **304** [1960] 276/95).

[42] Wannagat, U.; Kohnen, H. (Angew. Chem. **69** [1957] 783).

[43] Bolz, L. H.; Mauer, F. A.; Peiser, H. S. (J. Chem. Phys. **30** [1959] 349/50).

[44] Rice, F. O.; Ingalls, R. B. (J. Am. Chem. Soc. **81** [1959] 1856/9).

[45] Becker, E. D.; Pimentel, G. C.; Van Thiel, M. (J. Chem. Phys. **26** [1957] 145/50).

[46] Papazian, H. A. (J. Chem. Phys. **32** [1960] 456/60).

[47] Papazian, H. A. (J. Chem. Phys. **29** [1958] 448/9).

[48] Papazian, H. A.; Margozzi, A. P. (J. Chem. Phys. **44** [1966] 843/4).

[49] Gager, W. B.; Rice, F. O. (J. Chem. Phys. **31** [1959] 564).

[50] Pannetier, G.; Lecamp, M. (Bull. Soc. Chim. Fr. **1954** 1068/70).

[51] Paillard, C.; Dupré, G.; Combourieu, J. (J. Chim. Phys. Phys.-Chim. Biol. **70** [1973] 811/8).

[52] Guenebaut, H. (Bull. Soc. Chim. Fr. **1959** 962/1018).

[53] Aizatullin, T. A.; Voronkov, V. G.; Zubov, V. P. (Dokl. Akad. Nauk SSSR **140** [1961] 1356/7; Dokl. Phys. Chem. [Engl. Transl.] **136/141** [1961] 784/5).

[54] Paillard, C.; Dupré, G.; Lisbet, R.; Combourieu, J.; Fokeev, V. P.; Gvozdeva, L. G. (Acta Astronaut. **6** [1979] 227/42).

[55] Gray, P.; Waddington, T. C. (Nature **179** [1957] 576/7).

[56] Hajal, I.; Combourieu, J. (C. R. Hebd. Seances Acad. Sci. **253** [1961] 2346/8).

[57] Laffitte, P.; Hajal, I.; Combourieu, J. (10th Symp. Combust., Cambridge 1964 [1965], pp. 79/85; C.A. **64** [1966] 3275).

[58] Paillard, C.; Dupré, G.; Lisbet, R.; Combourieu, J. (1st Colloq. Int. Berthelot-Vieille-Mallard-Le Chatelier Actes, Talence, Fr., 1981, Vol. 2, pp. 449/54; C.A. **98** [1983] No. 128711).

[59] Paillard, C.; Dupré, G.; Lisbet, R.; Combourieu, J.; Fokeev, V. P.; Gvozdeva, L. G.; Bazhenova, T. V. (Prog. Astronaut. Aeronaut. **75** [1981] 134/49).

[60] Hajal, I.; Combourieu, J.; Guenebaut, H. (J. Chim. Phys. Phys.-Chim. Biol. **57** [1960] 941/6).

[61] Hajal, I.; Combourieu, J.; Guenebaut, H. (C. R. Hebd. Seances Acad. Sci. **250** [1960] 1043/5).

[62] Le Bras, G.; Hajal, I.; Combourieu, J.; Laffitte, P. (J. Chim. Phys. Phys.-Chim. Biol. **64** [1967] 1153/60).

[63] Pannetier, G.; Mignotte, P.; Chevillon, M. (Bull. Soc. Chim. Fr. **1960** 804/7).

[64] Rozenberg, A. S. (Zh. Fiz. Khim. **45** [1971] 2212/5; Russ. J. Phys. Chem. [Engl. Transl.] **45** [1971] 1252/4).

[65] Rozenberg, A. S.; Arsen'ev, Yu. N.; Voronkov, V. G. (Zh. Fiz. Khim. **44** [1970] 2057/8; Russ. J. Phys. Chem. [Engl. Transl.] **44** [1970] 1165/6).

[66] Rozenberg, A. S.; Arsen'ev, Yu. N.; Voronkov, V. G. (Zh. Fiz. Khim. **46** [1972] 1447/51; Russ. J. Phys. Chem. [Engl. Transl.] **46** [1972] 833/6).

[67] Hajal, I.; Combourieu, J. (J. Chim. Phys. Phys.-Chim. Biol. **63** [1966] 899/905).

[68] Bazhenova, T. V.; Gvozdeva, L. G.; Fokeev, V. P.; Paillard, C.; Combourieu, J.; Dupré, G.; Lisbet, R. (Fiz. Goreniya Vzryva **21** [1985] 120/4; Combust. Explos. Shock Waves [Engl. Transl.] **21** [1985] 114/8).

[69] Hajal, I.; Combourieu, J. (C. R. Hebd. Seances Acad. Sci. **255** [1962] 509/11).

[70] Kurbangalina, R. Kh.; Patskov, E. A.; Stesik, L. N.; Yakovleva, G. S. (PMTF Zh. Prikl. Mekh. Tekh. Fiz. **1970** No. 4, 160/5; J. Appl. Mech. Tech. Phys. [Engl. Transl.] **1970** 672/7).

[71] Yakovleva, G. S.; Kurbangalina, R. Kh. (Detonatsiya Mater. 6th Vses. Simp. Goreniyu Vzryvu, Alma-Ata 1980, pp. 56/60; C.A. **95** [1981] No. 100042).

[72] Yakovleva, G. S.; Apin, A. Ya.; Kurbangalina, R. Kh.; Stesik, L. N. (Dokl. Akad. Nauk SSSR **156** [1964] 152/3; Dokl. Phys. Chem. [Engl. Transl.] **154/159** [1964] 472/3).

[73] Joyner, A. R. (in: Taylor, J.; Detonation in Condensed Explosives, Oxford University Press, London 1952, pp. 158/9).

[74] Pepekin, V. I. (Pol. J. Chem. **55** [1981] 1405/10).

[75] Pepekin, V. I.; Lebedev, Yu. A. (Dokl. Akad. Nauk SSSR **234** [1977] 1391/4; Dokl. Phys. Chem. [Engl. Transl.] **232/237** [1977] 630/3).

[76] Yakovleva, G. S.; Kurbangalina, R. Kh. (Fiz. Goreniya Vzryva **12** [1976] 774/5; Combust. Explos. Shock Waves [Engl. Transl.] **12** [1976] 692/3).

2.3.1.10.1.2 Photolysis

Infrared Photolysis. Photolysis of HN_3-DN_3 mixtures (20 to 50 Torr) by a CO_2 laser generates after an induction period of 1 to 2 μs an orange flash, which is indicative of a decomposition reaction and represents the intrinsic light emission from the explosion. This is followed by a stronger, thermally initiated light emission with a maximum at ~250 μs. The rotational temperature of added HCl (which inhibits the reaction) showed initial heating to ~600 K by the laser pulse and an explosion temperature exceeding 3000 K [1]. Nitrogen and NH or ND are the initial products, and H_2 and N_2 are the final ones [1, 2].

The photolysis of a jet-cooled mixture of $D^{15}NNN$ and $DNN^{15}N$ with the $P(18)$ line from a CO_2 laser yielded exclusively ^{15}ND; the $DNN^{15}N$ isotopomer did not react [2].

Infrared multiphoton dissociation (IRMPD) of HN_3 and DN_3 results from exposure to the 946 cm^{-1} $P(18)$ line of CO_2 laser pulses under collision-free conditions (0.035 Torr or less) [2, 3]. The laser light weakly interacts with the P branches of the $\nu_2-\nu_4$ hot band of HN_3 and strongly with the P branches of the ν_4 fundamental of DN_3 [3].

The reaction of DN_3 along its $\tilde{X}\,^1A'$ surface requires the absorption of ~18 IR photons and shows product state selectivity [2]. The overtone photodissociation of vibrationally excited XN_3 (X = H, D) under collisionless conditions proceeds via the reaction channels:

$XN_3(\tilde{X}\,^1A') \rightarrow NX(X\,^3\Sigma^-) + N_2(X\,^1\Sigma_g^+)$ (spin-forbidden) [2, 4], $\Delta H = 63$ kJ/mol [5]

$XN_3(\tilde{X}\,^1A') \rightarrow NX(a\,^1\Delta) + N_2(X\,^1\Sigma_g^+)$ (spin-allowed) [2, 6], $\Delta H = 213$ kJ/mol [5]

The ND products were probed by laser-induced fluorescence to determine initial product state distributions. The yields of both ND states were found to have the same order of magnitude. ND(X) forms selectively in the symmetric spin-rotation states F_1 and F_3. Less than 6% of ND(X) are obtained in the antisymmetric F_2 state. The ND(X) population of vibrational states is below 3%. The rotational states follow a Boltzmann distribution with temperatures of 920 ± 100 (F_1, F_3 states) and 500 ± 200 K (F_2 states) and have a total rotational energy of ~620 cm^{-1}. The kinetic energy of 6430 cm^{-1} is known from the Doppler profiles of ND(X). In the spin-forbidden channel, ~94% (10100 cm^{-1}) of the available energy appears as kinetic energy, indicating that all the energy of the exit channel barrier plus substantial energy above threshold is released into translation. The spin-allowed ND(a) exhibits a low channel propensity; the population of the symmetric, e-labeled Λ-doublet levels slightly exceeds the population of the antisymmetric, f-labeled levels. The population of vibrationally excited levels is below 2%. The rotational state distribution is characterized by a temperature of ~425 K. The Doppler profiles demonstrate that ~80% of the product energy are released as kinetic energy amounting to 930 cm^{-1} and suggests a small exit barrier in the spin-allowed channel [2].

The spin-forbidden decomposition of $HN_3(\tilde{X}\,^1A')$ with formation of NH(X $^3\Sigma^-$) probably is significant only near the threshold as indicated by an extended CI calculation of the spin-orbit effects in this reaction [7]. The decomposition was analyzed by CASSCF (complete active space SCF) and MCSCF CI (multiconfiguration SCF CI) calculations. The multiphoton IR pumping leads to the products via a crossing from the $HN_3(\tilde{X}\,^1A')$ surface to the $HN_3(^3A'')$ surface. The energy minimum of the crossing for HN_3 occurs with a nearly linear N_3 backbone and the NH bond being nearly perpendicular to the N_3 group. The HN-NN bond is stretched, whereas the bond lengths in the N_2 and NH subunits are already similar to those of the separated molecules and indicate that both products form in their vibrational ground states [8, 9]. The calculated activation energy of 153 to 189 kJ/mol agrees with the experimental values (see p. 119); the spin-allowed decomposition to NH(a $^1\Delta$) and N_2 has a calculated activation energy of 170 to 219 kJ/mol. The potential energy surface in the exit channel of the spin-forbidden reaction implies a significant degree of rotational excitation in the departing N_2 fragment and insignificant rotational excitation of NH [10]. The observed formation of NH(X $^3\Sigma^-$) in the symmetric Λ states F_1 and F_3 by coplanar dissociation agrees with the theoretical expectations [8, 9].

A UV emission at about 336 nm, identified as the $^3\Pi \rightarrow {}^3\Sigma^-$ transition of ND, and a broad chemiluminescence, attributed to the $^2A_1 \rightarrow {}^2B_1$ transition of NH_2 and ND_2, were observed in earlier IRMPD investigations. Both types of fluorescent radicals stem from a complex scheme of secondary reactions which are initiated by the primary fragmentation product NH(D) (a $^1\Delta$) [3, 11]; see also [12 to 15].

Photolysis by Visible Light. The excitation of the H-N stretching overtone ($n\nu_1$) and the combination states in ground-state $HN_3(\tilde{X}\,^1A')$ by IR-visible, double-resonance pumping or by direct overtone pumping leads to dissociation. Excitation lies in the range of $5\nu_1$ (15120 cm^{-1}) to $7\nu_1$ (20070 cm^{-1}). The lifetimes of the combination bands show that the dissociation rates do not depend on the nominal participation of vibrations involving a motion along the reaction coordinate, but actually are average rates for the different kinds of molecular motions with the same total energy in agreement with the limited eigenstate character of the bands (cf. p. 112) [4, 6, 16]. The dissociation rate increases by a factor of 200 on going from the $5\nu_1$ level to the $6\nu_1$ level; statistical unimolecular reaction theory predicts a much smaller increase [17].

The overtone photodissociation of HN_3 yields NH and N_2 fragments by two channels which were also observed in infrared multiphoton dissociation of hydrogen azide; see above.

The asymptote of the NH singlet channel lies 12688.39 ± 0.10 cm^{-1} above that of the triplet channel which is the singlet-triplet splitting of both electronic states in their lowest quantum states [18]. The relative propensities for forming NH X $^3\Sigma^-$ and a $^1\Delta$ products for the different overtone and combination bands are as follows [6]:

band	$5\nu_1$ [4]	$6\nu_1$ [4]	$6\nu_1 + \nu_5$	$6\nu_1 + \nu_4$	$6\nu_1 + 2\nu_4$	$7\nu_1$
E_{vib} in cm^{-1}	15120	17670	18190	18755	19740	20070
NH(X $^3\Sigma^-$)	exclusively	>99%	>70%	~10%	–	–
NH(a $^1\Delta$)	–	–	–	~90%	>80%	>97%

The threshold for the spin-allowed channel lies between 18190 and 18755 cm^{-1}, but probably close to the upper limit. The energy release by the dissociation from $7\nu_1$ gives $\Delta H^\circ \leq 211$ kJ/mol for the spin-allowed reaction [6].

The Doppler profiles of the products formed by $5\nu_1$, $6\nu_1$, and $7\nu_1$ dissociations confirm that they all form exclusively in the vibrational ground state. The observed energy partitioning into rotation and translation with the average energies given in cm^{-1} (calculated values from energy partitioning models are given in the paper) are as follows [6]:

mode	$5\nu_1$	$6\nu_1$	$7\nu_1$
total translational energy	9000	7000 to 10000	1350
rotational energy of NH	200 (from [4])	400	230
rotational energy of N_2	–	>2000	>850

The NH(a) formed by dissociation from $7\nu_1$ has a rotational temperature of 330 ± 60 K. The rotational Λ-doublet components are observable from the rotational ground state with $J = 2$ up to a maximum value of $J = 7$ and have a Boltzmann-type distribution. The population ratio of NH(a) in the symmetric (Δ(A′)) and the antisymmetric (Δ(A″)) Λ states increases smoothly with J. The ratios indicate that planar dissociation processes predominate in producing the highest J(NH) fragments [6]:

J	2	4	5	6	7
Δ(A′)/Δ(A″)	1.0 ± 0.3	1.2 ± 0.3	1.7 ± 0.3	2.1 ± 0.3	4 ± 1

The population ratio of the Λ states as a function of J could be reproduced by complete active space SCF (CASSCF) calculations [19]. The Λ doublet of NH(a) formed from the $6\nu_1 + \nu_4$ state is equally populated for $J = 2$ [6].

Nascent NH(X) from $5\nu_1$ and $6\nu_1$ forms in about equal amounts in the symmetric F_1 and F_3 spin-rotation states [4]. The population of the F_2 state is about 3 to 4% [17]. More than 96% of the energy liberated is released by translation. The rotational distributions correspond to NH temperatures of 280 ± 50 K for dissociation from $5\nu_1$ and 570 ± 60 K for dissociation from $6\nu_1$, and the population of the vibrational ground level is >95% yielding an average increase of the internal energy by only 200 cm^{-1}. The decomposition from $5\nu_1$ and $6\nu_1$ is similar to that of DN_3 in the IRMPD experiments [4]; see above.

Ultraviolet Photolysis. Overall products of the photolysis of HN_3 (50 Torr) at 313 nm and 303 K are N_2, H_2, and NH_4N_3 in average quantum yields of 4.85, 0.494, and 0.842 independent of the light intensity. The conversion of HN_3 does not exceed 12.8% [20] in close agreement to the value found during flash photolysis of HN_3 diluted by H_2, N_2, or CO_2 [21]. The concentration ratio of formed H_2 and N_2 is 0.090 ± 0.005 and does not change with the pressure of HN_3 [22]. The influences of the HN_3 pressure and added Xe on the yields is moderate; see [20] for details. The rate of the photolysis increases with $p(HN_3)$ at pressures in the range of a few Torr and is independent of the pressure at $p > 100$

Torr. The inhibition of the photolysis by added CO_2 or hydrocarbons is attributed to the quenching of reactive intermediates [22].

The decomposition of gaseous HN_3, induced by irradiation at $\geq$248 nm, takes place from the $\tilde{A}\,^1A''$ state [23]. The states $\tilde{B}\,^1A'$ and $\tilde{C}\,^1A''$ of HN_3 are excited in addition at 193 nm [24]. The number of photons absorbed during the photolysis of HN_3 at 193 nm was determined as 1.0 ± 0.1 [25]. Dissociation times $\leq$120 fs for excited DN_3 and $\leq$160 fs for excited HN_3 during 308 nm photolysis [26] and $\leq$100 fs for HN_3 at 248 nm were estimated from the bipolar moments $\beta_{v\mu}$ derived from the vector $\mathbf{v}$ of the NH recoil velocity and the transition dipole moment $\boldsymbol{\mu}$ of hydrazoic acid [23] which has to be perpendicular to the molecular plane for symmetry reasons [27]. The possible channels leading to products during UV photolysis are given in Table 17. The complete active space SCF (CASSCF) method with inclusion of valence CI predicts exclusive formation of NH(a ^{1}A) by photolysis at >220 nm [28].

Table 17
Possible Dissociation Channels Accessible for the UV Photolysis of HN_3 [25].

reaction and products	dissociation energy[a] in cm^{-1}	threshold wavelength in nm
(1) $HN_3 \rightarrow NH(X) + N_2(X)$[b]	4000	2500
(2) $NH(a) + N_2(X)$	16590	603
(3) $NH(b) + N_2(X)$	25240	396
(4) $H(^2S) + N_3(^2\Pi_g)$	34610[c]	288.9[c]
(5) $N(^4S) + H(^2S) + N_2(X)$[b]	34770[c]	287.6[c]
(6) $NH(A) + N_2(X)$[b]	33780	296
(7) $NH(c) + N_2(X)$	47350	211
(8) $NH(X) + N_2(A)$	53760	186

[a] From the heats of product formation. — [b] The formation of these products violates spin conservation. — [c] Revised values from [24].

The observed primary products of the UV photolysis of HN_3 with quantum yields Φ, fraction of vibrational excitation, and translational energies are listed in Table 18. The predominant products are NH(a) and N_2 with varying amounts of NH(b) and NH(c). The concentration of NH(a) generated by photolysis at 248 nm is substantially less than at 193 nm at constant pulse energy. This reflects the significantly smaller absorption cross section at 248 nm [29]. The formation of NH(a) and NH(b) in vibrationally more highly excited states than those identified cannot be excluded. The uncertainty in Φ of NH(c) is 20% after photolysis at 193 nm, those of the other NH radicals are larger [25]. Other primary products are H and N_3 [30 to 32]. The observed H atoms (Table 18) form in accordance with the almost isoenergetic reactions (4) or (5) in Table 17 [24]. A definite assignment of the origin of H is not possible, because the observed $N_3(\tilde{X}\,^2\Pi_g, v=0)$ [21, 33] may also arise from the secondary reaction $HN_3 + NH \rightarrow N_3 + NH_2$ [34, 35].

Some of the identified products could be assigned unequivocally to secondary reactions. The time profile [34, 35] and the pressure dependence of the fluorescence [36] of the spin-forbidden by-product NH(A) observed during 121.6 nm photolysis [37] indicates its origin from the secondary reaction of HN_3 with electronically excited N_2. The concentration of NH(A) reaches 5% or less of the NH formed [36]. Other secondary products like NH_2 and excited NH(A) were found spectroscopically at a quantum yield close to 2 when the used

Table 18
Results of the UV Photolysis of HN_3 at Various Wavelengths [25].

wavelength	product	Φ (or yield)	vibrational state v	fraction N(v)/N	E_{trans} in cm^{-1}
121.6 nm[a]	NH(a)	(main product)	–	–	–
	NH(c)	($\leq$2%)	–	–	–
193 nm	NH(X)	$\leq$0.002	0	–	–
	NH(a)	0.40	0	0.79	26200
			1	0.21	23700
	NH(b)	0.02	0	$>$0.95	19800
	NH(A)	0.0002	0[b]	0.86	–
			1	0.14	–
	NH(c)	0.0006	0[b]	0.95	–
			1	~0.05	–
	H[c]	0.15(2)	–	–	–
248 nm	NH(a)[d]	1	0	0.58	10600
			1	0.42	11300
	NH(A)[d]	very low	0	–	–
	NH(a)[e]	–	0	0.32	–
			1	0.47	–
			2	0.17	–
			3	0.038	–
			4	$\ll$0.038	–
	H[c]	0.24(5)	–	–	–
266 nm	NH(a)[f]	~1	0	–	–
	NH(c)[f,g]	–	–	–	–
	NH(a)[h]	–	0	0.26	5450(1180)
		–	1	0.28	6950(1450)
		–	2	0.22	~7000
		–	3	0.24	–

[a] From [34 to 37]. – [b] The population of both rotational Λ states is about equal. – [c] From [24]. – [d] Reevaluated data from [38]; the value of the quantum yield is assumed. – [e] From [39]. – [f] From [40]. – [g] Additional product with low yield at high pulse energies by two-photon absorption. – [h] From [41].

pressure of HN_3 was too high; both products can be suppressed by using HN_3 at low pressures or adding Ar [25].

Detailed investigations were carried out on the dissociation of hydrazoic acid from the first excited state, $\tilde{A}\,^1A''$, at wavelengths above ~220 nm. The upper potential energy surfaces (PES) of HN_3 and DN_3 probably are very similar. The dynamic features of the dissociation are essentially independent of parent rotation [26]. The PES exhibits gradients in different molecular coordinates based on vector correlations of the products. The molecular motion before dissociation is influenced by forces which lead to in-plane as well as out-of-plane bending motions which are similar to those of the fundamentals ν_5 and ν_6 in the electronic ground state. Vector correlations at low rotational quantum numbers J of NH indicate a planar dissociation geometry [23, 27, 42, 43]. This movement in the molecular plane results in a strong, rotational excitation of N_2. An initial, linear-bent transition in the NNN frame similar to ν_6 was deduced for the dissociation process, resulting in high J values of NH accompanied by less rotational excitation of N_2. There seems to be a smooth transition between both modes of decomposition, which on the whole seems to take place by a torsional movement of the hydrazoic acid molecules [23, 27, 42, 44, 45]. A CASSCF calculation of the PES predicted a favored decomposition by in-plane bending at the HN-N_2 equilibrium distance and an increasing share of out-of-plane bending with increasing distance. The simultaneous decrease of N_2 rotation was also predicted correctly [28].

The general conclusions concerning the decomposition of electronically excited hydrazoic acid are confirmed by investigations on the population of the rotational Λ levels of NH. The equal occupation of the two levels of a $^1\Delta(A')$ and a $^1\Delta(A'')$ symmetry does not depend on the applied wavelength between 308 and 248 nm or on the rotational temperature of HN_3 in the range 10 to 300 K [23]. However, the vector correlations of both Λ states differ significantly. The effect is more pronounced in the case of DN_3. The asymmetric A″ level is occupied as the result of a planar dissociation process which is essentially (80%) an in-plane bending of excited hydrazoic acid. The rotation of NH (ND) is low [26]. A CASSCF calculation predicted little rotational excitation of NH(a) on account of the small dependence of the PES of the $HN_3(\tilde{A}\,^1A'')$ decomposition on the angle HNN [28]. The symmetric A′ state is occupied by NH (ND) of high rotational excitation. About half of it is generated by an internal torsional motion of hydrazoic acid which resembles an out-of-plane bending at the central nitrogen atom [26].

Energy distributions were determined for both hydrazoic acid fragments on the basis of NH(a) and ND(a) Doppler profiles. Excitation and fragment energies for HN_3 [43] (DN_3 [26]) in cm^{-1} are as follows:

photolysis at	excitation energy of HN_3 (DN_3)	NH (ND) energy kinetic	rotational	N_2 energy kinetic	rotational
248 nm	21950	6800	700	3640	10810
266 nm	19210	7040	700	3770	7700
283 nm	16970	6430	700	3440	6400
308 nm	14100	6950	690	3720	2740
	(13850)	(6430)	(1175)	3670	2580

The excess energy of the photolysis reappears in the rotational energy of N_2; the other energies of the fragments remain nearly constant upon changing the wavelength of the light used [43]. About half of the energy available from the photolysis of HN_3 at 308 nm [46], 266 nm [40, 41], and 248 nm and about 75% at 193 nm [25] is partitioned into the translational energies of the products as determined from the Doppler profiles of NH. A share of 34% for the translation energy from the time-of-flight mass-spectrometric profiles after photolysis at 283 nm is qualitatively similar [44]. The average recoil velocity of NH of 3320 m/s during photolysis at 266 nm is quite high, whereas the value for N_2 is only 1770 m/s [43]. Details are given in the following paragraphs.

Vibrational excitation of NH(a) with a population up to $v=3$ accounts for 21% of the energy available from photolysis at 266 nm. The occupation of all vibrational levels is rather similar and very different from the one that would be derived using the tabulated Franck-Condon factors for this transition; this may reflect the impulsive nature of the dissociative process [41]. Vibrationally excited NH(a) was also observed upon photolysis at 248 nm [39];

see Table 18 for the fractions of the vibrational levels. These observations of vibrationally excited NH(a) outdate earlier reports [47 to 49] which state a predominant formation of NH(a) in the vibrational ground state in photolyses at 248 to 315 nm.

Very similar rotational distributions of NH(a) were found for the photolysis of HN_3 at 308, 283, and 248 nm [43, 44]. The nascent, rotational distribution from photolysis at 266 nm is of the Gaussian type with a population inversion at $J<5$ and peaking at $J=5$ to 6 after including a vector correlation between the transition dipole momentum of HN_3 and the rotation of NH formed [40, 50]. A non-Boltzmann distribution of J values of NH was also noted for samples of HN_3 cooled to a rotational temperature of ~3 K by pulsed expansion before photolysis [47]. Photolysis of DN_3 at 308 nm leads to a Gaussian distribution of the ND rotation with the maximum at $J\approx9$ and the full width at half maximum (FWHM) $\Delta J\approx9$ [26]. The rotational temperature of NH cannot be given because of the Gaussian-type occupation of the rotational levels. The rotational temperatures given in [25, 46, 49, 50, 51] are based on Boltzmann distributions of the rotational states; these distributions could be shown experimentally to arise from partly relaxed samples [40, 50]. The bimodal, rotational distribution of partly relaxed NH(a) generated with 193 nm light in a mixture of 20 Torr HN_3 and 9 atm N_2 is described in [29].

The intensities of resonance-enhanced multiphoton ionization (REMPI) spectra suggest that the population of nascent N_2 in the vibrational ground state is larger than in the first excited state [44]. A rotational maximum of N_2 in the ground state at $J=70$ and a width ΔJ of 18 (FWHM) were determined at 248 nm [45]. The intensities of REMPI spectra yielded a maximum of the rotational population of N_2 in the ground state at $J\approx56$ with a spread of $\Delta J=12$ for the photolysis at 283 nm. The rotational energy amounts to ~60% of the total energy of 10500 cm^{-1} available to N_2 [44]. Calculations of the mean rotational quantum numbers of N_2 from NH energies yielded $J=73$ at 248 nm, $J=62$ at 266 nm, and $J=37$ at 308 nm [43].

The UV photolyses of HN_3 (DN_3) in **matrices** of Ne, Ar, Kr, Xe, and N_2 at 20 K or less led to the identification of NH [52 to 57], NH_2 [54, 56, 57], NH_3 [54, 55, 58], and the deuterated compounds, N_2H_2 [55], possibly N_3 [56], and the atoms N [52, 53, 57] and H [57]. Annealing of the samples at temperatures up to 74 K produced NH_4N_3 [54, 58]. The compounds were usually identified by UV spectroscopy except in [57], where ESR spectroscopy was used. The UV photolysis of undiluted, frozen HN_3 is described together with other investigations of the partly decomposed compound on p. 120.

During UV photolysis **aqueous** HN_3 decomposes to N_2 and NH_2OH, the latter probably resulting from the reaction of the intermediate NH with H_2O [59, 60]. The yield of NH_2OH is in the range 65 to 90% [60]. The rate with which N_2 is liberated was used to determine a reaction order of 2 and the rate constant [61, 62]. However, decomposition via $4\,HN_3 \rightarrow NH_4N_3 + 4\,N_2$ with a quantum yield $\Phi(N_2) \leq 2$ was found under similar conditions [63].

Solutions in the pH range 0.8 to 2.35 exclusively yield NH_2OH at quantum yields close to 1 and N_2 in the presence of $HClO_4$. The lower concentration of NH_2OH in the presence of Cl^- or allyl alcohol stems from scavenging an intermediate species, supposedly NH [64]. An attempt to identify the intermediates NH and N_3 in a flash photolyzed, acidic solution by absorption spectroscopy failed [65]. The photolysis of HN_3 in 2 N HNO_3 at 310 K yields N_2 and NH_4NO_3 exclusively [66]. An acidic solution of HN_3 containing Fe^{3+} also yields NH_3 and N_2. The product ratio approaches the maximum value of 0.25; the rate of formation depends almost linearly on the intensity of the incident light [67].

The photolysis of HN_3 in polar, **organic solvents** like alcohols and ethers yields mainly N_2 and NH_4N_3; the amounts of H_2 and N_2H_4 formed are small. NH_4N_3 results from a secondary reaction at $T > 220$ K only. The speed of the liberation of N_2 strongly depends on the concentration of HN_3 and indicates a bimolecular rate-determining step [63]. The photolysis in hydrocarbons yields products resulting from reactions with the solvents in addition to NH_3 and N_2; see p. 149.

Photolysis by Solar Radiation. Theoretical considerations suggest that the photodissociation of HN_3 in solar radiation fields yields H and N_3; the latter is converted to N and N_2 which then is ionized [68].

References:

[1] Avouris, P.; Bethune, D. S.; Lankard, J. R.; Ors, J. A.; Sorokin, P. P. (J. Chem. Phys. **74** [1981] 2304/12).
[2] Stephenson, J. C.; Casassa, M. P.; King, D. S. (J. Chem. Phys. **89** [1988] 1378/87).
[3] Hartford, A., Jr. (Chem. Phys. Lett. **57** [1978] 352/6).
[4] Foy, B. R.; Casassa, M. P.; Stephenson, J. C.; King, D. S. (J. Chem. Phys. **89** [1988] 608/9).
[5] Melius, C. (private communication, ref. 24 in [2]; ref. 6 in [4]).
[6] Casassa, M. P.; Foy, B. R.; Stephenson, J. C.; King, D. S. (J. Chem. Phys. **94** [1991] 250/61).
[7] Yarkony, D. R. (J. Chem. Phys. **92** [1990] 320/3).
[8] Alexander, M. H.; Werner, H.-J.; Dagdigian, P. J. (J. Chem. Phys. **89** [1988] 1388/400).
[9] Alexander, M. H.; Dagdigian, P. J. (AIP Conf. Proc. No. 191 [1988/89] 651/6).
[10] Alexander, M. H.; Werner, H.-J.; Hemmer, T.; Knowles, P. J. (J. Chem. Phys. **93** [1990] 3307/18).

[11] Simpson, T. B.; Mazur, E.; Lehmann, K. K.; Burak, I.; Bloembergen, N. (J. Chem. Phys. **79** [1983] 3373/81).
[12] Bloembergen, N.; Burak, I.; Simpson, T. B. (J. Mol. Struct. **113** [1984] 69/82).
[13] Bloembergen, N.; Burak, I.; Mazur, E.; Simpson, T. B. (Isr. J. Chem. **24** [1984] 179/86).
[14] Hartford, A., Jr. (Electro-Opt. Syst. Des. **11** [1979] 26/9; C.A. **91** [1979] No. 81519).
[15] Hartford, A., Jr. (Proc. Tech. Program-Electro-Opt./Laser Conf. Expo. **1978** 152/8; C.A. **90** [1979] No. 130597).
[16] Foy, B. R.; Casassa, M. P.; Stephenson, J. C.; King, D. S. (J. Chem. Phys. **92** [1990] 2782/9).
[17] Foy, B. R.; Casassa, M. P.; Stephenson, J. C.; King, D. S. (J. Chem. Phys. **90** [1989] 7037/45).
[18] Ram, R. S.; Bernath, P. F. (J. Opt. Soc. Am. B **3** [1986] 1170/4).
[19] Alexander, M. H.; Dagdigian, P. J.; Werner, H.-J. (Faraday Discuss. Chem. Soc. No. 91 [1991] 319/35).
[20] Kodama, S. (Bull. Chem. Soc. Jpn. **56** [1983] 2348/54).

[21] Thrush, B. A. (Proc. Roy. Soc. London A **235** [1956] 143/7).
[22] Konar, R. S.; Matsumoto, S.; Darwent, B. de B. (Trans. Faraday Soc. **67** [1971] 1698/706).
[23] Gericke, K.-H.; Theinl, R.; Comes, F. J. (J. Chem. Phys. **92** [1990] 6548/55).
[24] Gericke, K.-H.; Lock, M.; Comes, F. J. (Chem. Phys. Lett. **186** [1991] 427/30).
[25] Rohrer, F.; Stuhl, F. (J. Chem. Phys. **88** [1988] 4788/99).
[26] Gericke, K.-H.; Lock, M.; Fasold, R.; Comes, F. J. (J. Chem. Phys. **96** [1992] 422/32).
[27] Gericke, K.-H.; Theinl, R. (J. Chem. Soc. Faraday Trans. II **85** [1989] 1303/5).
[28] Meier, U.; Staemmler, V. (J. Phys. Chem. **95** [1991] 6111/7).
[29] Sauder, D. G.; Patel-Misra, D.; Dagdigian, P. J. (J. Chem. Phys. **91** [1989] 5316/23).

[30] Stuhl, F.; Welge, K. H. (unpublished results, ref. 4 in [37]).

[31] Stepanov, P. I.; Zamanskii, V. M.; Moskvitina, E. N.; Kuzyakov, Yu. Ya. (Vestn. Mosk. Univ. Ser. Khim. **28** [1973] 306/9; Moscow Univ. Chem. Bull. [Engl. Transl.] **28** No. 3 [1973] 36/8).
[32] Zamanskii, V. M.; Stepanov, P. I.; Kuzyakov, Yu. Ya.; Moskvitina, E. N. (Vestn. Mosk. Univ. Ser. Khim. **28** [1973] 412/5; Moscow Univ. Chem. Bull. [Engl. Transl.] **28** No. 4 [1973] 20/3).
[33] Douglas, A. E.; Jones, W. J. (Can. J. Phys. **43** [1965] 2216/21).
[34] Hikida, T.; Maruyama, Y.; Saito, Y.; Mori, Y. (Chem. Phys. **121** [1988] 63/71).
[35] Maruyama, Y.; Hikida, T.; Mori, Y. (Chem. Phys. Lett. **116** [1985] 371/3).
[36] Okabe, H. (J. Chem. Phys. **49** [1968] 2726/33).
[37] Welge, K. H. (J. Chem. Phys. **45** [1966] 4373/4).
[38] Kenner, R. D.; Rohrer, F.; Stuhl, F. (J. Chem. Phys. **86** [1987] 2036/43).
[39] Hack, W.; Mill, T. (J. Phys. Chem. **95** [1991] 4712/8).
[40] Gericke, K.-H.; Theinl, R.; Comes, F. J. (Chem. Phys. Lett. **164** [1989] 605/11).

[41] Nelson, H. H.; McDonald, J. R. (J. Chem. Phys. **93** [1990] 8777/83).
[42] Comes, F. J. (Angew. Chem. **104** [1992] 529/41; Angew. Chem. Int. Ed. Engl. **31** [1992] 516/27; Ber. Bunsen-Ges. Phys. Chem. **94** [1990] 1268/77).
[43] Gericke, K.-H.; Haas, T.; Lock, M.; Theinl, R.; Comes, F. J. (J. Phys. Chem. **95** [1991] 6104/11).
[44] Chu, J.-J.; Marcus, P.; Dagdigian, P. J. (J. Chem. Phys. **93** [1990] 257/67).
[45] Haas, T. (Dipl.-Arbeit Univ. Frankfurt am Main 1990 cited in [42]).
[46] Umemoto, H.; Kikuma, J.; Tsunashima, S.; Sato, S. (Chem. Phys. **120** [1988] 461/7).
[47] DeKoven, B. M.; Baronavski, A. P. (Chem. Phys. Lett. **86** [1982] 392/6).
[48] Piper, L. G.; Krech, R. H.; Taylor, R. L. (J. Chem. Phys. **73** [1980] 791/800).
[49] Baronavski, A. P.; Miller, R. G.; McDonald, J. R. (Chem. Phys. **30** [1978] 119/31).
[50] Hall, J. L.; Adams, H.; Kasper, J. V. V.; Curl, R. F.; Tittel, F. K. (J. Opt. Soc. Am. B **2** [1985] 781/5).

[51] McDonald, J. R.; Miller, R. G.; Baronavski, A. P. (Chem. Phys. Lett. **51** [1977] 57/60).
[52] Ramsthaler-Sommer, A.; Eberhardt, K. E.; Schurath, U. (J. Chem. Phys. **85** [1986] 3760/9).
[53] Esser, H.; Langen, J.; Schurath, U. (Ber. Bunsen-Ges. Phys. Chem. **87** [1983] 636/43).
[54] Van Thiel, M.; Pimentel, G. C. (J. Chem. Phys. **32** [1960] 133/40).
[55] Rosengren, K.; Pimentel, G. C. (J. Chem. Phys. **43** [1965] 507/16).
[56] Keyser, L. F.; Robinson, G. W. (J. Am. Chem. Soc. **82** [1960] 5245/6).
[57] Fischer, P. H. H.; Charles, S. W.; McDowell, C. A. (J. Chem. Phys. **46** [1967] 2162/6).
[58] Becker, E. D.; Pimentel, G. C.; Van Thiel, M. (J. Chem. Phys. **26** [1957] 145/50).
[59] Oliveri-Mandala, E.; Werber, G. (Gazz. Chim. Ital. **80** [1950] 177/9).
[60] Kawai, J.; Tsunashima, S.; Sato, S. (Chem. Lett. **1983** 823/6).

[61] Oliveri-Mandala, E.; Caronna, G. (Gazz. Chim. Ital. **81** [1951] 523/6).
[62] Oliveri-Mandala, E.; Valenti, G. (Ric. Sci. **21** [1951] 232/3).
[63] Koch, E. (Tetrahedron **23** [1967] 1747/68).
[64] Shapira, D.; Treinin, A. (J. Phys. Chem. **77** [1973] 1195/8).
[65] Treinin, A.; Hayon, E. (J. Chem. Phys. **50** [1969] 538/9).
[66] Zil'berman, B. Ya.; Lelyuk, G. A.; Mashkin, A. N.; Yasnovitskaya, A. L. (Radiokhimiya **30** [1988] 833/7; Sov. Radiochem. [Engl. Transl.] **30** [1988] 788/92).
[67] Trimm, D. L.; Williams, R. J. (Proc. Chem. Soc. **1962** 142/3).
[68] Cherednichenko, V. I. (Probl. Kosm. Fiz. No. 9 [1974] 155/9 from C.A. **83** [1975] No. 155439).

2.3.1.10.2 Interactions with Electrons

Investigations on HN_3 in noble-gas plasmas showed that HN_3 is a strong electronegatively attaching molecule on account of the high electron loss rates from the plasmas. The plasmas were generated by 600-keV electron beam pulses. The attachment rate constants at 296 K decreased from 10×10^{-11} to 5×10^{-11} cm^3/s, when the E/N values (E = electric field strength, N = Avogadro number) increased from 1×10^{-17} to 4×10^{-17} $V \cdot cm^2$ in Ar. The rate constants are slightly larger in Ne, larger in Kr, and much larger in He and Xe; this suggests a correlation with the electron velocity distribution. The discharges exhibit strong $N_2(C \rightarrow B)$ emissions in Ar, much weaker ones in Ne and Kr, and virtually none at all in He and Xe, implying a dependence on possible inert gas electronic or ionic resonances [1].

The intensity of ions in the 70-eV mass spectrum of HN_3 relative to the intensity of the molecular ion and their appearance potentials (AP) are as follows:

ion	HN_3^+	N_3^+	N_2H^+	N_2^+	N_3^{2+}	NH^+	N^+
intensity	100.0	5.8	8.3	7.3	2.6	16.8	4.9
AP in eV	10.3 ± 0.2	16.0 ± 0.2	13.8 ± 0.2	16.0 ± 0.1	–	14.4 ± 0.2	19.7 ± 0.3

The negative ions N_3^- and NH^- have appearance potentials of 1.1 ± 0.2 and 0.8 ± 0.3 eV. They originate from resonance capture processes at low voltages [2]. A more recent mass spectrum was obtained under different source and ion separation conditions and differed slightly from an earlier spectrum [3].

The decomposition of HN_3 to $NH(A\ ^3\Pi)$ and $N_2(X)$ predominates at moderate electron impact energies. The reaction has a threshold of 4.3 [4] or 4.5 ± 0.6 eV [5]; the NH(A) emission reaches a maximum at 10 to 15 eV. An additional, spin-forbidden reaction yielding NH(A) and $N_2(A\ ^3\Sigma_u^+)$ is important near the threshold and takes place after an electron-exchange excitation of HN_3 leading to a singlet-triplet transition. The formation of the minor product $NH(c\ ^1\Pi)$ increases with the electron impact energy [4] and prevails at energies exceeding ~17 eV. The experimentally determined threshold of the reaction yielding NH(c) and $N_2(X)$ is 6.5 ± 0.6 [5] or 6.8 eV [4]. Changes in the vibrational population and the rotational temperature of NH(A) suggest that it starts to form additionally via a different channel at 16 ± 2 eV. The ratio of NH(A) in the first vibrationally excited state to that in the ground state varies from 0.18 near the threshold to 0.33 at energies from 30 to 36 eV. The rotational temperature increases from 2800 ± 600 K at 7 eV to 4500 ± 400 K at energies exceeding 15 eV. Only the ground state of NH(c) was found because of predissociation in vibrationally excited states. The rotational temperature is 2000 ± 200 K [5].

References:

[1] Schlie, L. A.; Wright, M. W. (J. Chem. Phys. **92** [1990] 394/400).

[2] Franklin, J. L.; Dibeler, V. H.; Reese, R. M.; Krauss, M. (J. Am. Chem. Soc. **80** [1958] 298/302).

[3] Dupré, G.; Paillard, C.; Combourieu, J. (Dyn. Mass Spectrom. **4** [1976] 233/45).

[4] Fukui, K.; Fujita, I.; Kuwata, K. (J. Phys. Chem. **81** [1977] 1252/7).

[5] Tokue, I.; Ito, Y. (Chem. Phys. **79** [1983] 383/9).

2.3.1.10.3 Reactions with Elements and Element Ions

Noble Gases. Flames of HN_3 and electronically excited Ar, Kr, or Xe emit strong bands of rotationally excited $NH(A\ ^3\Pi)$. Additional bands of $N_2(B\ ^3\Pi_g)$ are found in flames with Ar and Kr [1].

Hydrogen. Spark ignition of HN_3 in excess H_2 yields more NH_3 than expected for the decomposition of HN_3 into NH_3 and N_2. This indicates an interaction between the starting materials [2].

Flames of HN_3 and H atoms in flow systems at total pressures less than 4 Torr are bright yellow with orange edges [3]. At ambient temperatures the reaction of the gases is quite fast [4]; fast freezing of the products yields a blue solid which resembles the product from incomplete decomposition of HN_3 [5]; see also p. 120. The reaction of frozen HN_3 and H atoms at 77 K is very slow [6].

The reaction of HN_3 or DN_3 with H atoms is best described in terms of a thermal decomposition of hydrazoic acid, induced by the heat liberated during recombination of the H atoms [7, 8]. Initial products are NH and ND in the A $^3\Pi$ state, indicative of excitation of hydrazoic acid to the triplet state before decomposition [7]. The rotational temperature of NH(A $^3\Pi$) in the 5500 K range causes the chemiluminescence of this reaction [3]. Emissions of NH [9] and ND [8] in the c $^1\Pi$ state, NH(b $^1\Sigma$) [10], NH_2 [9] and its deuterated isotopomers [7], N_2(a′ $^1\Sigma$) [11], and N_2(C $^3\Pi_u$) [12] were also observed and are supposed to result from secondary reactions. The rotational temperature of NH($^1\Pi$) of ~1400 K also is its flame temperature [3]. The electronically excited $NH_2(\tilde{A}\,^2A_1)$ is in the vibrational states $v_2=9$ to $v_2=15$ [10].

The reaction of HN_3 with less than the equimolar amount of H atoms in a flow system yields N_2 and H_2. Assuming a bimolecular reaction, a rate constant of $k=(6.4\pm2.0)\times10^{-14}$ $cm^3\cdot molecule^{-1}\cdot s^{-1}$ was determined at ambient temperature [13]. The reaction of HN_3 with excess H atoms yields up to 40% of NH_3 with respect to reacted HN_3 in addition to N_2 and H_2. The reaction rate increases with the concentration of H; the rate constant is $1.53\times10^{13}\exp[-(19.2\pm1.3)\ kJ\cdot mol^{-1}/RT]\ cm^3\cdot mol^{-1}\cdot s^{-1}$ in the temperature range 300 to 460 K. The activation energy indicates $HN_3+H\rightarrow NH_2+N_2$ to be the initial reaction [14]. Calculations of the structure of the supposed intermediate N_3H_2 are described on p. 156. The first-order dependence of the NH_2 emission on the concentrations of HN_3 and H suggests exclusive formation of NH_2 by this reaction [10].

The protonation of gaseous HN_3 by H_3O^+ and HN_3^+ in a mass spectrometer yields $N_3H_2^+$ in moderately exothermal reactions. The protonation by H_3^+ is highly exothermal; the reaction with CH_5^+ was also mentioned. $N_3H_2^+$ is probably a mixture of two isomers [15]; see p. 156 for details. The protonation of HN_3 at 195 K also succeeds with 10 to 15% solutions of the superacids HF-BF_3 and FSO_3H-SbF_5 in SO_2ClF [16] and with HF or HCl in the presence of Lewis acids. The formation of the aminodiazonium ion, H_2NNN^+, is substantiated by its NMR spectrum and an X-ray structure determination; see pp. 156/7. The protonation in aqueous solution is described on p. 152.

Oxygen. For the combustion via $HN_3(g)+1/4\ O_2\rightarrow1/2\ H_2O(g)+3/2\ N_2$, an enthalpy of −418 kJ/mol at 298 K was calculated [17]. Cocondensed mixtures of HN_3 or DN_3 and O_2 in an N_2 matrix at 20 K form *cis*- and *trans*-HONO, N_2O, NH_2OH, or the deuterated products during UV irradiation [18, 19]. The second-order rate constant for the reaction of HN_3 with O_3 at 293 K was found to be smaller than $4\times10^3\ L\cdot mol^{-1}\cdot s^{-1}$ in aqueous solution at pH 1.6 to 2.5 [20].

The reaction of HN_3 in He with $O_2(^1\Delta_g)$ does not take place at low pressures at 295 K. A rate constant of $k\leq4.4\times10^8\ cm^3\cdot mol^{-1}\cdot s^{-1}$ was estimated [21]. The quenching of O_2 in the singlet state by an aqueous solution of HN_3 is slower than by the azide ion by at least two orders of magnitude and possibly does not occur at all [22].

The reaction of excess, gaseous HN_3 with O(^{1}D) atoms generated by photolysis of O_3 yields NH(A $^3\Pi$), NO(A $^2\Sigma$), and OH(A $^2\Sigma$). The first step is probably $HN_3+O(^1D)\rightarrow OH(X\ ^2\Pi)+$

$N_3(^2\Pi)$ with a rate constant of $k=(3.2\pm1.0)\times10^{-10}$ $cm^3\cdot molecule^{-1}\cdot s^{-1}$ which was derived from a kinetic model. NO probably forms from N_3 and O atoms in a second step [23, 24]. The rate constant of the reaction $HN_3+O\rightarrow N_3+OH$ is $k=2\times10^{-13}$ $cm^3\cdot molecule^{-1}\cdot s^{-1}$ or less based on investigations in a discharge flow tube [25]. Early investigations of the reaction of HN_3 and DN_3 with O atoms identified the emissions of NO, NH, NH_2, and the deuterated radicals [7, 11].

Nitrogen. Gaseous HN_3 reacts with N_2 in the first electronically excited A $^3\Sigma_u^+$, v=0 state yielding $N_2(X)$, NH(X), and NH(A $^3\Pi$); the latter was identified by its (A→X) emission [26 to 29]. The standard enthalpy for the reaction leading to NH(X) and $N_2(X)$ is −553.1 kJ/mol and that for the formation of NH(A) and $N_2(X)$ is −144.4 kJ/mol [28]. The reaction with formation of NH(A) has a rate constant of $k=(0.13\pm0.02)\times10^{13}$ $cm^3\cdot mol^{-1}\cdot s^{-1}$. A branching fraction of 0.025±0.004 was obtained from k by using the total quenching rate constant of $k_q=(5.1\pm1.2)\times10^{13}$ $cm^3\cdot mol^{-1}\cdot s^{-1}$, probably at 300 K [26, 27]. A value of $k_q=(3.3\pm0.8)\times10^{13}$ $cm^3\cdot mol^{-1}\cdot s^{-1}$ at 298 K was determined in [28]. However, a reaction of HN_3 with $N_2(A)$ could not be detected in [30]. The reaction of HN_3 with active N_2, obtained by exposing N_2 to an electric discharge, increased the concentration of N atoms identified mass-spectrometrically [14].

The reaction of HN_3 and N atoms in a fast flow reactor yields N_2 and H_2 [14] and can be described as a thermolysis of HN_3, caused by the heat generated by the recombination of the N atoms [31]. The intensity of a yellow-green [30] to grey-orange luminescence [31] during the reaction depends linearly on the concentration of N [30]. The flame emits bands of vibrationally excited NH(A $^3\Pi$) with a rotational temperature of 2100 K (extrapolated to [N]=0) [30]. Bands of NH(c $^1\Pi$) and weak ones of NH_2 were also observed [31]. The analogous, deuterated products result from the reaction with DN_3 [11]. A blue solid can be isolated by quickly freezing the reacting mixture. The solid converts to NH_4N_3 during warming [31]; see also p. 120. The rate constant of the reaction of HN_3 with N, $k=3.0\times10^9$ $cm^3\cdot mol^{-1}\cdot s^{-1}$ at 293 K, was determined by measuring the decrease of N atoms [14].

The rate constant $k=2.0\times10^{-11}$ $cm^3\cdot molecule^{-1}\cdot s^{-1}$ for the reaction $HN_3+N_3\rightarrow H+3\,N_2$ in a flow system was determined by monitoring the absorption of N_3 [32].

Fluorine. An improved synthesis of N_3F from a diluted, gaseous mixture of HN_3 and F_2 in a stainless steel apparatus is described in [33]; this method also is suited to generate the ^{15}N-substituted isotopomers [34]. Earlier investigations of this reaction are given in "Fluorine" Suppl. Vol. 4, 1986, pp. 405/6, and "Fluor" Erg.-Bd. 1, 1959, p. 247. Annealing cocondensed HN_3 and F_2 in Ne or N_2 matrices results in formation of HF; other bands can be assigned to the $HN_3\cdots HF$ moiety [35].

Gaseous HN_3 (DN_3) and F atoms in a discharge flow apparatus yield the initial products HF (DF) and N_3 by a well-investigated reaction; details are given in the following paragraph. A second reaction channel leads to N_2 and HNF (DNF) which was identified by laser fluorescence excitation. The product branching ratio could not be determined [36].

The reaction of HN_3 with an approximately equimolar amount of F atoms is accompanied by the dull red emission typical for $N_2(B)$; an excess of F leads to the bright green flame of NF(b) [37]. A refined investigation of the reaction of HN_3 and F was done at ~300 K in a reactor with a halocarbon wax coating in order to suppress N_3 decomposition [38]. The initial step consists in the formation of N_3(X $^2\Pi$) [39] and HF; the latter was found in the states v=1 to 4 with an average, nascent distribution of 39:36:22:6. The share of HF(v=0) was unknown and was estimated to be similar to that of HF(v=1). In this case, the reaction has a rate constant of $k=(1.1\pm0.1)\times10^{-10}$ $cm^3\cdot molecule^{-1}\cdot s^{-1}$ [38]. A rate constant of $(1.6\pm0.2)\times10^{-10}$ $cm^3\cdot molecule^{-1}\cdot s^{-1}$ was determined by following the decay of the $N_2(B)$ emission [40]. The secondary reaction of F and N_3 then yields ~85% of NF(a) with respect to HN_3 and an insignificant amount of NF(b) [38]. A seventyfold increase of NF(b) results upon adding H_2 to the mixture of HN_3 and excess F because of the increased formation of vibrationally excited HF [41]. A CNDO/2 calculation showed that for F to approach one of the terminal N atoms of HN_3 is energetically more favorable than to approach in a direction collinear with the HN bond [42]. An energy transfer process between NF(a) and vibrationally excited HF leads to NF(b), but is missing when HN_3 is replaced by DN_3; see "Fluorine" Suppl. Vol. 4, 1986, pp. 267/8, for details of earlier investigations. However, a transient formation of NF(b) in the reaction of DN_3 and F atoms results in the presence of iodine atom precursors, when iodine recombination is prevented by optical pumping [43].

The reactions of HN_3 with F atoms were also investigated in the presence of other atomic halogens. The reaction of HN_3 with an excess mixture of F and Cl atoms results in the bright red emission typical for NCl(b). It increases linearly with the concentrations of HN_3 and Cl. The proposed reaction sequence is $HN_3 + F \rightarrow HF(v) + N_3$ followed by $N_3 + Cl \rightarrow NCl(b) + N_2$. The origin of the second product, NCl(a), is unknown [44]. The reaction of HN_3 and a mixture of atomic F and Br proceeds with the intense, red emission of vibrationally excited NBr(b) and seems to resemble the reaction with Cl [45]. The reaction in the presence of atomic I results in the bright yellow emission typical for vibrationally excited IF(b) which forms from IF(X) by an energy transfer from the observed NF(b). The bands of NF(a) could also be identified [41, 46].

The gas phase reaction of HN_3 and F^- with formation of N_3^- was monitored with an ion cyclotron resonance spectrometer [47].

Chlorine. The reaction of HN_3 with Cl atoms yields the brilliant, red emission typical for NCl(b) in vibrationally excited states with $v \leq 10$. The initial step is $HN_3 + Cl \rightarrow HCl + N_3$, and the consecutive reaction is $Cl + N_3 \rightarrow NCl(b) + N_2$. The reaction rate is slower than in the presence of F atoms and linear in the concentrations of HN_3 and Cl [44]. A rate constant of $k = (8.9 \pm 1.0) \times 10^{-13}\ cm^3 \cdot molecule^{-1} \cdot s^{-1}$ was determined from the decay of the first positive emission of N_2 [48] and is in a range which was estimated from the formation of NCl(b) [44].

The expected exothermal reaction of HN_3 with Cl^- in the gas phase could not be observed by ion cyclotron resonance spectrometry [47].

Br_2^-. A rate constant of $5 \times 10^8\ L \cdot mol^{-1} \cdot s^{-1}$ was determined for the reaction of HN_3 with the Br_2^- radical anion in aqueous solution. The temperature and the products were not given [49].

Si. An absorption of gaseous HN_3 nearly parallel to the Si(110) surface at 120 K is suggested by the weak angular dependence of the vibrational peak intensity in the high-resolution electron energy loss (HREEL) spectra. The dissociation into absorbed NH and desorbed N_2 starts upon annealing at 220 K [50].

Ca. Sr. Gaseous HN_3 and vapors of Ca or Sr yield gaseous CaN_3 or SrN_3 in powerful reactions with a bright, blue-orange chemiluminescence [51]. However, spectroscopic measurements under nearly single-collision conditions showed that the primary products are CaNH or SrNH. The observed MN_3 (M = Ca, Sr) stems in part from a secondary reaction between MNH and HN_3 and yields NH_2 in the ground state as the second product. Other products from reactions of HN_3 with as-formed MN_3 and MNH are MH and excited metal atoms [52].

V^{2+}. The reduction of HN_3 by V^{2+} can be formulated by $HN_3 + 2\ V^{2+} + 3\ H^+ \rightarrow NH_4^+ + 2\,V^{3+} + N_2$. The rate law in acidic solution has a first-order dependence in both reactants; the rate constant is $k = (2.83 \pm 0.32) \times 10^{-2}\ L \cdot mol^{-1} \cdot s^{-1}$ at 298.2 K. Investigations in the range 292.1 to 308.5 K yield the activation parameters $\Delta H^{\ddagger} = 60.2 \pm 2.5$ kJ/mol and $\Delta S^{\ddagger} = -72.4 \pm 8.4\ J \cdot mol^{-1} \cdot K^{-1}$ [53].

Cr^{2+}. The reaction of HN_3 and Cr^{2+} can be described by $HN_3 + 2\,Cr^{2+} + 2\,H^+ \rightarrow NH_3 + N_2 + 2\ Cr^{3+}$ [54]. A dimeric chromium complex is an additional product with a yield of ~10% in the presence of HCl [53]. The rate law is first order in HN_3 and Cr^{2+} and has a rate constant of $k = 14.0\ L \cdot mol^{-1} \cdot s^{-1}$ at 298 K and an ionic strength of 1.0. Adding between 0.0004 and 1.0 mol/L $HClO_4$ has no effect [54, 55]. A later investigation yielded $k = 17.8 \pm 2.4\ L \cdot mol^{-1} \cdot s^{-1}$ which qualitatively confirms the earlier result [53]. The reaction has an activation energy of 56.9 kJ/mol; the preexponential factor of the rate constant is 1.4×10^{11} at 298 K. The entropy of activation of $-31.4\ J \cdot mol^{-1} \cdot K^{-1}$ in [54] disagrees with a value of $-120.9 \pm 12.1\ J \cdot mol^{-1} \cdot K^{-1}$ [53] which was determined at 285.1 to 308.0 K. The activation energy is 29.7 ± 3.3 kJ/mol [53]. Activation parameters of $\Delta H^{\ddagger} = 19.2 \pm 2.5$ kJ/mol and $\Delta S^{\ddagger} = -149.0 \pm 8.4\ J \cdot mol^{-1} \cdot K^{-1}$ were determined at 288 to 303 K [56] and agree with the results in [55].

The rate constant of the reduction increases in the presence of Cl^- or Br^-; values are given in [54, 55]. This effect may be due to the formation of chromium complexes of increased reactivity. Addition of F^- or SO_4^{2-} also accelerates the reaction and in addition results in changed kinetics [55]. A moderate increase of the reaction rate in the presence of I^- and a strong increase in the presence of SCN^- were also noted [56]. The rate constant decreases with increasing amounts of added alcohol. *tert*-C_4H_9OH has the strongest effect, *i*-C_3H_7OH a smaller one, and CH_3OH the smallest [57].

Mo. A second-order rate constant of $k = 70 \pm 20\ L \cdot mol^{-1} \cdot s^{-1}$ at 298 K for the reduction $HN_3 + Mo^{4+} + 3\ H^+ \rightarrow NH_4^+ + N_2 + Mo^{6+}$ was estimated from the dependence of the catalytic current during polarography of Mo^{6+} in HCl solution on the concentration of added HN_3. A rate constant of $45 \pm 15\ L \cdot mol^{-1} \cdot s^{-1}$ was deduced for the corresponding reduction of HN_3 by Mo^{3+} [58].

Mn^{3+}. Tc. Re. The oxidation of HN_3 by an equimolar amount of Mn^{3+} in aqueous solution yields H^+, N_2, and Mn^{2+}. The intermediate formation of free radicals induces the polymerization of added acrylonitrile [59]. Kinetic investigations in [59 to 61] failed to completely identify the rate law of the reaction. The reaction becomes faster with increasing concentration of H^+ and is first order in Mn^{3+} [60, 61]. A second-order dependence in the concentration of HN_3 was found in $HClO_4$ solution [60]. The first-order dependence on the total concentration of azide in an acetic-acid-buffered solution becomes more complicated at $[N_3^-] > 0.225$ mol/L [61]. Earlier results are given in "Mangan" C 3, 1975, pp. 263/4.

An aqueous solution of HN_3 in HNO_3 does not react with Tc ions at 313 K [62].

The catalytic decomposition of HN_3 in He on the surface of elemental Re yields N_2 and NH_4N_3 in the temperature range 320 to 360 K [63].

Fe. Co. Ni. The exothermal decomposition of HN_3 in He on Fe, Co, or Ni surfaces at ~370 K yields the respective metal nitride surface layers. They exhibit no activity for HN_3 decomposition between 370 and 530 K [63].

The red $[Fe(H_2O)_5N_3]^{2+}$ is the exclusive product of the reaction of Fe^{3+} in aqueous solution, even in the presence of excess HN_3. The equilibrium constant of $Fe^{3+} + HN_3 \rightleftharpoons [FeN_3]^{2+} + H^+$ is $K = 1.67$ at 296 K, extrapolated to zero ionic strength and infinitely diluted $HClO_4$ solution. K is constant at $0.01 < [H^+] < 0.50$ mol/L and then decreases slightly with increased acidity. The increase of K with temperature indicates an endothermic reaction; an enthalpy change of ~8 kJ/mol was estimated [64]. Rate constants at 298.2 K are 4.0 ± 1.0 $L \cdot mol^{-1} \cdot s^{-1}$ for the formation of $[FeN_3]^{2+}$ from HN_3 with Fe^{3+} and $(6.8 \pm 0.5) \times 10^3$ $L \cdot mol^{-1} \cdot s^{-1}$ for the reaction of HN_3 with $FeOH^{2+}$ in 1.5 mol/L $HClO_4$ solution. The rates increase linearly with the concentration of H^+ [65]. Results of stopped-flow experiments on the formation of $[Fe(H_2O)_5N_3]^{2+}$ in H_2O and in H_2O-DMSO were used for a kinetic model of this reaction [66].

The oxidation of $H^{15}NN^{15}N$ by Co^{3+} in $HClO_4$ solution is given by $H^{15}NN^{15}N + Co^{3+} \rightarrow N^{15}N + 0.5\ {}^{15}N_2 + Co^{2+} + H^+$ and proceeds with quantitative liberation of N_2 and without random mixing of the N isotopes [67]. The intermediate formation of free radicals leads to an accelerated polymerization of added acrylonitrile [68]. The rate law for the reaction of nearly equal concentrations of HN_3 and Co^{3+} is given by $k'[HN_3][Co^{3+}]$ with $k' = 17.5 \pm 0.2$ $L \cdot mol^{-1} \cdot s^{-1}$ at 298 K. The dependence of the rate constant on the acidity of the solution follows the relation $\log k' = \log k + (0.973 \pm 0.026) \cdot \log [H^+]$ at 298 K. The apparent activation energy is 106.3 ± 1.3 kJ/mol between 278 and 298 K [67], later refined to 113.4 ± 0.8 kJ/mol in [69]. The reaction of excess HN_3 with Co^{3+} is first order in $[Co^{3+}]$, second order in $[HN_3]$, and independent of $[H^+]$. The rate constant has an average value of $(1.25 \pm 0.08) \times 10^3$ $L^2 \cdot mol^{-2} \cdot s^{-1}$ at 273 K. An activation energy of 55.6 ± 2.5 kJ/mol and an entropy of activation of 6.7 ± 8.4 $J \cdot mol^{-1} \cdot K^{-1}$ were calculated for the range 273 to 309 K [70] by including corrected rate constants from [68].

Ru to Pt. The reaction of gaseous HN_3 with Pd or Pt surfaces produces highly explosive layers of azides at ambient temperature [71]. The catalytic decomposition of HN_3 in He on the surface of the heavier metals of the platinum group at 320 to 360 K quantitatively yields N_2 and NH_4N_3 [63]. The precipitation of Pd^{2+} from aqueous HNO_3 as $Pd(N_3)_2$ is complete, when at least twice the molar quantity of HN_3 is used [72].

Cu. Gaseous HN_3 oxidizes Cu or brass to solid CuN_3 with formation of NH_3 and N_2 when air and moisture are excluded. Their presence leads to the formation of solid $Cu(N_3)_2 \cdot Cu(OH)_2$ [71].

Ce^{4+}. The oxidation of HN_3 by an acidic solution of Ce^{4+} yields N_2, H^+, and Ce^{3+} [73] and is commonly used for disposing of HN_3; see p. 94. The reaction of $H^{15}NN^{15}N$ yields a mixture of $N^{15}N$ and ${}^{15}N_2$ in a ratio of 2:1 without random mixing of N [67]. The rate of the oxidation is first order in the concentration of Ce^{4+} and seems to be determined by the decomposition of an intermediate. The average rate constant of $(2.6 \pm 0.4) \times 10^2$ s^{-1} at 298.8 K does not depend on the concentration of HN_3 and the acidity, and is insensitive to changes in temperature [73].

Actinides. The reduction of HN_3 by U^{3+} in an acidic, aqueous solution follows the stoichiometry $2\ U^{3+} + HN_3 + 3\ H^+ \rightarrow N_2 + NH_4^+ + 2\ U^{4+}$. The reaction rate is first order in U^{3+} and in HN_3. The rate constant is 8.8×10^{-2} $L \cdot mol^{-1} \cdot s^{-1}$ at 298 K in 0.4 M HCl solution. The rate constant decreases slightly with increasing acidity and does not depend on the ionic strength. Sulfate ions catalyze the reaction; the rate constant reaches a maximum in solutions containing 15 to 25% of CH_3OH, C_2H_5OH, or i-C_3H_7OH [74]. The reduction of HN_3 by U^{3+} in a solution containing *tert*-butanol seems to proceed by an outer-sphere mechanism [75]. The oxidation of U^{IV} in solution by HNO_3 is slower in the presence of HN_3 [76].

The reduction of Np^{VI} to Np^{V} by HN_3 in 1 M HNO_3 is slow. Both Np^{V} and Np^{IV} seem to be inert towards HN_3 [76].

The complex formed by HN_3 and Pu^{IV} in aqueous HNO_3 [76] is weak [77]. There seems to be no redox reaction of HN_3 with Pu^{III}, Pu^{IV}, and Pu^{VI} [76].

References:

[1] Stedman, D. H. (J. Chem. Phys. **52** [1970] 3966/70).
[2] Rozenberg, A. S.; Arsen'ev, Yu. N.; Voronkov, V. G. (Fiz. Goreniya Vzryva **6** [1970] 302/10; Combust. Explos. Shock Waves [Engl. Transl.] **6** [1970] 271/7).
[3] Guenebaut, H.; Latour, M. (J. Chim. Phys. **59** [1962] 970/9).
[4] Combourieu, J.; Le Bras, G.; Laverdet, G. (C. R. Seances Acad. Sci. C **268** [1969] 1335/8).
[5] Pannetier, G.; Guenebaut, H.; Hajal, I. (Bull. Soc. Chim. Fr. **1959** 1690/1).
[6] DeCarlo, V. J.; Rice, F. O. (J. Phys. Chem. **65** [1961] 1913/4).
[7] Guenebaut, H. (Bull. Soc. Chim. Fr. **1959** 962/1018).
[8] Pannetier, G.; Guenebaut, H.; Gaydon, A. G. (C. R. Seances Acad. Sci. **246** [1958] 88/90).
[9] Pannetier, G.; Guenebaut, H. (C. R. Seances Acad. Sci. **245** [1957] 929/31).
[10] Kajimoto, O.; Kawajiri, T.; Fueno, T. (Chem. Phys. Lett. **76** [1980] 315/8).

[11] Pannetier, G.; Guenebaut, H. (Acta Chim. Acad. Sci. Hung. **18** [1959] 347/64).
[12] Pannetier, G.; Goudmand, P.; Dessaux, O.; Guenebaut, H. (C. R. Seances Acad. Sci. **256** [1963] 3082/5).
[13] Combourieu, J.; Le Bras, G.; Barassin, J. (Bull. Soc. Chim. Fr. **1970** 1271/4).
[14] Le Bras, G.; Combourieu, J. (Int. J. Chem. Kinet. **5** [1973] 559/76).
[15] Cacace, F.; Attinà, M.; De Petris, G.; Grandinetti, F.; Speranza, M. (Gazz. Chim. Ital. **120** [1990] 691/700).
[16] Mertens, A.; Lammertsma, K.; Arvanaghi, M.; Olah, G. A. (J. Am. Chem. Soc. **105** [1983] 5657/60).
[17] Gray, P.; Waddington, T. C. (Proc. R. Soc. London A **235** [1956] 106/19).
[18] Baldeschwieler, J. D.; Pimentel, G. C. (J. Chem. Phys. **33** [1960] 1008/15).
[19] Pimentel, G. C. (J. Am. Chem. Soc. **80** [1958] 62/4).
[20] Hoigné, J.; Bader, H.; Haag, W. R.; Staehelin, J. (Water Res. **19** [1985] 993/1004).

[21] Fiedler, E. (Ber. Max-Planck-Inst. Strömungsforsch. **1986** No. 15, pp. 1/97, 81/4; C.A. **107** [1987] No. 77134).
[22] Haag, W. R.; Mill, T. (Photochem. Photobiol. **45** [1987] 317/21).
[23] Neumann, D. K.; Coombe, R. D.; Ongstad, A. P.; Stech, D. J. (Proc. SPIE Int. Soc. Opt. Eng. **875** [1988] 142/8).
[24] Ongstad, A. P.; Coombe, R. D.; Neumann, D. K.; Stech, D. J. (J. Phys. Chem. **93** [1989] 549/52).
[25] Ongstad, A. P.; Henshaw, T. L.; Lawconnell, R. I.; Thorpe, W. G. (J. Phys. Chem. **94** [1990] 6724/30).
[26] Cao, D. Z.; Setser, D. W. (J. Phys. Chem. **92** [1988] 1169/78).
[27] Cao, D. Z.; Setser, D. W. (DE-88005414 [1987] 1/51; C.A. **110** [1989] No. 104686).
[28] Böhmer, E.; Hack, W. (Z. Phys. Chem. [Munich] **170** [1991] 15/30).
[29] Stedman, D. H.; Setser, D. W. (Chem. Phys. Lett. **2** [1968] 542/4).
[30] Dessaux, O.; Picavet-Bernard, G.; Goudmand, P. (C. R. Seances Acad. Sci. C **276** [1973] 635/8).

[31] Guenebaut, H. (C. R. Seances Acad. Sci. **249** [1959] 2778/9).
[32] Paur, R. J.; Bair, E. J. (Int. J. Chem. Kinet. **8** [1976] 139/52).
[33] Gholivand, K.; Schatte, G.; Willner, H. (Inorg. Chem. **26** [1987] 2137/40).
[34] Christen, D.; Mack, H. G.; Schatte, G.; Willner, H. (J. Am. Chem. Soc. **110** [1988] 707/12).
[35] Pritt, A. T., Jr. (AD-A 121190 [1982] 1/48, 41/2; C.A. **99** [1983] No. 21860).
[36] Chen, J.; Dagdigian, P. J. (J. Chem. Phys. **96** [1992] 7333/43).
[37] David, S. J.; Coombe, R. D. (J. Phys. Chem. **90** [1986] 3260/3).

[38] Habdas, J.; Wategaonkar, S.; Setser, D. W. (J. Phys. Chem. **91** [1987] 451/8).
[39] Dyke, J. M.; Jonathan, N. B. H.; Lewis, A. E.; Morris, A. (Mol. Phys. **47** [1982] 1231/40).
[40] David, S. J.; Coombe, R. D. (J. Phys. Chem. **89** [1985] 5206/12).

[41] Pritt, A. T., Jr.; Patel, D.; Benard, D. J. (Chem. Phys. Lett. **97** [1983] 471/5).
[42] Sloan, J. J.; Watson, D. G.; Wright, J. S. (Chem. Phys. **43** [1979] 1/8).
[43] Benard, D. J.; Chowdhury, M. A.; Pritt, A. T. (J. Appl. Phys. **60** [1986] 4051/8).
[44] Pritt, A. T., Jr.; Coombe, R. D. (Int. J. Chem. Kinet. **12** [1980] 741/53).
[45] Pritt, A. T., Jr.; Patel, D.; Coombe, R. D. (J. Mol. Spectrosc. **87** [1981] 401/15).
[46] Pritt, A. T. (AD-A169781 [1986] 77 pp.; C.A. **106** [1987] No. 75423).
[47] Pellerite, M. J.; Jackson, R. L.; Brauman, J. I. (J. Phys. Chem. **85** [1981] 1624/6).
[48] Yamasaki, K.; Fueno, T.; Kajimoto, O. (Chem. Phys. Lett. **94** [1983] 425/9).
[49] Lind, J.; Shen, X.; Eriksen, T. E.; Merényi, G.; Eberson, L. (J. Am. Chem. Soc. **113** [1991] 4629/33).
[50] Bu, Y.; Chu, J. C. S.; Lin, M. C. (Surf. Sci. **264** [1992] L151/L156).

[51] Brazier, C. R.; Bernath, P. F. (J. Chem. Phys. **88** [1988] 2112/6).
[52] Chen, J.; Dagdigian, P. J. (J. Phys. Chem. **96** [1992] 1284/8).
[53] Linck, R. G. (Inorg. Chem. **11** [1972] 61/4).
[54] Wells, C. F.; Salam, M. A. (Chem. Ind. [London] **1967** 2079/80).
[55] Wells, C. F.; Salam, M. A. (J. Chem. Soc. A **1968** 1568/75).
[56] Sevcik, P.; Biresova, D. (Collect. Czech. Chem. Commun. **39** [1974] 2168/74).
[57] Sevcik, P.; Tkac, J. (Collect. Czech. Chem. Commun. **46** [1981] 1554/9).
[58] Viste, A.; Klopf, L.; Mundhenke, J. A. (Proc. S. D. Acad. Sci. **63** [1984] 22/6).
[59] Wells, C. F.; Mays, D. (Inorg. Nucl. Chem. Lett. **4** [1968] 61/3).
[60] Wells, C. F.; Mays, D. (J. Chem. Soc. A **1968** 1622/5).

[61] Treindl, L.; Mrakavova, M. (Chem. Zvesti **31** [1977] 145/52).
[62] Zil'berman, B. Ya.; Lelyuk, G. A.; Mashkin, A. N.; Yasnovitskaya, A. L. (Radiokhimiya **30** [1988] 833/7; Sov. Radiochem. [Engl. Transl.] **30** [1988] 788/92).
[63] Muetterties, E. L.; Evans, W. J.; Sauer, J. C. (J. Chem. Soc. Chem. Commun. **1974** 939/40).
[64] Wallace, R. M.; Dukes, E. K. (J. Phys. Chem. **65** [1961] 2094/7).
[65] Seewald, D.; Sutin, N. (Inorg. Chem. **2** [1963] 643/5).
[66] Krishnamoorthy, G.; Prabhananda, B. S. (Proc. Indian Acad. Sci. Chem. Sci. **95** [1985] 337/44).
[67] Murmann, R. K.; Sullivan, J. C.; Thompson, R. C. (Inorg. Chem. **7** [1968] 1876/9).
[68] Wells, C. F.; Mays, D. (J. Chem. Soc. A **1969** 2175/9).
[69] Thompson, R. C.; Sullivan, J. C. (Inorg. Chem. **9** [1970] 1590/2).
[70] Wells, C. F.; Mays, D. (J. Inorg. Nucl. Chem. **33** [1971] 3855/9).

[71] Lamnevik, S. (Symp. Chem. Probl. Connected Stabil. Explos. 1967 [1968] 21/33; C.A. **70** [1969] No. 98403).
[72] Zil'berman, B. Ya.; In'kova, E. N.; Lelyuk, G. A.; Mashkin, A. N. (Radiokhimia **32** No. 4 [1990] 45/9; Sov. Radiochem. [Engl. Transl.] **32** [1990] 342/4).
[73] Wells, C. F.; Husain, M. (J. Chem. Soc. A **1969** 2981/4).
[74] Adamcikova, L.; Treindl, L. (Chem. Zvesti **30** [1976] 593/8).
[75] Treindl, L.; Adamcikova, L. (Collect. Czech. Chem. Commun. **45** [1980] 3266/9).
[76] Zil'berman, B. Ya.; Lelyuk, G. A.; Mashkin, A. N.; Fedorov, Yu. S. (Radiokhimiya **30** [1988] 837/40; Sov. Radiochem. [Engl. Transl.] **30** [1988] 792/4).
[77] Mayankutty, P. C.; Pillai, N. S.; Shinde, S. S.; Ravi, S.; Nadkarni, M. N. (Prepr. Invited Talks Contrib. Pap.-Symp. Solvent Extr. Met., Bombay, India, 1979, pp. III A3/1-III A3/15, III A3/5; C.A. **92** [1980] No. 170149).

2.3.1.10.4 Reactions with Inorganic Compounds

Alkali and Alkaline Earth Compounds. Azides of the alkali and alkaline earth elements can be prepared by treating their hydroxides or carbonates with aqueous HN_3. The azides are obtained with LiOH, KOH, Rb_2CO_3, Cs_2CO_3 [1], $Mg_2(OH)_2CO_3$ [2], $Ca(OH)_2$, $SrCO_3$, and $Ba(OH)_2$ or $BaCO_3$. A second treatment of the crude product with aqueous HN_3 is occasionally required [1]. Gaseous HN_3 can be used instead of the solution [3]. Solutions of the mixed azides are formed from HN_3 and suspended mixtures of Rb_2CO_3 and $CaCO_3$ [4] or Cs_2CO_3 and $SrCO_3$ [5].

Reacting excess gaseous HN_3 with solid MF (M = Na, K, Rb, Cs, and $N(CH_3)_4$) yields a mixture of MN_3 and MHF_2. Intermediates could not be identified; the reaction is attributed to the high proton affinity of F^- which is larger than that of N_3^-, whereas the more acidic HF_2^- is not replaced by the weak acid HN_3 [6].

Boron Compounds. Boranes and HN_3 react by substituting hydrogen. A frozen ether solution of HN_3 and excess B_2H_6 yield a mixture of $BH_n(N_3)_{3-n}$ with n = 0, 1, 2 upon warming [7]. The reaction $4\ HN_3 + LiBH_4 \rightarrow LiB(N_3)_4 + 4\ H_2$ in ether goes to completion upon warming to ambient temperature [8]. A 2:1 molar ratio of HN_3 and $BH_3 \cdot N(CH_3)_3$ yields $B(N_3)_2H \cdot N(CH_3)_3$, whereas $B(N_3)_3 \cdot N(CH_3)_3$ results with a sixfold amount of HN_3. The adducts $B(N_3)H_2 \cdot L$ with $L = N(C_2H_5)_3$ or pyridine form predominantly from HN_3 and $BH_3 \cdot L$ in equimolar amounts. Using double the molar quantity of HN_3 converts $(CH_3)_3N \cdot BH_2N(CH_3)_2 \cdot BH_3$ to $(CH_3)_3N \cdot BH(N_3)N(CH_3)_2 \cdot B(N_3)H_2$ with limited reproducibility [9]. Excess HN_3 and $B_{10}H_{12}[S(CH_3)_2]_2$ yield 60% of *arachno*-$B_{10}H_{12}(N_3)\mu$-NH_2 in toluene at ambient temperature [10].

AlH_3. GaH_3. $LiAlH_4$. $Al(BH_4)_3$. Cocondensed ether solutions of HN_3 and AlH_3 (molar ratio 3:1) [11] or GaH_3 [12] yield $Al(N_3)_3$ or $Ga(N_3)_3$ and H_2 during melting. The trialkylamine adducts of AlH_3 yield $(NR_3H)Al(N_3)_4$ and $(NR_3H)_2Al(N_3)_5$ under the same conditions [11]. The substitution of all H atoms in $LiAlH_4$ and $Al(BH_4)_3$ by HN_3 in ether solution with formation of $LiAl(N_3)_4$ and $Al[B(N_3)_4]_3$ was mentioned [13].

CO_2. CO. C_3O_2. The photolysis of HN_3 or DN_3 in a CO_2 matrix results in dissociation to NH (ND) and N_2 and in NH reacting with CO_2 yielding HNO (DNO) and CO [14]. The vacuum UV-photolysis of HN_3 in a CO matrix yields a high concentration of NCO, a considerable amount of HCO, and some HNCO [15]. Mercury light yields mainly HNCO, some HCO, and a trace of HOCN [16]. Photolysis of a gaseous mixture of HN_3 and C_3O_2 at 193 nm yields the primary product $CN(B\ ^2\Sigma)$ via the initially formed radicals C and N_3 [17].

ClCN. BrCN. Treating ClCN with a solution of HN_3 yields 5-azido-tetrazole [18]. The reaction of excess HN_3 in ether solution with BrCN at ~330 K stops at the stage of 5-bromotetrazole [19].

SiH_4. HN_3 does not react with SiH_4 below 298 K in the gas phase and in ether solution [20].

$SnCl_2$. The reduction of the mixture of $H^{15}NNN$ and $HNN^{15}N$ by $SnCl_2$ in acidic solution yields mainly NH_3 and N_2 and some N_2H_4. The reaction proceeds without scrambling of the nitrogen atoms; half of the ^{15}N atoms appear in NH_3 and the other half in N_2 [21, 22].

NH. NH_2. The intermediate formation of NH and NH_2 during photolysis of HN_3 in organic solvents is frequently proposed to explain the formation of organic products and the by-product NH_3; see [23, 24] for examples.

N_2H_4. Bubbling moist HN_3 in N_2 through an aqueous solution of N_2H_4 yields suspended crystals of $N_2H_5N_3$ in a safe reaction. The product can be filtered and dried [25]; see also p. 180. The reaction can also be carried out with pure N_2H_4 or with aqueous solutions of both reactants [26].

NH_3. For the formation of NH_4N_3, see p. 172. The admixture of NH_3 to gaseous HN_3 before decomposition in a glow discharge increases the amount of N_2H_4 formed (and isolated as $N_2H_5N_3$) by a factor ten to yield 3 to 4% [27]. The presence of NH_3 during the photolysis of HN_3 in CH_3OH solution at 195 K also raises the yield of N_2H_4 [28].

N_2O. The photolysis of HN_3 (DN_3) in an N_2O matrix induces dissociation to NH (ND) and N_2 and formation of HNO (DNO) [14].

NO. Condensation of HN_3-NO mixtures in Ar at 12 K to a moderate extent results in formation of a product which is believed to be an adduct of the starting materials. Reactions via $NH(^1\Delta)$ are induced by photolysis [29]; see "Nitrogen" Suppl. Vol. B 1. The photolysis of HN_3 and NO in SF_6 at ambient temperature yields N_2O and H_2O. The reaction involves the intermediate formation of $NH(^1\Delta)$. The decrease of as-formed N_2O with the ratio of $NO:HN_3$ is counterbalanced by an increase in the yield of H_2O [30].

$NOSO_3H$. An ethereal solution of HN_3 and $NOSO_3H$ in H_2SO_4 at 213 to 223 K forms thermally instable NON_3 in low yield [31].

NO_2. The reaction $HN_3+2\ NO_2 \rightarrow N_2O+N_2+HNO_3$ in the gas phase is first order in HN_3 and second order in NO_2. The rate constant is $2.28 \times 10^6\ L^2 \cdot mol^{-2} \cdot s^{-1}$ at 293 K and changes with $\log k = -1.18+2212/T$ between 293 and 323 K. The decrease of the reaction rate with increasing temperature yields an activation energy of −42.3 kJ/mol which indicates a preceding, exothermal equilibrium reaction. The rate of the reaction is not influenced by the presence of dry air or the size of the surface [32].

HNO_2. NO_2^-. The well-known reaction $HN_3+HNO_2 \rightarrow N_2O+N_2+H_2O$ proceeds with N in HNO_2 becoming the central N in N_2O, while the terminal N in N_2O stems from a terminal position of the N_3 group in HN_3. The other terminal and the central N atoms of HN_3 become N_2, as demonstrated with ^{15}N-labeled reactants [33]. The rate v of the reaction is given by $v=k_a[HNO_2]^2$ at $[H^+]<0.04$ mol/L in $HClO_4$ solution. The rate constant is $k_a=0.80+33.7[H^+]\ L \cdot mol^{-1} \cdot s^{-1}$ at 273 K. The rate in moderately acidic solution at $[H^+]>0.1$ mol/L can be described by $v=k_b[HN_3][HNO_2][H^+]$ with $k_b=33.7\ L^2 \cdot mol^{-2} \cdot s^{-1}$ at 273 K. The rate-determining steps for both rate laws were discussed [34]. A later investigation gave a value of $k_b=160\ L^2 \cdot mol^{-2} \cdot s^{-1}$ at 298 K in agreement with the earlier value [35]. A value of $253\ L^2 \cdot mol^{-2} \cdot s^{-1}$ at 298 K and higher acidity and the rate constant at 273 K yield an approximate activation energy of 54.5 kJ/mol. The dependence of the rate constant on the Hammett parameter of $HClO_4$ was also described [36].

The efficiency of the nitrite trap HN_3 increases strongly with the concentration of H^+ and less strongly with that of the nucleophilic catalyst Br^- [37]. Other nucleophilic catalysts are Cl^-, SCN^-, and $(NH_2)_2CS$. Their effect was attributed to the intermediate formation of NO^+ adducts with HNO_2 in the presence of acid. The results of the kinetic investigations are described in [35].

HNO_3. The oxidation of HN_3 by moderately concentrated HNO_3 at 370 K is described by $HN_3+0.486\ HNO_3 \rightarrow 1.15\ N_2+0.27\ NO+0.46\ N_2O+0.73\ H_2O$ from an analysis of the gases formed and based on the fact that NH_4^+ is absent. The reaction is first order in HN_3. The rate increases linearly from 5.1 min^{-1} at $[HNO_3]=6.21$ mol/L to 249 min^{-1} at $[HNO_3]=10.7$ mol/L. The activation energy is 89 kJ/mol [38]. There is practically no oxidation of HN_3 in diluted HNO_3 even in the presence of Tc^{VII} ions. However, the reaction is initiated by adding a small quantity of N_2H_4. The oxidation of HN_3 by HNO_3 is initially the main process; reduction of Tc^{VII} and oxidation of N_2H_4 are less important. An $N_2H_5NO_3:HN_3$ ratio of 1.5 to 2.0 is established; it remains constant during further oxidation [39].

The reaction of HN_3 and HNO_3 in strong H_2SO_4 at 298 K yields N_2 (containing NO) and N_2O [40]. The stoichiometry can be formulated $4\ HN_3 + 2\ NO_2^+ \rightarrow 4\ N_2 + 3\ N_2O + H_2O + 2\ H^+$; the intermediately formed NO_2^+ was deduced from polarographic measurements [41].

N_2F_4. Flash photolysis of gaseous HN_3 and N_2F_4 mixtures in ratios from 2 to 0.1 at 5 Torr of N_2F_4 yields NF_3 with excess N_2F_4. The intermediates NH, NF, NF_2, and vibrationally excited HF were detected [42].

$SbCl_5$. Undiluted HN_3 and $SbCl_5$ at 255 to 278 K form a precipitate of the adduct $HN_3 \cdot SbCl_5$ which eliminates HCl at ambient temperature. The reaction of a large excess of HN_3 with $SbCl_5$ during warming the cooled CH_2Cl_2 solution proceeds via $4\ HN_3 + SbCl_5 \rightarrow NH_4SbN_3Cl_5 + 4\ N_2$. A maximum yield of 53% is achieved with the reactant ratio given by the equation; the product and NH_4SbCl_6 precipitate from the solution. At a ratio of $HN_3:SbCl_5$ of 2:1 or less the products form via $4\ HN_3 + 2\ SbCl_5 \rightarrow NH_4SbCl_6 + 1/2\ [SbN_3Cl_4]_2 + 4\ N_2$. The product is isolated after filtering the precipitated ammonium salt [43].

H_2O. The reaction of HN_3 (DN_3) and dissociated H_2O in the gas phase yields the primary products NH (ND) and N_2 and the secondary product NH_2 (ND_2) [45].

H_2S. The reaction of HN_3 with a saturated solution of H_2S in diluted H_2SO_4 requires a minimum concentration of ~2 mol/L in HN_3 to start and yields a precipitate of sulfur. The effervescent N_2 corresponds to 15 to 30% yield with respect to the initial concentration of H_2S; only a trace of NH_3 forms. The equation for the reaction is unknown [46].

H_2SO_4. Hydrazine sulfate was detected when HN_3 was bubbled through concentrated H_2SO_4 [47]. The decomposition of HN_3 in aqueous H_2SO_4 is first order in HN_3; the acid-catalyzed process starts with formation of $H_2N_3^+$. The rate constant at 333 K decreases from $k = 5.12 \times 10^{-3}\ min^{-1}$ in 73.8 to 83.6% H_2SO_4 to $4.72 \times 10^{-3}\ min^{-1}$ in 95.1 to 98.7% H_2SO_4. The activation energy at 323 to 353 K changes from 130.5 kJ/mol in 75.9% H_2SO_4 to 97.1 kJ/mol in 86.3% H_2SO_4 and to 82.8 kJ/mol in 96.3% H_2SO_4 which may result from a partial change in the mechanism of decomposition [48]. The decomposition of DN_3 in 67 to 98% D_2SO_4 is similar to that of HN_3 and has a rate constant of $1.86 \times 10^{-2}\ min^{-1}$ at 333 K [49].

HF. The protonation of HN_3 in HF solution requires (roughly) equimolar quantities of the Lewis acids BF_3, AsF_5, or SbF_5. The protonation takes place when the frozen mixtures are warmed from 77 K to ambient temperature. The aminodiazonium salts $H_2NNN^+Y^-$ formed with $Y = BF_4$, AsF_6, and SbF_6 can be isolated by evaporating the volatiles [63]; see also p. 156.

HCl. The protonation of HN_3 in CH_2Cl_2 solution at 195 K by gaseous HCl requires an equimolar quantity of $SbCl_5$. $H_2NNNSbCl_6$ thus formed precipitates and can be isolated at 263 K [44]; see also p. 156.

HI. The reduction of ^{15}N end-labeled HN_3 by aqueous HI yields a mixture of NH_3, N_2, some N_2H_4, and I_2. The reaction proceeds without scrambling of the nitrogen atoms; half of the ^{15}N atoms are converted to NH_3 and the other half to N_2 [21, 22].

BrO_3^-. The redox reaction of HN_3 with BrO_3^- yields considerable amounts of N_2 and N_2O [50]. The oxidative part of the reaction with excess HN_3 in aqueous $HClO_4$ is $2\ HN_3 + H_2O \rightarrow 2\ N_2 + N_2O + 4\ H^+ + 4\ e^-$, while BrO_3^- is reduced to BrO^- which then is scavenged by added allyl alcohol. A tracer study with ^{18}O revealed that most of the O in

N_2O is derived from the solvent. The reaction is first order in both reactants. The rate law is $-d[BrO_3^-]/dt = k_0[BrO_3^-][HN_3][H^+]$ with $k_0 = 0.0622(6)$ $L^2 \cdot mol^{-2} \cdot s^{-1}$ at an ionic strength of 2.0 and 298 K. Experiments at 283 to 305 K yield the activation energy of 59.0 ± 0.8 kJ/mol, the enthalpy of activation of 56.5 ± 0.8 kJ/mol, and the entropy of activation of -78.2 ± 2.5 $J \cdot mol^{-1} \cdot K^{-1}$. The stoichiometry of the reaction becomes very complicated at $[HN_3]:[BrO_3^-] < 2.00$ and higher oxidation states of nitrogen are produced [51].

XeF_2. The mixture of HN_3 and XeF_2 in He reacts within a characteristic time period of ~50 s with formation of HF, N_2, and Xe. The photoinitiation of a reaction in the gaseous mixture of HN_3 and excess XeF_2 in He produces the excited species XeF(B), XeF(C), NF(a), N_2(b), and NH(A) [52]. See p. 94 for the application of the reaction in lasers.

$[Cr(NH_3)_5H_2O]^{3+}$. The kinetics of the formation of $[Cr(NH_3)_5N_3]^{2+}$ was investigated at pH 2.5 to 4.5, where HN_3 is mostly undissociated. The product forms simultaneously via: (1) $[Cr(NH_3)_5H_2O]^{3+} + N_3^- \rightarrow [Cr(NH_3)_5N_3]^{2+} + H_2O$ with $k_1 = 3.2 \times 10^{-4}$ $L \cdot mol^{-1} \cdot s^{-1}$ and (2) $[Cr(NH_3)_5H_2O]^{3+} + HN_3 \rightarrow [Cr(NH_3)_5N_3]^{2+} + H^+ + H_2O$ with $k_2 = 6.1 \times 10^{-6}$ $L \cdot mol^{-1} \cdot s^{-1}$ at 323 K and an ionic strength of 1.0 mol/L. The rate constants k_1 and k_2 were calculated from the overall rate constant and the dissociation constant of HN_3. Parameters of activation are $\Delta H_1^{\ddagger} = 96.2 \pm 1.7$, $\Delta H_2^{\ddagger} = 109.2 \pm 9.2$ kJ/mol, $\Delta S_1^{\ddagger} = -15.1 \pm 5.0$, and $\Delta S_2^{\ddagger} = -8.4 \pm 2.9$ $J \cdot mol^{-1} \cdot K^{-1}$; they were determined at 313 to 333 K [53].

$MoO(S_2L)_2$. An aqueous solution of HN_3 oxidizes $MoO(S_2CNR_2)_2$ with R = organic substituent in $CHCl_3$ or aqueous dimethylformamide in the presence of HCl. Products are N_2 and $MoO_2(S_2CNR_2)_2$ at low acidity and $MoO(Cl)_2(S_2CNR_2)_2$ at high acidity [54, 55]. The reaction of equimolar HN_3 and $MoO[S_2P(OC_2H_5)_2]$ in CH_2Cl_2 and H_2O in the presence of HCl yields N_2 and 63% of $Mo_2O_3(NH)[S_2P(OC_2H_5)_2]$. Excess HN_3 oxidizes both the metal and the ligand; the reaction yields N_2, Mo^V, $(C_2H_5O)_2P(S)SSP(S)(OC_2H_5)_2$, and NH_3 [55, 56].

MnO_4^-. The mixture of $H^{15}NNN$ and $HNN^{15}N$ is oxidized by MnO_4^- in acidic solution. Half of ^{15}N is found in thus formed HNO_3 and the other half in N_2 [21, 22].

$[Mn(2,2'\text{-bipyridine})_2]^{3+}$. The oxidation of HN_3 via $2\,HN_3 + 2\,Mn(bipy)_2^{3+} \rightarrow 2\,Mn(bipy)_2^{2+} + 3\,N_2 + 2\,H^+$ involves free radicals and probably two different Mn-azide complexes. Pseudo-first-order rate constants for $Mn(bipy)_2^{3+}$ and excess HN_3 at different $[H^+]$ are listed. A kinetic model of the reaction and the calculated parameters of activation are given [57].

$[ReO(CN)_4H_2O]^-$. The ligand substitution $HN_3 + [ReO(CN)_4H_2O]^- \rightarrow [ReO(CN)_4N_3]^{2-}$ has a rate constant of $(6.4 \pm 0.2) \times 10^{-3}$ $L \cdot mol^{-1} \cdot s^{-1}$ at 298 K and pH < 2 in aqueous solution. The large, negative entropy of activation of -87 ± 6 $J \cdot K^{-1} \cdot mol^{-1}$ suggests an associative activation [58].

$[Co(CN)_5(H_2O)]^{2-}$. An acidic solution of HN_3 and $[Co(CN)_5(H_2O)]^{2-}$ yields $[Co(CN)_5N_3]^{3-}$. The thermal reaction at 298 K with excess HN_3 is first order in the Co complex. Experimental rate constants are listed; an activation energy of ~109 kJ/mol is given. A similar investigation of the photochemical reaction at 274 K was described; the activation energy is in the range 8 to 12 kJ/mol [59].

$[Co(en)_2(ONO)_2]^+$. The reaction of HN_3 with aqueous $[Co(en)_2(ONO)_2]^+$ (en = 1,2-diaminoethane) is supposed to take place in two consecutive steps. The initial bimolecular reaction with the rate constant k_1 is $HN_3 + [Co(en)_2(ONO)_2]^+ \rightarrow [Co(en)_2(OH)ONO]^+ + N_2O + N_2$. After immediate protonation of the complex, the bimolecular reaction $[Co(en)_2(OH_2)ONO]^{2+} + HN_3 \rightarrow [Co(en)_2(H_2O)OH]^{2+} + N_2O + N_2$ follows. Values for the rate constants in $L \cdot mol^{-1} \cdot min^{-1}$ are as follows [60]:

	cis-$[Co(en)_2(ONO)_2]^+$		*trans*-$[Co(en)_2(ONO)_2]^+$	
	10^3 k_1	10^3 k_2	10^3 k_1	10^3 k_2
at 274 K	121	26.9	–	–
at 278 K	185	39.5	58.3	12.1
at 283 K	313	69.5	96.5	19.8
at 288 K	–	–	166	35.5
E_a in kJ/mol	68.2±0.4	67.8±4.6	69.9±2.5	71.5±5.0
$\log(A/L\cdot mol^{-1}\cdot min^{-1})$	10.3±0.3	9.5±0.9	10.1±0.5	9.7±1.0

$[Ni(2,2'\text{-bipyridine})_3]^{3+}$. The oxidation of HN_3 is given by $2\ HN_3+2\ [Ni(bipy)_3]^{3+} \rightarrow 2\ [Ni(bipy)_3]^{2+}+3\ N_2+2\ H^+$. The rate law is $k[HN_3][Ni(bipy)_3^{3+}][H^+]^{-1}$ with $k=104\pm4\ s^{-1}$ at 298 K. The dependence on $[H^+]$ suggests a participation of N_3^- in the rate-determining step. Investigations at 290 to 309 K yield the overall parameters of activation $\Delta H^{\ddagger}=51\pm3$ kJ/mol and $\Delta S^{\ddagger}=-36\pm10\ J\cdot mol^{-1}\cdot K^{-1}$. The large value of the entropy of activation stems from the transfer of a proton from HN_3 to the aqueous solution [61].

$[Ru(NH_3)_5(H_2O)]^{2+}$. A two-electron reduction of HN_3 proceeds via $HN_3+2\ H^++2\ [Ru(NH_3)_5(H_2O)]^{2+} \rightarrow [Ru(NH_3)_6]^{3+}+[Ru(NH_3)_5(H_2O)]^{3+}+N_2+H_2O$ in acidic solution. The additional product NH_3 substitutes H_2O in half of the Ru complexes [62].

References:

[1] Gray, P.; Waddington, T. C. (Trans. Faraday Soc. **53** [1957] 901/8).
[2] Mautner, F. A.; Krischner, H.; Kratky, C. (Z. Naturforsch. **41b** [1986] 935/7).
[3] Krischner, H.; Maier, H. E. (Z. Anorg. Allg. Chem. **460** [1980] 217/20).
[4] Mautner, F. A.; Krischner, H.; Kratky, C. (Z. Naturforsch. **43b** [1988] 497/8).
[5] Krischner, H.; Hofer, V. F. (Z. Anorg. Allg. Chem. **455** [1979] 60/4).
[6] Christe, K. O.; Wilson, W. W.; Bau, R.; Bunte, S. W. (J. Am. Chem. Soc. **114** [1992] 3411/4).
[7] Wiberg, E.; Michaud, H. (Z. Naturforsch. **9b** [1954] 497/9).
[8] Wiberg, E.; Michaud, H. (Z. Naturforsch. **9b** [1954] 499).
[9] Litzow, M.; Schaeffer, R. (Section 3 in: Schaeffer, H.; AD-701129 [1970] 66 pp.; C.A. **73** [1970] No. 41404).
[10] Müller, J.; Paetzold, P.; Boese, R. (Heteroat. Chem. **1** [1990] 461/5).

[11] Wiberg, E.; Michaud, H. (Z. Naturforsch. **9b** [1954] 495/6).
[12] Wiberg, E.; Michaud, H. (Z. Naturforsch. **9b** [1954] 502/3).
[13] Wiberg, E. (ref. 36 in: Gaylord, N. G.; Reduction with Complex Metal Hydrides, Interscience, New York 1956, p. 36).
[14] Milligan, D. E.; Jacox, M. E.; Charles, S. W.; Pimentel, G. C. (J. Chem. Phys. **37** [1962] 2302/10).
[15] Milligan, D. E.; Jacox, M. E. (J. Chem. Phys. **47** [1967] 5157/68).
[16] Milligan, D. E.; Jacox, M. E. (J. Chem. Phys. **41** [1964] 2838/41).
[17] May, D. J.; Coombe, R. D. (J. Phys. Chem. **93** [1989] 520/5).
[18] Dynamit, A. G. (Fr. 843916 [1939] from C. **1939** II 3228 and U.S. 2179783 [1939] from C.A. **1940** 1827).
[19] Oliveri-Mandala, E. (Gazz. Chim. Ital. **41** I [1911] 59/63).
[20] Wiberg, E.; Michaud, H. (Z. Naturforsch. **9b** [1954] 500).

[21] Clusius, K.; Huerzeler, H. (Helv. Chim. Acta **36** [1953] 1326/32).
[22] Clusius, K. (Angew. Chem. **66** [1954] 497/506).

[23] Kawai, J.; Tsunashima, S.; Sato, S. (Chem. Phys. Lett. **110** [1984] 655/8).
[24] Kawai, J.; Tsunashima, S.; Sato, S. (Bull. Chem. Soc. Jpn. **55** [1982] 3312/6).
[25] Pannetier, G.; Margineanu, F.; Dereigne, A.; Bonnaire, R. (Bull. Soc. Chim. Fr. **1972** 2617/22).
[26] Pannetier, G. (Ger. Offen. 2249893 [1973] 8 pp., addn. to Ger. Offen. 2128686; C.A. **79** [1973] No. 21064).
[27] Wannagat, U.; Kohnen, H. (Z. Anorg. Allg. Chem. **304** [1960] 276/95; Angew. Chem. **69** [1957] 783).
[28] Koch, E. (Tetrahedron **23** [1967] 1747/68).
[29] Yokoyama, K.; Kitaike, H.; Fueno, T. (Bull. Chem. Soc. Jpn. **64** [1991] 1731/7).
[30] Fueno, T.; Fukuda, M.; Yokoyama, K. (Chem. Phys. **124** [1988] 265/72).

[31] Lucien, H. W. (J. Am. Chem. Soc. **80** [1958] 4458/60).
[32] Seel, F.; Birnkraut, W.; Lange, E. (Chem. Ber. **94** [1961] 1436/42).
[33] Clusius, K.; Effenberger, E. (Helv. Chim. Acta **38** [1955] 1843/7).
[34] Stedman, G. (J. Chem. Soc. **1959** 2943/9).
[35] Fitzpatrick, J.; Meyer, T. A.; O'Neill, M. E.; Williams, D. L. H. (J. Chem. Soc. Perkin Trans. II **1984** 927/32).
[36] Perrott, J. R.; Stedman, G. (J. Inorg. Nucl. Chem. **39** [1977] 325/7).
[37] Ellison, G.; Williams, D. L. H. (J. Chem. Soc. Perkin Trans. II **1981** 699/702).
[38] Maya, B. M.; Stedman, G. (J. Chem. Soc. Dalton Trans. **1983** 257/9).
[39] Mashkin, A. N.; Zil'berman, B. Ya. (Radiokhimia **33** No. 2 [1991] 43/51; Sov. Radiochem. [Engl. Transl.] **33** [1991] 143/9).
[40] Masek, J. (Collect. Czech. Chem. Commun. **27** [1962] 667/79).

[41] Masek, J. (Nature **191** [1961] 166/7).
[42] Moskvitina, E. N.; Zamanskii, V. M.; Kuzyakov, Yu. Ya. (Vestn. Mosk. Univ. Khim. **29** [1974] 486/7; Moscow Univ. Chem. Bull. [Engl. Transl.] **29** No. 4 [1974] 76/7).
[43] Schmidt, A. (Z. Anorg. Allg. Chem. **381** [1971] 31/9).
[44] Schmidt, A. (Chem. Ber. **99** [1966] 2976/83).
[45] Pannetier, G.; Guenebaut, H. (Acta Chim. Acad. Sci. Hung. **18** [1959] 347/64).
[46] Lieber, E.; Kawalko, J. (Chem. Ind. **1959** 1093).
[47] Reitzner, B.; Manno, R. P. (NASA-N-63-16521 [1963] 13 pp. from C.A. **60** [1964] 6462).
[48] Agibalova, N. D.; Ostrovskii, V. A.; Koldobskii, G. I.; Enin, A. S. (Zh. Org. Khim. **9** [1973] 1580/5; J. Org. Chem. USSR [Engl. Transl.] **9** [1973] 1605/9).
[49] Shirokova, N. P.; Smirnova, T. I.; Koldobskii, G. I.; Ostrovskii, V. A.; Gidaspov, G. V. (Zh. Org. Khim. **11** [1975] 1805/8; J. Org. Chem. USSR [Engl. Transl.] **11** [1975] 1815/8).
[50] Murmann, R. K.; Sullivan, J. C.; Thompson, R. C. (Inorg. Chem. **7** [1968] 1876/9).

[51] Thompson, R. C. (Inorg. Chem. **8** [1969] 1891/4).
[52] Mead, R. D.; Baughcum, S. L.; Fisher, C. H.; Kushner, M. J.; Ewing, J. J. (Proc. SPIE Int. Soc. Opt. Eng. **875** [1988] 149/62).
[53] Castillo-Blum, S.; Sykes, A. G. (Inorg. Chem. **23** [1984] 1049/52).
[54] Maatta, E. A.; Wentworth, R. A. D. (Inorg. Chem. **17** [1978] 922/6).
[55] Edelblut, A. W.; Haymore, B. L.; Wentworth, R. A. D. (J. Am. Chem. Soc. **100** [1978] 2250/1).
[56] Edelblut, A. W.; Wentworth, R. A. D. (Inorg. Chem. **19** [1980] 2006/10).
[57] Heyward, M. P.; Wells, C. F. (J. Chem. Soc. Dalton Trans. **1988** 1331/5).
[58] Purcell, W.; Roodt, A.; Leipoldt, J. G. (Transition Met. Chem. [London] **16** [1991] 339/43).
[59] Viaene, L.; D'Olieslager, J.; De Jaegere, S. (Bull. Soc. Chim. Belg. **85** [1976] 89/102).
[60] Seel, F.; Meyer, D. (Z. Anorg. Allg. Chem. **408** [1974] 283/92).

[61] Brown, J. K.; Fox, D.; Heyward, M. P.; Wells, C. F. (J. Chem. Soc. Dalton Trans. **1979** 735/9).

[62] Sheridan, P. S.; Basolo, F. (Inorg. Chem. **11** [1972] 2721/4).

[63] Christe, K. O.; Wilson, W. W.; Dixon, D. A.; Khan, S. I.; Bau, R.; Metzenthin, T.; Lu, R. (J. Am. Chem. Soc. **115** [1993] 1836/42).

2.3.1.10.5 Reactions with Organoelement Compounds

$Be(CH_3)_2$. $Mg(C_2H_5)_2$. The reaction of pure $Be(CH_3)_2$ and cocondensed excess HN_3 in $(C_2H_5)_2O$ commences upon melting with liberation of CH_4 and precipitation of $Be(N_3)_2$ with a yield of 90.3% [1]. The analogous reaction with $Mg(C_2H_5)_2$ in ether-dioxane begins below 273 K and is complete at ambient temperature. The yields of $Mg(N_3)_2$ and C_2H_6 are nearly quantitative [2].

$Al(CH_3)_3$. Excess HN_3 and $Al(CH_3)_3$ slowly form CH_4 and a precipitate of $Al(N_3)_2CH_3$ in ether solution at ambient temperature [3].

$Tl(CH_3)_2OH$. The neutralization of HN_3 by $Tl(CH_3)_2OH$ in aqueous solution at 360 K yields $Tl(CH_3)_2N_3$ which precipitates nearly quantitatively during cooling [4].

$R_2Sn(NR'_2)_2$. $R_3SnNR'_2$. The reaction of HN_3 with $R_2Sn(NR'_2)_2$ and $R_3SnNR'_2$ (R' = organic substituent) in ether solution yields $R_2Sn(N_3)_2$ and R_3SnN_3 with $R = CH_3$, C_2H_5, n-C_4H_9, C_6H_5 nearly quantitatively. Stannanes with more than two azide groups in the molecule cannot be obtained by this method [5].

NRH_2. NR_2H. The gas phase reaction of HN_3 with $N(CH_3)H_2$, $N(C_2H_5)H_2$, and $N(CH_3)_2H$ yields the white, solid ammonium azides [6].

NR_4OH. The neutralization of aqueous solutions of NR_4OH (R = organic substituent) by gaseous HN_3 yields tetraalkyl ammonium azides. Hydroxyl groups in the substituents do not react [7].

Tris(*p*-methoxyphenyl)phosphane. The reaction of excess HN_3 and tris(*p*-methoxyphenyl)phosphane in ether at ambient temperature yields impure tris(*p*-methoxyphenyl)phosphanimine after treating the nonvolatile residue with an additional quantity of the phosphane at 430 K [8].

$P{\equiv}C(t\text{-}C_4H_9)$. The cycloaddition of HN_3 to $PC(t\text{-}C_4H_9)$ in ether solution at 293 K yields 3-*H*-1,2,3,4-triazaphosphole [9].

$Cl{\sim}P{=}C(C_6H_5)Si(CH_3)_3$. The reaction of HN_3 with $ClPC(C_6H_5)Si(CH_3)_3$ yields 3,5-diphenyl-1-*H*-1,2,4-diazaphosphole. The product seems to form by fragmentation of the primary product in the presence of traces of moisture and by cycloaddition of the fragments [10].

$Sb(CH_3)_3$. $Bi(CH_3)_3$. An ether solution of HN_3 and $Bi(CH_3)_3$ yields CH_4 and a precipitate of $Bi(CH_3)_2N_3$ with a yield of 75%. A mixture of HN_3 and $Sb(CH_3)_3$ does not react [4].

$Sb(CH_3)_2NR_2$. $Bi(CH_3)_2NR_2$. The reaction of HN_3 and $Bi(CH_3)_2N[Si(CH_3)_3]_2$ in ether at 273 K yields $N[Si(CH_3)_3]_2H$ and a crystalline precipitate of $Bi(CH_3)_2N_3$ in a yield of 86%. The analogous reaction of $Sb(CH_3)_2N(CH_3)_2$ yields $Sb(CH_3)_2N_3$ and $NH_2(CH_3)_2N_3$ [11].

References:

[1] Wiberg, E.; Michaud, H. (Z. Naturforsch. **9b** [1954] 502).

[2] Wiberg, E.; Michaud, H. (Z. Naturforsch. **9b** [1954] 501/2).

[3] Wiberg, E.; Michaud, H. (Z. Naturforsch. **9b** [1954] 497).

[4] Müller, J. (Z. Anorg. Allg. Chem. **381** [1971] 103/15).
[5] Lorberth, J.; Krapf, H.; Nöth, H. (Chem. Ber. **100** [1967] 3511/9).
[6] Kodama, S. (Bull. Chem. Soc. Jpn. **56** [1983] 2355/62).
[7] Broh-Kahn, R. H.; Fand, T. I.; Tenenbaum, L. E.; Nepera Chemical Co., Inc. (U.S. 2755291 [1956] 2 pp.; C.A. **1957** 2024).
[8] Yolles, S.; Woodland, J. H. R. (J. Organomet. Chem. **93** [1975] 297/308).
[9] Rösch, W.; Regitz, M. (Angew. Chem. **96** [1984] 898/9).
[10] Märkl, G.; Troetsch-Schaller, I.; Hölzl, W. (Tetrahedron Lett. **29** [1988] 785/8).

[11] Müller, J.; Müller, U.; Loss, A.; Lorberth, J.; Donath, H.; Massa, W. (Z. Naturforsch. **40b** [1985] 1320/6).

2.3.1.10.6 Survey of the Reactions with Organic Compounds

Being a very reactive molecule, hydrogen azide takes part in a wide variety of organic reactions. In these reactions HN_3 functions as an acid, a nucleophile, a bipolar molecule, or as a source of NH in the Schmidt reaction in the presence of concentrated H_2SO_4. The acid HN_3 forms azide salts with dissolved organic bases [1]. The formation of the azide salt in the case of pyridine goes to completion at 298 K, whereas Lewis bases like ethers, propene oxide, and acetonitrile react incompletely [2]. The following paragraphs describe the basic reactions with principal types of organic compounds; only reviews and examples of typical papers are cited.

The explosion of gaseous mixtures of HN_3 and alkanes, olefines, or arenes yields soot, unsaturated hydrocarbons, H_2, N_2, and small quantities of NH_3 and HCN [3, 4]. The photolysis of HN_3 and alkanes mainly leads to N_2 and amines which form by insertion of the intermediate NH into C-H bonds. NH_3 and H_2 are minor products [5, 6]. The decomposition of HN_3 to N_2 and NH_3 prevails in the copyrolysis with alkanes [7].

The addition of HN_3 to nonactivated alkenes with formation of the saturated azides requires drastic conditions and a catalyst. Olefinic double bonds activated by conjugated, electron-withdrawing groups like -CN, $-NO_2$, or -C(O)R react easily [8, 9]. The photolysis [10] and the pyrolysis [7] of HN_3 with alkenes yields nitriles, N_2, and decomposition products. The reaction of HN_3 with alkines usually leads to 1,2,3-triazoles. Single or double addition with formation of vinyl azides or saturated diazides are rare [8, 9]. Arenes and HN_3 form aniline derivatives directly and efficiently in the presence of trifluoroacetic acid and the strongly acidic trifluoromethanesulfonic acid [11]. The yield is frequently low in the presence of H_2SO_4 [1].

The reactions of HN_3 with cyclic alcohols to yield mixtures of ketones, amines, and products with an enlarged ring are catalyzed by H_2SO_4 [1]. Tertiary alcohols are converted to azides in the presence of acid [12] or $TiCl_4$ [13]. Aldehydes and ketones with HN_3 undergo a Schmidt-type reaction by liberating N_2 and inserting NH in the presence of H^+ or Lewis acids [14]. Ketones yield secondary amides and, in the case of cyclic ketones, lactames. Aldehydes are converted to nitriles or N-formylamines. Tetrazole derivatives result with excess HN_3 [1, 15]. However, α-azido ethers are obtained from aldehydes and HN_3 in the presence of alcohols by catalysis of $TiCl_4$ [16]. Carboxylic acids and anhydrides form amines, N_2, and CO_2 in Schmidt reactions with HN_3. Intermediates are carbamic acids which form by insertion of NH into the R-COOH bond [1, 14]. High yields result for acids of arenes [17].

Tetrazoles form by adding HN_3 to nitriles. Cyclic products also result from the addition of HN_3 to the cumulated double bonds of cyanates, thiocyanates, carbodiimines, or ketoketenes [1, 8, 18].

Sulfoxides are oxidized to sulfoximides by HN_3 in the presence of H_2SO_4 [1, 19]. The nucleophilic substitution of chloride by azide is accelerated, when the solution of HN_3 and alkyl halide is allowed to react in a column filled with acidic Al_2O_3 [20]. The exchange of halide substituents of arenes by azide requires activating groups in other positions of the aromatic system. Pyridine derivatives frequently yield tetrazoles [8]. Aromatic C-nitroso compounds and twice the molar quantity of HN_3 form the aromatic azide, N_2, and H_2O [1]. The influence of the nitrite trap HN_3 on the Fischer-Hepp rearrangement of N-nitrosoaniline [21], on its denitrosation by an excess of a secondary amine [22], and on other reactions of the starting material [23] were investigated.

References:

[1] Mason, K. G. (in: Mellor's Comprehensive Treatise on Inorganic and Theoretical Chemistry, Vol. VIII, Supplement II, Longmans, London 1967, pp. 1/15).
[2] Nelson, J.; Spratt, R.; Nelson, S. M. (J. Chem. Soc. A **1970** 583/7).
[3] Rozenberg, A. S. (Zh. Fiz. Khim. **45** [1971] 2212/5; Russ. J. Phys. Chem. [Engl. Transl.] **45** [1971] 1252/4).
[4] Rozenberg, A. S.; Arsen'ev, Yu. N.; Voronkov, V. G. (Fiz. Goreniya Vzryva **6** [1970] 302/10; Combust. Explos. Shock Waves [Engl. Transl.] **6** [1970] 271/7).
[5] Kodama, S. (Bull. Chem. Soc. Jpn. **56** [1983] 2355/62).
[6] Tsunashima, S.; Hotta, M.; Sato, S. (Chem. Phys. Lett. **64** [1979] 435/9).
[7] Richardson, W. C.; Setser, D. W. (Can. J. Chem. **47** [1969] 2725/7).
[8] Grundmann, C. (in: Houben-Weyl; Methoden Org. Chem. 4th Ed. **10** Pt. 3 [1965] 777/836, 785/804).
[9] Scherer, H.; Regitz, M. (Methodicum Chimicum, Vol. 6, Academic, New York 1975, pp. 309/36, 310/1).
[10] Cornell, D. W.; Berry, R. S.; Lwowski, W. (J. Am. Chem. Soc. **88** [1966] 544/50).

[11] Takeuchi, H.; Adachi, T.; Nishiguchi, H. (J. Chem. Soc. Chem. Commun. **1991** 1524/5).
[12] Geneste, P.; Herrmann, P.; Kamenka, J. M.; Pons, A. (C. R. Seances Acad. Sci. C **279** [1974] 1163/5).
[13] Poetsch, E.; Reiffenrath, V.; Weber, G.; Scheuble, B.; Kurmeier, H.-A.; Merck Patent GmbH (Ger. Offen. 3731619 [1988] 16 pp.; C.A. **109** [1988] No. 220242).
[14] Caronna, G. (Atti Accad. Sci. Lett. Arti Palermo I [4] **25** [1964] 47/52).
[15] Challis, B. C.; Challis, J. A. (in: Sutherland, I. O.; Comprehensive Organic Chemistry, Vol. 2, Pergamon, Oxford 1979, pp. 957/1065, 968/9, 978/9).
[16] Hassner, A.; Fibiger, R.; Amarasekara, A. S. (J. Org. Chem. **53** [1988] 22/7).
[17] Lindsay, A. J. (in: Sutherland, I. O.; Comprehensive Organic Chemistry, Vol. 2, Pergamon, Oxford 1979, pp. 131/84, 137).
[18] Grimmett, M. R. (in: Sammes, P. G.; Comprehensive Organic Chemistry, Vol. 4, Pergamon, Oxford 1979, pp. 357/410, 407/8).
[19] Johnson, C. R. (in: Neville Jones, D.; Comprehensive Organic Chemistry, Vol. 3, Pergamon, Oxford 1979, pp. 223/32, 225).
[20] Hudlicky, M. (J. Org. Chem. **39** [1974] 3460).

[21] Williams, D. L. H. (J. Chem. Soc. Perkin Trans. II **1982** 801/4).
[22] Biggs, I. D.; Williams, D. L. H. (J. Chem. Soc. Perkin Trans. II **1976** 601/5).
[23] Williams, D. L. H. (J. Chem. Soc. Perkin Trans. II **1977** 128/32).

2.3.1.11 Solutions of HN_3

2.3.1.11.1 Aqueous Solution

Heat of Solution. Gaseous HN_3 dissolves vigorously in H_2O. The experimental heat of solution is -40.6 ± 0.4 kJ/mol at ambient temperature [1]. The values of $\Delta H = -33.89 \pm 1.3$ kJ/

mol and $\Delta S = -93.3 \pm 4.6$ $J \cdot K^{-1} \cdot mol^{-1}$ at 298.15 K were calculated from vapor pressure measurements of HN_3 over its aqueous solution [2]. The decreasing volume upon mixing indicates an intermolecular interaction of HN_3 and H_2O [3].

Density. The density of aqueous HN_3 at 290 K is given by $\varrho_{290} = 0.999 + 0.212\,\alpha - 0.132\,\alpha^2 + 0.048\,\alpha^3$, where α is the weight fraction of HN_3 [3]. Experimental values at 290 ± 1 K are [3, 4]:

ϱ_{290} in g/cm^3	1.125	1.121	1.116	1.109	1.098	1.089	1.077	1.057	1.032
α	0.983	0.931	0.882	0.820	0.686	0.600	0.495	0.329	0.161

Dissociation. The pH value of aqueous HN_3 increases at 298 K from 3.0 for a 0.05 M solution to 2.8 for a 0.1 M solution, and to 2.5 for a 0.5 M solution [5]. The acid strength of HN_3 is similar to that of acetic acid. The dissociation constant pK_a of HN_3 decreases linearly with increasing temperature [6] and changes with ionic strength μ as follows:

pK_a	T in K	μ in mol/L	method	Ref.
4.70 ± 0.02	293	0 (extrapolated)	potentiometric titration with HCl	[6]
4.64 ± 0.02	299	0 (extrapolated)		
4.58 ± 0.04	306	0 (extrapolated)		
4.47 ± 0.11	295	1.0	potentiometric titration with $HClO_4$	[7]
4.36 ± 0.15	313	1.0		
4.30 ± 0.15	323	1.0		
4.25 ± 0.24	333	1.0		
4.261 ± 0.031	298	0.5	potentiometric titration with HCl	[8]
4.44	298	1	potentiometric titration with $HClO_4$	[9]
4.79	298	3		

Individual values of pK_a at 298 K in [10 to 13] agree with these results. A pK_a value for DN_3 of 5.0 ± 0.5 at 293 K, extrapolated to zero ionic strength, was determined potentiometrically [11].

The rate constant of the dissociation of HN_3 of 1.15×10^6 s^{-1} was calculated from the dissociation constant and the rate of H^+ and N_3^- recombination. It has a rate constant of $(6.0 \pm 1.6) \times 10^{10}$ $L \cdot mol^{-1} \cdot s^{-1}$ which was determined by a relaxation method [14].

Approximate [6] thermodynamic data of the dissociation of HN_3 in H_2O were calculated from the temperature dependence of the dissociation constant at 293 to 333 K [6, 7]; the calorimetric value of ΔH from the reaction of NaN_3 and HCl in water and an earlier dissociation constant were used in [15]:

ΔG in kJ/mol	ΔH in kJ/mol	ΔS in $J \cdot mol^{-1} \cdot K^{-1}$	Ref.
26.6 ± 2.5	15.9	−36.0	[6]
24.77	15.06 ± 0.21	−32.64	[15]
–	10.92 ± 0.33	−48.5 ± 1.3	[7]

Other thermodynamic data of aqueous HN_3 are given on p. 115.

Vapor Pressure. Henry's Law Constant. The vapor pressure of HN_3 over the aqueous solution rises with temperature and concentration from 1.8 Torr for a 0.1023 molal solution at 273.15 K to 228.8 Torr at 322.61 K for a 1.397 molal solution [2]. The partition coefficients (Henry's law constants) $\kappa' = p(HN_3)/[HN_3]$ in Torr·L/mol of 51 at 291 K [16], 84 at 298 K [17], 76 at 303 K [18], and 120 at 308 K were determined [17]. A smaller constant in $HClO_4$ at $[HClO_4] > 8$ mol/L results from the protonation of HN_3 [18]. The Henry's law constant of HN_3 in aqueous HNO_3 at 298 to 333 K increases moderately with the concentration of HNO_3 and agrees well with older results [19].

Basicity. The protonation of HN_3 in H_2SO_4 of 68% or more yields the thermodynamic constant pK_a for $H_2N_3^+ \rightleftharpoons HN_3 + H^+$, when the acidity function H_0 of the solvent is taken into consideration. The determination by various methods gives agreeing results [20]:

pK_a	T in K	method	Ref.
−7.19	298	UV absorption	[20]
−6.6 (−7.02*⁾)	303	pressure of the vapor over the solution	[18]
−6.21 (−6.9*⁾)	298	distribution $HCCl_3$-aqueous H_2SO_4	[21]
−6.6	283	kinetics of reaction with acetone	[22]

*⁾ The values in parentheses were recalculated in [20] to the H_0 scale of acidity.

The corresponding thermodynamic constant of DN_3 is −7.56 at 298 K and was determined by UV spectroscopy in D_2SO_4-D_2O [23].

References:

[1] Günther, P.; Meyer, R.; Müller-Skjold, F. (Z. Phys. Chem. A **175** [1935] 154/69).
[2] D'Orazio, L. A.; Wood, R. H. (J. Phys. Chem. **67** [1963] 1435/8).
[3] Kurbangalina, R. Kh.; Yakovleva, G. S. (Zh. Fiz. Khim. **43** [1969] 2649/50; Russ. J. Phys. Chem. [Engl. Transl.] **43** [1969] 1490/1).
[4] Kurbangalina, R. Kh.; Patskov, E. A.; Stesik, L. N.; Yakovleva, G. S. (PMTF Zh. Prikl. Mekh. Tekh. Fiz. **1970** No. 4, 160/5; J. Appl. Mech. Tech. Phys. [Engl. Transl.] **1970** 672/7).
[5] Oguma, K.; Maruyama, T.; Kuroda, R. (Anal. Chim. Acta **74** [1975] 339/45).
[6] Boughton, J. H.; Keller, R. N. (J. Inorg. Nucl. Chem. **28** [1966] 2851/9).
[7] Castillo-Blum, S.; Sykes, A. G. (Inorg. Chem. **23** [1984] 1049/52).
[8] Hirata, R.; Do Amaral, L. (An. Acad. Bras. Cienc. **54** [1982] 77/86).
[9] Maggio, F.; Romano, V.; Pellerito, L. (Ann. Chim. [Rome] **57** [1967] 191/202).
[10] McDonald, J. R.; Rabalais, J. W.; McGlynn, S. P. (J. Chem. Phys. **52** [1970] 1332/40).

[11] Bunn, D.; Dainton, F. S.; Duckworth, S. (Trans. Faraday Soc. **57** [1961] 1131/9).
[12] Burns, E. A.; Chang, F. D. (J. Phys. Chem. **63** [1959] 1314/7).
[13] Wells, C. F.; Salam, M. A. (J. Chem. Soc. A **1968** 1568/75).
[14] Auborn, J. J.; Warrick, P., Jr.; Eyring, E. M. (J. Phys. Chem. **75** [1971] 3026/8).
[15] Gray, P.; Waddington, T. C. (Proc. R. Soc. London A **235** [1956] 106/19).
[16] Feitknecht, W.; Sahli, M. (Helv. Chim. Acta **37** [1954] 1431/6).
[17] Lamnevik, S. (Symp. Chem. Probl. Connected Stab. Explos. 1967 [1968] 21/33; C.A. **70** [1969] No. 98403).
[18] Templeton, J. C.; King, E. L. (J. Am. Chem. Soc. **93** [1971] 7160/6).
[19] Maya, B. M.; Stedman, G. (J. Chem. Soc. Dalton Trans. **1983** 257/9).
[20] Agibalova, N. D.; Ostrovskii, V. A.; Koldobskii, G. I.; Enin, A. S. (Zh. Org. Khim. **9** [1973] 1580/5; J. Org. Chem. USSR [Engl. Transl.] **9** [1973] 1605/9).

[21] Bak, T. A.; Praestgaard, E. L. (Acta Chem. Scand. **11** [1957] 901/2).

[22] Ostrovskii, V. A.; Enin, A. S.; Koldobskii, G. I.; Bagal, L. I. (Zh. Org. Khim. **8** [1972] 456/9; J. Org. Chem. USSR [Engl. Transl.] **8** [1972] 460/2).

[23] Shirokova, N. P.; Smirnova, T. I.; Koldobskii, G. I.; Ostrovskii, V. A.; Gidaspov, B. V. (Zh. Org. Khim. **11** [1975] 1805/8; J. Org. Chem. USSR [Engl. Transl.] **11** [1975] 1815/8).

2.3.1.11.2 HN_3 in Organic Solvents and Their Mixtures with Water

The preparation of solutions of HN_3 in $(C_2H_5)_2O$ [1], CH_2Cl_2, and $CHCl_3$ [2] by acidification of aqueous NaN_3 in the presence of the organic solvent was described. The codistillation of HN_3 and $(C_2H_5)_2O$ or CH_2Cl_2 requires appropriate precautions [2].

Contacting HN_3 in aqueous HNO_3 with tributyl phosphate (TBP) in dodecane extracts most HN_3 into the organic phase. The extraction is enhanced by the adduct formed by HN_3 and TBP [3]. This process is described by $HN_3+TBP \rightleftharpoons HN_3 \cdot TBP$ and has an average constant of extraction of $K_{av}=[HN_3(org)]/[HN_3(aq)][TBP(org)]=10.6 \pm 1.6$ L/mol for an excess of 30% TBP in dodecane, probably at ambient temperature. The constant of extraction decreases to around 9 L/mol when HNO_3 is added to the solution, whereas $UO_2(NO_3)_2$ has no effect. The composition of the adduct was confirmed by measuring the dependence of the distribution coefficient on the concentration of TBP [4]. Stability constants for $HN_3(l)+TBP(l) \rightleftharpoons HN_3 \cdot TBP(l)$ in hexadecane from ~100 L/mol at 298 K to ~40 L/mol at 338 K were determined by a gas-chromatographic method. The constants yield $\Delta H° = -19.2$ kJ/mol and $\Delta S° = -26.3$ $J \cdot K^{-1} \cdot mol^{-1}$ for the formation of the complex [5].

The distribution coefficients of HN_3 at 294 K are 0.69 for $HCCl_3$-H_2O and 7.3 for $(C_2H_5)_2O$-H_2O [6]. Thermodynamic parameters for the transfer of HN_3 from water to mixtures of 10 to 40% dioxane in water at 298 K were calculated from the standard potentials of the $Ag|AgN_3$ electrode in the mixtures [7].

The dissociation constant $pK_a = 7.9 \pm 0.2$ was determined for HN_3 in dimethyl sulfoxide (DMSO) at 298 K by titration of NaN_3 with *p*-toluene sulfonic acid [8]. A pK_a value of 7.5 at 298 K was used in [9]; the linear change from pK_a in water to pK_a in DMSO with addition of DMSO to the aqueous solution was mentioned.

References:

[1] Grundmann, C. (in: Houben-Weyl; Methoden Org. Chem. 4th Ed. **10** Pt. 3 [1965] 777/836, 782).

[2] Hassner, A. (in: Houben-Weyl; Methoden Org. Chem. 4th Ed. E **16**a [1990] 1243/90, 1245).

[3] Kelmers, A. D.; Browning, D. N. (Inorg. Nucl. Chem. Lett. **13** [1977] 505/10).

[4] Zil'berman, B. Ya.; Lelyuk, G. A.; Mashkin, A. N.; Fedorov, Yu. S. (Radiokhimia **31** No. 5 [1989] 53/7; Sov. Radiochem. [Engl. Transl.] **31** [1989] 574/7).

[5] Furton, K. G.; Purnell, J. H.; Stedman, G. (J. Chem. Soc. Faraday Trans. **86** [1990] 3561/5).

[6] Sandell, K. B. (Naturwissenschaften **51** [1964] 336).

[7] Das, R. C.; Misra, M. K.; Nanda, B. K. (J. Chem. Soc. Faraday Trans. I **78** [1982] 3485/92).

[8] Ritchie, C. D.; Uschold, R. E. (J. Am. Chem. Soc. **89** [1967] 1721/5).

[9] Krishnamoorthy, G.; Prabhananda, B. S. (Proc. Indian Acad. Sci. Chem. Sci. **95** [1985] 337/44).

2.3.2 The Hydrogen Azide Cation, HN_3^+

CAS Registry Numbers: HN_3^+ *[58852-14-5]*, DN_3^+ *[58852-15-6]*

The formation of HN_3^+ and DN_3^+ was observed during mass spectrometric (p. 134) and photoelectron (PE) spectroscopic investigations (p. 98) on hydrazoic acid. The number of PE bands observed is consistent with the bent N_3 group in the cations [1, 2] and with C_s symmetry. The following electronic term energies T_0 in cm^{-1} of both ions were obtained [3] from the PE spectra [1, 2, 4] in the gas phase:

state	$\tilde{X}\,^2A''$	$\tilde{A}\,^2A'$	$\tilde{B}\,^2A'$	$\tilde{C}\,^2A'$	$\tilde{D}\,^2A''$	$\tilde{E}\,^2A'$
T_0	0	7750(320)	38000(320)	48890(320)*)	77130(1000)*)	87620(1000)*)

*) From the vertical ionization potential.

The fundamental vibrations of the cations were assigned on the basis of the vibrational splitting of the first three PE bands by comparison with the fundamentals of the parent molecules. Frequencies in cm^{-1} and the PE band of their origin (in parentheses) given on p. 98 are as follows:

cation	ν_1	ν_2	ν_3	ν_4	ν_5	Ref.
HN_3^+	3320 ($\tilde{X}$)	2060 ($\tilde{X}$), 2360 ($\tilde{B}$)	940 ($\tilde{X}$), 930 ($\tilde{B}$)	460 ($\tilde{A}$)	540 ($\tilde{B}$)	[5]
	~2260 ($\tilde{B}$)	–	~980 ($\tilde{X}$)	890 ($\tilde{B}$)	~570 ($\tilde{A}$), 560 ($\tilde{B}$)	[4]
	–	1850 ($\tilde{X}$)	850 ($\tilde{X}$)	–	480 ($\tilde{A}$), 570 ($\tilde{B}$)	[2]
DN_3^+	2440 ($\tilde{X}$)	2060 ($\tilde{X}$), 2380 ($\tilde{B}$)	930 ($\tilde{X}$), 890 ($\tilde{B}$)	320 ($\tilde{A}$)	520 ($\tilde{B}$)	[5]
	–	1850 ($\tilde{X}$)	850 ($\tilde{X}$)	–	400 ($\tilde{A}$), 490 ($\tilde{B}$)	[2]

Vibrational progressions in the PE band $\tilde{B}$ of 2380 and 930 cm^{-1} for HN_3^+ and 2300 and 900 cm^{-1} for DN_3^+ were assigned to combination bands [2]. Some bands of both cations are also given in [1]; earlier results for HN_3^+ are described in [6].

References:

[1] Cradock, S.; Ebsworth, E. A. V.; Murdoch, J. D. (J. Chem. Soc. Faraday Trans. II **68** [1972] 86/100).

[2] Bastide, J.; Maier, J. P. (Chem. Phys. **12** [1976] 177/90).

[3] Jacox, M. E. (J. Phys. Chem. Ref. Data **17** [1988] 269/511, 376/7).

[4] Lee, T. H.; Colton, R. J.; White, M. G.; Rabalais, J. W. (J. Am. Chem. Soc. **97** [1975] 4845/51).

[5] Cvitas, T.; Klasinc, L. (J. Chem. Soc. Faraday Trans. II **72** [1976] 1240/4).

[6] Eland, J. H. D. (Philos. Trans. R. Soc. London A **268** [1970] 87/96).

2.3.3 Cyclotriazene (Triazirine), c-N_3H, and Ions

CAS Registry Numbers: c-N_3H *[157-29-9]*, c-N_3H^{2+} *[84988-32-9]*

The cyclic isomer of linear HN_3 is **triazirine**; it has an N_α-N_β double bond opposite to the NH group, and the H atom is bent out of the $NN_\alpha N_\beta$ plane (C_s symmetry). Neither c-N_3H nor organic derivatives seem to have been detected spectroscopically [1]. However, an intermediate formation of c-N_3H was suggested based on the scrambling of nitrogen isotopes during the formation of HN_3 via the reaction of $^{15}N_2H_4$ with excess HNO_2 [2].

An MP3 (third-order Møller-Plesset perturbation theory) calculation predicts that the triazirine ground state is 126 kJ/mol more energetic than the ground state of linear HN_3 [3]. An ab initio SCF CI calculation predicts an excess energy of ~230 kJ/mol for triazirine; thus, immediate dissociation into NH and N_2 can be expected [4]. An MP2 calculation did not yield a minimum for c-N_3H on the potential energy surface [5].

Optimized geometries for the triazirine ground state with C_s symmetry and for the energetically less favorable, planar isomer with C_{2v} symmetry were calculated at the SCF/6-31G* level [1] and were confirmed for the energetically favorable isomer in [3]; distances in Å and angles in degree (where Φ is the angle of the N-H bond relative to the N_3 plane) are as follows [1]:

symmetry	$r(N-N_{\alpha,\beta})$	$r(N_\alpha-N_\beta)$	$r(N-H)$	$\angle N_\alpha NN_\beta$	$\angle NN_\alpha N_\beta$	$\angle N_\alpha NH$	Φ
C_s	1.489	1.161	1.007	45.9	67.0	104.6	74.1
C_{2v}	1.402	1.189	0.983	50.1	64.9	154.9	0

The inversion barrier for the H-carrying nitrogen via the planar state was calculated by using the MP2 and MP3 methods with various extended 6-31G basis sets to be 234 to 251 kJ/mol. The ground state is stabilized by the stronger N_α-N_β bond and a simultaneous decrease in the N-N_α and N-N_β π-antibonding character of this molecular orbital [1]. The nonaromatic character of c-N_3H is evidenced by a ring current index of 1.240 which was calculated by the semiempirical SINDO1 method [6]. Calculated dipole moments are 1.77 [3] and 1.69 D for c-N_3H in the ground state and 1.61 D in the planar state [1]. A protonation energy of 774 to 787 kJ/mol was calculated for the NH group of c-N_3H in the nonplanar ground state [1]. Molecular data were also calculated at the HF level [7].

A calculation with the semiempirical SINDO1 method yields a ring current index of 1.720 for **c-N_3H^{2+}** indicative of an aromatic ion. The anion **c-N_3H^{2-}** was found to be unstable, however [6].

References:

[1] Alcami, M.; De Paz, J. L. G.; Yáñez, M. (J. Comput. Chem. **10** [1989] 468/78).
[2] Phelan, K. G.; Stedman, G. (J. Chem. Soc. Chem. Commun. **1981** 299/300).
[3] Chaban, G. M.; Klimenko, N. M.; Charkin, O. P. (Zh. Neorg. Khim. **37** [1992] 191/5; Russ. J. Inorg. Chem. [Engl. Transl.] **37** [1992] 102/4).
[4] Sevin, A.; Le Roux, J. P.; Bigot, B.; Devaquet, A. (Chem. Phys. **45** [1980] 305/14).
[5] Zavoruev, S. M.; Rakauskas, R.-I. I. (Astron. Zh. **66** [1989] 1013/23).
[6] Jug, K. (J. Org. Chem. **48** [1983] 1344/8).
[7] Lathan, W. A.; Radom, L.; Hariharan, P. C.; Hehre, W. J.; Pople, J. A. (Fortschr. Chem. Forsch. **40** [1973] 1/45).

2.3.4 The Triazenyl Radical, N_3H_2, and Ions

The Radicals 1-Triazenyl, H_2NNN, and 2-Triazenyl, HNNNH

CAS Registry Numbers: H_2NNN *[73947-29-2]*, HNNNH *[73947-28-1]*

The N_3H_2 radical is supposed to form intermediately during the reaction of HN_3 with H atoms; see p. 135. An ab initio SCF calculation on this reaction gave an activation barrier of 18 kJ/mol and an enthalpy change of −268 kJ/mol for the formation of H_2NNN. The radical is unstable; the decomposition to $NH_2(\tilde{X}\,^2B_1)$ and N_2 is most favorable and associated with an enthalpy change of −177 kJ/mol [1]. Ab initio calculations for the first electronically excited Σ state showed that H_2NNN is more stable than the HNNNH isomer by 128 kJ/mol. The Σ state of HNNNH is 66.9 kJ/mol higher in energy than the Π ground state [2]. Geometric parameters for the flat radicals from ab initio calculations (CI/STO-3G [2] and HF/4-31G [1]) are as follows:

isomer	state	distances in Å N_α-N_β	 N_β-N_γ	 H-N_α	angles in degree $N_\alpha N_\beta N_\gamma$	 HNN	Ref.
$H_2N_\alpha N_\beta N_\gamma$	–	1.352	1.227	0.991, 0.985*⁾	120.2	121.6, 115.8*⁾	[1]
$H_2N_\alpha N_\beta N_\gamma$	Σ	1.40	1.28	–	117	–	[2]
$HN_\alpha N_\beta N_\gamma H$	Π	1.39	1.39	–	107	102	[2]
$HN_\alpha N_\beta N_\gamma H$	Σ	1.32	1.32	–	126	107	[2]

*⁾ For the H substituent in trans arrangement with respect to the terminal nitrogen.

The Triazadienium Ion, $N_3H_2^+$

CAS Registry Numbers: $N_3H_2^+$ *[85990-23-4]*, H_2NNN^+ *[43422-90-8]*, D_2NNN^+ *[43422-91-9]*

Formation. Gaseous $N_3H_2^+$ is obtained by protonation of HN_3 under the conditions of chemical ionization mass spectrometry. Protonations by H_3O^+ and HN_3^+ are moderately and those with H_3^+ are highly exothermal. Other reactants are CH_5^+ and protonated $C_2H_5N_3$. Tandem mass spectrometric techniques involving collisionally activated dissociation (CAD) and metastable ion kinetic energy (MIKE) were used to investigate the isomers formed. The moderately exothermal reactions yield only one isomer of $N_3H_2^+$, probably the aminodiazonium ion H_2NNN^+, as indicated by the almost exclusive formation of the fragment NH_2^+. The formation of an additional isomer in the reactions of high exothermicity is suggested by the fragment N_2H^+ which is assigned to the iminodiazenium ion $HNNNH^+$ in line with the energies calculated for the isomers (see below) [3].

Protonation of HN_3 by superacids in SO_2ClF solution yields the aminodiazonium ion H_2NNN^+; see p. 135. This cation is also obtained from $(CH_3)_3SiN_3$ and HSO_3F-SbF_5 (6:1) in SO_2ClF solution at 195 K. The in situ formation of the cation from $(CH_3)_3SiN_3$ or NaN_3, a 1.1 molar quantity of $AlCl_3$, and excess HCl [4] or from $(CH_3)_3SiN_3$ and excess trifluoromethanesulfonic (triflic) acid [5] in arenes is a convenient procedure for electrophilic aromatic aminations. The protonation of HN_3 (DN_3) in aqueous H_2SO_4 (D_2SO_4) is described on p. 152; the experimentally determined basicity constants of the reactants are also listed there.

Solid aminodiazonium salts are formed by protonation of HN_3. This reaction proceeds in HF solution in the presence of roughly equimolar quantities of the Lewis acids BF_3, AsF_5, or SbF_5 after warming the initially cooled mixture to ambient temperature. Evaporation of the volatiles leaves the colorless solids $H_2NNN^+Y^-$ where $Y = BF_4$, AsF_6, or SbF_6 [10]. A colorless precipitate of $H_2NNNSbCl_6$ forms from HN_3 in CH_2Cl_2 solution at 195 K in the presence of an equimolar quantity of $SbCl_5$, when HCl is bubbled through the solution. The product can be isolated and is dried at 263 K [11]. The aminodiazonium salts are very sensitive to moisture; they decompose slowly at ambient temperature with loss of N_2 [10, 11].

Properties. The heat of formation in the gas phase of the energetically most favorable isomer of $N_3H_2^+$, probably the H_2NNN^+ isomer, is calculated from the experimental proton affinity of HN_3 at 343 K to be 1085.3 kJ/mol [3]. A value of 1075 kJ/mol at 298 K was derived with the estimated proton affinity [6].

The ^{15}N NMR spectrum in SO_2ClF solution at 183 K of $N_3H_2^+$ enriched with ^{15}N in the terminal positions demonstrates the aminodiazonium structure of the cation by separate signals and different N-H coupling of the terminal N atoms. The chemical shifts towards high field relative to external, anhydrous NH_3 are $\delta = 68.61$ ppm (t) with $^1J(NH) = 100.0$ Hz for the protonated nitrogen and $\delta = 266.15$ ppm (s) for the other terminal N atom. The ^1H NMR spectrum consists of a signal with $\delta = 9.83$ ppm at 193 K, whereas a singlet at 253 K originates from rapid proton exchange between $N_3H_2^+$ and HSO_3F [4].

The structural parameters of the aminodiazonium ion obtained by X-ray crystallography of salts are given together with the calculated structures of the $N_3H_2^+$ isomers below (p. 158). The fundamental vibrations of the aminodiazonium ion in cm^{-1} were determined from the IR [10, 11] and Raman spectra [10] of the salts; C_s symmetry was assigned to the ion:

vibration (approximate description)	H_2NNNY [10] ($Y = AsF_6$, SbF_6)	$H_2NNNSbCl_6$ [11]	$D_2NNNSbCl_6$ [11]
ν_1 (A', $\nu_s(NH_2)$)	3170 vs	2970 m	2330 m
ν_2 (A', $\nu(N{\equiv}N)$)	2318 s	2290 s	2240 vs
ν_3 (A', $\delta_{sciss}(NH_2)$)	1547 vs	1522 vs	1163 s
ν_4 (A', $\nu(N{-}N)$)	1129 w	–	–
ν_5 (A', $\delta_{in\text{-}plane}(NNN)$)	530 m	–	–
ν_6 (A', $\delta_{wag}(NH_2$ inversion))	489 w	–	–
ν_7 (A'', $\nu_{as}(NH_2)$)	3280 vs	3080 s	2438 m
ν_8 (A'', $\delta_{as}(NH_2)$)	1259 m	–	–
ν_9 (A'', $\delta_{out\text{-}of\text{-}plane}(NNN)$)	418 w	–	–

While the assignment in [11] is rather tentative, the fundamentals in [10] were identified by using the fundamentals calculated by local density functional (LDF) theory as guides. However, the assignment of ν_5 and ν_6 may have to be changed. Some combination bands and overtones were also identified; force constants calculated by the LDF method were also given [10].

Ab initio calculations at the MP2/6-31G* level for the various isomers, likely to result from the protonation of HN_3, demonstrated that the formation of the aminodiazonium ion H_2NNN^+ is most favorable with $\Delta_rH = -737$ kJ/mol. This value is close to the experimental protonation energy of HN_3. The iminodiazenium ion $HNNNH^+$ forms with $\Delta_rH = -636$ kJ/mol. The formation of the cyclic isomer with geminal protons ($\Delta_rH = -566$ kJ/mol) and of the acyclic $HNN(H)N^+$ ($\Delta_rH = -168$ kJ/mol) are energetically less favorable [3]. An MP4[SDTQ]/6-311G** calculation also demonstrated that H_2NNN^+ is energetically more favorable by 163 kJ/mol than the cyclic isomer with geminal H substituents; the activation barrier for the conversion to the cyclic isomer was predicted to be 226 kJ/mol. Slightly different results for the conversion mechanism were obtained at the HF and MP2(full) levels [7]. The formation of the isomers of c-$N_3H_2^+$ with geminal and vicinal hydrogen substituents was studied at the MP2/6-31G(d, p)+P level. The values for $\Delta_fH_0^\circ$ are 1228 and 1398 kJ/mol, respectively. The formation of the geminal isomer from N_2^+ with NH_2 and from N_2 with NH_2^+ proceeds with standard heats of reaction of -468 kJ/mol and -36 kJ/mol, respectively [8]. The formation of the vicinal isomer from N_2H^+ with either $NH(^3\Sigma^-)$ or with $NH(^1\Delta)$ was predicted to be endothermal, $\Delta_rH_0^\circ = 107$ and 32 kJ/mol [8].

An X-ray diffraction analysis proved that $N_3H_2AsF_6$ and $N_3H_2SbCl_6$ contain the aminodiazonium ion with C_s symmetry. The cation has a pyramidal NH_2 group; the nitrogen internuclear distances indicate $[H_2N{-}N{\equiv}N]^+$ to be the prevalent structure with only a small contribution from the resonance structure $[H_2N{=}N{=}N]^+$ [10]. The structure analysis confirmed the predictions of ab initio calculations. Activation barriers for amino inversion are in the range 2 to 4 kJ/mol at the RHF and MP2 levels [7]. Experimental results for H_2NNN^+ and calculated structural data for the $N_3H_2^+$ isomers (distances r in Å) [3] are as follows:

isomer	$r(H\text{-}N_\alpha)$	$r(N_\alpha\text{-}N_\beta)$	$r(N_\beta\text{-}N_\gamma)$	$\angle HN_\alpha N_\beta$	$\angle N_\alpha N_\beta N_\gamma$	remarks
H_2NNN^+	1.043[a]	1.295(5)	1.101(6)	107(6)°	175.3(5)°	experimental result[b]
	1.007	1.308	1.078	112.1°	175.1°	C_s symmetry
	1.026	1.300	1.136	113.47°	174.04°	[c], $\angle HNH = 118.28°$, C_s symmetry
$HNN(H')N^+$	1.015	1.207	1.327	113.4°	131.9°	$r(H'\text{-}N_\beta) = 1.030$, $\angle H'N_\beta N_\gamma = 110.4°$
$HNNNH^+$	1.019	1.156	1.156	116.5°	170.2°	symmetr., nonplanar
$c\text{-}N_3H_2^+$	1.007	1.466	1.160	–	(60°)	$\angle HN_\alpha H = 121.8°$
	1.027	1.493	1.234	115.94°	65.58°	[c], $\angle HN_\alpha H = 122.58°$

[a] Calculated by the LDF theory; the experimental value is unreliable. – [b] Investigation of $N_3H_2SbCl_6$ at 20 K; $\angle HN_\alpha H = 118(8)°$ [10]. – [c] From [7].

Reactions. Gaseous H_2NNN^+ reacts with the n- and π-type nucleophiles H_2O, CF_3CH_2OH, CH_3ONO_2, CH_2O, and C_6H_6 exclusively as a Brønsted acid [3]. Electrophilic substitution by H_2NNN^+ in arene solution gives with the reactants $NaN_3\text{-}AlCl_3\text{-}HCl$ moderate to good yields [4] and with $(CH_3)_3SiN_3$-triflic acid good to very good yields of arylamines. Arenes with electron-withdrawing groups react less smoothly [5]. The loss of N_2 from H_2NNN^+ was predicted to be endothermal with values ranging from 216 kJ/mol at the RHF level [9] to 334 kJ/mol at the MP4[SDTQ] level [7].

The Triazenide Ion, $N_3H_2^-$

CAS Registry Number: *[70102-56-6]*

$N_3H_2^-$ is treated as the conjugate base of triazene, N_3H_3; see p. 161.

References:

[1] Fueno, T. (Seisan to Gijutsu **35** [1983] 44/9; C.A. **99** [1983] No. 128949).

[2] Baird, N. C.; Taylor, K. F. (Can. J. Chem. **58** [1980] 733/8).

[3] Cacace, F.; Attinà, M.; De Petris, G.; Grandinetti, F.; Speranza, M. (Gazz. Chim. Ital. **120** [1990] 691/700).

[4] Mertens, A.; Lammertsma, K.; Arvanaghi, M.; Olah, G. A. (J. Am. Chem. Soc. **105** [1983] 5657/60).

[5] Olah, G. A.; Ernst, T. D. (J. Org. Chem. **54** [1989] 1203/4).

[6] Lias, S. G.; Bartmess, J. E.; Liebman, J. F.; Holmes, J. L.; Levin, R. D.; Mallard, W. G. (J. Phys. Chem. Ref. Data, Suppl. **17** No. 1 [1988] 1/861, 620).

[7] Glaser, R.; Choy, G. S.-C. (J. Phys. Chem. **95** [1991] 7682/93).

[8] Zavoruev, S. M.; Rakauskas, R.-I. I. (Astron. Zh. **66** [1989] 1013/23).

[9] Glaser, R.; Choy, G. S.-C.; Horan, C. J. (J. Org. Chem. **57** [1992] 995/9).

[10] Christe, K. O.; Wilson, W. W.; Dixon, D. A.; Khan, S. I.; Bau, R.; Metzenthin, T.; Lu, R. (J. Am. Chem. Soc. **115** [1993] 1836/42).

[11] Schmidt, A. (Chem. Ber. **99** [1966] 2976/83).

2.3.5 Compounds of the Composition N_3H_3

The formation of N_3H_3 and related ions without specifying the isomers involved was described for the following reactions: Decomposition of gaseous N_2H_4 in a fast-flow system by an electrodeless discharge yields N_3H_3 in addition to fragments of the reactant [1]. The yield of N_3H_3 reaches a maximum of ~2% when 20 to 35% of N_2H_4 are decomposed [2]. The formation of N_3H_3 in a mixture of NH_3 and other nitrogen-hydrogen compounds was detected mass-spectrometrically after exposing gaseous N_2H_4 at 233 K to a microwave discharge [3]. N_3H_3 also forms when N_2H_4 reacts with the products of microwave discharges in H_2 or N_2. The N_3H_3 thus formed was identified with a mass spectrometer and has an ionization potential of 9.6 ± 1 eV [1]. The formation of N_3H_3, possibly with triazene structure, in incompletely decomposed HN_3 (see p. 120) and in solid N_2H_4 during bombardment by ions and electrons [4] was discussed.

Choosing 3/2 ($N_2 + H_2$) as the reference point, the relative energies of the molecules on the N_3H_3 hypersurface were calculated using ab initio coupled-cluster and many-body perturbation theories (MBPT). Triazene is most favorable with an energy of 192 kJ/mol. Azimine (triimide) has an energy of 265 kJ/mol, and triaziridine can be expected to be even less stable with an energy of 365 kJ/mol. The cis isomers of triimide and triaziridine, which have all hydrogens on the same side of the N_3 unit, are about 10 to 15% higher in energy than the regular isomers [5, 6]. Individual isomers of N_3H_3 and the corresponding ions are described separately below, starting with the acyclic compounds.

Triazene, $HNNNH_2$, and Its Conjugate Base

CAS Registry Numbers: $HNNNH_2$ *[15056-34-5]*, *cis*-$HNNNH_2$ *[58729-78-5]*, *trans*-$HNNNH_2$ *[58729-79-6]*

Formation. The intermediate N_3H_3 and its conjugated acid $N_3H_4^+$ (described on p. 166) and base $N_3H_2^-$ are supposed to form during one-electron oxidation of aqueous N_2H_4, conveniently done by pulse radiolysis. The reaction probably starts with the formation of the hydrazyl radical followed by $2\ N_2H_3 \rightarrow N_4H_6$, $N_4H_6 \rightarrow NH_3 + N_3H_3$, and $N_3H_3 \rightarrow NH_3 + N_2$. The observed UV absorption of an intermediate is attributed to N_3H_3 in the triazene form and to $N_3H_4^+$ or $N_3H_2^-$ depending on the pH of the solution. The absorptions assigned to N_3H_3 (pH range 7.2 to 8.7) and $N_3H_4^+$ (pH range 1.5 to 3.0) peak at ~225 nm; the maximum absorption of $N_3H_2^-$ could not be determined. Extinction coefficients at 230 nm range from 4.2×10^3 to 5.2×10^3 $L \cdot mol^{-1} \cdot cm^{-1}$ for N_3H_3, from 3.1×10^3 to 3.9×10^3 $L \cdot mol^{-1} \cdot cm^{-1}$ for $N_3H_4^+$, and from 40 to 50 $L \cdot mol^{-1} \cdot cm^{-1}$ for $N_3H_2^-$. A kinetic model for the N_2H_4 oxidation yielded the equilibrium constants at 295 K and rate constants of the decomposition [7]:

$$N_3H_3 \rightleftharpoons N_3H_2^- + H^+$$

with $pK = 11.37$ and an estimated $k \leq 10^{-3}\ s^{-1}$ at 297 K,

$$N_3H_4^+ \rightleftharpoons N_3H_3 + H^+$$

with $pK = 4.95$ and $k = 1.97 \times 10^{11} \exp(-52.7\ kJ \cdot mol^{-1}/RT)\ s^{-1}$ for the reaction yielding N_2 and NH_4^+ (see above) at pH 2.30 and 274 to 300 K, and

$$N_3H_2^- + H_2O \rightarrow N_2 + NH_3 + OH^-$$

with $k = 2.14 \times 10^{14} \exp(-80.3\ kJ \cdot mol^{-1}/RT)\ s^{-1}$ at pH 11.9 and 274 to 303 K.

An earlier kinetic investigation was described in [8]. The older literature on the possible formation of N_3H_3 via radiolysis of N_2H_4 was briefly discussed in [7, 8].

Properties. Ab initio calculations predict that the cis isomer of triazene is energetically less favorable than the trans isomer by 23 to 30 kJ/mol. Activation energies for the cis → trans inversion in the range 200 to 380 kJ/mol were calculated for various transition states at the HF/6-31G** level [9]. For an earlier theoretical study on this inversion, see [10].

The trans isomer of triazene, $HN_\alpha N_\beta N_\gamma HH'$, was predicted at the MBPT(2) level to have a ^1A ground state and to be almost planar. The internuclear distances are $r(N_\alpha\text{-}N_\beta) = 1.274$, $r(N_\beta\text{-}N_\gamma) = 1.365$, $r(H\text{-}N_\alpha) = 1.029$, $r(H\text{-}N_\gamma) = 1.012$, and $r(H'\text{-}N_\gamma) = 1.021$ Å. The bond angles were calculated to be $\angle NNN = 111.59°$, $\angle HN_\alpha N_\beta = 103.82°$, $\angle HN_\gamma H' = 114.81°$, $\angle HN_\gamma N_\beta = 110.52°$, $\angle H'N_\gamma N_\beta = 113.57°$, $\angle HN_\alpha N_\beta N_\gamma = 176.09°$, and $\angle H'N_\gamma N_\beta N_\alpha = 21.21°$. A bond order analysis confirms the expected double bond between N_α and N_β and the single bond between N_β and N_γ [5]. However, an interaction between the double bond and the lone electron pair of the NH_2 group is evidenced by the rotation barrier around the N-N single bond. A value of 94 kJ/mol was calculated at the HF/3-21G* level for the planar conformer [11]; a value in the range of 55 kJ/mol resulted at the HF/3-21G level [12]. The transition to a nonplanar molecule shortens the double bond, lengthens the N-N single bond, and slightly decreases $\angle NNN$ [11]. The vibrational spectrum of *trans*-$HNNNH_2$ was predicted to show the out-of-plane deformation of H' at 684 cm^{-1} as the strongest band [5]. A UV transition at 280 nm was predicted for *trans*-$HNNNH_2$ from an SCF CI calculation using a minimal basis [13].

The most favorable dimer of *trans*-triazene was predicted to form by simultaneous approach of the hydrogen of N_γ to N_α of the second molecule; dissociation of the dimer can lead to the tautomeric triazenes [12]. The tautomerization of triazenes by a [1,3]-H shift probably has a high energy barrier [9]. The thermodynamically favored protonation site of *trans*-triazene is N_α, and N_β is the one least favored [12, 14]. Kinetic reasons suggest a protonation at N_γ, because the resulting cation can be considered a complex of an ammonia molecule and a diazonium ion, products which also result from the protonation of organic triazenes [14].

Organically substituted triazenes are commonly prepared by nucleophilic alkylation of azides or by reacting diazonium salts with amines [15]. Only the trans isomers were found in crystallographic investigations. The flatness expected for the molecules was confirmed experimentally in one case; the torsional angle of 175.6° along the R-N=N-N chain approaches the ideal value of 180° [16]. The mutual influence of the adjacent N-N single and double bonds tends to decrease their different lengths [17] from the difference of (at least) 0.1 Å usually observed [18]. Some of the structural parameters of RN=N-NR'R'' are:

triazene[a]	bond length in Å		angles in degree			Ref.
	N=N	N-N	NNN	RNN	NNR', NNR''	
A	1.25(7)	1.34(8)	115	114.5	120[b]	[18]
B	1.259(7)	1.338(7)	114.4(5)	112.5(5)	112.9(5), 122.6(4)	[16]
C	1.27	1.32	115	114.5	120[b]	[19]
D	1.281(7)	1.3099(7)	113.3(5)	111.7(8)	115.6(5), 123.8(5)	[20]

[a] A: $C_6H_5NNN(4\text{-}NO_2C_6H_4)H$; B: N-phenylazo-2,6-dimethylpiperidine; C: $C_6H_5NNN(C_6H_5)H$; D: $2\text{-}NH_2C(O)C_6H_4NNN(CH_3)_2$. – [b] The angle NNH is not given.

^{15}N NMR spectra were only described for 1-aryl-3,3-dialkyltriazenes. The signal due to the central nitrogen in $RN_\alpha N_\beta N_\gamma R'_2$ appears at the lowest field. The average shifts of the other nitrogens with respect to N_β are 97 to 115 ppm for N_α and 258 to 293 ppm for N_γ [21 to 23]. A comparison with the shifts of free amines and azo compounds shows for the triazenes a low-field shift of the amine resonances [22] and a high-field shift of the N_α resonance; both indicate conjugation in the nitrogen chain [21, 22]. A direct comparison of the chemical shifts is hampered by the influence of the substituents and the use of different standards. Some examples of ^{15}N NMR shifts of $RN_\alpha N_\beta N_\gamma R'_2$ (positive low-field shifts) in ppm are as follows:

R, R'_2	standard	N_α	N_β	N_γ	solvent	Ref.
C_6H_5, $(CH_3)_2$*)	CH_3NO_2	−25.49	69.22	−224.23	DMSO	[23]
C_6H_5, pentamethylene	$^{15}NO_3^-$	−16.98	73.54	−206.23	not given	[22]
4-$NO_2C_6H_4$, $(CH_3)_2$	$^{15}NH_4Cl$	320.0	428.0	138.0	$CDCl_3$	[21]

*) The shifts agree qualitatively with earlier results in [21], where the coupling constants $^1J(N_\alpha N_\beta) = 12.8$ Hz and $^1J(N_\beta N_\gamma) = 14.0$ Hz were additionally given.

The ^1H resonances of the N-bonded protons in RNNN(H)R were found at $\delta = 7.10$ ppm for $R = CH_3$ and at $\delta = 7.0$ ppm in $CDCl_3$ [24], and at $\delta = 8.49$ ppm for $R = Si(t\text{-}C_4H_9)$ in C_6D_6 [25]. A shift of $\delta = 7.66$ ppm was given for $C_4H_9NNN(H)C_2H_5$ [26].

Typical IR bands of RNNN(H)R′ are ν(NH) at ~3300 cm^{-1}, δ(NH) at ~1500 cm^{-1}, ν_{as}(N=N) at ~1400 cm^{-1}, ν_s(N-N) at ~1200 cm^{-1}, and δ(NNN) at ~650 cm^{-1} [26, 27]. The bands were assigned by comparing them with those of the ^{15}N-labeled triazenes in [27].

The UV absorption of an intermediate during the oxidation of N_2H_4 at ~225 nm (see above) is possibly that of N_3H_3, probably the $HNNNH_2$ isomer. The $\pi^* \leftarrow \pi_n$ absorption of the NNN chain of $(t\text{-}C_4H_9)_3SiNNN(H)Si(t\text{-}C_4H_9)_3$ in hexane was found at 259 nm (ε = 15900) [25], whereas in 1,3-diaryltriazanes this absorption was observed at 340 to 350 nm (ε ranges from 17500 to 18200) [28]. A weak band of the silylated triazene at 384 nm (ε = 60) was assigned to the $\pi^* \leftarrow n$ transition of the NNN group [25].

The **triazenide** ion is known only in $Os_3(\eta\text{-}N_3H_2)(\mu\text{-}H)(CO)_{10}$ which forms from $(CH_3)_3SiN_3$ and $Os_3H_2(CO)_{10}$ in hexane. The coordinated $N_3H_2^-$ has an N-N distance of 1.32 ± 0.02 Å and an angle NNN of 118° ± 1° [29]. The UV absorption of the $\pi^* \leftarrow \pi$ transition of RNNNHR ($R = C_6H_5$; 2,4,5-$Cl_3C_6H_2$) shifts to longer wavelengths in alkaline ethanol; the anions have maxima at 402 nm (ε = 22400) for $R = C_6H_5$ and at 439 nm (ε = 29600) for R = 2,4,5-$Cl_3C_6H_2$ [30]. Coordination compounds of organically substituted triazenides are numerous; they were reviewed in [31].

Azimine (Triimide), HNN′(H)NH

Ab initio calculations for the isomers of azimine predicted a planar arrangement of all 6 atoms and a bent chain of the 3 N atoms. The energetically favored (Z,Z) isomer (A) of azimine was calculated to have a $^1A_1$ ground state and C_{2v} symmetry [5, 9]. The (E,E) isomer (B) of azimine also has C_{2v} symmetry and its energy is higher by 41 kJ/mol at the SCF level.

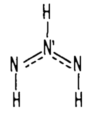

(A)

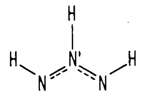

(B)

Internuclear distances in Å and bond angles in degree at the MBPT(2) level are as follows:

isomer	r(N′-N)	r(H-N′)	r(H-N)	∠NN′N	∠HN′N	∠HNN′
(A)	1.305	1.023	1.033	135.87	112.07	105.35
(B)	1.258	1.013	1.005	125.25	117.37	107.37

The higher energy of the isomer (B) is a result of mutual repulsion of the positively charged hydrogens and the negatively charged nitrogens. The planar structure of azimine allows strong π bonding in the N_3 chain; the bonds are halfway between single and double bonds. The compound has less biradical character than ozone. A calculation predicted the strongest band in the vibrational spectrum to be at 1093 cm^{-1} for the isomer (A) and at 1413 cm^{-1} for the isomer (B) [5].

An activation energy of 260 to 280 kJ/mol for the conversion of azimine to triazene via [1,2]-H shift was predicted by an SCF/6-31G** calculation and makes the process unlikely to occur under thermal conditions [9]. Based on calculations the dimer of azimine, formed preferentially by the hydrogen atom at N′ simultaneously approaching the terminal nitrogen of the other molecule and vice versa, is remarkably lower in energy than the separate molecules. The hydrogen transfer reaction in dimeric azimine has an activation energy of only 4 kJ/mol and yields a triazene dimer. Azimine is therefore kinetically too unstable to be isolable [12].

Organically substituted, configurational isomers of azimines were obtained stereospecifically by reacting (E)- or (Z)-configurated azo compounds with nitrenes. The (E) isomers of the azimines (designation with respect to the N-N bond of the azo reactant) are thermodynamically less stable and convert slowly to the (Z) isomers. Both isomers of 1-alkoxycarbonyl-2,3-diisopropylazimines have UV absorptions at 280 to 290 nm with $\varepsilon = 7000 \pm 600$ [32]. Crystallographic investigations of the isomers of $C_6H_5N_\alpha N_\beta(C_6H_5)N_\gamma R$ with R being a thiazole derivative indicate a double bond between N_α and N_β and a dipolar structure in which N_γ and N_β have formally negative and positive charges. Both molecules have an almost planar geometry at the central N atom. The structural parameters are as follows:

configuration	bond length in Å		angles in degree			Ref.
	$N_\alpha N_\beta$	$N_\beta N_\gamma$	$CN_\alpha N_\beta$	$N_\alpha N_\beta N_\gamma$	$N_\beta N_\gamma R$	
(1Z,2E)	1.279 ± 0.004	1.323 ± 0.003	116.7 ± 0.3	123.4 ± 0.3	115.0 ± 0.2	[33]
(1E,2Z)	1.286 ± 0.003	1.311 ± 0.003	118.8 ± 0.2	122.3 ± 0.2	117.0 ± 0.2	[34]

Cyclotriazane (Triaziridine), c-N_3H_3, and Its Conjugate Acid. Ions

CAS Registry Numbers: c-N_3H_3 *[6572-31-2]*, *cis*-c-N_3H_3 *[108739-42-0]*, *trans*-c-N_3H_3 *[108691-97-0]*, c-$N_3H_5^{2+}$ *[73870-52-7]*

The formation of **c-N_3H_3** (and N_3H_5) in the capillaries of a fully Ag^+-exchanged zeolite upon exposure to NH_3 gas at ambient temperature was established by crystallographic and mass-spectrometric techniques. The reaction, possibly catalyzed by Ag, is not fully understood, because the expected quantity of liberated H_2 was not observed. Triaziridine acts as a trihapto ligand in $Ag(N_3H_3)^+$. The N-N bond length of 1.49 ± 0.08 Å is that of a single bond. Additional stabilization of c-N_3H_3 is provided by H bridges to neighboring NH_3 molecules which are H-bonded to the zeolite framework. The weakness of the complex is demonstrated by a long N_3H_3-Ag^+ separation and an easy removability of triaziridine. The mass spectrum of the gas evolved from the zeolite crystal shows peaks due to $N_3H_3^+$

and $N_3H_2^+$; they remain unchanged between 300 and 343 K and indicate a stable $c\text{-}N_3H_3$ molecule in the gas phase [35]. Other syntheses of cyclotriazane are not known.

The trans isomer of triaziridine has a $^1A'$ ground state and C_s symmetry according to an MBPT (many-body perturbation theory) calculation. The hydrogen at N′ is located above the N_3 ring and the others are below it. The internuclear distances were calculated to be r(N′-N) = r(N-N) = 1.470, r(H-N′) = 1.025, and r(H-N) = 1.027 Å. The bond angles are ∠NN′N = 59.98°, ∠N′NN = 60.01°, ∠HN′N = 102.59°, ∠HNN′ = 102.39°, ∠HNN = 107.33°, ∠HN′NH = 159.58°, and ∠NNN′H = 97.40°. The symmetry of *cis*-triaziridine is C_{3v}; all hydrogens are on the same side of the nitrogen ring. The N-N bond length of 1.419 Å is nearly the same as in the trans isomer. The N-H distance is 1.007 Å. The bond angles ∠NNN = 60.00°, ∠HNN = 109.62°, and ∠HNNN = 101.88° were calculated [5]. Other calculations on the structures were performed at the SCF level [36, 37]. An activation energy of 125 kJ/mol for the inversion at an N atom yielding *trans*-triaziridine was calculated in an SCF study [9].

An MBPT calculation of the vibrational spectrum of *trans*-triaziridine predicted a most intense vibration at 1118 cm^{-1} and two strong, similar ones at 1287 and 1295 cm^{-1}. The strongest vibration of the cis isomer can be expected at 1561 cm^{-1} [5]. Complete sets of fundamentals of both isomers, but without intensities, were also obtained at the SCF level [37]. An MP2 calculation yielded rotational constants and microwave frequencies that can be used for the identification of $c\text{-}N_3H_3$ in interstellar space [38].

Calculated values of $\Delta_fH°$ for *trans*- and *cis*-triaziridine at 0 K are 386.9 and 434.6 kJ/mol at the MP2 level. Values of $\Delta_rH_0^\circ$ in kJ/mol for the following reactions are [38]:

reaction	trans isomer	cis isomer
trans-$N_2H_2 + NH(^1\Delta) \rightarrow c\text{-}N_3H_3$	−254.3	−206.5
cis-$N_2H_2 + NH(^1\Delta) \rightarrow c\text{-}N_3H_3$	−290.3	−242.5

A calculation using the semiempirical SINDO1 method yields ring current indices of 1.14 for $c\text{-}N_3H_3$ and 1.01 for **$c\text{-}N_3H_3^{2+}$** which indicate the antiaromatic character of these nonplanar systems. The nonplanar **$c\text{-}N_3H_3^{2-}$** was found to be unstable [39]. The stabilization of $c\text{-}N_3H_3$ caused by arranging the H substituents out of the N_3 plane was used to qualify the nonaromatic character of the molecule [40].

An SCF/STO-3G calculation for **$c\text{-}N_3H_3^{2+}$**, including configuration interaction, predicted that the ion should be a ground-state singlet with C_s symmetry having one pyramidal nitrogen N′ with a localized pair of electrons and an ethylenic π bond between the other nitrogens. The internuclear distances r(N-N′) = 1.622 and r(N-N) = 1.279 Å were calculated for a fixed N-H distance of 1.106 Å; the out-of-plane hydrogen bond angles are 74.7° at N′ and −2.9° at N. The N-N bond lengths in the low-lying excited states of the ion become almost identical in spite of the fact that the pyramidalization at N′ is retained [41].

Organic monocyclic triaziridines are commonly obtained by photolytic cyclization of azimines [42]; the prevailing isomer of the product is determined by the configuration of the starting material [43]. These products are stable enough to allow the preparation of derivatives. Titration of *trans*-diisopropyltriaziridine with $HClO_4$ revealed a low basicity of the N_3 system; titration with $(C_4H_9)_4NOH$ led to $pK_a > 14$ corresponding to a low acidity [44]. The triaziridines reconvert slowly into azimines; the activation energy of the ring opening reaction is ~100 kJ/mol [42]. Heating in $CDCl_3$ yields azimines, triazenes, and products containing fragments of the N_3 framework [45].

A crystallographic investigation of 1-methoxycarbonyl-2,3-(cyclopenta-1,3-diyl)triaziridine revealed a tetrahedral configuration of the nitrogens with angles NNC of 107 ± 3.5°. The interatomic distances are $r(N_1\text{-}N_2) = 1.479 \pm 0.002$, $r(N_1\text{-}N_3) = 1.458 \pm 0.002$, and $r(N_2\text{-}N_3) = 1.490 \pm 0.002$ Å [46]. The ^{15}N chemical shifts with a standard deviation of 0.5 ppm (and ^1J in Hz) of the cis and trans isomers of 2,3-diisopropyltriaziridines in $CDCl_3$ solution with respect to external, liquid NH_3 are as follows [47]:

N_1 substituent; isomer	$\delta(N_1)$, $^1J(NH)$	$\delta(N_2)$	$\delta(N_3)$	temperature
H; cis	119.9, 58.1 ± 0.5	144.0	144.0	249 K
H; trans	131.1, 51.7 ± 0.5	141.2*⁾	139.0*⁾	297 K
$CH_3O(O)C$; cis	145.0, –	164.9	164.9	246 K
$CH_3O(O)C$; trans	155.4, –	166.8	153.0	251 K

*⁾ Tentative assignment.

The pyramidal N atoms in diisopropyltriaziridine are stable towards inversion on the NMR time scale. The disappearance of the ^1H and ^{15}N resonances of the NH group after adding CF_3COOH can be attributed to fast, reversible protonation of the N atom [48]. The broad singlet of the hydrogen substituent of diisopropyltriaziridine in $CDCl_3$ solution has a shift of $\delta = 3.50$ ppm for the cis isomer and of $\delta = 2.61$ ppm for the trans isomer [44].

The NH vibrations of diisopropyltriaziridine in $CHCl_3$ solution produce weak IR bands at 3300 to 3400 cm^{-1} for an associated NH group (in the dimer) and at ~3200 cm^{-1} for a free one [44]. The maximum UV absorptions of triaziridines were observed at 200 to 220 nm; their low intensities with ε ranging from 20 to 800 indicate the loss of π conjugation with respect to the acyclic azimines [43, 44]. Bands in the photoelectron spectra of highly substituted, bicyclic triaziridines at 10.4 to 10.6 eV and at 10.9 to 11.0 eV were assigned to the highest occupied orbitals n_A and n_S of the N_3 ring. The high ionization potentials agree qualitatively with the results of semiempirical MNDO [49] and ab initio SCF calculations [9] for $c\text{-}N_3H_3$ and indicate the low availability of the nitrogen lone-pair electrons [49].

The isomers of $\mathbf{c\text{-}N_3H_4^+}$, resulting from protonation of $c\text{-}N_3H_3$, were investigated at the MP2 level. Two (unspecified) isomers derived from *trans*-triaziridine have $\Delta_fH°$ values of 1125 and 1146 kJ/mol, respectively. The latter value was also calculated for the isomer derived from protonation of *cis*-triaziridine. The standard enthalpies $\Delta_rH_0^\circ$ in kJ/mol for the formation of $c\text{-}N_3H_4^+$ by the following reactions are [38]:

reaction	protonated *trans*-triaziridine	protonated *cis*-triaziridine
$trans\text{-}N_2H_2 + NH_2^+ \rightarrow c\text{-}N_3H_4^+$	−358.0	−337.1
$cis\text{-}N_2H_2 + NH_2^+ \rightarrow c\text{-}N_3H_4^+$	−394.0	−373.1
$N_2H_2^+ + NH_2 \rightarrow c\text{-}N_3H_4^+$	−209.5	−188.6

References:

[1] Foner, S. N.; Hudson, R. L. (J. Chem. Phys. **29** [1958] 442/3).

[2] Foner, S. N.; Hudson, R. L. (Adv. Chem. Ser. **36** [1962] 34/49).

[3] Wiberg, N.; Fischer, G.; Bachhuber, H. (unpublished, ref. 1 in: Wiberg, N.; Chimia **30** [1976] 426).

[4] Papazian, H. A. (J. Phys. Chem. **65** [1961] 53/5).

[5] Magers, D. H.; Salter, E. A.; Bartlett, R. J.; Salter, C.; Hess, B. A., Jr.; Schaad, L. J. (J. Am. Chem. Soc. **110** [1988] 3435/46).
[6] Bartlett, R. J. (AD-A184451 [1987] 27 pp.; C.A. **109** [1988] No. 116207).
[7] Sutherland, J. W. (J. Phys. Chem. **83** [1979] 789/95).
[8] Hayon, E.; Simic, M. (J. Am. Chem. Soc. **94** [1972] 42/7).
[9] Nguyen, M. T.; Kaneti, J.; Hoesch, L.; Dreiding, A. S. (Helv. Chim. Acta **67** [1984] 1918/29).
[10] Howell, J. M.; Kirschenbaum, L. J. (J. Am. Chem. Soc. **98** [1976] 877/85).

[11] Korkin, A. A. (Int. J. Quantum Chem. **38** [1990] 245/52).
[12] Nguyen, M. T.; Hoesch, L. (Helv. Chim. Acta **69** [1986] 1627/37).
[13] Ditchfield, R.; Del Bene, J. E.; Pople, J. A. (J. Am. Chem. Soc. **94** [1972] 703/7).
[14] Schmiedekamp, A.; Smith, R. H., Jr.; Michejda, C. J. (J. Org. Chem. **53** [1988] 3433/6).
[15] Engel, A. (Houben-Weyl; Methoden Org. Chem. 4th Ed. E **16**a Pt. 2 [1990] 1182/226).
[16] Lunazzi, L.; Cerioni, G.; Foresti, E.; Macciantelli, D. (J. Chem. Soc. Perkin Trans. II **1978** 686/91).
[17] Benson, F. R. (The High Nitrogen Compounds, Wiley, New York 1984, pp. 265/6).
[18] Kondrashev, Yu. D. (Zh. Strukt. Khim. **15** [1974] 517/22; J. Struct. Chem. [Engl. Transl.] **15** [1974] 441/6).
[19] Gladkova, V. F.; Kondrashev, Yu. D. (Kristallografiya **17** [1972] 33/40; Sov. Phys.-Crystallogr. [Engl. Transl.] **17** [1972/73] 23/8).
[20] Edwards, S. L.; Chapuis, G.; Templeton, D. H.; Zalkin, A. (Acta Crystallogr. B **33** [1977] 276/8).

[21] Axenrod, T.; Mangiaracina, P.; Pregosin, P. S (Helv. Chim. Acta **59** [1976] 1655/60).
[22] Patrick, T. B.; Willaredt, R. P. (J. Org. Chem. **48** [1983] 4415/6).
[23] Wilman, D. E. V. (Magn. Reson. Chem. **28** [1990] 729/31).
[24] Smith, R. H., Jr.; Michejda, C. J. (Synthesis **1983** 476/7).
[25] Wiberg, N.; Fischer, G.; Karampatses, P. (Angew. Chem. **96** [1984] 58/9; Angew. Chem. Int. Ed. Engl. **23** [1984] 59).
[26] Danilov, S. N.; Yastrebov, L. N.; Burova, L. N. (Zh. Obshch. Khim. **40** [1970] 2248/50; J. Gen. Chem. USSR [Engl. Transl.] **40** [1970] 2235/6).
[27] Kübler, R.; Lüttke, W.; Weckherlin, S. (Z. Elektrochem. **64** [1960] 650/8).
[28] Day, B. F.; Campbell, T. W.; Coppinger, G. M. (J. Am. Chem. Soc. **73** [1951] 4687/8).
[29] Johnson, B. F. G.; Lewis, J.; Raithby, P. R.; Sankey, S. W. (J. Organomet. Chem. **228** [1982] 135/8).
[30] Zaitsev, B. E.; Alister, P. I.; Zaitseva, V. A.; Ezhov, A. I.; Lisitsina, E. S. (Zh. Neorg. Khim. **32** [1987] 2994/9; Russ. J. Inorg. Chem. [Engl. Transl.] **32** [1987] 1736/9).

[31] Moore, D. S.; Robinson, S. D. (Adv. Inorg. Chem. Radiochem. **30** [1986] 1/68).
[32] Leuenberger, C.; Hoesch, L.; Dreiding, A. S. (Helv. Chim. Acta **65** [1982] 217/28).
[33] Boyd, G. V.; Norris, T.; Lindley, P. F. (J. Chem. Soc. Perkin Trans. I **1977** 965/71).
[34] Boyd, G. V.; Norris, T.; Lindley, P. F.; Mahmoud, M. M. (J. Chem. Soc. Perkin Trans. I **1977** 1612/5).
[35] Kim, Y.; Gilje, J. W.; Seff, K. (J. Am. Chem. Soc. **99** [1977] 7057/9).
[36] Lathan, W. A.; Radom, L.; Hariharan, P. C.; Hehre, W. J.; Pople, J. A. (Fortschr. Chem. Forsch. **40** [1973] 1/45).
[37] Zavoruev, S. M.; Rakauskas, R.-I. I. (Liet. Fiz. Rinkinys **27** [1987] 117/20; Sov. Phys. Collect. [Engl. Transl.] **1987** 95/7).
[38] Zavoruev, S. M.; Rakauskas, R.-I. I. (Astron. Zh. **66** [1989] 1013/23).
[39] Jug, K. (J. Org. Chem. **48** [1983] 1344/8).
[40] Gimarc, B. M.; Trinajstic, N. (Pure Appl. Chem. **52** [1980] 1443/58).

[41] Borden, W. T.; Davidson, E. R.; Feller, D. (J. Am. Chem. Soc. **102** [1980] 5302/11).
[42] Hoesch, L.; Leuenberger, C.; Hilpert, H.; Dreiding, A. S. (Helv. Chim. Acta **65** [1982] 2682/96).
[43] Hilpert, H.; Hoesch, L.; Dreiding, A. S. (Helv. Chim. Acta **68** [1985] 1691/7).
[44] Hilpert, H.; Hoesch, L.; Dreiding, A. S. (Helv. Chim. Acta **69** [1986] 2087/97).
[45] Hilpert, H.; Dreiding, A. S. (Helv. Chim. Acta **71** [1988] 277/91).
[46] Prewo, R.; Bieri, J. H. (Acta Crystallogr. A **37** [1981] C 208).
[47] Hilpert, H.; Hollenstein, R. (Helv. Chim. Acta **69** [1986] 136/40).
[48] Hilpert, H.; Hoesch, L.; Dreiding, A. S. (Helv. Chim. Acta **70** [1987] 381/9).
[49] Kaupp, G.; Döhle, J. A.; Burger, K.; Rademacher, P.; Poppek, R. (J. Phys. Org. Chem. **1** [1988] 267/73).

2.3.6 Compounds of the Composition N_3H_4

The Triazyl (1-Aminohydrazyl) Radical, N_3H_4

CAS Registry Number: *[114045-17-9]*

The semiempirically calculated formation of the H_2NNNH_2 radical from N_3H_5 by reacting with CH_3 has an activation energy of 6.7 kJ/mol and a standard enthalpy of −149 kJ/mol. The N-N bond length of the H_2NNNH_2 radical of 1.386 Å was obtained in an ab initio SCF calculation [1]. An angle of 107.8° at the central nitrogen was calculated [2]. The standard heat of formation of 278 kJ/mol at 298.15 K was obtained by a semiempirical relation. A stabilization energy of 84 kJ/mol, the difference between the heat of atomization and the sum of the bond energies, indicates a thermodynamically stable radical; it was also predicted to be stable towards dimerization to N_6H_8 [1], probably because of electronic effects [2]; see also p. 185. The activation energy at ambient temperature for the dimerization was calculated to be 91 to 96 kJ/mol which would correspond to a small rate constant [2, 3].

The Triazenium Ion, $N_3H_4^+$

CAS Registry Numbers: $N_3H_4^+$, $[H_2NNNH_2]^+$ *[70102-55-5]*, *cis*-$HNNNH_3^+$ *[115246-90-7]*, *trans*-$HNNNH_3^+$ *[115246-89-4]*

The dominant species of protonated triazene was found to be $[H_2NNNH_2]^+$ by ab initio SCF calculations, the cis and trans isomers of $HNNNH_3^+$ being less favorable (no details were given) [4]. The ion $[H_2NNNH_2]^+$ was predicted to be planar and to have C_{2v} symmetry. Structural parameters are r(N-N) = 1.247 Å, r(H-N) = 1.006 Å for the hydrogen atoms on the outside of the angular N_3 skeleton and 1.010 Å for the other ones, $\angle$NNN = 120.0°, $\angle$HNN = 116.2° and 123.7°. The four π electrons form a delocalized, allylic system. The ion has a singlet ground state; the triplet state is 445 kJ/mol higher in energy [5]. Calculations showed that the formation of *cis*-$HNNNH_3^+$ by protonation of *cis*-$HNNNH_2$ is accompanied by the synchronous breakage of the HNN-NH_3^+ bond [4].

The Cyclotriazanium Ion, c-$N_3H_4^+$

The cyclotriazanium ion is treated as the conjugated acid of c-N_3H_3 on p. 164.

References:

[1] Leroy, G.; Sana, M.; Wilante, C.; Peeters, D.; Dogimont, C. (J. Mol. Struct. **153** [1987] 249/67 [THEOCHEM **38**]).
[2] Sana, M.; Leroy, G.; Vinson, L. K.; Dannenberg, J. J. (J. Mol. Struct. **205** [1990] 89/95 [THEOCHEM **64**]).

[3] Sana, M.; Leroy, G. (Ann. Soc. Sci. Bruxelles I **101** [1988] 23/57).

[4] Schmiedekamp, A.; Smith, R. H., Jr.; Michejda, C. J. (J. Org. Chem. **53** [1988] 3433/6).

[5] Schoeller, W. W.; Busch, T. (Chem. Ber. **123** [1990] 971/3).

2.3.7 Triazane (Aminohydrazine), N_3H_5

CAS Registry Number: *[14451-01-5]*

The formation of N_3H_5 (and $c\text{-}N_3H_3$) in the capillaries of a fully Ag^+-exchanged zeolite upon exposure to NH_3 gas at ambient temperature was established by crystallographic and mass-spectrometric techniques. The reaction, possibly catalyzed by Ag, is not fully understood, because the expected quantity of liberated H_2 was not observed. The N_3H_5 molecules form triple bridges via the terminal nitrogens between the Ag^+ atoms in the complex $Ag_2(N_3H_5)_3^{2+}$. Additional stabilization of N_3H_5 comes from bridges formed by all hydrogens to the oxygens of the zeolite framework. The mass spectrum of the gas evolved from the zeolite crystal at 348 K contains weak $N_3H_5^+$ and $N_3H_4^+$ peaks. The angle ∠NNN of 107±8° and the N-N bond length of 1.6±0.1 Å of N_3H_5 in the Ag^+ complex are in the range normal for N-N single bonds [1]. An N-N bond length of 1.399 Å was calculated for free N_3H_5 at the ab initio SCF level [2].

The standard heat of formation for N_3H_5 of 205 kJ/mol at 298.15 K was obtained by a semiempirical relation. A stabilization energy of −3.6 kJ/mol, the difference between the heat of atomization and the sum of bond energies, indicates an unstable molecule. A dissociation energy of 270 kJ/mol was estimated for the $H\text{-}N(NH_2)_2$ bond [2].

Organic triazanes are not numerous. They can be prepared by adding amines to azoesters [3]; other methods were also used, for example the thermolysis of *cis*-azimines [4]. A broad singlet of H bonded to nitrogen in $C_2H_5OOC(H)NN(COOC_2H_5)N(C_2H_5)_2$ was observed at $\delta = 7.43$ ppm. The IR spectra of 1,2-bis(ethoxycarbonyl)-3,3-dialkyltriazanes contain medium-to-strong bands assigned to ν(N-H) at 3240 to 3265 cm^{-1} and to ν(N-N) at 1025 to 1048 cm^{-1} [3]. The maximum UV absorption of $ROOC(H)NN(i\text{-}C_3H_7)NC(CH_3)_2$ with $R = CH_3$, C_2H_5 was found at 255 nm ($\varepsilon = 710$ to 730) [4].

References:

[1] Kim, Y.; Gilje, J. W.; Seff, K. (J. Am. Chem. Soc. **99** [1977] 7057/9).

[2] Leroy, G.; Sana, M.; Wilante, C.; Peeters, D.; Dogimont, C. (J. Mol. Struct. **153** [1987] 249/67 [THEOCHEM **38**]).

[3] Linke, K.-H.; Göhausen, H. J. (Chem. Ber. **104** [1971] 301/6).

[4] Hilpert, H.; Hoesch, L.; Dreiding, A. S. (Croat. Chem. Acta **58** [1985/86] 559/67).

2.3.8 The Triazanium Ion, $N_3H_6^+$

A precipitate of $N_3H_6SO_4H$ forms upon adding an equimolar quantity of dry N_2H_4 to hydroxylamido-O-sulfuric acid in dry CH_3OH at 273 K. Addition of excess N_2H_4 leads to decomposition [1]. The $N_3H_6^+$ salt dissolves in water; approximately 0.1 N solutions containing counter ions other than SO_4H^- can be prepared at 273 K by adding barium salts, whereupon $BaSO_4$ precipitates. The half-life of N_3H_6X in solution decreases from 2040 min for $X = SO_4H^-$ to 1260 min for $X = ClO_4^-$, to 380 min for $X = CH_3COO^-$, and to 14 min for $X = OH^-$. The stability of the solutions decreases with the concentration of H^+ based on the strength of the acids formed by the counter ions. The isolation of $N_3H_6^+$ salts from the aqueous solutions yields only products containing $BaSO_4$ [2]. Solid $N_3H_6SO_4H$ decomposes slowly at ambient temperature with liberation of N_2 and formation of hydrazinium and ammonium sulfate in a ratio of 5:2 [1]; other triazanium salts are more sensible to temperature. The reduction of $N_3H_6^+$ in acidic iodide solution can be described by $N_3H_6^+ + 3\ H^+ + 2\ I^- \rightarrow NH_4^+ + N_2H_5^+ + I_2$ and can be used for its titrimetric determination. Liquid NH_3 decomposes solid $N_3H_6SO_4H$ [2].

Organic triazanium salts $H_2NNR_2NH_2^+$ are synthesized similarly by amination of organically substituted hydrazines [3]. The proton resonances of the NH_2 groups appear at $\delta = 5.7$ to 6.7 ppm in solution [4, 5]. The ^{15}N resonances of the terminal NH_2 groups have high-field shifts of -260 to -275 ppm and coupling constants $^1J(NH)$ around -69 Hz. A shift of the central NR_2 unit of -256 ppm for $R = i\text{-}C_3H_7$ is probably less influenced by the substituents than a shift of -326 ppm for $R = C_6H_5CH_2$ (standard not given) [5]. The IR spectra contain absorptions from the symmetric and antisymmetric NH_2 stretching vibrations at 3300 to 3100 cm^{-1}, from the NH_2 deformation vibration at $\sim 1600\ cm^{-1}$, and a band at $\sim 1100\ cm^{-1}$ which was assigned tentatively to the NNN stretching vibration [4, 5]. The maximum UV absorption of $H_2NN(CH_3)_2NH_2Cl$ shifts from 240 nm at pH 11.25 to 234 nm at pH 13.79 [6].

References:

[1] Fehér, F.; Linke, K.-H. (Z. Anorg. Allg. Chem. **344** [1966] 18/22).
[2] Linke, K.-H.; Turley, R. (Z. Anorg. Allg. Chem. **377** [1970] 139/43).
[3] Benson, F. R. (The High Nitrogen Compounds, Wiley, New York 1984, pp. 584/5).
[4] Utvary, K.; Sisler, H. H. (Inorg. Chem. **5** [1966] 1835/6).
[5] Khatib, A. A.; Sisler, H. H. (Inorg. Chem. **29** [1990] 3158/61).
[6] Mathur, M. A.; Sisler, H. H.; Morgenthaler, L. N. (Inorg. Chem. **18** [1979] 2350/4).

2.4 Tetranitrogen Compounds

2.4.1 1,3-Tetrazadiene, N_4H_2, and 1,3-Dihydrocyclotetrazene, c-N_4H_2

CAS Registry Numbers: N_4H_2 *[27730-49-0]*, c-N_4H_2 *[127399-21-7]*

The formation of **N_4H_2** in a mixture of NH_3 and other nitrogen-hydrogen compounds was detected with a mass spectrometer after exposing gaseous N_2H_4 at 233 K to a microwave discharge [1]. Formation of N_4H_2 was discussed to be a possible reaction during photolysis of HN_3 in matrices [2]. The compound could not be isolated so far.

Analysis by the graph theoretical technique showed similar electron densities and bonds in the isoelectronic systems tetrazadiene and butadiene [3]. The molecular orbital levels of N_4H_2 were calculated with regard to a complex formed with the iron tricarbonyl group [4]. The maximum UV absorption of the $\pi^* \leftarrow \pi$ band at 204 nm was predicted on the basis of ab initio SCF and CNDO/S calculations [5].

Organic derivatives of tetrazadienes in the free state are not known. A number of their complexes have been isolated, however. Tetrazadiene acts as a chelating ligand in most of them; see [6] for a review.

Ab initio HF calculations for **c-N_4H_2** with the hydrogens in the 1- and 3-positions predicted that the isomer with the hydrogens above and below the N_4 plane (C_{2h} symmetry) is energetically more favorable than the planar isomer (D_{2h} symmetry) by only 4 kJ/mol. The conformational flexibility corresponds to the nonaromatic character of the molecule. Structural parameters with distances in Å are:

symmetry	r(N′-H)	r(N-N′)	∠NN′N	∠HN′, NN′N
C_{2h}	0.997	1.322	48.1°	22.3°
D_{2h}	0.993	1.319	96.4°	–

Harmonic frequencies of the planar isomer of 523 cm^{-1} (B_{1u}), 978 cm^{-1} (B_{2u}), and 1117 cm^{-1} (B_{3u}) were calculated [7].

References:

[1] Wiberg, N.; Fischer, G.; Bachhuber, H. (unpublished, ref. 1 in: Wiberg, N.; Chimia **30** [1976] 426).

[2] Milligan, D. E.; Jacox, M. E. (J. Chem. Phys. **41** [1964] 2838/41).

[3] Singh, S.; Mishra, R. K.; Mishra, B. K. (Indian J. Chem. A **27** [1988] 653/6).

[4] Armstrong, D. R.; Perkins, P. G.; Scott, J. M.; Stewart, J. J. P. (Theor. Chim. Acta **26** [1972] 237/48).

[5] Petukhov, V. A.; Agafonov, N. E.; Abronin, I. A. (Izv. Akad. Nauk SSSR Ser. Khim. **1984** 450/4; Bull. Acad. Sci. USSR Div. Chem. Sci. [Engl. Transl.] **33** [1984] 414/7).

[6] Moore, D. S.; Robinson, S. D. (Adv. Inorg. Chem. Radiochem. **30** [1986] 1/68, 41/59).

[7] Van Zandwijk, G.; Janssen, R. A. J.; Buck, H. M. (J. Am. Chem. Soc. **112** [1990] 4155/64).

2.4.2 Compounds of the Composition N_4H_4

2.4.2.1 Tetrazenes

CAS Registry Number: *[27120-23-6]*

The decomposition of gaseous N_2H_4 by an electrodeless discharge in a fast flow system and fast cooling of the products to 78 K led to the formation of N_4H_4 which was identified with a mass spectrometer in the vapors set free during warmup [1]; see also [2].

Only the trans isomer of 2-tetrazene was experimentally identified. Derivatives of the other isomers of N_4H_4 are mostly known either as organic or coordination compounds. Results for individual isomers of N_4H_4 are described separately in the following paragraphs.

1-Tetrazene, $HNNNHNH_2$

CAS Registry Number: *[14097-21-3]*

No paper dealing with $HNNNHNH_2$ seems to have been published. Organic derivatives can be prepared by reacting diazonium salts with hydrazines which are substituted at one nitrogen. The number of the compounds known is limited; see [3] for a review.

2-Tetrazene, H_2NNNNH_2

CAS Registry Numbers: *trans*-N_4H_4 *[54410-57-0]*, *cis*-N_4H_4 *[69996-02-7]*

Formation. The trans isomer of 2-tetrazene was obtained with 90% yield by protolysis of *trans*-tetrakis(trimethylsilyl)tetraz-2-ene with the stoichiometric amount of CF_3COOH in CH_2Cl_2 at 195 K. A colorless product precipitated and was separated at 195 K by fractional condensation. The product was purified by repeated sublimation in vacuum with a temperature gradient of 258 to 195 K [4]. The trans isomer also forms by protolysis of bis(trimethylsilyl)diazene with H_2SO_4 in diethyl ether at 195 K via acid-catalyzed dimerization of N_2H_2. The tetrazene is set free from the intermediately formed $N_4H_5^+$ salt by reaction with NH_3 or $N(C_2H_5)_3$ at 243 K [5]. Single crystals of *trans*-2-tetrazene were obtained by slow sublimation in vacuum; recrystallization from $(C_2H_5)_2O$ or CH_2Cl_2 yielded only microcrystals [6].

The intermediate formation of the cis isomer of 2-tetrazene is supposed to occur during protolysis of 5,5-dimethyl-1,4-bis(trimethylsilyl)-4,5-dihydro-1*H*-5-silatetrazole by a four-molar quantity of CF_3COOH in CH_2Cl_2 at 195 K. However, only the decomposition products NH_3 and HN_3 were identified [7].

Properties. The trans configuration at the double bond of 2-tetrazene is known from a crystal structure determination by a photographic method at 183 K. The tetrazene crystallizes in the triclinic space group $P1-C_i^1$ (No. 2) with the lattice constants $a=10.23\pm0.03$, $b=7.12\pm0.02$, $c=4.19\pm0.02$ Å, $\alpha=102.0\pm0.8°$, $\beta=90.0\pm0.8°$, and $\gamma=106.5\pm0.8°$. All of the crystals isolated were twinned at the (100) plane. The crystallographic density is 1.40 g/cm^3. Atomic positions are listed in the original paper. The structure was refined to $R=0.12$. Each unit cell contains four individual molecules of C_i symmetry with planar nitrogen frames. The average internuclear distances $r(N-N)=1.429\pm0.005$ and $r(N=N)=1.205\pm0.016$ Å indicate isolated single and double bonds. The angle $\angle NNN$ is $109\pm2°$. The N-H distance was fixed at 1.02 Å; related angles are $\angle NNH=101\pm4°$ and $118\pm3°$ and a fixed value of $\angle HNH=109.8°$. The hydrogens of each NH_2 group have average angles of 27.9° and 29.0° with respect to the N_4 plane. The conformation of the NH_2 groups is "pseudo-gauche" [6]. This conformation was also found to be the most favorable one in CEPA and CI calculations [8]. The N_4H_4 molecules in the crystal are linked by hydrogen bridges to amino nitrogens and also by bridges which additionally involve imino nitrogens [6].

The vertical ionization potentials (IP) in the He I photoelectron spectrum of *trans*-2-tetrazene were assigned with the aid of a CNDO/S calculation (assuming sp^3 hybridization at the amino nitrogens):

IP in eV	8.99	10.04	11.62	13.31	14.7	16.1	18.2	19.6
assignment	π	n_+	π	n_-	π	σ	σ	σ

The first band exhibits a vibrational splitting of 650 cm^{-1}. The π character of the highest occupied MO was taken to indicate a considerable amount of conjugation along the nitrogen chain [9].

Crystals of *trans*-2-tetrazene liquefy quickly at 273 K with vigorous liberation of N_2 [6]. The decomposition of the solid leads to N_2H_4 and N_2 with 75% yield and the tetrazene structural isomer NH_4N_3 with 25% yield; the product ratio was about 40:60 in CH_3OH solution [4]. Large single crystals of NH_4N_3 started to grow after a short time in the liquid formed from crystalline N_4H_4 [6]. The tetrazene is metastable at ambient temperature in the gas phase [4]; decomposition causes single crystals of $N_2H_5N_3$ to grow on the walls of the reaction vessel [6].

The mass spectrum of *trans*-2-tetrazene contains the molecular ion and its fragments $N_mH_n^+$. The reactions of N_4H_4 with $(CH_3)_3EN(C_2H_5)_2$ (E = Ge, Sn) yield $[(CH_3)_3E]_2NNNN[E(CH_3)_3]_2$ [4]. Metallation of N_4H_4 by LiC_4H_9 (1:4) in diethyl ether at 195 K yields solid Li_4N_4 [10].

Organic tetraz-2-enes are mainly prepared by oxidizing hydrazines with organic substituents at one N atom [3]. The ^{14}N NMR resonance of the amino nitrogen in R_2NNNNR_2 is shifted by 270 to 350 ppm towards high field relative to the signal of the azo nitrogen [11, 12]. The latter has a shift of about 45 to -30 ppm with respect to external aqueous $NaNO_3$ [12]. The shift of the hydrogens bonded to nitrogen in $[(CH_3)_3Si]_2NNNNH_2$ is $\delta = 6.3$ ppm [13].

The IR band assignments for neat, liquid $[(CH_3)_3Si]_2NNNNH_2$ in cm^{-1} are $\nu_{as}(NH_2) = 3395$ w, $\nu_s(NH_2) = 3260$ vw, $\delta(NH_2) = 1585$ w [14], $\nu(N{=}N) = 1493$ vw, and $\nu(N{-}N) = 1125$ w, 1055 s [13].

Based on the observed intensities, the first UV absorptions of R_2NNNNR_2 can be assigned to the energetically closely related $\pi^* \leftarrow \pi$ and $\pi^* \leftarrow n$ transitions [12]. The maximum absorption was found in the range 277 to 292 nm with extinction values ranging from 5800 to 8300 $L \cdot mol^{-1} \cdot cm^{-1}$ [12, 15, 16].

Isotetrazene, $(H_2N)_2NN$

The deprotonated nitrogen framework of isotetrazene was identified by an X-ray structure determination of $[Cl_5W(\mu\text{-}N_4)WCl_5]^{2-}$ which forms by thermolysis of the tungsten azide complex in the presence of azide. The bridging involves the singly bonded N atoms. Internuclear distances are $r(N{-}N) = 1.48 \pm 0.02$, 1.50 ± 0.02, and $r(N{=}N) = 1.23 \pm 0.02$ Å. The angles $\angle N{-}N{-}N = 109 \pm 1°$ and $\angle N{-}N{=}N = 125 \pm 2°$, $126 \pm 1°$ were determined. The IR spectrum contains an N=N stretching vibration at 1640 cm^{-1} [17]. Other compounds with an isotetrazene framework do not seem to have been described.

Cyclotetrazane (Tetrazetidine), c-N_4H_4, and the Ion c-$N_4H_4^{2+}$

CAS Registry Numbers: c-N_4H_4 *[58674-00-3]*, c-$N_4H_4^{2+}$ *[127421-11-8]*

Neither **c-N_4H_4** itself nor organic derivatives were identified experimentally. However, there are indications that a *cis,trans*-cyclotetrazane forms intermediately in a side reaction during photolysis of an azobenzenophane. Ab initio MO calculations on energies and structural parameters of cyclotetrazane isomers predicted for the most stable isomer a bent N_4 frame and trans arrangement of the hydrogens. Structural parameters are $r(N{-}N) = 1.44$, $r(N{-}H) = 1.00$ Å, and $\angle NNH = 107°$. The conformer with a planar N_4 frame is less stable by only 1.5 kJ/mol and has almost identical structural parameters. Both conformers have no dipole moment. Configurational isomers with cis arrangement of some or all hydrogens are considerably less stable. Even the most favorable of these isomers is destabilized by 138 kJ/mol with respect to two separate molecules of *trans*-diazene [18].

A calculation showed the planar ion **$c\text{-}N_4H_4^{2+}$** with D_{4h} symmetry to be stabilized by its aromatic character. Internuclear distances of the square ion are r(N-N) = 1.30 Å and r(N-H) = 1.02 Å. Harmonic frequencies of 178 cm^{-1} (E_g), 487 cm^{-1} (B_{2u}), and 1115 cm^{-1} (E_u) were predicted [19].

References:

[1] Foner, S. N.; Hudson, R. L. (J. Chem. Phys. **29** [1958] 442/3).
[2] Foner, S. N.; Hudson, R. L. (Adv. Chem. Ser. **36** [1962] 34/49).
[3] Lang-Fugmann, S. (Houben-Weyl; Methoden Org. Chem. 4th Ed. E **16**a [1990] 1227/38).
[4] Wiberg, N.; Bayer, H.; Bachhuber, H. (Angew. Chem. **87** [1975] 202/3; Angew. Chem. Int. Ed. Engl. **14** [1975] 177/8).
[5] Wiberg, N.; Häring, H.-W.; Vasisht, S. K. (Z. Naturforsch. **34b** [1979] 356/7).
[6] Veith, M.; Schlemmer, G. (Z. Anorg. Allg. Chem. **494** [1982] 7/19).
[7] Wiberg, N.; Ziegleder, G. (Chem. Ber. **111** [1978] 2123/9).
[8] Schoeller, W. W.; Staemmler, V. (Inorg. Chem. **23** [1984] 3369/73).
[9] Kroner, J.; Wiberg, N.; Bayer, H. (Angew. Chem. **87** [1975] 203/4; Angew. Chem. Int. Ed. Engl. **14** [1975] 178/9).
[10] Wiberg, N.; Vasisht, S. K. (unpublished, ref. 38 in: Wiberg, N.; Adv. Organomet. Chem. **24** [1985] 179/248, 239).

[11] Mason, J.; Vinter, J. G. (J. Chem. Soc. Dalton Trans. **1975** 2522/6).
[12] Kroner, J.; Schneid, W.; Wiberg, N.; Wrackmeyer, B.; Ziegleder, G. (J. Chem. Soc. Faraday Trans. II **74** [1978] 1909/19).
[13] Wiberg, N.; Meyers, R.; Vasisht, S. K.; Bayer, H. (Chem. Ber. **117** [1984] 2886/99).
[14] Wiberg, N.; Bayer, H.; Vasisht, S. K.; Meyers, R. (Chem. Ber. **113** [1980] 2916/27).
[15] McBride, W. R.; Kruse, H. W. (J. Am. Chem. Soc. **79** [1957] 572/6).
[16] Bull, W. E.; Seaton, J. A.; Audrieth, L. F. (J. Am. Chem. Soc. **80** [1958] 2516/8).
[17] Massa, W.; Kujanek, R.; Baum, G.; Dehnicke, K. (Angew. Chem. **96** [1984] 149).
[18] Ritter, G.; Häfelinger, G.; Lüddecke, E.; Rau, H. (J. Am. Chem. Soc. **111** [1989] 4627/35).
[19] Van Zandwijk, G.; Janssen, R. A. J.; Buck, H. M. (J. Am. Chem. Soc. **112** [1990] 4155/64).

2.4.2.2 Ammonium Azide, NH_4N_3

Other name: Ammonium trinitride

CAS Registry Number: *[12164-94-2]*

NH_4N_3, under ambient conditions a white crystalline solid, is one of the more stable azides, but has been reported to detonate with considerable violence when heated in a sealed tube [1, 2]. NH_4N_3 can be used as a detonation initiator [3].

Preparation and Formation. The preparation of NH_4N_3 from NH_3 and HN_3 [4, 5] was already described in "Ammonium" 1936, p. 80. A product yield of 74% could be achieved by using a solution of dry HN_3 in ether to which gaseous NH_3 was added [6]. Heating a dry mixture of NaN_3 and NH_4NO_3 to 473 K yielded about 85 to 95% of pure NH_4N_3. To avoid detonations it is recommended to prepare only small amounts of NH_4N_3 by the latter method [6]. Larger quantities of NH_4N_3 may conveniently be prepared by the reaction of NaN_3 with $(NH_4)_2SO_4$ [1] or NH_4Cl [7] in N,N-dimethylformamide between 358 to 393 K at a reduced pressure. The product is distilled together with the solvent from the reaction mixture. The yield is about 50% [7].

NH_4N_3 is formed by thermally decomposing 5-aminotetrazole via the intermediate NH_2CN [8]. Small amounts of NH_4N_3 were found in the reaction mixture of SO_2 and NH_3 in humid air with $(NH_3)_2 \cdot SO_2$ and $NH_3 \cdot SO_2$ being the main products [9]. NH_4N_3 is one of the decomposition products of lead azide in the presence of water [10]. The formation of NH_4N_3 as a decomposition product of diazene is described on p. 61, of tetrazene on p. 171, and of hydrazoic acid on pp. 120, 131.

Structure. NH_4N_3 crystallizes in the orthorhombic space group Pmna $-$ D_{2h}^7 (No. 53; the setting Pman was used in an earlier X-ray diffraction study [11]) with the unit cell parameters a = 8.948(3), b = 3.808(2), c = 8.659(3) Å, and Z = 4 at ambient temperature determined by neutron diffraction on single crystals. Half of a formula unit of NH_4N_3 represents the asymmetric unit with the ammonium nitrogens lying on a twofold axis, 1/4 of one azide group is lying on a mirror plane and 1/4 of the other on a twofold axis. Both azide groups have C_{2h} site symmetry and are perpendicular to each other. Each ammonium ion is bridged tetrahedrally to four nitrogens of four azide ions. The structure can be described as a distorted CsCl lattice with layers of azide ions parallel to the c axis. The structure model was refined to a reliability factor of 0.054 with 233 observed neutron reflections, treating the azide groups as rigid bodies. The following bond distances and angles resulted for the ammonium ion (the estimated standard deviations are given in parentheses): r(NH) = 1.037(10) and 1.001(9) Å; angles HNH = 106.0(1.1)°, 110.3(0.7)°, 110.3(0.7)°, 109.6(1.0)°. The corrected NN distance for the two crystallographically independent azide ions is 1.186(4) Å. The ammonium and azide ions are connected by N-H···N hydrogen bonds with N-N distances of 2.975(4) and 2.967(3) Å [12].

The crystal lattice energies were estimated to be 160 kcal/mol [13] and 175 kcal/mol [14].

Possible phase transitions between 90 and 348 K were excluded by comparing the infrared spectra at 90 K and ambient temperature [15], and the inelastic neutron scattering spectra at 293 and 348 K [16]. Two different phases obtained by sublimation of NH_4N_3 onto cold AgCl windows at 68 K were interpreted to result from the formation of disordered crystals which became ordered on warming [4].

Binding Energies. Solid NH_4N_3 was studied at 170 K by X-ray photoelectron spectroscopy. Three overlapping bands were recorded at 398.0, 400.3, and 402.3 eV. The first band was assigned to the terminal nitrogen atoms of the azide ion, the second band to the ammonium nitrogen, and the third band to the central nitrogen of the azide ion [17].

Internal and Lattice Vibrations. Infrared and Raman spectroscopic investigations were only performed on crystalline NH_4N_3. The symmetry of free NH_4^+ (T_d) and free N_3^- ($D_{\infty h}$) is reduced to the site symmetry C_2 and C_{2h} in the crystal lattice. The site group analysis for the NH_4^+ ion and the two crystallographically independent N_3^- ions is given in [4].

The asymmetric stretching and bending modes ν_3 and ν_4, which are triply degenerate in free NH_4^+, are split in the crystal. At 69 K infrared absorption bands at 3160, 3040, and 2880 cm^{-1} are attributed to ν_3 and bands at 1441, 1428, and 1420 cm^{-1} to ν_4. Additionally, a band at 1671 cm^{-1} was assigned to the symmetric bending mode ν_2 [4]. At ambient temperature no splitting could be observed and only one band at 3140 and at 1414 cm^{-1} was assigned to ν_3 and ν_4, respectively [5]. The spectra were recorded on powdered samples mulled with Nujol [5] and on NH_4N_3 sublimed onto an AgCl window [4].

Bands observed at 69 K at 420 cm^{-1} [4] and at ambient temperature at 396 cm^{-1} [5] were assigned to a torsional motion of the NH_4^+ ion at its lattice site. This observation indicates that the rotation of the NH_4^+ ion is hindered in the crystal lattice due to hydrogen bonds [4]. The torsional frequency was also observed at about 400 cm^{-1} by inelastic neutron scattering at 293 and 384 K. A shoulder at 300 cm^{-1} in the spectrum is attributed to a transition between the first and the second excited state of the torsional oscillator NH_4^+. The intensity ratio of the two peaks varied with temperature and supported the assignment. The NH_4^+ ions are therefore torsionally oscillating in a very anharmonic potential well with the energy levels of the first and the second excited state at 400 and 700 cm^{-1} above the ground state, respectively. The height of the potential barrier was estimated to be about 25 kJ/mol [16].

A strong band at 2030 cm^{-1} and a weak one at 1345 cm^{-1} in the IR spectrum at 69 K were assigned to the antisymmetric and the symmetric stretching vibrations ν_3 and ν_1 of the azide ion, respectively. The bands at 664 and 652 cm^{-1} are associated with the bending mode ν_2 [4]. The bending mode was also observed in the inelastic neutron scattering spectrum at 680 cm^{-1} [16]. The regions around ν_2 and ν_1 were also studied by far-IR and Raman spectroscopy at ambient temperature and interpreted by a factor group analysis. ν_2 was split into several peaks: 623 and 630 cm^{-1} (B_{1u}), 652 and 664 cm^{-1} (B_{2u} and B_{3u}). The strong peak in the Raman spectrum at 1355 cm^{-1} was assigned to $\nu_1(A_{1g})$, while the weak shoulder at 1375 cm^{-1} is likely due to $\nu_1(B_{1g})$. The spectral results show only one-half of the calculated internal mode splittings, suggesting that the observed N_3^- internal mode spectra are determined by the correlation field interaction between the two types of N_3^- sites, enhanced to some extent by hydrogen bond perturbations [15].

Frequencies of the $\vec{k}\approx 0$ lattice modes were obtained from Raman and IR spectra in the range 30 to 700 cm^{-1} [15] and by inelastic neutron scattering (INS) [16] and assigned as follows (T denotes the translational and R the librational modes) [15]:

	frequencies in cm^{-1}		assignments
Raman	infrared	INS	
89 s, 101 m, sh	–	104 w	$R(N_3^-)$, B_{2g}, B_{3g}
117 m, 130 m	–	136 w	$R(N_3^-)$, A_{1g}, B_{1g}
–	92 s	–	$T(N_3^-)$, B_{1u}
–	128 s, 162 m	168 w	$T(N_3^-)$, B_{2u}, B_{3u}
–	194 m, 228 m, br	192 w, 220 w	$T(NH_4^+)$
205 m, 240 w, sh	–	–	$T(NH_4^+)$
–	405 w	400 s	$R(NH_4^+)$

Force constants (in 10^5 dyn/cm) in mass-weighted cartesian coordinates were calculated for the N_3^- unit in solid NH_4N_3 from the stretching vibrations to be $F_{11}=F_{33}=13.130$, $F_{13}=F_{31}=-1.796$, $F_{22}=22.668$, $F_{12}=F_{21}=F_{23}=F_{32}=-11.334$ and from the bending vibrations to be $F'_{11}=F'_{13}=F'_{31}=0.584$, $F'_{12}=F'_{21}=F'_{23}=F'_{32}=-1.168$, $F'_{22}=2.336$ [18].

Diamagnetic Susceptibility. $\chi_m=-34.0\times10^{-6}$ cm^3/mol was determined from measurements at 296 ± 1 K using KCl as a calibrant [19].

Density. The calculated and measured densities of NH_4N_3 crystals, 1.352 g/cm^3 at 299 K, agree with one another [11, 12]. A density of 1.350 g/cm^3 was measured at 298 K [20].

Molar Refraction. From the extrapolated refractive index $n=1.573$ at λ_∞, the molar refraction of 14.66 cm^3/mol was determined at ambient temperature [20].

Sublimation. NH_4N_3 sublimes at 406 K [6], 407 K [21]. A condensation temperature of NH_4N_3 vapor of 418 K was determined from differential scanning calorimetric (DSC) cooling diagrams. The sublimation was investigated by thermogravimetric and DSC cooling diagrams. The isothermal sublimation kinetics was studied by weight-loss measurements between 360 to 389 K. The sublimation follows a zero-order kinetics with an activation energy of 93.7 kJ/mol and a frequency factor of 4.8×10^{11} s^{-1}. The enthalpy of sublimation, $\Delta_{subl}H° = 73.6$ kJ/mol, at 418 K was obtained from DSC cooling diagrams [22]. This value is close to a value of 65.8 kJ/mol which was derived from vapor pressure data between 288 and 407 K taken from [23]. It was suggested that NH_4N_3 sublimes by forming NH_4N_3 vapor which subsequently dissociates into NH_3 and HN_3 above 418 K [22]. A significantly larger value for the sublimation enthalpy, 163.4 kJ/mol, is probably derived from measurements on the dissociation of NH_4N_3 [21].

Thermodynamic Data of Formation. The standard ($p° = 0.1$ MPa) molar enthalpy of formation for crystalline NH_4N_3 was derived from measurements of the energy of combustion in oxygen: $\Delta_fH°(NH_4N_3, cr) = 114.14 \pm 0.94$ kJ/mol at 298.15 K [24]. Earlier values are 112.1 kJ/mol [17, 25] and 139 kJ/mol [13] and tabulated values $\Delta_fH° = 115.5$ kJ/mol, $\Delta_fG° = 274.2$ kJ/mol, and $S° = 112.5$ $J \cdot mol^{-1} \cdot K^{-1}$ at 298.15 K and 0.1 MPa [26]. Combined with the measured enthalpy of solution, $\Delta_{sol}H°(NH_4N_3, cr, \infty\ H_2O) = 27.23 \pm 0.06$ kJ/mol, the enthalpy of formation in aqueous solution was derived to be $\Delta_fH°(NH_4N_3, aq, \infty) = 141.37 \pm 0.94$ kJ/mol [24]. A value of 142.7 kJ/mol was tabulated earlier together with $\Delta_fG° = 268.7$ kJ/mol and $S° = 221.3$ $J \cdot mol^{-1} \cdot K^{-1}$ at 298.15 K and 0.1 MPa [26]. The enthalpy of formation of gaseous NH_4N_3 at 298.15 K was obtained to be 185.6 [22] or 179.7 kJ/mol [24] by adding the enthalpy of sublimation (values given above) to the enthalpy of formation of crystalline NH_4N_3.

Heat Capacity. DSC measurements between 328 and 363 K were used to determine the specific heat capacity, obtaining $c_p = (2.09 \pm 0.41)$ $J \cdot g^{-1} \cdot K^{-1}$ at 298.15 K by extrapolation [24].

Chemical Behavior. The monomeric NH_4N_3 vapor was found to dissociate into NH_3 and HN_3 above 418 K. The reaction enthalpy was calculated to be 67.7 kJ/mol [22].

NH_4N_3 is considered a "weak explosive" causing considerable shattering because of the large volume of the gaseous explosion products [2]. The explosion reaction can be represented by the equation $NH_4N_3(s) \rightarrow NH_3(g) + 1/2\ H_2(g) + 3/2\ N_2(g)$ with a reaction enthalpy of -158 kJ/mol [27]. An activation energy of decomposition of $E_a = 110.11$ kJ/mol was derived from a linear relationship between E_a and the heat of explosion of inorganic azides (130.5 kJ/mol was used as heat of explosion for NH_4N_3) [3]. The explosion hazard of aqueous solutions, due to precipitation of solid NH_4N_3 following evaporation of water, was studied on single drops of the solutions. Safety and danger zones were estimated depending on the droplet velocity and temperature [28].

Decomposition via $3\ NH_4N_3 \rightarrow 4\ NH_3 + 4\ N_2$ is induced by irradiation at wavelengths below 300 nm. Therefore, NH_4N_3 was proposed as a propellant in photochemical microrockets for altitude control [29].

The enthalpy of combustion of NH_4N_3 in oxygen via $NH_4N_3(cr) + O_2(g) \rightarrow 2\ H_2O(l) + 2\ N_2(g)$ was measured calorimetrically to give $\Delta H = -685.8 \pm 0.9$ kJ/mol [24]. NH_4N_3 is reduced by Cu, Fe, and Al in aqueous solution, whereby triazene is the probable reaction product [30]. The combustion rate of the reaction $Mo + B \rightarrow MoB$ is reduced in the presence of NH_4N_3 [31].

When powdered NH_4N_3, covered by purified cyclohexane under an N_2 or Ar atmosphere, was photolyzed at 303 K, the main decomposition products were cyclohexyl and cyclohexylidene amines. The extent of decomposition increased from 11.4 to ~18% after 12 h of irradiation and to 52% after 72 h of irradiation [32].

NH_4N_3 reacts with *cis*- or *trans*-thiobenzoyl chloride S-oxide in ethanolic solution to give benzonitrile, nitrogen, chloride, sulfur, and sulfur dioxide. Thiobenzoyl azide S-oxide could be isolated as an intermediate product [33].

The 1,3 cycloaddition of N_3^- (from NH_4N_3) to nitrile compounds is a convenient method to prepare substituted tetrazoles. The reaction is normally performed at 373 K in dimethylformamide as solvent; see e.g. [34 to 36].

References:

[1] Obenland, C. O.; Mangold, D. J.; Marino, M. P. (Inorg. Synth. **8** [1966] 53/6).

[2] Yakovleva, G. S.; Kurbangalina, R. K.; Stesik, L. N. (Fiz. Goreniya Vzryva **13** [1977] 473/5; Combust. Explos. Shock Waves [Engl. Transl.] **13** [1977] 405/7).

[3] Zeman, S.; Dimun, M.; Truchlik, S.; Kabatova, V. (Thermochim. Acta **80** [1984] 137/41).

[4] Dows, D. A.; Whittle, E.; Pimentel, G. C. (J. Chem. Phys. **23** [1955] 1475/9).

[5] Waddington, T. C. (J. Chem. Soc. **1958** 4340/4).

[6] Frierson, W. J.; Filbert, W. F. (Inorg. Synth. **2** [1946] 136/8).

[7] Evans, L.; Yoffe, A. D.; Gray, P. (Chem. Rev. **59** [1959] 515/68).

[8] Gao, A.; Oyumi, Y.; Brill, T. B. (Combust. Flame **83** [1991] 345/52).

[9] Hartley, E. M., Jr.; Matteson, M. J. (Ind. Eng. Chem. Fundam. **14** [1975] 67/72).

[10] Reitzner, B. (J. Phys. Chem. **65** [1961] 948/52).

[11] Frevel, L. K. (Z. Kristallogr. **94** [1936] 197/211).

[12] Prince, E.; Choi, C. S. (Acta Crystallogr. B **34** [1978] 2606/8).

[13] Kaganyuk, D. S. (Zh. Neorg. Khim. **23** [1978] 2003/8; Russ. J. Inorg. Chem. [Engl. Transl.] **23** [1978] 1099/102).

[14] Gray, P.; Waddington, T. C. (Proc. R. Soc. London A **235** [1956] 481/95).

[15] Iqbal, Z.; Malhotra, M. L. (Spectrochim. Acta A **27** [1971] 441/6).

[16] Boutin, H.; Trevino, S.; Prask, H. (J. Chem. Phys. **45** [1966] 401/2).

[17] Colton, R. J.; Rabalais, J. W. (J. Chem. Phys. **64** [1976] 3481/6).

[18] Mou, C. Y.; Chen, T. (J. Chin. Chem. Soc. [Taipei] **17** [1970] 193/206).

[19] Dobramysl, W.; Fritzer, H. P. (Inorg. Nucl. Chem. Lett. **14** [1978] 269/73).

[20] Batsanov, S. S. (Kristallografiya **1** [1956] 328/33; Sov. Phys.-Crystallogr. [Engl. Transl.] **1** [1956] 254/7).

[21] Luft, N. W. (Ind. Chem. **31** [1955] 502/4).

[22] Ng, W. L.; Field, J. E. (Thermochim. Acta **84** [1985] 133/40).

[23] Frost, W. S.; Cothran, J. C.; Browne, A. W. (J. Am. Chem. Soc. **55** [1933] 3516/8).

[24] Finch, A.; Gardner, P. J.; Head, A. J.; Wu, X. (J. Chem. Thermodyn. **22** [1990] 301/5).

[25] Gray, P.; Waddington, T. C. (Proc. R. Soc. London A **235** [1956] 106/19).

[26] Wagman, D. D.; Evans, W. H.; Parker, V. B.; et al. (J. Phys. Chem. Ref. Data **11** [1982] 2-65).

[27] Gray, P.; Waddington, T. C. (Research [London] **8** [1955] S56/S57).

[28] Gerstein, M.; Choudhury, P. R. (Prog. Astronaut. Aeronaut. **95** [1984] 455/63; C.A. **102** [1985] No. 116038).

[29] Maycock, J. N.; Verneker, V. R. P. (J. Spacecr. Rockets **6** [1969] 336/7).

[30] Papazian, H. A. (J. Chem. Phys. **32** [1960] 456/60).

[31] Novikov, N. P.; Borovinskaya, I. P.; Boldyrev, V. V. (Fiz. Goreniya Vzryva **13** [1977] 342/8; Combust. Explos. Shock Waves [Engl. Transl.] **13** [1977] 281/4).

[32] Marcantonio, A. F.; Thekkekandamm, J. T. (J. Am. Chem. Soc. **93** [1971] 1524/6).

[33] Holm, A.; Carlsen, L. (Tetrahedron Lett. **1973** 3203/4).

[34] Finnegan, W. G.; Henry, R. A.; Lofquist, R. (J. Am. Chem. Soc. **80** [1958] 3908/11).

[35] Kaczmarek, J.; Smagowski, H.; Grzonka, Z. (J. Chem. Soc. Perkin Trans. II **1979** 1670/4).
[36] Seldes, A. M.; Thiel, I. M. E.; Deferrari, J. O. (Carbohydr. Res. **39** [1975] 47/51).

2.4.3 Tetrazane, N_4H_6

CAS Registry Number: *[6054-69-9]*

Tetrazane seems to form in addition to equimolar amounts of H_2 and N_2 upon thermolysis of ~0.5 Torr of N_2H_4 at around 1120 K. A substance can be isolated by rapidly freezing the less volatile products at 78 K. A stable, bright yellow solid results, which consists of the supposed N_4H_6 in a mixture with NH_3 also formed, in addition to unreacted N_2H_4. The formation of N_4H_6 is evidenced by the properties of the product and its decomposition. The absent paramagnetism of the solid and a half-life of the gaseous product of ~0.01 s at ambient temperature preclude the formation of a radical. The exothermic decomposition starts at 95 K and yields N_2 and NH_3. Experiments with ^{15}N-labeled N_2H_4 show some randomization of the N_2 formed [1]. The intermediate formation of N_4H_6 is considered one reaction channel in the decomposition of the N_2H_3 radical in the gas phase. The assumption is based on the partial scrambling of the N_2 formed when mixtures of ^{15}N-labeled N_2H_4 are used. Details and the earlier literature are given in [2]. The existence of isolable N_4H_6 seems not to have been confirmed later.

Tetrazane is possibly a precursor of N_3H_3 in the one-electron oxidation of aqueous N_2H_4; see also p. 159. The formation of N_4H_6 is postulated on the basis of the second-order decay of the hydrazyl radical. A first-order decay of N_4H_6 with formation of NH_3 and instable N_3H_3 was suggested by the formation of a second intermediate. The slowing of N_3H_3 formation when increasing the pH from 8 to 11 probably can be attributed to a decay after N_4H_6 protonation with formation of $N_4H_7^+$ and $N_4H_8^{2+}$. The pK_a constants of the ions are possibly in the range 5 to 9 [3].

The heat of formation of N_4H_6 was estimated by a semiempirical relation to be 342 kJ/mol at 298 K. A stabilization energy of −27.6 kJ/mol is indicative of a thermodynamically unstable molecule. It was predicted to be stable towards dissocation into H_2NNH radicals [4]. A limited number of completely substituted tetrazanes is known; see [5] for a review.

References:

[1] Rice, F. O.; Scherber, F. (J. Am. Chem. Soc. **77** [1955] 291/3).
[2] Stief, L. J. (J. Chem. Phys. **52** [1970] 4841/5).
[3] Hayon, E.; Simic, M. (J. Am. Chem. Soc. **94** [1972] 42/7).
[4] Leroy, G.; Sana, M.; Wilante, C.; Peeters, D.; Dogimont, C. (J. Mol. Struct. **153** [1987] 249/67 [THEOCHEM **38**]).
[5] Benson, F. R. (The High Nitrogen Compounds, Wiley-Interscience, New York 1984, pp. 1/679, 126/8).

2.5 Penta- and Polynitrogen Compounds

2.5.1 Compounds of the Composition N_5H

Neither the cyclic nor the acyclic isomers of N_5H have been observed experimentally; only organic derivatives of cyclopentazadiene, c-N_5H, are known, but their thermal stability is low. The acyclic isomers of N_5H are supposed to consist of a double-bonded N_2 unit with a hydrogen and an N_3 substituent. Each of the (Z) and (E) isomers forms an s-cis or s-trans conformer depending on the spatial arrangement of the approximately linear N_3 unit with respect to the N-N double bond. An ab initio SCF MO calculation at the STO-3G level showed that cyclopentazadiene is the most stable isomer of N_5H, followed by the (E) s-trans isomer of acyclic N_5H and the (Z) s-trans, the (E) s-cis, and the (Z) s-cis isomers. The decomposition to HN_3 and N_2 is exothermal for all isomers of N_5H. A mutual conversion between the (Z) and (E) isomers is predicted not to occur [1].

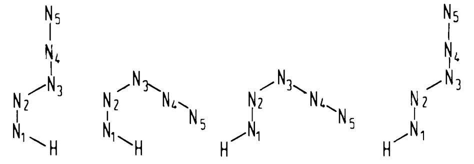

(Z) s-trans (Z) s-cis (E) s-cis (E) s-trans

Cyclopentazadiene (Pentazole), c-N_5H

CAS Registry Number: *[289-19-0]*

The formation of c-N_5H by 1,3-dipolar cycloaddition of N_2 to HN_3 or by cyclization of the (E) s-cis isomer of N_5H was studied in ab initio SCF and limited CI calculations [1]. A heat of formation of 891 kJ/mol was obtained from an MNDDO/1 calculation [2]. The structural parameters of (planar) c-N_5H with C_{2v} symmetry were optimized in an HF calculation at the 6-21G level [3]; results of a calculation by the many-body perturbation theory (MBPT(2)/DZP) were also given [4]. Internuclear distances and angles are listed below:

internuclear distances in Å				angles in degree				Ref.
H-N_1	N_1-N_2	N_2-N_3	N_3-N_4	HN_1N_2	$N_5N_1N_2$	$N_1N_2N_3$	$N_2N_3N_4$	
0.989	1.323	1.276	1.367	124.3	111.3	105.6	108.7	[3]
0.996	1.298	1.264	1.330	124.05	–	–	–	[4]

Vertical ionization potentials of 11.53 eV for σ ionization and 11.75 eV for π ionization and a dipole moment of 4.10 D were calculated [3]. Polarizabilities [5], the ^{15}N chemical shift, the diamagnetic susceptibility, and Dewar and Hess-Schaad resonance energies were also calculated [6]. A very strong fundamental with A_1 symmetry at 3922 cm^{-1} (SCF/DZP) or at 3700 cm^{-1} (MBPT(2)/DZP) was predicted [4].

The decomposition reactions c-$N_5H \rightarrow HN_3 + N_2$ and c-$N_5H \rightarrow NN(H)N + N_2$ have MBPT(2) barriers of 82.8 and 224.7 kJ/mol, applying estimates for the zero-point and internal energy corrections [4]. The small value for the first reaction indicates a questionable kinetic stability of N_5H [1, 7]; see also [2]. Cyclopentazadiene is predicted to be strongly acidic [8]. Deprotonation [9] and absolute protonation energies were calculated; the most basic center, N_3, is protonated preferentially [3]. Protonation and deprotonation energies of pentahydrated cyclopentazadiene are given in [9]. A stable Li^+ complex of pentazole was predicted to be obtainable only upon coordination at the 3-position [10].

Organically substituted pentazoles form from arenediazonium salts and alkali azides; see [11] for a review. The reactions in aqueous solution at ambient temperature are strictly first order in each of the reactants; intermediates were not detected [12]. An almost planar N_5 ring in *p*-(dimethylamino)phenyl pentazole was deduced from a single-crystal X-ray investigation. Internuclear distances are $r(N_1\text{-}N_2) = 1.321$, $r(N_2\text{-}N_3) = 1.309$, and $r(N_3\text{-}N_4) = 1.347$ Å; their values are intermediate between single- and double-bond lengths and indicate aromaticity. Angles measured are $\angle RN_1N_2 = 123.9°$, $\angle N_1N_2N_3 = 105.1°$, and $\angle N_2N_3N_4 = 108.8°$ [13]. The substituted pentazole in $CDCl_3$ solution at 238 K has ^{15}N NMR shifts of $\delta = -80.0 \pm 0.3$ ppm for N_1, $\delta = -27.1 \pm 0.3$ ppm for N_2, and $\delta = 4.9 \pm 0.3$ ppm for N_3 (negative high-field shifts) from external CH_3NO_2 [14]. A ^{14}N chemical shift of $\delta = -70 \pm 1$ ppm was assigned to N_1 in $CH_3OH\text{-}CH_2Cl_2$ at 305 K. (Shifts of N_5H of $\delta = -75 \pm 9$ ppm for N_1, $\delta = 7 \pm 15$ ppm for N_2, and $\delta = -13 \pm 14$ ppm for N_3 were predicted by an empirical rule [15].) The decomposition of aryl pentazoles yields aryl azides and N_2 [11].

1,2,4-Pentazatriene, N_5H

CAS Registry Numbers: *[72635-51-9]*, (*E*)-N_5H *[77269-51-3]*, (*Z*)-N_5H *[77269-50-2]*

The formation of (*E*)-N_5H from HN_3 and N_2 has an activation energy of 99.2 and an enthalpy of 89.1 kJ/mol at the STO-3G level. Structural parameters of the planar, acyclic N_5H isomers were calculated at the STO-3G level. Dipole moments in the range of 1.2 ((E) s-cis isomer) to 3.0 D ((Z) s-cis isomer) were calculated with inclusion of CI.

Barriers to a s-trans → s-cis conversion of the conformers by rotation around the $N_2\text{-}N_3$ bond were calculated to be less strongly endothermic than the (Z) → (E) inversion. However, decomposition to HN_3 and N_2 is exothermic [1].

References:

[1] Sana, M.; Leroy, G.; Nguyen, M.-T.; Elguero, J. (Nouv. J. Chim. **3** [1979] 607/21).
[2] Carrion, F. (unpublished, ref. 18 in: Dewar, M. J. S.; Pure Appl. Chem. **44** [1975] 767/82).
[3] Mó, O.; de Paz, J. L. G.; Yáñez, M. (J. Phys. Chem. **90** [1986] 5597/604).
[4] Ferris, K. F.; Bartlett, R. J. (J. Am. Chem. Soc. **114** [1992] 8302/3).
[5] Waite, J.; Papadopoulos, M. G. (J. Phys. Chem. **94** [1990] 1755/8).
[6] Katritzky, A. R.; Barczinsky, P. (J. Prakt. Chem. **332** [1990] 885/97).
[7] Janoschek, R. (Angew. Chem. **105** [1993] 242/4; Angew. Chem. Int. Ed. Engl. **32** [1993] 230).
[8] Catalán, J.; De Paz, J. L. G.; Yáñez, M.; Elguero, J. (Chem. Scr. **24** [1984] 84/91).
[9] Catalán, J.; Sanchez-Cabezudo, M.; De Paz, J. L. G.; Elguero, J. (J. Mol. Struct. **166** [1988] 415/20 [THEOCHEM **43**]).
[10] Alcami, M.; Mó, O.; Yáñez, M. (J. Phys. Chem. **93** [1989] 3929/36).

[11] Ugi, I. (in: Katritzky, A. R.; Rees, C. W.; Comprehensive Heterocyclic Chemistry, Vol. 5, Pergamon, Oxford 1984, pp. 839/45).
[12] Ritchie, C. D.; Wright, D. J. (J. Am. Chem. Soc. **93** [1971] 2429/32).
[13] Wallis, J. D.; Dunitz, J. D. (J. Chem. Soc. Chem. Commun. **1983** 910/1).
[14] Müller, R.; Wallis, J. D.; v. Philipsborn, W. (Angew. Chem. **97** [1985] 515/7; Angew. Chem. Int. Ed. Engl. **24** [1985] 513).
[15] Witanowski, M.; Stefaniak, L.; Januszewski, H.; Bahadur, K.; Webb, G. A. (J. Cryst. Mol. Struct. **5** [1975] 137/40).

2.5.2 The Cyclopentazadienium Ion, $c\text{-}N_5H_2^+$

CAS Registry Number: *[103692-66-6]*

The structural parameters of the (planar) cyclopentazadienium ions formed by protonation at the 2-position (**a**) or 3-position (**b**) of cyclopentazadiene were calculated at the HF/6-31G level. Internuclear distances and angles are as follows [1]:

bond	$H\text{-}N_1$	$H\text{-}N_{2(3)}$	$N_1\text{-}N_2$	$N_2\text{-}N_3$	$N_3\text{-}N_4$	$N_4\text{-}N_5$	$N_5\text{-}N_1$
distance in Å for **a**	1.004	1.004	1.321	1.288	1.317	1.317	1.288
distance in Å for **b**	1.001	1.001	1.281	1.281	1.350	1.262	1.350

angle	HN_1N_2	$HN_{2(3)}N_{3(4)}$	$N_5N_1N_2$	$N_1N_2N_3$	$N_2N_3N_4$	$N_3N_4N_5$	$N_4N_5N_1$
value in deg. for **a**	126.8	124.7	108.6	108.6	107.1	108.7	107.1
value in deg. for **b**	124.2	123.3	112.5	103.0	112.5	106.0	106.0

The pK_a values of -15.74 for **a** and of -9.36 for **b** were obtained from an empirical equation on the basis of the calculated proton affinities [2].

References:

[1] Mó, O.; de Paz, J. L. G.; Yáñez, M. (J. Phys. Chem. **90** [1986] 5597/604).

[2] Andrianov, V. G.; Shokhen, M. A.; Eremeev, A. V. (Khim. Geterotsikl. Soedin. **1989** 508/11; Chem. Heterocycl. Compd. [Engl. Transl.] **25** [1989] 423/5).

2.5.3 Hydrazinium(1+) Azide, $N_2H_5N_3$, and Its Monohydrazinate, $N_2H_5N_3 \cdot N_2H_4$

Other names: Hydrazonium azide, hydrazine azide

CAS Registry Numbers: $N_2H_5N_3$ *[14662-04-5]*, $N_2H_5N_3 \cdot N_2H_4$ *[14546-45-3]*

Preparation and Formation. Colorless crystals of $N_2H_5N_3$ are prepared after the modified method of Curtius (see "Ammonium" 1936, p. 549) by bubbling a gaseous HN_3-N_2 mixture through an aqueous hydrazine solution. Based on the amount of the starting material NaN_3, which is also used to prepare HN_3, a yield of at least 85% was achieved [1]. The compound may also be prepared by adding N_2H_4 to an excess of dilute HN_3 [1] or by reacting stoichiometric amounts of NH_4N_3 with anhydrous N_2H_4 [2] or aqueous N_2H_4 [3]. Crystals suitable for single-crystal X-ray analysis are obtained by slowly evaporating an aqueous $N_2H_5N_3$ solution in the presence of dehydrating agents [4]. The crystals are hygroscopic and need to be handled in a dry atmosphere [3].

$N_2H_5N_3$ was observed during the thermal decomposition of 5-aminotetrazole (CN_5H_3) [5] and *trans*-2-tetrazene (see also p. 171) [6]. Besides NH_4N_3 traces of $N_2H_5N_3$ were formed at 148 K in glow-discharged HN_3 [7].

Because of its explosive nature, $N_2H_5N_3$ was proposed to be used in propellant mixtures; see e.g. [8 to 12]. The oxidizing properties can be applied in the chemical vapor deposition of semiconducting materials for electronic devices; see e.g. [13 to 15].

Physical Properties. $N_2H_5N_3$ crystallizes in the monoclinic space group $P2_1/b - C_{2h}^5$ (No. 14) with four formula units in the unit cell and the cell parameters $a = 5.663(2)$, $b = 12.436(3)$, $c = 5.506(2)$ Å, $\gamma = 114.0(0.1)°$ [4], or in the equivalent space group $P2_1/n$ with $a = 5.665(2)$, $b = 5.522(2)$, $c = 11.401(4)$ Å, $\beta = 93.00(4)°$ [1, 16]. The structure was derived from single-crystal X-ray diffractometric data and refined to a reliability factor of 0.044. The structure is built up of N_3^- and $N_2H_5^+$ ions held together by a three-dimensional framework of N-H···N hydrogen bonds. The hydrazinium ions with an intraionic N-N distance of 1.45 Å exhibit an almost perfectly staggered conformation of H atoms. The ions are connected via hydrogen bonds to form infinite chains along a twofold screw axis. The azide ion forms a quasi-linear chain (angle NNN = 179.3°) with an N-N distance of 1.17 Å. In this structure the typical N-N distances within the N-H···N hydrogen bonds range from 2.8 up to 3.4 Å [4].

The infrared spectrum of solid $N_2H_5N_3$ was recorded by [3, 16]. By comparing this spectrum with that of KN_3, the characteristic frequencies of the N_3^- moiety ($D_{\infty h}$) were found at 2036 (ν_3) and at 635 cm^{-1} (ν_2). Based on a comparison with the spectrum of N_2H_5Cl, the remaining frequencies were assigned to the $N_2H_5^+$ moiety. The band at 950 cm^{-1} (960 cm^{-1} in [3]) was assigned to ν(NN); additional strong bands were found at 1620 and at 1100 cm^{-1} and a medium one at 3170 cm^{-1} [16].

The density of crystalline $N_2H_5N_3$ was measured to be 1.400 g/cm^3 at 298 K [16] (1.40 g/cm^3 [1, 4]) and calculated to be 1.407 g/cm^3 [4].

The melting points reported for $N_2H_5N_3$ differ from each other. The hygroscopicity and a probable mix-up with $N_2H_5N_3 \cdot N_2H_4$ may have caused errors in determining the melting point. The highest reported value of 355 K stems from a thermoanalytic study [17], but is in conflict with a lower value of 348 K reported earlier by the same group [3] and by others [18, 19]. The even lower, thermoanalytically determined value of 343.6 K was claimed to be reliable, because in that case the formation of $N_2H_5N_3 \cdot N_2H_4$ was excluded [1, 16].

$N_2H_5N_3$ is reported to volatilize at ~443 K without any violent reaction [17]. This conflicts with the results of other investigations which report a violent decomposition at ~403 K [19] or at 408 K [16]. Compared to other hydrazinium compounds, such as $N_2H_5NO_3$ and N_2H_5Cl, the vapor pressure over $N_2H_5N_3$ is high (~525 Torr at 433 K) due to the low acidity and high volatility of HN_3 formed via $N_2H_5N_3 \rightleftharpoons N_2H_4 + HN_3$ [18]. Vapor pressures of less than 1 Torr at room temperature and of less than 100 Torr at 333 K were reported [20].

The enthalpy of formation, $\Delta_fH°(s)$, was determined to be 246.4 ± 1.6 kJ/mol [21]. The enthalpy and entropy of fusion of $N_2H_5N_3$ are 15.82 ± 0.25 kJ/mol and 45.6 ± 0.8 $J \cdot mol^{-1} \cdot K^{-1}$, respectively [19].

A mixture of 23% $N_2H_5N_3$ in hydrazine has a conductivity of 0.18 S/cm at 298 K [22].

Thermal Decomposition. Decomposition of $N_2H_5N_3$ in the liquid phase between 400.3 to 443.8 K proceeds through initial dissociation into N_2H_4 and HN_3. The reaction rate is dependent mainly on the rate of interaction of the salt with HN_3. $N_2H_5N_3$ exhibits autocatalytic behavior below 443 K with NH_3, N_2H_4, and N_2 being the final products. The first-order autocatalytic decomposition follows the rate law $d\eta/dt = k_1(1-\eta) + k_2\eta(1-\eta)$, where $k_1 = 10^8 \exp(-100\ kJ \cdot mol^{-1}/RT)\ s^{-1}$ and $k_2 = 10^4 \exp(-67\ kJ \cdot mol^{-1}/RT)\ s^{-1}$. The decomposition essentially follows the overall equation $N_2H_5N_3 \rightarrow 0.25\ N_2H_4 + 1.33\ NH_3 + 1.58\ N_2$, and the calculated heat of reaction of 288 to 297 kJ/mol at 298 K is close to the experimentally obtained value of 285 ± 8 kJ/mol between 418.7 to 443.8 K [18]. Earlier, the Arrhenius expression $k = 10^8 \exp(-100\ kJ \cdot mol^{-1}/RT)\ s^{-1}$ was derived from the initial decomposition rates determined at 393, 423, and 473 K [23].

The decomposition of solid $N_2H_5N_3$ in argon at a pressure of $\sim 2.3 \times 10^4$ Torr proceeds via $N_2H_5N_3(s) \rightarrow 2.18\ N_2(g) + 1.52\ H_2(g) + 0.65\ NH_3(g)$ with a reaction enthalpy of -276.1 ± 0.8 kJ/mol [21]. The dry, powdered compound is reported to detonate on contact with a heated wire [24]. Depending on the experimental conditions, two pathways were proposed for the decomposition: $N_2H_5N_3 \rightarrow 2.5\ N_2 + 2.5\ H_2$ and $N_2H_5N_3 \rightarrow 1.666\ NH_3 + 1.66\ N_2$ [25].

Electrochemical Decomposition. A mixture of 23% $N_2H_5N_3$ with hydrazine was investigated with platinum, graphite, and stainless steel electrodes. The cathodic products were N_2, NH_3, and H_2. With a platinum electrode, only N_2 and H_2 were produced, thus indicating a catalytic decomposition on the surface. Nitrogen was the only anodic product [22]. The rate-limiting anodic reaction is the decomposition of hydrazine molecules. Azide ions are discharged during the initial stage, but the polarization for this reaction shifts the potential to a point where simple hydrazine discharge predominates. The cathodic and anodic reactions are both diffusion-controlled [26].

Titration. The existence of $N_2H_5N_3$ can be demonstrated by oxidation with IO_3^- via $3\,N_2H_5N_3 + 2\,KIO_3 \rightarrow 3\,N_2 + 2\,KI + 6\,H_2O + 3\,HN_3$ [1].

Systems with N_2H_4 and $N_2H_4 \cdot H_2O$. In the binary system N_2H_4-$N_2H_5N_3$ a eutecticum was found at 257.1 K and 22.7% $N_2H_5N_3$ using technical-grade hydrazine with about 1% H_2O [27] and at 258.1 K and 23.8% $N_2H_5N_3$ using strictly anhydrous hydrazine. Densities and kinematic viscosities were determined on mixtures of $N_2H_5N_3$ with 72.4 to 80% N_2H_4 [11]. The resulting addition compound $N_2H_5N_3 \cdot N_2H_4$ is described below.

The ternary system $N_2H_5N_3$-N_2H_4-H_2O was studied within the ranges 1.0 to 12.6% H_2O, 72.5 to 76.4% N_2H_4, and 14.9 to 23.6% $N_2H_5N_3$. The ternary system appears to be a pseudobinary system of $N_2H_4 \cdot H_2O$ and $N_2H_5N_3$. The temperature of the eutectic melt decreased from 257.1 K for 22.7% $N_2H_5N_3$ and 1% H_2O to 245.8 K for 15.9% $N_2H_5N_3$ and 12.6% H_2O. The densities of the ternary mixtures at 298 K increased linearly with the $N_2H_5N_3$ content [27].

Hydrazinium(1+) Azide Monohydrazinate. As already described in "Ammonium" 1936, p. 549, the addition compound $\mathbf{N_2H_5N_3 \cdot N_2H_4}$ forms in the binary system $N_2H_5N_3$-N_2H_4 and can be precipitated with absolute alcohol from a saturated solution of $N_2H_5N_3$ in N_2H_4. It is used as an additive to propellants [8, 9, 28] because it lowers the combustion temperature [8].

The decomposition of the solid compound under an argon pressure of 2.3×10^4 Torr was found to proceed according to $N_2H_5N_3 \cdot N_2H_4(s) \rightarrow 2.63\,N_2(g) + 1.91\,H_2(g) + 1.73\,NH_3(g)$ with a reaction enthalpy of -373.6 ± 2.1 kJ/mol. Therefrom its enthalpy of formation, $\Delta_fH°(s) = 294.1 \pm 3.3$ kJ/mol, was derived [21].

The thermal decomposition of $N_2H_5N_3 \cdot H_4N_2$ was investigated in the liquid phase at 430 and 439 K; initial rates were determined to be 4.5×10^{-6} and $13.7 \times 10^{-6}\ s^{-1}$, respectively. Under these conditions N_2H_4, NH_3, and N_2 are the final decomposition products. In contrast to hydrazinium azide (cf. p. 181), whose decomposition is determined by the rate of reaction of the salt with formed HN_3, the initial rate of the $N_2H_5N_3 \cdot H_4N_2$ decomposition is lower and almost entirely depends on the decomposition of the intermediately formed complex $N_2H_5^+ \cdot N_2H_4$ [18].

References:

[1] Pannetier, G.; Margineanu, F.; Dereigne, A.; Bonnaire, R. (Bull. Soc. Chim. Fr. **1972** 2617/22).

[2] Müller, E. (Ger. 634688 [1936]; C.A. **1937** 511; cited as ref. 22 in [1]).

[3] Patil, K. C.; Soundararajan, R.; Verneker, V. R. P. (Proc. Indian Acad. Sci. A **87** [1978] 281/4).

[4] Chiglien, G.; Etienne, J.; Jaulmes, S.; Laruelle, P. (Acta Crystallogr. B **30** [1974] 2229/33).

[5] Reimlinger, H. (Chem. Ind. [London] **1972** 294/5).

[6] Veith, M.; Schlemmer, G. (Z. Anorg. Allg. Chem. **494** [1982] 7/19).

[7] Wannagat, U.; Kohnen, H. (Angew. Chem. **69** [1957] 783).
[8] Rausch, D. A. (U.S. 3288659 [1924/66]; C.A. **66** [1967] No. 30647).
[9] Rausch, D. A. (U.S. 3309248 [1924/67]; C.A. **67** [1967] No. 4515).
[10] Paustian, J. E.; Fein, M. M. (U.S. 3459607 [1912/69] from C.A. **71** [1969] No. 83179).

[11] Seamans, T. F.; Kahrs, J.; Huson, G. R. (J. Spacecr. Rockets **8** [1971] 1080/3).
[12] Burwell, W. G.; Oickle, C., Jr.; to United Aircraft Corp. (U.S. 3694770 [1972] 9 pp. from C.A. **77** [1972] No. 158689).
[13] Ohtoshi, H.; Hanna, J.; Shimizu, I. (Eur. Appl. 228295 [1986/87] 39 pp. from C.A. **107** [1987] No. 145776).
[14] Kanai, M.; Hanna, J.; Shimizu, I. (Ger. 3644652 [1986/87] 13 pp. from C.A. **108** [1988] No. 14906).
[15] Kanai, M.; Hanna, J.; Shimizu, I. (Fr. 2592524 [1986/87] 25 pp. from C.A. **108** [1988] No. 86325).
[16] Pannetier, G.; Margineanu, F.; Dereigne, A.; Bonnaire, R. (Bull. Soc. Chim. Fr. **1972** 2623/5).
[17] Patil, K. C.; Soundararajan, R.; Verneker, V. R. P. (Thermochim. Acta **31** [1979] 259/61).
[18] Rubtsov, Y. I.; Manelis, G. B. (Izv. Akad. Nauk SSSR Ser. Khim. **1984** 296/9; Bull. Acad. Sci. USSR Div. Chem. Sci. [Engl. Transl.] **33** [1984] 260/3).
[19] Abello, L.; Margineanu, F. (C. R. Séances Acad. Sci. C **274** [1972] 916/8).
[20] Axworthy, A. E.; Wagner, R. I. (AD-750900 [1972] 78 pp.; C.A. **78** [1973] No. 99926).

[21] Kirpichev, E. P.; Alekseev, A. P.; Rubtsov, Y. I.; Manelis, G. B. (Zh. Fiz. Khim. **47** [1973] 2942; Russ. J. Phys. Chem. [Engl. Transl.] **47** [1973] 1654).
[22] Brown, C. T.; McMahon, D. G.; Russell, S.; Fondrk, T.; Reed, I. (AD-745993 [1972] 187 pp.; C.A. **78** [1973] No. 74318).
[23] Rubtsov, Y. I. (Gorenie Vzryv Mater. 3rd Vses. Simp., Leningrad 1971 [1972], pp. 771/4; C.A. **79** [1973] No. 35519).
[24] Yakovleva, G. S.; Kurbangalina, R. K.; Stesik, L. N. (Fiz. Goreniya Vzryva **10** [1974] 270/4; Combust. Explos. Shock Waves [Engl. Transl.] **10** [1974] 233/5).
[25] Apin, A. Ya.; Lebedev, Yu. A.; Nefedova, O. I. (Zh. Fiz. Khim. **32** [1958] 819/23).
[26] Brown, C. T. (Propr. Hydrazine Ses Appl. Source Energ. Colloq. Int., Poitiers, Fr., 1974 [1975], pp. 245/65; C.A. **85** [1976] No. 110741).
[27] Pannetier, G.; Margineanu, F. (Bull. Soc. Chim. Fr. **1972** 3725/8).
[28] Texaco Development Corp. (Fr. 2203940 [1972/74]; C.A. **82** [1975] No. 61422).

2.5.4 Compounds of the Composition N_6H_2

A compound with the composition N_6H_2 in a mixture of NH_3 and other nitrogen-hydrogen compounds was detected with a mass spectrometer after exposing gaseous N_2H_4 at 233 K to a microwave discharge [1]. The formation of dimeric adducts of HN_3 is described on pp. 96/7.

Cyclohexazadiene-1,4 (1,4-Dihydrohexazine), c-N_6H_2

CAS Registry Number: *[102101-04-2]*

An MNDO calculation of the geometry of the 1,4-isomer of dihydrohexazine revealed a stable boat conformer. The dihedral angle of the molecular halves, which are joined at the sp^3 nitrogens, is 149°. The sum of the angles at these atoms is 335°. The internuclear distances are $r(N\text{-}N) = 1.379$ Å and $r(N{=}N) = 1.232$ Å. An enthalpy of formation of 371.5 kJ/mol was calculated. The relatively high ionization potential of 10.83 eV indicates that the interaction of the 8 π electrons is moderate [2].

Aminocyclopentazadiene (Aminopentazole), $c\text{-}N_5(NH_2)$

The molecular structure of aminopentazole was calculated at the SCF level. The molecule has a C_s symmetry with a tetrahedral amino nitrogen and the hydrogens above and below the plane of the nitrogen atoms. Internuclear SCF distances in Å are r(H-N′) = 1.000, r(N′-N_1) = 1.374, r(N_1-N_2) = 1.299, r(N_2-N_3) = 1.265, r(N_3-N_4) = 1.326; the angles $\angle N'N_1N_2$ = 124.21° and $\angle HN'N_1$ close to 120° are also given. The barrier to decomposition into N_2 and N_4H_2 is expected to be lower than the barrier to decomposition of cyclopentazadiene [3].

References:

[1] Wiberg, N.; Fischer, G.; Bachhuber, H. (unpublished, ref. 1 in: Wiberg, N.; Chimia **30** [1976] 426).

[2] Kaim, W. (J. Chem. Soc. Perkin Trans. II **1985** 1633/7).

[3] Ferris, K. F.; Bartlett, R. J. (J. Am. Chem. Soc. **114** [1992] 8302/3).

2.5.5 The Ion $c\text{-}N_6H_3^{3+}$

The cation $c\text{-}N_6H_3^{3+}$ can be considered a cyclic trimer of protonated nitrogen, N_2H^+. A C_3 symmetry of the N_6 ring was assumed in semiempirical calculations. A minimum of the potential energy surface was found by the MNDO method. However, the ion is strongly destabilized with respect to the decomposition into 3 N_2H^+. The low stability of the cation is attributed to mutual repulsion of the positive charges which a calculation of the atomic charges showed to be delocalized over the N_6 ring atoms.

Reference:

Gal'pern, E. G.; Stankevich, I. V.; Chistyakov, A. L.; Shur, V. B.; Vol'pin, M. E. (Dokl. Akad. Nauk SSSR **302** [1988] 1384/8; Dokl. Chem. [Engl. Transl.] **298/303** [1988] 302/5).

2.5.6 Cyclohexazane (Hexahydrohexazine), $c\text{-}N_6H_6$

CAS Registry Number: *[60221-91-2]*

Ab initio SCF MO calculations showed that the $c\text{-}N_6H_6$ isomer with the chair conformation is lower in energy than three *cis*-N_2H_2 molecules, whereas octahedral N_6H_6 was found to be considerably higher in energy. The $c\text{-}N_6H_6$ molecule might be stable, because the 2+2+2 dissociation is symmetry-forbidden [1].

Calculations for the 13 chair-N_6H_6 conformers differing by the axial or equatorial arrangement of the hydrogen substituents were performed at the double zeta plus polarization (DZP) level. Minima on the potential surface were found for all conformers. The conformer with all hydrogens in axial positions was confirmed to be the most stable one; the spacious, equatorial positions are occupied by the nitrogen lone electron pairs. The most unfavorable chair conformer has all hydrogens in equatorial positions and is higher in energy by 155 kJ/mol than the most favorable one [2].

The most and least favorable chair conformers of $c\text{-}N_6H_6$ have D_{3d} symmetry. Their internuclear distances d in Å and bond angles calculated at the DZP level are as follows:

conformer	r(N-H)	r(N-N)	∠NNH	∠NNNN (torsion)
only axial H atoms	1.001	1.399	53.3°	40.9°
only equatorial H atoms	1.005	1.435	68.3°	69.3°

The geometrical variations reflect the steric strain caused by axial lone-pair interaction. Structural parameters of the other conformers are listed in the original paper. Twenty out of the expected 30 harmonic vibrational frequencies of the favored conformer are also given. The exothermal decomposition $c\text{-}N_6H_6 \rightarrow 3\ N_2 + 3\ H_2$ has an enthalpy of −696 kJ/mol [2].

References:

[1] Van der Meer, K.; Mulder, J. J. C. (Theor. Chim. Acta **41** [1976] 183/6).
[2] Blahous, C. P.; Schaefer, H. F. (J. Mol. Struct. **200** [1989] 591/610 [THEOCHEM **59**]).

2.5.7 2,3-Diaminotetrazane, $(H_2N)_2NN(NH_2)_2$

CAS Registry Number: *[114045-09-9]*

The heat of formation of $(H_2N)_2NN(NH_2)_2$ was estimated by a semiempirical relation to be 575.6 kJ/mol at 298.15 K. A stabilization energy of −53.9 kJ/mol, being the difference between the heat of atomization and the sum of bond energies, indicates an unstable molecule. Instability with respect to formation of the $(H_2N)_2N$ radical was also predicted [1]; see also p. 166. The equilibrium length of the central N-N bond of 1.470 Å was calculated by an ab initio SCF method [2]. The terminal N-N bonds were predicted to be 1.403 Å long. Angles NNN of 110.1° and 107.0° at the central and 111.4° at the more peripheral nitrogens were calculated. A bond dissociation energy of 20 to 44 kJ/mol at 0 K was predicted for the central N-N bond [3].

References:

[1] Leroy, G.; Sana, M.; Wilante, C.; Peeters, D.; Dogimont, C. (J. Mol. Struct. **153** [1987] 249/67 [THEOCHEM **38**]).
[2] Sana, M.; Leroy, G. (Ann. Soc. Sci. Bruxelles I **101** [1988] 23/57).
[3] Sana, M.; Leroy, G.; Vinson, L. K.; Dannenberg, J. J. (J. Mol. Struct. **205** [1990] 89/95 [THEOCHEM **64**]).

2.5.8 c-N_9H_3

CAS Registry Number: *[112055-75-1]*

The N_9H_3 molecule results from trimerization of HN_3 and consists of an N_6 ring with negatively charged NH substituents in the 1-, 3-, and 5-positions of the ring atoms which are positively charged. A C_3 symmetry of the N_6 ring was assumed in semiempirical calculations. The N_9H_3 was calculated to be stable and energetically not too different from three individual HN_3 molecules. The endocyclic and exocyclic N-N bonds were predicted to be intermediate between single and double bonds. A calculation of the atomic charges shows a separation of the positive charges by localization at the substituted ring atoms which seems to cause the relative stability of N_9H_3. The potential barrier to decomposition into 3 HN_3 is high; the decomposition into hexazine and NH in the triplet state is endothermal.

Reference:

Gal'pern, E. G.; Stankevich, I. V.; Chistyakov, A. L.; Shur, V. B.; Vol'pin, M. E. (Dokl. Akad. Nauk SSSR **302** [1988] 1384/8; Dokl. Chem. [Engl. Transl.] **298/303** [1988] 302/5).

3 Compounds of Nitrogen with Hydrogen and Noble Gases

A few compounds composed of nitrogen, hydrogen, and noble gases are known. The major portion of these compounds are van der Waals complexes between ammonia and a noble gas, such as $NH_3 \cdot He$, $NH_3 \cdot Ar$, or $NH_3 \cdot Kr$. A description of these complexes between ammonia and noble gas is beyond the scope of the present volume.

3.1 The NH_2He^+ Ion

CAS Registry Number: *[65114-22-9]*

Ab initio self-consistent field (SCF) calculations were made on NH_2He^+ to estimate the stability of the product resulting from $T \rightarrow He^+$ β^--decay of tritium-labeled ammonia NH_2T [1] and to check the possibility that NH_2He^+ can be detected in interstellar space [2]. Assuming C_s symmetry, the structural parameters $r(N\text{-}He) = 1.89$ Å, $r(N\text{-}H) = 1.10$ Å, $\angle HeNH = 90.1°$, and $\angle HNH = 107.6°$ were obtained [2]. The ion was found to be weakly bound with a well depth of about 250 cm^{-1} [1, 2]. Thus, it was concluded that NH_2He^+, the daughter ion of NH_2T, is not stable, but dissociates into He and NH_2^+ [1] and that detecting it in interstellar space is unlikely [2].

References:

[1] Ikuta, S.; Yoshihara, K.; Shiokawa, T. (J. Nucl. Sci. Technol. **14** [1977] 720/2).

[2] Cooper, D. L.; Wilson, S. (Mol. Phys. **44** [1981] 161/72).

3.2 Other Ions

$N_mH_nX^+$ (X = Ar, Kr, Xe) ions, formed by electron ionization of mixtures of ammonia and a noble gas, could be detected in mass-spectrometric measurements at high resolving power and by collision-induced dissociation of mass-selected ions using kinetic energy spectroscopy. In addition to the NH_3X^+ ions, there also is evidence for the ions $NHKr^+$, $NHXe^+$, NH_2Xe^+, NH_4Xe^+, and $N_2H_4Xe^+$.

Reference:

Jonathan, P.; Brenton, A. G.; Beynon, J. H.; Boyd, R. K. (Int. J. Mass Spectrom. Ion Processes **71** [1986] 257/82).

Physical Constants and Conversion Factors

Avogadro constant N_A (or L) $= 6.02214 \times 10^{23}\ \text{mol}^{-1}$
Faraday constant $F = 9.64853 \times 10^{4}$ C/mol
molar gas constant $R = 8.31451\ \text{J} \cdot \text{mol}^{-1} \cdot \text{K}^{-1}$
molar volume (ideal gas) $V_m = 2.24141 \times 10^{1}$ L/mol
(273.15 K, 101325 Pa)

Planck constant $h = 6.62608 \times 10^{-34}\ \text{J} \cdot \text{s}$
elementary charge $e = 1.60218 \times 10^{-19}$ C
electron mass $m_e = 9.10939 \times 10^{-31}$ kg
proton mass $m_p = 1.67262 \times 10^{-27}$ kg

1 kg $= 2.205$ pounds
1 m $= 3.937 \times 10^{1}$ inches $= 3.281$ feet
1 m^3 $= 2.642 \times 10^{2}$ gallons (U.S.)
1 m^3 $= 2.200 \times 10^{2}$ gallons (Imperial)

Force	N	dyn	kp
1 N	1	10^{5}	1.019716×10^{-1}
1 dyn	10^{-5}	1	1.019716×10^{-6}
1 kp	9.80665	9.80665×10^{5}	1

Pressure	Pa	bar	kp/m^2	at	atm	Torr	lb/in^2
1 Pa $= 1$ N/m^2	1	10^{-5}	1.019716×10^{-1}	1.019716×10^{-5}	9.86923×10^{-6}	7.50062×10^{-3}	1.450378×10^{-4}
1 bar $= 10^{6}$ dyn/cm^2	10^{5}	1	1.019716×10^{4}	1.019716	9.86923×10^{-1}	7.50062×10^{2}	1.450378×10^{1}
1 kp/m^2 $= 1$ mm H_2O	9.80665	9.80665×10^{-5}	1	10^{-4}	9.67841×10^{-5}	7.35559×10^{-2}	1.422335×10^{-3}
1 at (technical)	9.80665×10^{4}	9.80665×10^{-1}	10^{4}	1	9.67841×10^{-1}	7.35559×10^{2}	1.422335×10^{1}
1 atm $= 760$ Torr	1.01325×10^{5}	1.01325	1.033227×10^{4}	1.033227	1	7.60×10^{2}	1.469595×10^{1}
1 Torr $= 1$ mmHg	1.333224×10^{2}	1.333224×10^{-3}	1.359510×10^{1}	1.359510×10^{-3}	1.315789×10^{-3}	1	1.933678×10^{-2}
1 lb/in^2 $= 1$ psi	6.89476×10^{3}	6.89476×10^{-2}	7.03069×10^{2}	7.03069×10^{-2}	6.80460×10^{-2}	5.17149×10^{1}	1

Work, Energy, Heat	J	kW·h	kcal	Btu	eV
1 J = 1 W·s = 1 N·m = 10^7 erg	1	2.778×10^{-7}	2.39006×10^{-4}	9.4781×10^{-4}	6.242×10^{18}
1 kW·h	3.6×10^{6}	1	8.604×10^{2}	3.41214×10^{3}	2.247×10^{25}
1 kcal	4.1840×10^{3}	1.1622×10^{-3}	1	3.96566	2.6117×10^{22}
1 Btu (British thermal unit)	1.05506×10^{3}	2.93071×10^{-4}	2.5164×10^{-1}	1	6.5858×10^{21}
1 eV	1.602×10^{-19}	4.450×10^{-26}	3.8289×10^{-23}	1.51840×10^{-22}	1

1 $\text{cm}^{-1} = 1.239842\times10^{-4}$ eV

1 hartree = 27.2114 eV

1 Hz = 4.135669×10^{-15} eV

1 eV ≙ 23.0578 kcal/mol

Power	kW	hp	$\text{kp}\cdot\text{m}\cdot\text{s}^{-1}$	kcal/s
1 kW = 10^3 J/s	1	1.35962	1.01972×10^{2}	2.39006×10^{-1}
1 hp (horsepower, metric)	7.3550×10^{-1}	1	7.5×10^{1}	1.7579×10^{-1}
1 $\text{kp}\cdot\text{m}\cdot\text{s}^{-1}$	9.80665×10^{-3}	1.333×10^{-2}	1	2.34384×10^{-3}
1 kcal/s	4.1840	5.6886	4.26650×10^{2}	1

References:

Mills, I. (Ed.), International Union of Pure and Applied Chemistry, Quantities, Units and Symbols in Physical Chemistry, Blackwell Scientific Publications, Oxford 1988.
The International System of Units (SI), National Bureau of Standards Spec. Publ. 330 [1972].
Landolt-Börnstein, 6th Ed., Vol. II, Pt. 1, 1971, pp. 1/14.
ISO Standards Handbook 2, Units of Measurement, 2nd Ed., Geneva 1982.
Cohen, E. R., Taylor, B. N., Codata Bulletin No. 63, Pergamon, Oxford 1986.

Key to the Gmelin System of Elements and Compounds

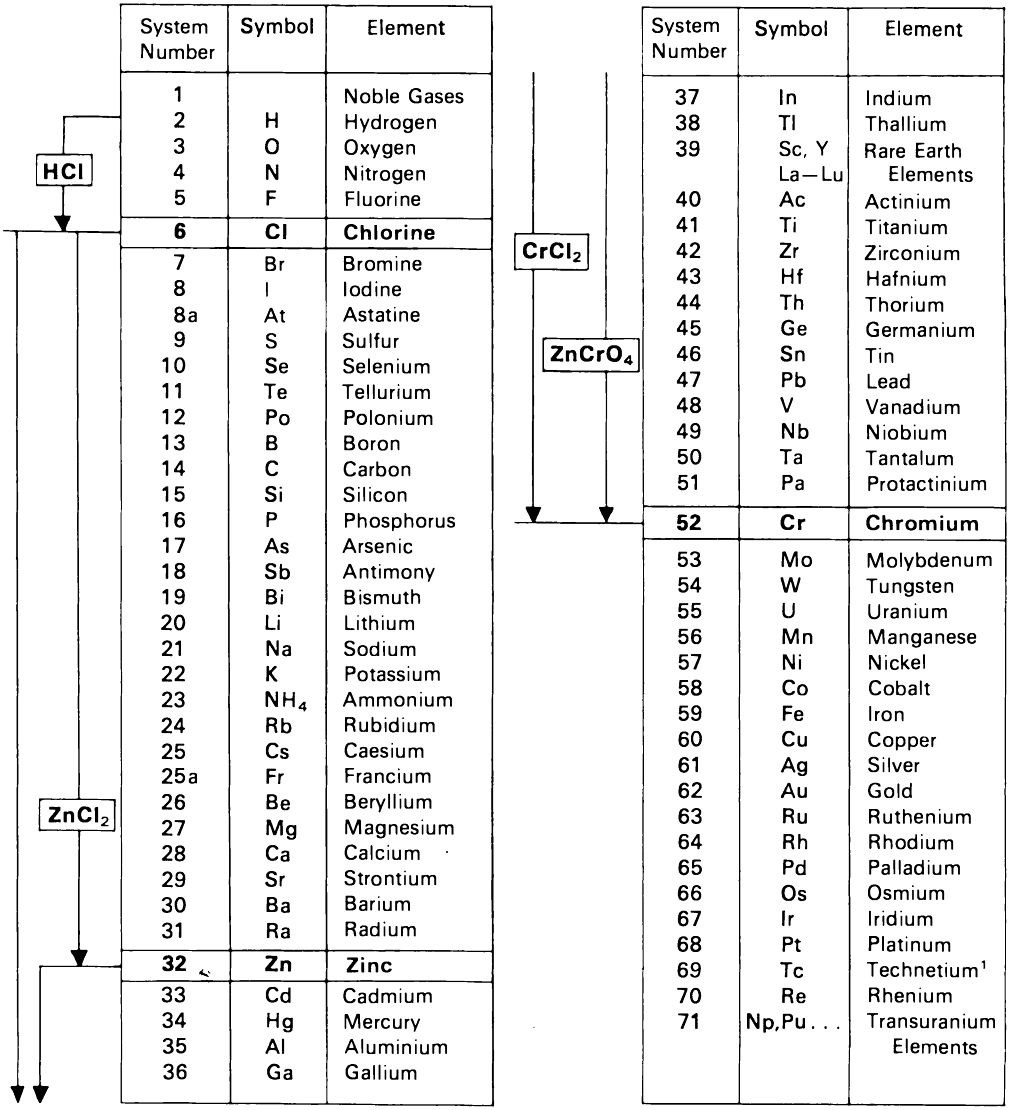

System Number	Symbol	Element
1		Noble Gases
2	H	Hydrogen
3	O	Oxygen
4	N	Nitrogen
5	F	Fluorine
6	**Cl**	**Chlorine**
7	Br	Bromine
8	I	Iodine
8a	At	Astatine
9	S	Sulfur
10	Se	Selenium
11	Te	Tellurium
12	Po	Polonium
13	B	Boron
14	C	Carbon
15	Si	Silicon
16	P	Phosphorus
17	As	Arsenic
18	Sb	Antimony
19	Bi	Bismuth
20	Li	Lithium
21	Na	Sodium
22	K	Potassium
23	NH_4	Ammonium
24	Rb	Rubidium
25	Cs	Caesium
25a	Fr	Francium
26	Be	Beryllium
27	Mg	Magnesium
28	Ca	Calcium
29	Sr	Strontium
30	Ba	Barium
31	Ra	Radium
32	**Zn**	**Zinc**
33	Cd	Cadmium
34	Hg	Mercury
35	Al	Aluminium
36	Ga	Gallium

System Number	Symbol	Element
37	In	Indium
38	Tl	Thallium
39	Sc, Y La—Lu	Rare Earth Elements
40	Ac	Actinium
41	Ti	Titanium
42	Zr	Zirconium
43	Hf	Hafnium
44	Th	Thorium
45	Ge	Germanium
46	Sn	Tin
47	Pb	Lead
48	V	Vanadium
49	Nb	Niobium
50	Ta	Tantalum
51	Pa	Protactinium
52	**Cr**	**Chromium**
53	Mo	Molybdenum
54	W	Tungsten
55	U	Uranium
56	Mn	Manganese
57	Ni	Nickel
58	Co	Cobalt
59	Fe	Iron
60	Cu	Copper
61	Ag	Silver
62	Au	Gold
63	Ru	Ruthenium
64	Rh	Rhodium
65	Pd	Palladium
66	Os	Osmium
67	Ir	Iridium
68	Pt	Platinum
69	Tc	Technetium[1]
70	Re	Rhenium
71	Np,Pu. . .	Transuranium Elements

Material presented under each Gmelin System Number includes all information concerning the element(s) listed for that number plus the compounds with elements of lower System Number.

For example, zinc (System Number 32) as well as all zinc compounds with elements numbered from 1 to 31 are classified under number 32.

---

[1] A Gmelin volume titled "Masurium" was published with this System Number in 1941.

A Periodic Table of the Elements with the Gmelin System Numbers is given on the Inside Front Cover